Mechanisms underlying retinogeniculate synapse formation in mouse visual thalamus

Aboozar Monavarfeshani

Dissertation submitted to the faculty of the Virginia Polytechnic Institute and State University in partial fulfillment of the requirements for the degree of

Doctor of Philosophy
In
Biological Sciences

Michael A. Fox (Committee Chair)
Michael J. Friedlander
Gregorio Valdez
Ignacio Moore
Robert Gourdie

December 18th, 2017
Roanoke, Virginia

Keywords: Lateral Geniculate Nucleus, Synaptic Organizer, Retinogeniculate, LRRTM1

Mechanisms underlying retinogeniculate synapse formation in mouse visual thalamus

Aboozar Monavarfeshani

Abstract

Retinogeniculate (RG) synapses connect retinal ganglion cells to the thalamic relay cells of the dorsal lateral geniculate nucleus (dLGN). They are critical for regulating the flow of visual information from retina to primary visual cortex (V1). RG synapses in dLGN are uniquely larger and stronger than their counterparts in other retinorecipient regions. Moreover, in dLGN, RG synapses can be classified into two groups: simple RG synapses, which contain glia-encapsulated single RTs synapsing onto relay cell dendrites, and complex RG synapses, which contain numerous RTs that converge onto the shared regions of relay cell dendrites. To identify target-derived molecules that direct the transformation of RTs into unique RG synapses in dLGN, I used RNAseq to obtain the whole transcriptome of dLGN and its adjacent retinorecipient nucleus, vLGN, at different time points during RG synapses development. Leucine-Rich Repeat Transmembrane Neuronal 1 (LRRTM1), a synaptogenic adhesion molecule, was the candidate I selected based on its expression pattern. Here, I discovered that LRRTM1 regulates the development of complex RG synapses. Mice lacking LRRTM1 (*lrrtm1*$^{-/-}$) not only show a significant reduction in the number of complex RG synapses but they exhibit abnormal visual behaviors. This work reveals, for the first time, a high level of retinal convergence onto dLGN relay cells in thalamus and the functional significance of this convergence for vision.

Mechanisms underlying retinogeniculate synapse formation in mouse visual thalamus

Aboozar Monavarfeshani

General audience abstract

Our relationship with the environment is heavily reliant on vision, an intricately wired sensory system, much like a circuit. This circuit begins at the eyes, with the retina, and spreads to different visual centers in the brain. Retinal ganglion cells (RGCs) send their wires, called axons, carrying information about the visual world to over 40 different regions in the brain. A major target of these axons is the dorsal lateral geniculate nucleus (dLGN), a region critical to our ability to perceive the visual world. The sites where RGCs connect to the dLGN cells are called retinogeniculate (RG) synapses, and my studies focused on understanding how these RG synapses develop and how they function. I am the first to discover the fact that more than a dozen distinct RGC axons cluster within the same neighborhood of one shared target cell in the dLGN. Unique to the dLGN, these clusters, termed complex RG synapses, are not seen in any other RGC target regions in the brain. Moreover, I demonstrated a new molecular mechanism that forms these synapses by identifying a protein called LRRTM1, as a critical molecule required for the formation of these complex RG synapses in the dLGN. By studying the visual behavior of mutant mice lacking LRRTM1, I demonstrated that complex RG synapses are important for performing complex visual tasks. The discoveries detailed within this dissertation add to current efforts to restore vision in patients suffering from severe visual impairments, via regenerative therapies, by furthering our understanding of how neural wires connect in the visual circuit to reveal everything we will ever know about the visual world.

Acknowledgements

I am grateful to Dr. Fox for his incredible mentorship over the years, and for providing me with valuable opportunities during my PhD training. From him, I not only learned how to ask and answer scientific questions, but also how to write and talk about science. More importantly, I learned, hopefully, from Mike how to be patient for a scientific discovery and how to work effectively with others as a team to tackle a question. I am also thankful for the tremendous support and guidance of my committee members, Dr. Friedlander, Dr. Gourdie, Dr. Moore and Dr. Valdez. Whenever I needed, they provided me with their excellent expertise. Their short and occasional comments on my work can be classified into two groups: favorable comments which were truly inspiring and unfavorable comments which were truly instructive. Additionally, I am thankful for being surrounded by supportive people at VTCRI and having wonderful colleagues and friends at Fox, Valdez, Mukherjee and Sontheimer labs. I must particularly thank Dr. Mukherjee, whom I'd often consulted and found to be a source of valuable comments and science discussions.

Despite being 7000 miles away from me, my family (fortunately I have a big family but it makes it hard to mention them by name) always supported my efforts through Skype, so I am truly thankful to them too. I am grateful to my father and my mother who did all they could to make sure I become the first scientist in my family.

Above all, I'm grateful and indebted to my beautiful wife, Marjan, who sacrificed her career for this work and who bears the difficulty of missing her family and friends while we have been here for my PhD. I dedicate this work to her.

Table of Contents

List of Figures

Chapter 1

Chapter 2

Chapter 3

1. General introduction

1.1. **Overview of the mouse visual system**

Retina, the neural tissue within the eye, detects, processes and transmits light-derived information to many retinorecipient regions in the brain. This light-derived information regulates a diverse collection of biological processes. The most evident function of the retina and its light-derived output is vision. Sighted animals utilize this information to perceive the size, shape, color, direction and motion of the objects and other organisms in their surrounding environment. In addition to this "image-forming" function, light-derived signals regulate many other physiological processes such as photo-entrainment of the circadian rhythm, pupillary reflexes and heart rate in mammals.

The retina contains 5 main neural cell types: photoreceptors, 3 types of interneurons and retinal ganglion cells. Photoreceptors (PRs) lie in the outermost layer of retina (the ONL) where they detect and convert photons of lights into neural signals. PRs then transmit those light-derived signals to the inner nuclear layer (the INL) of the retina where retinal interneurons which include bipolar cells, horizontal cells and amacrine cells, process and shape the visual signals and transmit them to retinal ganglion cells (RGCs) in the innermost layer of the retina. RGCs extract and transmit distinct aspects of visual information to many different subcortical regions in the brain, based on their classes (Fig. 1). Retinal projections that carry image-forming information necessary for vision innervate many subcortical regions including the dorsal Lateral Geniculate Nucleus (dLGN) in the thalamus and Superior Colliculus (SC) in the midbrain. These two regions are the most well-studied retinorecipient regions in mammals. The dLGN (called simply LGN or DLG in carnivores and primates) relays image-forming visual information to the primary visual cortex (V1), primarily to layers 1 and 4. From V1, visual information enters one

of the two less known cortical pathways, the ventral and dorsal streams, through anterolateral (AL) and lateromedial (LM) visual areas, respectively (Wang et al., 2012). The visual information of the ventral and dorsal stream, along with inputs from other sensory systems, ultimately guides animal's sight-dependent navigation in their environment.

More details regarding the components of rodent visual circuitry which are important for studies in this dissertation will be discussed below. At this point, however, it is important to note that studying the circuitry of the visual system and the mechanisms by which visual information is generated, processed, and transmitted to the brain is necessary not only to enhance our fundamental understanding of vision, but also to develop novel therapeutic interventions for patients suffering from devastating disorders of the visual system such as glaucoma.

1.2. Visual impairments and future regenerative therapies

Blindness and other visual impairments affect millions of people worldwide and in the United States (Stevens et al., 2013; Tham et al., 2014) and they represent a significant economic burden (Köberlein et al., 2013; Rein et al., 2006). According to world health organization (WHO) estimation, currently, about 36 million people worldwide are blind and 217 million more suffer from moderate to severe visual impairment. Additionally, the National Eye Institute (NEI) projects that 4 million Americans will be blind and upwards of 12 million will suffer from visual impairment by the year 2050. One of the main causes of blindness and severe visual impairment is glaucoma, a condition caused by blockage of the Schlemm's canal and increased pressure inside the anterior and vitreous chambers of the eyes. This increased pressure leads to permanent damage to the optic nerve and eventual death of RGCs (thus, disconnecting the eyes from the

brain). In the US alone, it has been projected that the number of people affected by glaucoma will exceed 6 million by 2050 (NIH).

Unfortunately, there are no cures or effective treatments for glaucoma (Tham et al., 2014). However, the emergence of regenerative therapeutics has opened the door to the potential treatments of severe visual impairment and blindness caused by this disease and other neurodegenerative disorders of the visual system such as optic nerve hypoplasia (ONH) (Kong et al., 2012; Ryabets-Lienhard et al., 2016) as well as traumatic optic nerve injuries, in which the neural connections between RGCs and target regions in the brain are disrupted. The driving principle of regenerative therapeutics is to re-establish neural connections between RGCs and retinorecipient regions in the brain (Sieving, 2012; Yucel and Gupta, 2015). To restore vision through this regenerative approach, we need to: (1) regenerate RGCs from stem cells, (2) regrow their axons into the brain, (3) guide them to the correct target nuclei in the brain – and correct cell types – and, most importantly, (4) program them into building the correct type and functional synapses. While not fully successful yet, the generation of some RGCs or the whole retina (in the form of organoids) from embryonic stem (ES) or induced pluripotent stem cells (iPSCs) have been accomplished by a few groups (Gill et al., 2016; Maekawa et al., 2016; Nakano et al., 2012; Ohlemacher et al., 2016; Reichman et al., 2014; Zhong et al., 2014). Similarly, regeneration and regrowth of RGC axons into the retinorecipient regions of the brain have been only achieved for a very small percentage of RGCs with minor functional recoveries of visual behaviors (Benowitz et al., 2017).

Currently, a major obstacle in visual circuit regeneration is the significant gap in the knowledge about molecules and mechanisms required for guiding retinal axons to their targets and molecular mechanisms that regulate the assembly of appropriate and functional synapses

(Crair and Mason, 2016; Goldberg and Guido, 2016). Therefore, understanding how synaptic connections form between retinal axons and relay cells in the dLGN by filling this gap serves a crucial step for developing regenerative therapies for visual impairments. For this reason, I have focused on trying to identify molecules and mechanisms that underlie the formation and differentiation of retinogeniculate (RG) synapses; the synapses that connect RGCs to the principal relay cells in the dLGN.

In the following sections, I will introduce key concepts regarding the circuitry and cytoarchitecture of the mouse retina and dLGN and their respective mechanisms involved in receiving, processing and transmitting visual sensory information. It is important to note that some parts of this section are excerpts from a review that I co-authored (Monavarfeshani et al., 2017). The full version of this manuscript is available online. After a general introduction to the RG circuit, I will introduce key concepts in known molecular mechanisms that govern synaptogenesis (mainly at other synapses in the brain).

1.3. Retinal processing of light-derived signals in mice

In mouse retina, three types of PRs exist in the outer nuclear layer (Fig. 1): Rods which possess a high level of sensitivity to light and, therefore, are responsible for vision in low-light conditions; and 2 types of cones, which respond best to bright lights and each contain distinct photopigments that enable them to detect specific wavelengths of light (color). One type of rods and two types of cones have been characterized in the mouse retina based on the presence of different opsins in their outer segments. S cones, which express short wavelength-sensitive (S) opsins and are able to detect UV light (unlike S cones in primates which detect blue light); and S/M cones, which contain both S and M (middle-to-long-wavelengths, also called L opsin) opsin

photopigments and are able to detect both UV and green colors (mice cannot detect red light) (Baden et al., 2013; Jacobs et al., 2004; Ortín-Martínez et al., 2014). Thus, in the ONL of retina, one can assume at least 3 separate entrance channels for different visual information (i.e. rod channel, S-cone channel and S/M-cone channel).

The INL of the retina harbors at least 12 (but likely more) types of bipolar cells, as well as many other types of horizontal and amacrine cells (Macosko et al., 2015; Masland, 2001; Shekhar et al., 2016). Bipolar cells that connect with rods are called rod bipolar cells (RBC), while those that receive input solely from cones are called cone bipolar cells (CBC). Typically, around 20-80 rod PRs converge onto a single RBC, and similarly (but to a lesser extent), a single CBC receives converging input from multiple cone PRs (only from S cones, or from a mixture of S and S/M cones). CBCs are classified as ON (depolarize in response to stimulus) or OFF (hyperpolarize in response to stimulus) bipolar cells depending on their response to the presence of light. Horizontal cells in the outer plexiform layer (OPL) connect to PRs synaptic terminals. It has been thought that horizontal cells, through an inhibitory feedback mechanism onto the PRs, generate lateral inhibition. The highly precise neural circuit that forms in the inner plexiform layer (IPL) among different classes of the 3 main retinal cells types, bipolar, amacrine and ganglion cells, assembles a computational substrate that underlies the complex processing of visual information before they sent to the brain through RGC axons (Euler et al., 2014; Wässle, 2004).

About 30 classes of RGCs have been characterized based on their morphology, circuitry, physiological properties and molecular identities (Sanes and Masland, 2015), although single cell transcriptome analyses suggest this number could exceed 45 and analyses in zebrafish have proposed ~80 classes of RGCs (Robles et al., 2013). For those classes that have been studied in

detail, layer-specific dendritic stratification and the pattern of dendritic branching of RGCs in the IPL, soma size, and gene expression patterns are all important criteria by which RGC classes are defined. Each class of RGCs is optimized to respond best to a particular feature of the visual world varying from detection of a simple center-surround spot (e.g. by alpha RGCs, the largest RGCs) to detection of directional movement of both light and dark edges (e.g. by ON-OFF DSGCs). Thus, different features of the visual information are encoded by RGCs, sorted into distinct channels, and transferred to subcortical regions in the brain through separate pathways. Beyond being a powerful light detector, the retina process and parses out different features of the visual world before transmitting them through RGC axons to the brain.

1.4. dLGN: the main target region of image-forming RGC projections

RGC axons exit the eye from the optic disc and reach the brain through the optic nerve. In both nocturnal and diurnal rodents, these axons innervate approximately 40 different retinorecipient regions, more than ten of which are located within the thalamus (Martersteck et al., 2017; Morin and Studholme, 2014). In nocturnal rodents, thalamic nuclei directly innervated by retinal axons include the dLGN, ventral lateral geniculate nucleus (vLGN), intergeniculate leaflet (IGL), lateral posterior thalamic nucleus (LP; analogous to the pulvinar in higher mammals), anterodorsal thalamic nucleus (AD), centrolateral thalamic nucleus (CL), para-habenular zone (PHb), peripeduncular nucleus (PP), zona incerta (ZI), and subgeniculate nucleus (SubG) (Morin and Studholme, 2014). (Fig. 2). In addition to these retinorecipient regions, some thalamic nuclei, such as the thalamic reticular nucleus (TRN), process visual information but do not receive direct input from RGCs. Despite the plethora of retinorecipient targets in mice brain,

the vast majority of image-forming RGC axons innervate the dLGN. Here, I review the cytoarchitecture and circuitry of the dLGN in mouse (and other rodents).

1.4.1. Cytoarchitectural organization of dLGN

The dLGN receives, processes, and relays classical image-forming visual information and, for this reason, has received the most attention of all retinorecipient thalamic nuclei. In higher mammals, the dLGN has a distinctive cytoarchitecture with layers that receive eye- and function-specific retinal inputs. While cells in the dLGN of highly visual diurnal rodents, such as squirrels, are separated into at least five layers (Kaas et al., 1972; Van Hooser and Nelson, 2006), the dLGN of nocturnal rodents lacks gross cytoarchitecture lamination, despite having eye-specific domains (Godement et al., 1984; Jaubert-Miazza et al., 2005; Muir-Robinson et al., 2002; Reese and Cowey, 1983) (Fig. 3). Nevertheless, evidence that the dLGN of rats (Reese, 1988), mice (Grubb and Thompson, 2004; Krahe et al., 2011), and hamsters (Emerson et al., 1982) are not anatomically homogenous emerged. The possibility that “hidden laminae” existed in rodent dLGN first arose from studies demonstrating the dorsolateral “shell” and ventromedial “core” regions of rodent dLGN contain population of retinal terminals (RTs) that are morphologically separable (Erzurumlu et al., 1988; Hammer et al., 2015; Reese, 1988). Hidden laminae have become more apparent with techniques that label individual classes of RGCs (Baden et al., 2016; Sanes and Masland, 2015). A series of studies in transgenic reporter mice (each of which labels a single class of RGCs) have demonstrated the existence of several RGC class-specific retinorecipient sublaminae in dLGN (Hong and Chen, 2011; Huberman et al., 2008a; Huberman et al., 2009; Kay et al., 2011; Kim et al., 2010; Kim et al., 2008) (Fig. 3).

In addition to a heterogeneous distribution of retinal afferents, neuronal subtypes within the rodent dLGN are differentially distributed. Two main types of neurons exist in dLGN, both of which are innervated by retinal afferents. Principal neurons, or thalamocortical (TC) relay cells, are excitatory projection neurons that originate from the caudal progenitor domain within the thalamic ventricular zone (i.e. prosomer 2) (Altman and Bayer, 1989; Puelles and Rubenstein, 2003; Vue et al., 2007) during rodent embryogenesis. Ultimately TC progenitor cells differentiate into at least three morphologically distinct classes in nocturnal rodents – biconical X-like cells, symmetrical Y-like cells and hemispheric W-like TC cells (Krahe et al., 2011; Ling et al., 2012). These classes of TC relay cells closely resemble those reported in cats (Friedlander et al., 1981) and higher mammals (Irvin et al., 1993). Just as classes of relay cells are differentially distributed in cat and primate dLGN (Nassi and Callaway, 2009; Sherman, 1985), they are uniquely distributed in mouse dLGN: W-like cells occupy the dorsolateral shell of mouse dLGN and X- and Y-like cells occupy the ventromedial dLGN core (Krahe et al., 2011). While all three classes of TC relay cells project axons to visual cortex, recent evidence has demonstrated that regionally restricted cell types participate in functionally distinct parallel visual pathways in mice (Bickford et al., 2015; Cruz-Martín et al., 2014).

Beside principal relay cells, rodent dLGN contains a small percentage (10-20%) of inhibitory interneurons, a cell type absent from most other dorsal thalamic regions (Arcelli et al., 1997; Jaubert-Miazza et al., 2005). The arrival of these interneurons occurs postnatally, after retinal inputs have targeted dLGN, formed immature connections, and begun to undergo activity-dependent refinement (Golding et al., 2014; Jager et al., 2016; Jones and Rubenstein, 2004; Singh et al., 2012). The precise origin of these interneurons is currently under debate, with studies suggesting they arise from a rostral progenitor domain within the thalamus (i.e. prosomer

3) or from tectum (Golding et al., 2014; Jager et al., 2016; Virolainen et al., 2012). Evidence is also emerging that dLGN interneurons are not a homogeneous population in mice, and can instead be divided into at least two classes based on soma size, membrane capacitance and neuronal nitric oxide synthase (nNOS) expression (Leist et al., 2016). Similar interneuron diversity has been reported in rats (Gabbott and Bacon, 1994), cats (Montera and Zempel, 1985; Montero and Singer, 1985), and primates (Braak and Bachmann, 1985). At present, however, it remains unclear whether classes of local inhibitory interneurons exhibit regional preferences in the nocturnal rodent dLGN.

1.4.2. Afferent projections of dLGN: Retinal Afferents

In mammals, the primary excitatory drive onto TC relay cells is provided by retinal inputs (Petrof and Sherman, 2013; Sherman, 2005). Anatomically, retinal projections to dLGN are spatially organized in (at least) three fundamental ways. First, retinal afferents are segregated into non-overlapping eye-specific domains in an activity-dependent manner (Huberman et al., 2008a; Zhang et al., 2012). The dLGN of nocturnal rodents receives a relatively small contribution (5-10%) of retinal afferents from the ipsilateral retina and these projections are confined to a ventromedial core region of the dLGN (Gaillard et al., 2013; Jaubert-Miazza et al., 2005; Morin and Studholme, 2014) (Fig. 3B). Second, retinal projections to dLGN are organized topographically– so that neighboring RGCs provide input to neighboring TC relay cells and provide a continuous and faithful representation of spatial information from retina to brain (Cang and Feldheim, 2013; Feldheim et al., 1998; Huberman et al., 2008a; Pfeiffenberger et al., 2006) (Fig. 3C). Third, and perhaps most remarkably, retinal projections undergo class-specific segregation in rodent dLGN (Fig. 3D). Although more than 30 classes of RGCs exist in

nocturnal rodents only a subset innervate dLGN (Baden et al., 2016; Ellis et al., 2016; Sanes and Masland, 2015). This suggests that targeting mechanisms exist that guide some classes of RGC axons into dLGN and exclude others. Once appropriate classes of retinal axons enter dLGN, they are further segregated into a newly-appreciated laminar organization (Dhande and Huberman, 2014; Hong and Chen, 2011; Sanes and Masland, 2015). The presence of these stereotyped class-specific retinal projections has been elegantly revealed by transgenic reporter mice in which individual RGC classes are labeled with reporter proteins (Dhande et al., 2013; Hattar et al., 2006; Huberman et al., 2008b; Huberman et al., 2009; Kay et al., 2011; Kim et al., 2010; Kim et al., 2008; Rivlin-Etzion et al., 2011; Triplett et al., 2014). While only a small set of individual RGC projections have been mapped with this approach, some rules are beginning to emerge. First, projections of direction-selective classes of RGCs arborize in more dorsolateral regions of dLGN, including the shell of dLGN (Cruz-Martín et al., 2014; Huberman et al., 2009; Kim et al., 2008; Rivlin-Etzion et al., 2011). Second, there is considerable overlap in the laminar termination zones of RGC axons (Fig. 3D), and taken in the context of recent ultrastructural and circuit tracing experiments in dLGN (Hammer et al., 2015; Morgan et al., 2016; Rompani et al., 2017), this raises the possibility that individual TC relay cells may receive inputs from multiple classes of RGCs.

In addition to being segregated based on eye of origin, topography, and RGC class, retinal inputs in dLGN are structurally and functionally distinct from retinal inputs in other retinorecipient nuclei, even other thalamic nuclei (Hammer et al., 2014; Sherman, 2005). Specifically, RTs onto dLGN TC relay cells are significantly larger than all other terminals in dLGN (and larger than RTs in all other retinorecipient nuclei), and exhibit unique ultrastructural morphology and function (Bickford et al., 2010; Guido, 2008; Guillery, 1969; Hong and Chen,

2011; Lund and Cunningham, 1972; Sherman, 2004). It is worth pointing out, however, that at least two distinct types of RG synapses have been identified in rodent dLGN: “simple encapsulated” RG synapses, in which a single retinal terminal synapses onto a TC relay cell dendrite, and “complex encapsulated” RG synapses in which axons from numerous RGCs converge to innervate adjacent region of TC relay cell dendrite (Hammer et al., 2015; Lund and Cunningham, 1972; Morgan et al., 2016). Finally, it is important to point out that retinal projections not only innervate TC relay cells, but also local interneurons in nocturnal rodents (Seabrook et al., 2013b; Sherman, 2004).

1.4.3. Afferent projections of dLGN: Non-Retinal Afferents

While retinal inputs provide the excitatory drive to TC relay cells, they account for only 5-10% of the total inputs onto a relay cell and are far outnumbered by non-retinal inputs (Bickford et al., 2010; Cetin and Callaway, 2014; Sherman and Guillery, 2002). A summary of the main inputs to rodent dLGN is depicted in Fig. 4.

While many non-retinal inputs onto dLGN TC relay cells have modulatory or inhibitory roles, a recent study identified a novel glutamatergic non-retinal source of “driver-like” input onto dLGN TC relay cells (Bickford et al., 2015). These inputs arise from the ipsilateral superior colliculus (SC) and terminate onto W-like TC relay cells in the dorsolateral shell of dLGN (Bickford et al., 2015; Harting et al., 1991a). Circuit tracing experiments indicate these excitatory tectogeniculate connections contribute to the processing and transmission of direction-selective visual information (Bickford et al., 2015).

While tectogeniculate inputs represent a minor source of inputs to dLGN, a more significant portion of non-retinal glutamatergic inputs arise from cortical projection neurons in

layer VI of primary visual cortex (Sherman, 2016). Corticothalamic inputs are small, located on distal portions of TC relay cell dendrites, and generate weak excitatory postsynaptic potentials (EPSPs) in relay cells (Petrof and Sherman, 2013; Sherman and Guillery, 2002). For this reason, it is likely that these inputs are insufficient for the relay of information alone and are, therefore, modulatory in nature (Petrof and Sherman, 2013). Despite these features, corticothalamic inputs do significantly influence RG transmission by affecting the gain of signal transmission and the sharpening of receptive field properties of TC relay cells (Bickford, 2015; Briggs and Usrey, 2008; Olsen et al., 2012; Sherman and Guillery, 2002).

In addition to tectal and cortical glutamatergic inputs, TC relay cells in higher mammals receive modulatory cholinergic, serotonergic, noradrenergic and dopaminergic inputs from a variety of sources in the brainstem including parabigeminal nucleus, pedunculopontine region, locus coeruleus, dorsal raphe nucleus of the midbrain, and the midbrain reticular formation (De Lima and Singer, 1987; de Lima et al., 1985; Jones, 2012; Mackay-Sim et al., 1983; McCormick, 1992; Papadopoulos and Parnavelas, 1990a, b). At present, some of these afferent projections have been demonstrated in nocturnal rodents (Hallanger et al., 1987; Harting et al., 1991b), but additional studies are needed to map specific sources of these inputs and to understand their role in signal processing in rodents.

Finally, the last significant source of non-retinal inputs to dLGN are inhibitory GABAergic inputs that arise from both local inhibitory neurons and projection neurons in the thalamic reticular nucleus (TRN), a region that forms a lateral shell around dorsal thalamus in nocturnal rodents (Guillery and Harting, 2003; Hale et al., 1982; Pinault, 2004). Inhibitory neurons in the ipsilateral pretectum also project to dLGN (Born and Schmidt, 2007), however

evidence suggests that these projections innervate dLGN interneurons not TC relay cells (Born and Schmidt, 2007; Wang et al., 2002), adding further complexity to dLGN circuitry.

An interesting facet of the convergence of retinal and non-retinal inputs in dLGN is that their development appears tightly coordinated. Retinal axons target and innervate dLGN prior to the arrival of non-retinal inputs and play instructive roles in the establishment of non-retinal circuitry (Brooks et al., 2013; Golding et al., 2014; Grant et al., 2016; Seabrook et al., 2013a). Likewise, non-retinal inputs contribute to the development and function of retinogeniculate synapses. For example the presence of corticothalamic axons and corticogeniculate synapses play essential roles in the establishment, refinement, and maintenance of retinal inputs (Shanks et al., 2016; Thompson et al., 2016).

1.4.5. Efferent projections of dLGN

The relative simplicity of efferent projections from dLGN is striking and emphasizes a singular function of dLGN in processing and transferring image-forming visual information. TC relay cells project axons to only two ipsilateral regions in nocturnal rodents: primary visual cortex and TRN (Crabtree and Killackey, 1989; Jurgens et al., 2012; López-Bendito and Molnár, 2003; Rafols and Valverde, 1973; Reese and Cowey, 1983; Towns et al., 1982). Recent studies in mice have demonstrated that projections to visual cortex exhibit class-specificity, with W-like relay cells in the dorsolateral shell of dLGN, conveying direction-selective visual information to layer I and Y-like and X-like relay cells projecting to layer IV of primary visual cortex (Bickford et al., 2015; Cruz-Martín et al., 2014). At present, it remains unclear whether these three classes of TC relay cells make unique connections with TRN neurons in nocturnal rodents. It is worth mentioning that, in cat, Y-cells provide the predominant dLGN input to the perigeniculate

nucleus, the visual sector of cat TRN which overlies dLGN (Dubin and Cleland, 1977; Friedlander et al., 1980).

1.5. Molecular mechanism underlying synapse formation

Synapses are the main routes of communication between neurons. They are specialized asymmetric cell-cell junctions that permit the exchange of chemical signals (i.e. neurotransmitters) between pre- and post-synaptic neurons. The formation of synapse is a highly regulated process which takes place in a series of interrelated steps (Waites et al., 2005). Axons of the presynaptic neurons navigate through the complex and crowded neural tissues and target appropriate postsynaptic cells. Attractive and repulsive guidance cues (also called targeting cues) regulate this stage of synaptic development. These targeting cues ensure the striking specificity of synaptic connections. Not only do growing axons target an appropriate cell, but they also form synapses on a specific subcellular portion of their targets (e.g. proximal dendrites or soma) (Sanes and Yamagata, 2009). After the initial contact between axons and postsynaptic targets, molecules expressed by presynaptic and/or postsynaptic neurons (and even by neighboring glia cells) promote the differentiation of nascent neural contacts into mature synapses (Fox and Umemori, 2006). These molecules, called synaptic organizers (or synaptogenic factors), direct the transformation of unspecialized presynaptic membrane into a complex structure (i.e. active zone) which is highly specialized for releasing neurotransmitter through an exocytotic pathway. On the other side, they also transform the postsynaptic membranes into specialized domains that contain clusters of neurotransmitter receptors as well as a variety of other extracellular, transmembrane and cytoplasmic proteins (i.e. postsynaptic density scaffold). Since an excessive number of synapses form early in development, synapses either mature by expanding their

synaptic components (e.g. the presynaptic terminal size, number of synaptic vesicles, active zone area, spine head volume, post synaptic density area) or they undergo an activity-dependent elimination process which is thought to rely on sensory experiences (Flavell and Greenberg, 2008; Fox and Umemori, 2006; Sanes and Lichtman, 2001).

An increasing number of molecules involved in synaptic development have been identified (Brose, 2009; Chia et al., 2013; Fox and Umemori, 2006; Lee and Sheng, 2000; Waites et al., 2005; Yogev and Shen, 2014). Synaptic adhesion molecules and secreted factors are two main classes of synaptic organizing proteins (Fig. 5). Secreted synaptogenic factors are expressed by presynaptic axon or postsynaptic neurons, by neighboring neurons or even by glia cells. For example, postsynaptic neurons secrete Fibroblast Growth Factor 22 (FGF22) which can induce presynaptic differentiation of excitatory synapses in many regions of the nervous system including skeletal muscle (Fox et al., 2007), cerebellum (Umemori et al., 2004), hippocampus (Terauchi et al., 2010) and dLGN (Singh et al., 2011). Other examples of secreted factors are members of Thrombospondins (TSPs) which are likely to be exclusively released by glia cells and promote the formation and maturation of nearby synapses (Christopherson et al., 2005).

On the other hand, synaptic adhesion molecules mediate different stages of synaptic development by facilitating adhesive interaction between synaptic partners. Obviously, they stabilize synaptic structures by physically linking pre- and postsynaptic partners, but by being expressed on the surface of cell membranes, they can also specify (tag) neurons or distinct subcellular portion of neurons as the appropriate targets for axons, therefore, acting as targeting cues. Synaptic adhesion molecules can also promote the differentiation of nascent synaptic structures into mature synapses by providing a signaling bridge between synaptic partners

(Bukalo and Dityatev, 2012; Siddiqui and Craig, 2011; Yamagata et al., 2003). Some of these synaptic adhesion molecules include members of the cadherin family, neurexins and neuroligins, ephrins, and Eph receptors, and leucine-rich repeat (LRR)–containing cell adhesion molecules such as netrin-G ligands, synaptic adhesion–like molecules and leucine-rich repeat transmembrane neuronal proteins (LRRTMs).

1.6. Rationale, hypothesis and experimental design

Data from my first study in the Fox lab suggested that RTs in the dorsal lateral geniculate nucleus (dLGN) are uniquely larger than their counterparts in all other major retinorecipient nuclei (Fig. 6). Similarly, electrical stimulation of the optic tract coupled to the recording from relay cells revealed fewer, but stronger, retinal inputs onto relay cells in dLGN compared to those in vLGN. This lower level of retinal convergence onto dLGN relay cells has been reported in mice and higher mammals (Chen and Regehr, 2000; Cleland et al., 1971; Cleland and Lee, 1985; Jaubert-Miazza et al., 2005; Sincich et al., 2007; Usrey et al., 1999; Yeh et al., 2009). However, our electron microscopy data (Hammer et al. 2014) showed that multiple RTs in dLGN participate in forming complex retinogeniculate synapses, a synaptic structure that have been found in other rodents and higher mammals (Guillery and Scott, 1971; Jones and Powell, 1969; Lund and Cunningham, 1972; So et al., 1985; Wilson et al., 1984) (see Hammer et al. 2014). To be consistent with physiological data, which shows that each relay cell receives only a few strong RG inputs, these RTs clustering on a portion of postsynaptic neurons must originate from a small number (~1-2) of RGCs.

Therefore, one of my aims was to test the **hypothesis** that retinal terminals in complex retinogeniculate synapses originated from one (or a few) RGCs. To test this hypothesis, I studied

RTs in dLGN of adult (P35-42) wild type mice using serial block-face scanning electron microscopy (SBFSEM) and AAV viral tracing. Our data presented in chapter 2 of this dissertation (following chapter) showed that, to our surprise, our hypothesis was incorrect. In fact, we discovered that as many as a dozen distinct retinal axons converge onto a single relay cell at the sites of complex RG synapses.

Overall, results from Hammer *et al.* 2014 and Hammer *et al.* 2015 showed that in dLGN, not only RTs were larger compared to their counterparts in all other retinorecipient nuclei, but a large subset of RTs were clustered into complex RG synapses. As I mentioned above, different classes of RGCs exist. Therefore, different retinorecipient regions (e.g. dLGN) may receive inputs from distinct classes of RGCs which are intrinsically able to generate different retinal terminals in their exclusive target region. Although intrinsic properties of RGCs cannot be ruled out, several lines of evidence suggest that extrinsic target-derived signals are responsible for the unique differentiations of RTs in dLGN. First, while almost all RGCs innervating dLGN send a collateral branch to the SC, their RTs in the dLGN is significantly larger than those in SC (Ellis et al., 2016; Hammer et al., 2014). Second, it has been shown that a single RGC axon can form RTs varying in size and morphology depending on the target cells they contact with (Hamos et al., 1987). Third, rerouting RGC axons from the dLGN adopt a “target-like” morphology and form RTs similar to the boutons existing in their new destination (Campbell and Frost, 1987, 1988), suggesting the existence of target-derived signals regulating the unique development of RTs in their target regions (e.g. dLGN). Moreover, we found that RTs originating from one specific class of RGCs (which are transgenically labeled in HB9-gfp mice) end up making dramatically larger terminals in dLGN compared to those in SC. Interestingly, collateral axons from a single RGC have been shown to contain distinct anatomical features (e.g. larger

terminals) in the dLGN compared to superior colliculus (Dhande et al., 2011). These observations suggested the existence of extrinsic mechanisms regulating the transformation of RTs in different retinorecipient target regions. Therefore, we **hypothesized** that specific target-derived signals must exist in dLGN in order to transform RTs into unique RG synapses in dLGN. To test this hypothesis, I identified synaptic organizers that are differentially expressed during different stages of retinal terminal development in dLGN. To narrow the potential list of candidate organizing cues, I compared dLGN transcriptome to the transcriptome of its adjacent retinorecipient region (vLGN) in which retinal terminals do not undergo the same morphological enlargement as retinal terminals in dLGN.

Using RNAseq, I obtained the whole transcriptome of mouse dLGN and vLGN at four different ages which correspond to distinct stages of retinal terminal (i.e. the presynaptic sides of retinogeniculate synapses) development. Postnatal day 3 (P3) is an age corresponding to the initial stages of RG synapse formation, P8 and P12 are ages corresponding to the refinement and maturation of RG synapses, and P25 is the age by which RG synapses have matured and acquired adult-like morphology. To select potential target-derived candidates regulating the unique transformation of RG synapses in dLGN, I first screened all genes that had a higher level of expression at p12, the age when we observed the emergence of large retinal terminals in dLGN. Next, I focused on genes of with a significant two fold enrichment in dLGN compared to vLGN. Finally, I ranked my list of genes based their known function in their involvement in (any aspect of) synapse development according to previous reports. For the top 30 candidates, I performed qPCR and (for some) designed riboprobes in order to validate the expression pattern obtained by RNAseq. This unbiased screen led me to final list of several growth factors and synaptic adhesion molecules (Fig. 7) including Leucine-Rich Repeat Transmembrane neuronal

proteins 1 (LRRTM1) and Neuritin (NRN1, also known as candidate plasticity gene 15 or CPG15) which I will discuss in this dissertation (chapter 2).

LRRTM proteins are potent synaptogenic molecules (Linhoff et al., 2009) that are predominantly expressed in the central nervous system and they show distinct regional expression patterns (Laurén et al., 2003). There are four LRRTM paralogues (LRRTM1–4) in mammals which are typical cell surface adhesion proteins. They contain an N-terminal signal peptide, an extracellular region containing (a potential) N-linked glycosylation sites and a hydrophobic transmembrane region followed by a cytoplasmic region containing a C-terminal PDZ-binding motif that is required for binding to the postsynaptic scaffolding protein PSD-95 (Fig. 5) (Laurén et al., 2003). Recent studies have identified LRRTMs as postsynaptic ligands of presynaptic protein neurexins (de Wit et al., 2009; Ko et al., 2009a; Siddiqui et al., 2010). Our potential candidate, *Lrrtm1*, has been shown to be localized in the postsynaptic side of excitatory synapses made by hippocampal neurons and to be important for the normal distribution of vesicular glutamate transporter 1 (VgluT1) positive terminals in specific regions of hippocampal formation in mice (Linhoff et al., 2009). Other studies reported an overlapping cooperative role for postsynaptic partners of neurexins (including *Lrrtm1*) in the formation of excitatory synapse (Ko et al., 2011; Soler-Llavina et al., 2011). Recently, some conflicting behavioral deficits have been reported for mice lacking *Lrrtm1* including increased social interaction, delayed learning, and avoidance from small enclosures (Takashima et al., 2011; Voikar et al., 2013). Interestingly, *Lrrtm1* has been linked to human handedness and schizophrenia (Francks et al., 2007; Ludwig et al., 2009).

Similarly, *Nrn1* is a cell surface protein (Naeve et al., 1997) which was firstly identified in the rat dentate gyrus after experimentally induced seizure (Nedivi et al., 1993). *Nrn1* is an

activity-dependent gene and it accelerates the maturation of glutamatergic synapses *in vivo* (Cantallops et al., 2000; Corriveau et al., 1999; Nedivi, 1998; Nedivi et al., 1996). *Nrn1* also has been shown to play an important role in modulating the neurite outgrowth *in vitro* (Cappelletti et al., 2007) and to promote the migration of neurons (Zito et al., 2012). Effects of *Nrn1* on dendritic growth and survival of cortical neurons has been suggested to occur in a cell type-specific manner (Sato et al., 2012). Moreover, *Nrn1* is associated with synapse stabilization and learning (Fujino et al., 2011) and has been linked to cognitive dysfunction in schizophrenia (Chandler et al., 2010).

Figure 1.1. Overview of the image-forming neural pathways in the mouse brain.

A. Sagittal view of the mouse brain depicting retinal connections (red) between retina (yellow tissue at the back of eye) and dLGN (orange) in the thalamus. Thalamocortical relay cells from in dLGN project (green) to the layers 4 (and less to layer 1) of the primary visual cortex. B. Different layers of the retina are separated by dash lines. Rods (R; gray) and cone (C; green and blue) photoreceptors located in the outer-nuclear layer of the retina convert photons of light into neural activates and send them to the bipolar cells (B; yellow) in the inner-nuclear of the retina through synaptic connections that are limited to outer plexiform layer. In the INL, visual information undergoes a processing step which shapes visual information through interaction among horizontal (H; purple) and amacrine (A; dark blue) and bipolar cells. Layer specific connections between RGC (red) and bipolar cells in the IPL are the synaptic sites for sorting visual information before it exit they from RGC axons (red). C. TC relay cells (green) in dLGN receive visual information from retinal axons, integrate it with multiple other information coming from other sources such feedback projections from layer 6 V1 (dark gray), TRN projections (yellow), brainstem (blue) and then transfer it output to the V1 (layers 4 and to a lesser extent to layer 1).

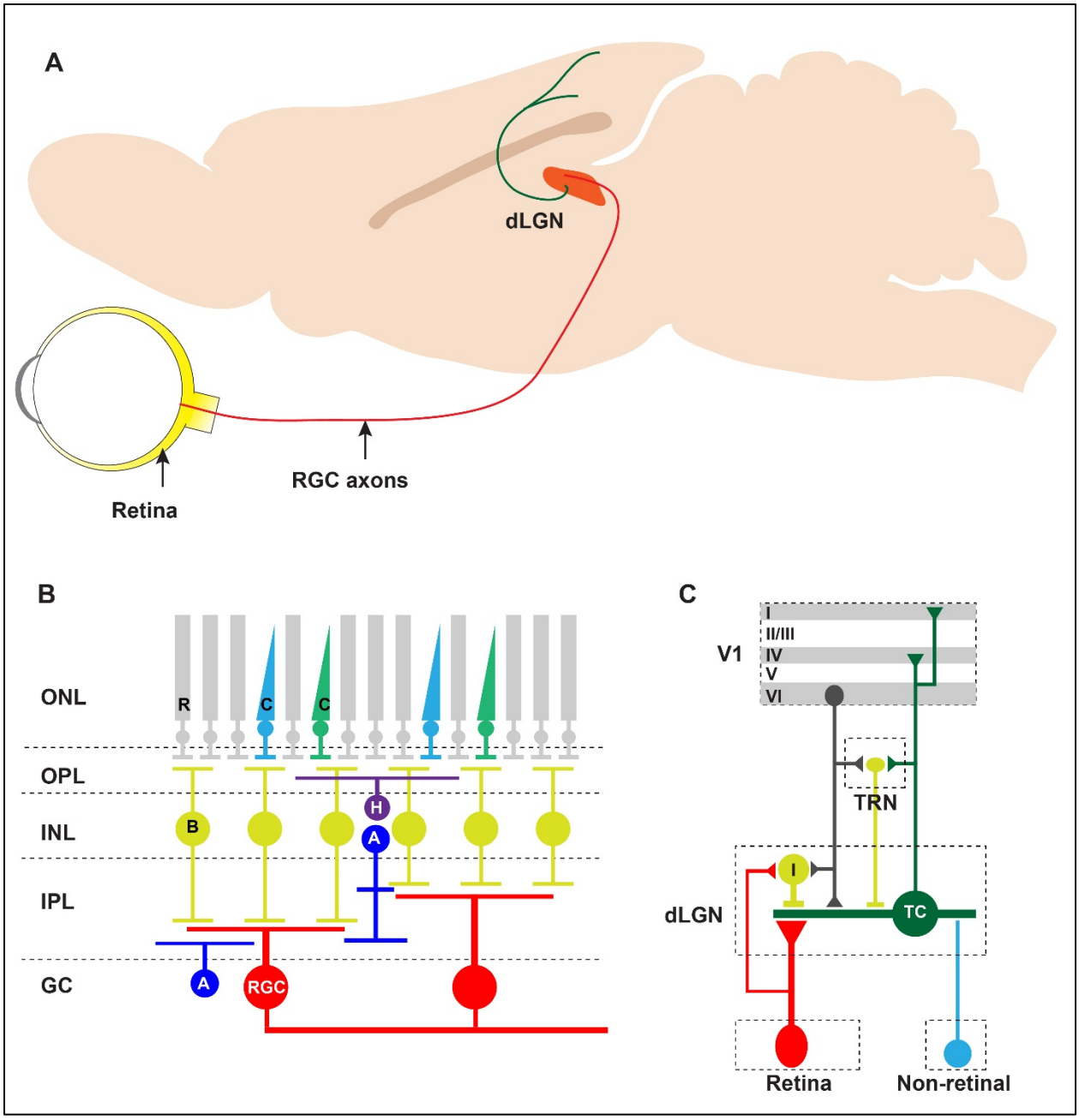
A
dLGN
RGC axons
Retina
B
ONL
OPL
INL
IPL
GC
R
C
C
H
B
A
A
RGC
C
V1
I
II/III
IV
V
VI
TRN
dLGN
I
TC
Retina
Non-retinal

Figure 1.2. Retinorecipient nuclei of nocturnal rodents.

This schematic illustrates the variety and distribution of brain nuclei innervated by retinal ganglion cells (see Morin and Studholme, 2014). Thalamic retinorecipient nuclei are colored in orange; other retinorecipient regions are colored grey. dLGN, dorsal lateral geniculate nucleus; IGL, intergeniculate leaflet; vLGNe, ventral lateral geniculate nucleus, external division; AD, anterodorsal thalamic nucleus; LP, lateral posterior thalamic nucleus; CL, centrolateral thalamic nucleus; PP, peripeduncular nucleus; PHb, para-habenular zone; ZI, zona incerta; SubG, subgeniculate nucleus; SGN, suprageniculate nucleus; SON, supraoptic nucleus; SCN, suprachiasmatic nucleus; RCH, retrochiasmatic area; SBPV, subparaventricular zone; AHN, anterior hypothalamic area; LHA, lateral hypothalamic area; MeA, medial amygdala, anterior; MePV, medial amygdala, posteroventral; AAV, anterior amygdaloid area, ventral; SI, substantia innominata; MT, medial terminal nucleus; LT, lateral terminal nucleus; DT, dorsal terminal nucleus; PN, paranigral nucleus; MRN, midbrain reticular nucleus; PB, parabrachial nucleus; DR, dorsal raphe nucleus; PAG, periaqueductal gray; CPT, commissural pretectal nucleus; MPT, medial pretectal nucleus; PPT, posterior pretectal nucleus; APT, anterior pretectal nucleus; OPN, olivary pretectal nucleus; NOT, nucleus of optic tract; SC, superior colliculus; DCIC, dorsal cortex of the inferior colliculus; RGC, retinal ganglion cell.

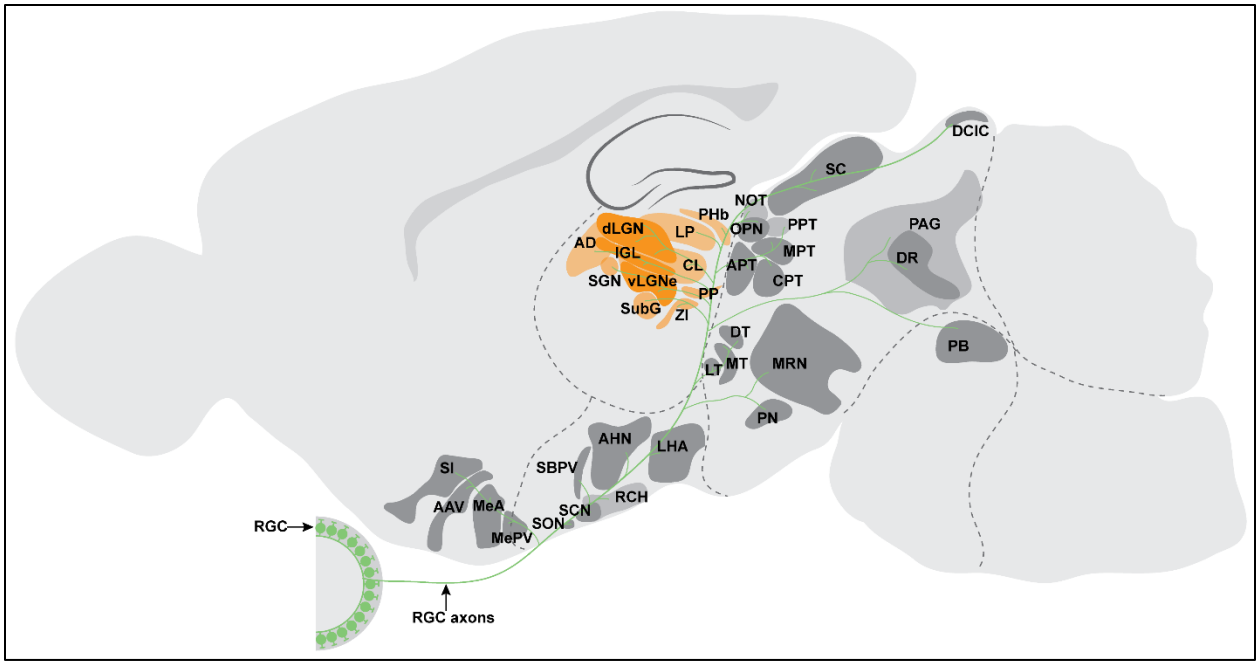
DCIC
SC
NOT
PHb
OPN
PPT
PAG
dLGN
LP
AD
IGL
MPT
DR
CL
APT
CPT
SGN
vLGNe
PP
SubG
ZI
DT
PB
MT
MRN
LT
PN
AHN
LHA
SBPV
SI
RCH
AAV
MeA
SCN
SON
MePV
RGC
RGC axons

Figure 1.3. Organization of retinal projections in nuclei of the lateral geniculate complex.

A. Coronal view of a Nissl-stained mouse brain. Arrows indicate the location of dLGN, IGL, and vLGN. Image is from the Allen Brain Atlas (http://www.brain-map.org). B-D. Schematic representation of coronal section through the lateral geniculate complex of nocturnal rodents. B depicts eye-specific segregation of retinal projections in dLGN, IGL and vLGN. Terminals of ipsilateral retinal projections are depicted as green dots; terminals of contralateral retinal projections are depicted as orange dots. RGCs from which these projections arise are shown in the retinal cross sections. Dotted line in dLGN depicts the approximate boundary separating the dorsolateral shell (s) from the ventromedial core (c). The dotted line in vLGN depicts the boundary separating the external layer (e) from the internal layer (i). C depicts topographic mapping of retinal arbors in dLGN, vLGN and IGL. Colors represent temporal (T) to nasal (N) location of RGCs in the retina (Feldheim et al., 1998; Huberman et al., 2008a; Pfeiffenberger et al., 2006). D depicts class-specific targeting of RGC axons to distinct sublamina of dLGN, vLGN and IGL. Colors represent some classes of RGCs studied with transgenic reporter mice. Names of these reporter mouse lines are indicated in parentheses (see Kim et al. 2008; Kim et al. 2010; Huberman et al. 2009; Rivlin-Etzion et al. 2011; Hattar et al. 2006; Osterhout et al. 2011). Color-filled dots in the dLGN, IGL and vLGN represent RTs (and are not meant to indicate that these terminals innervate distinct cells). dLGN, dorsal lateral geniculate nucleus; IGL, intergeniculate leaflet; vLGN, ventral lateral geniculate nucleus; dsRGC, direction-selective retinal ganglion cell; ipRGC, intrinsically photosensitive retinal ganglion cell.

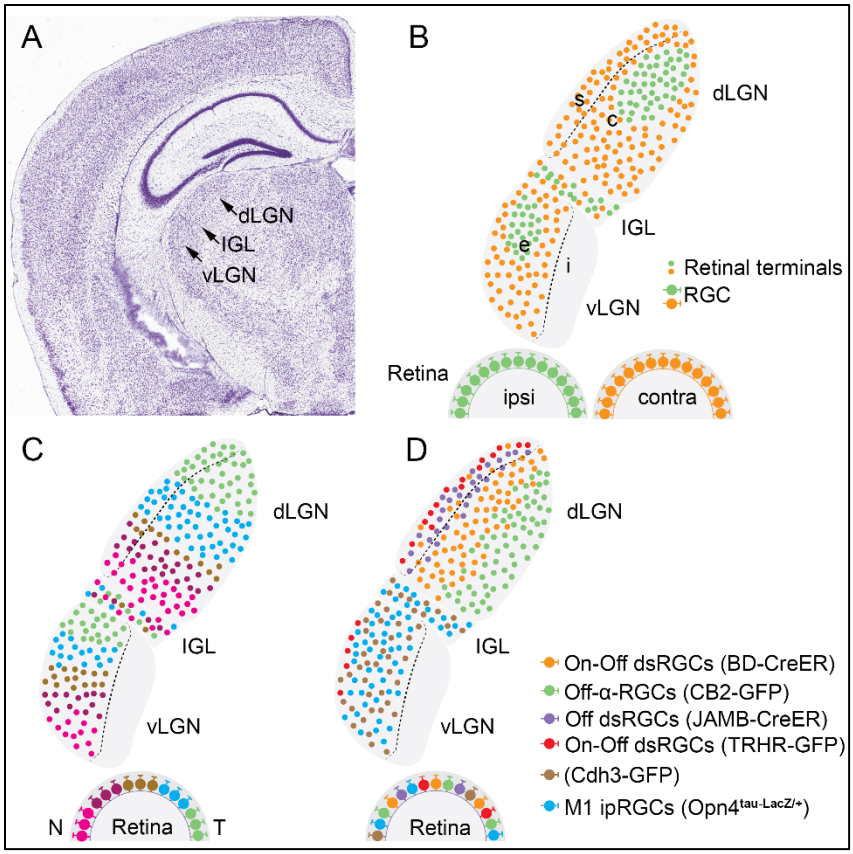
A
dLGN
IGL
vLGN
B
dLGN
s
c
IGL
e
i
vLGN
Retinal terminals
RGC
Retina
ipsi
contra
C
dLGN
IGL
vLGN
N
Retina
T
D
dLGN
IGL
vLGN
Retina
On-Off dsRGCs (BD-CreER)
Off-α-RGCs (CB2-GFP)
Off dsRGCs (JAMB-CreER)
On-Off dsRGCs (TRHR-GFP)
(Cdh3-GFP)
M1 ipRGCs (Opn4tau-LacZ/+)

Figure 1.4. Afferent and efferent projections of rodent dLGN.

A. Sources of afferent projections to dLGN are colored green. B. Brain regions innervated by dLGN efferents are colored in orange. dLGN, dorsal lateral geniculate nucleus; vLGN, ventral lateral geniculate nucleus; TRN, thalamic reticular nucleus; SC, superior colliculus; PRT, pretectal region; MRN, midbrain reticular nucleus; DR, dorsal raphe nucleus; PPN, pedunculopontine nucleus; PBG, parabigeminal nucleus; PB, parabrachial nucleus; LC, locus ceruleus; VIS1, visual cortex, layer I; VIS4, visual cortex, layer IV; VIS6, visual cortex, layer VI; RGC, retinal ganglion cell.

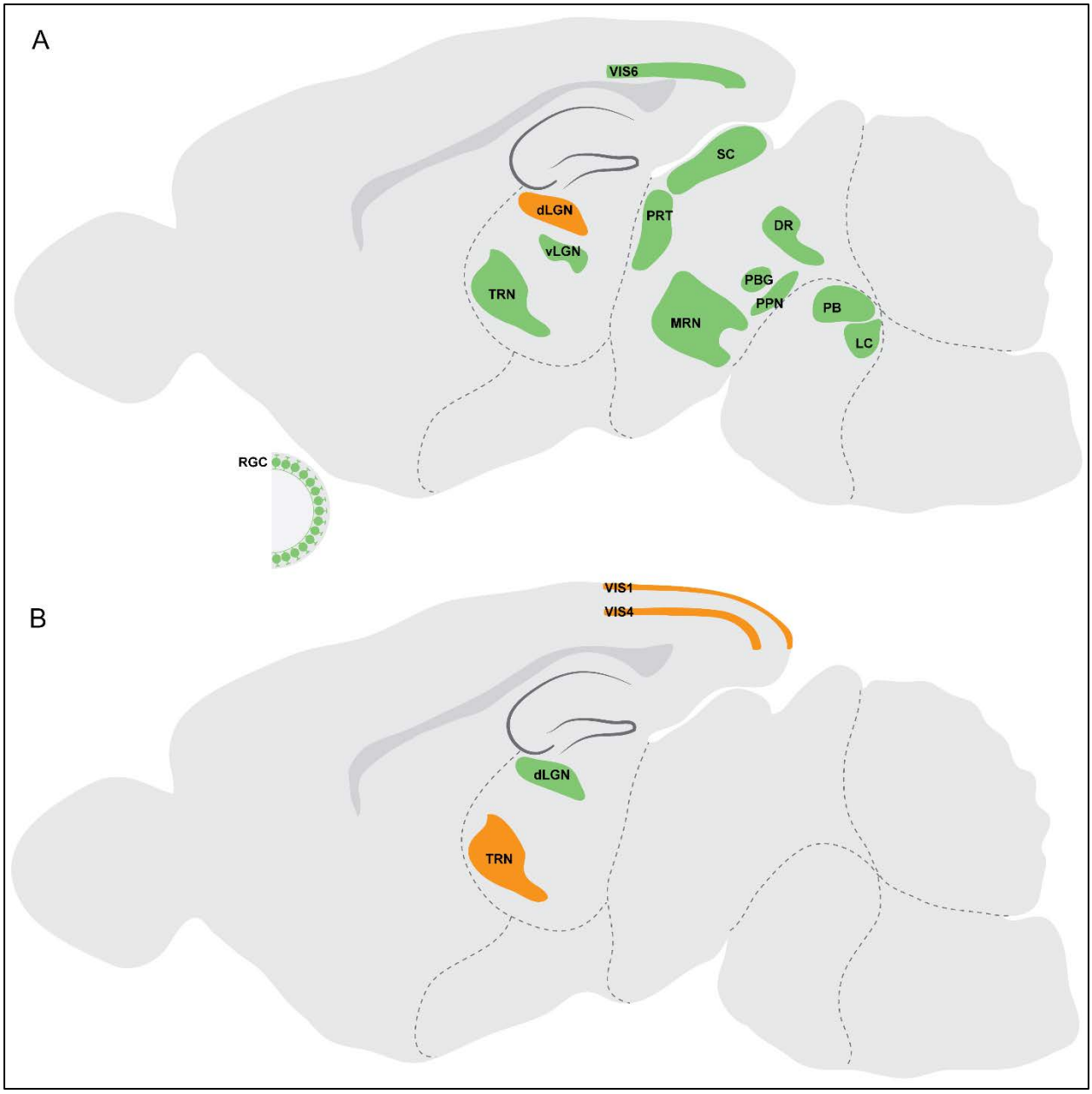
A
VIS6
SC
dLGN
PRT
DR
vLGN
PBG
TRN
PPN
PB
MRN
LC
RGC
B
VIS1
VIS4
dLGN
TRN

Figure 1.5. An inventory of synaptogenic molecules.

This figure and its legend are taken from (Siddiqui and Craig, 2011) without modification. An inventory of synaptogenic molecules, defined here as proteins that induce presynaptic (←) or postsynaptic (→) differentiation when presented to axons or dendrites, respectively. Many of the adhesion complexes have bidirectional synaptogenic activity (↔). The main receptors are also shown for the secreted synaptogenic factors. PDZ domain binding sites and common protein domains are indicated.

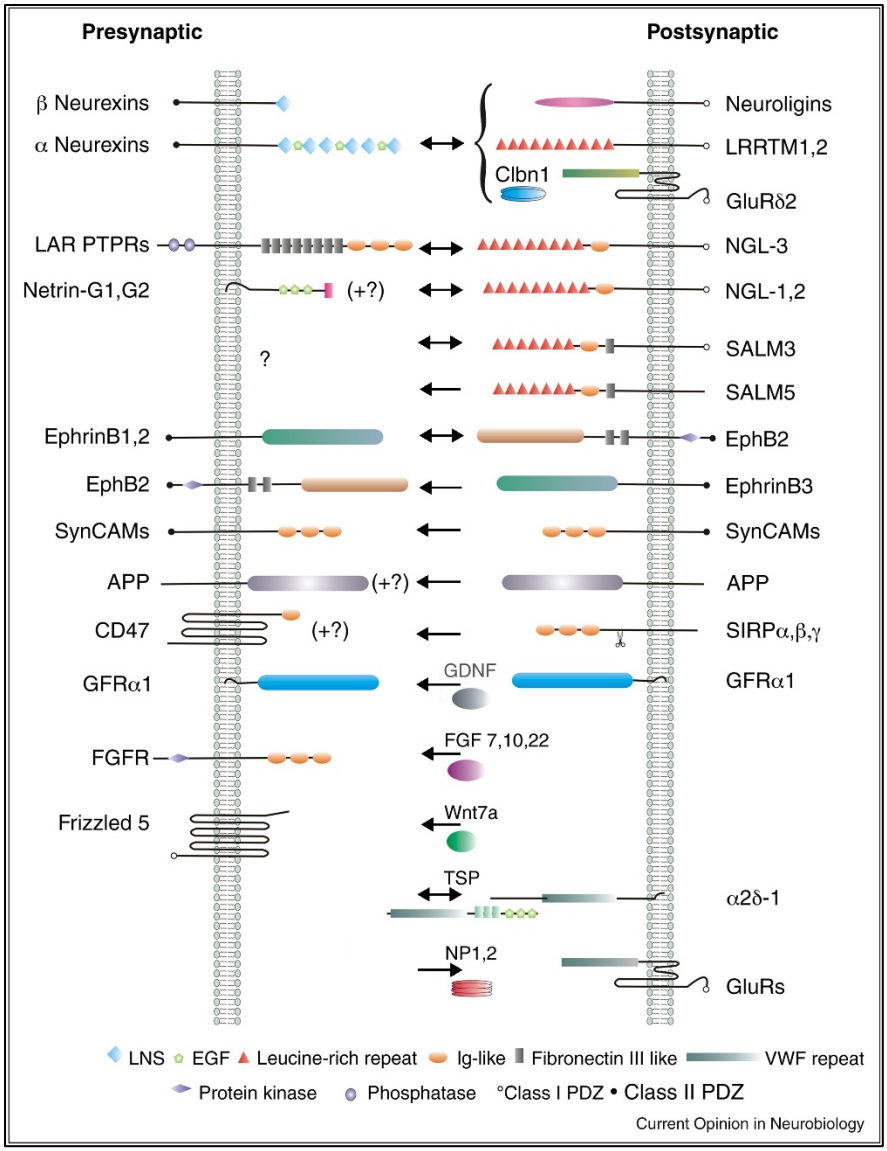
Presynaptic
Postsynaptic
β Neurexins
α Neurexins
Neuroligins
LRRTM1,2
Clbn1
GluRδ2
LAR PTPRs
NGL-3
Netrin-G1,G2
(+?)
NGL-1,2
?
SALM3
SALM5
EphrinB1,2
EphB2
EphB2
EphrinB3
SynCAMs
SynCAMs
APP
(+?)
APP
CD47
(+?)
SIRPα,β,γ
GDNF
GFRα1
GFRα1
FGF 7,10,22
FGFR
Wnt7a
Frizzled 5
TSP
α2δ-1
NP1,2
GluRs
LNS
EGF
Leucine-rich repeat
Ig-like
Fibronectin III like
VWF repeat
Protein kinase
Phosphatase
°Class I PDZ
• Class II PDZ
Current Opinion in Neurobiology

Figure 1.6. Anterograde labeling of retinal terminals in other retinorecipient nuclei.

A. Retinal projections in P35 wild-type mice were labeled by intraocular injection of fluorescently conjugated cholera toxin subunit B (CTB). Left eyes were injected with Alexa Fluor 555 CTB (magenta) and right eyes were injected with Alexa Fluor 488 CTB (green). LGN from right hemispheres are shown. 'Contra' denotes projections originating from the contralateral retina and 'ipsi' denotes projections originating from the ipsilateral retina. Confocal images were acquired from dLGN, IGL, vLGN, SCN, OPN, SC. IGL is outlined by white dots. B. High magnification images of both contralateral and ipsilateral retinal projections to each region are shown (note – contralateral and ipsilateral panels are not all from the same image). Scale bar in A = 200 μm and in B = 20 μm.

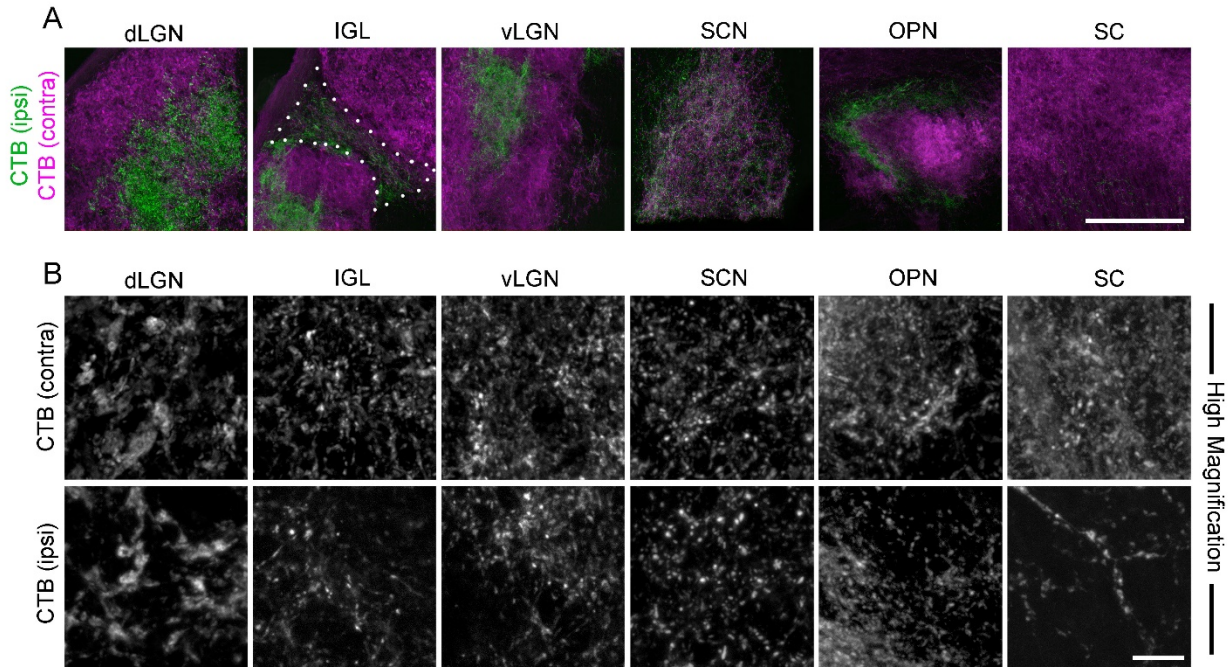
A
dLGN
IGL
vLGN
SCN
OPN
SC
CTB (ipsi)
CTB (contra)
B
dLGN
IGL
vLGN
SCN
OPN
SC
CTB (contra)
CTB (ipsi)
High Magnification

Figure 1.7. Top candidate genes screened out from the RNAseq

This figure is presented in next four panels. First two panels (with only black bars) are showing the ratio of RNAseq normalized expression in dLGN versus vLGN. Age of mice has been shown on x axis. First column: Panels 3 and 4 are comparison between RNAseq data and qPCR data. Black bars are fold change ratio of dLGN versus vLGN obtained by RNAseq and gray bars are the same ratio measured by qPCR. Dotted lines in panels 3 and 4 separate P3 and P12 measurements.

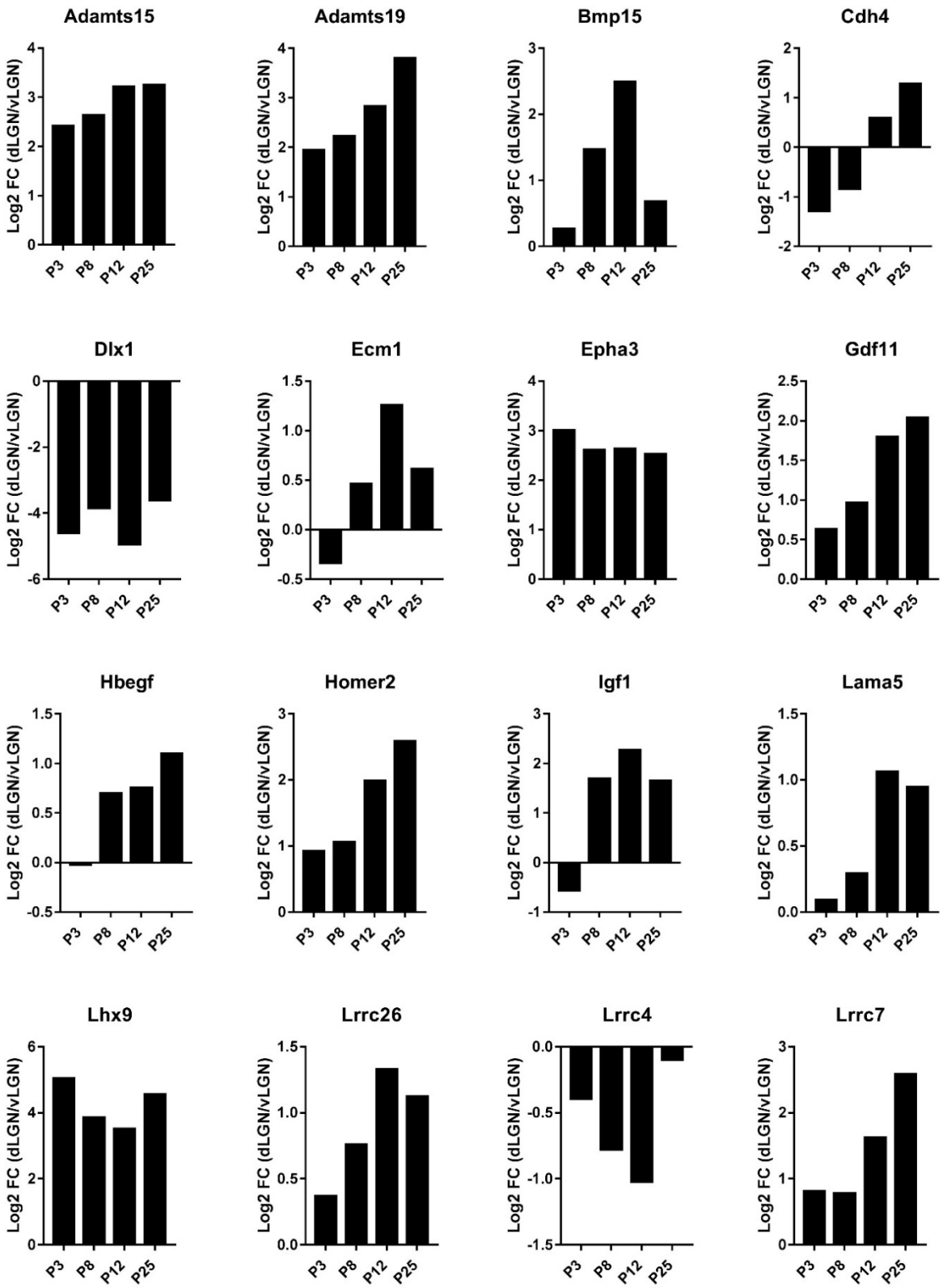
Adamts15
Adamts19
Bmp15
Cdh4
Dlx1
Ecm1
Epha3
Gdf11
Hbegf
Homer2
Igf1
Lama5
Lhx9
Lrrc26
Lrrc4
Lrrc7
Log2 FC (dLGN/vLGN)
P3
P8
P12
P25

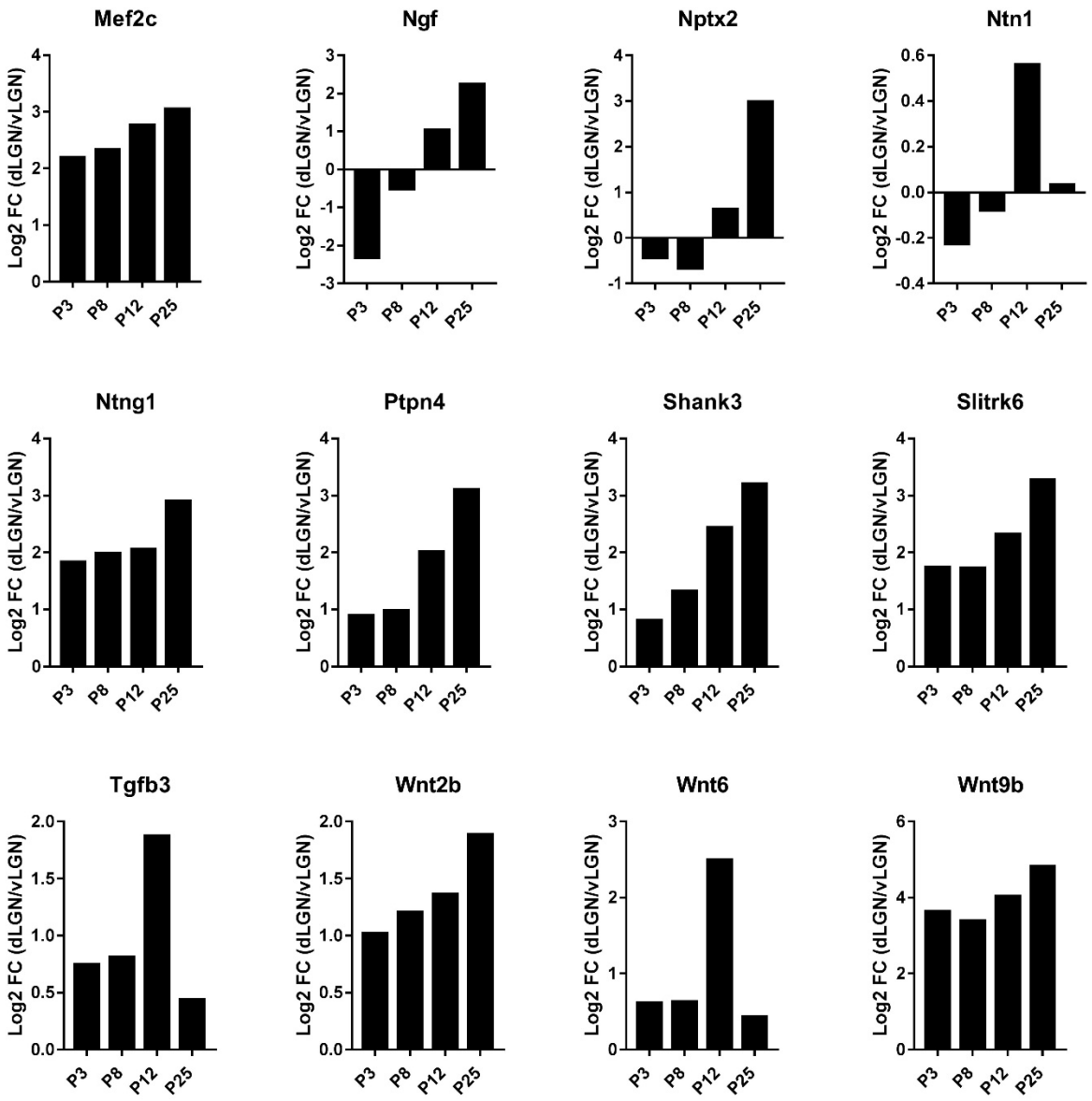
Mef2c
Ngf
Nptx2
Ntn1
Ntng1
Ptpn4
Shank3
Slitrk6
Tgfb3
Wnt2b
Wnt6
Wnt9b
Log2 FC (dLGN/vLGN)
P3
P8
P12
P25

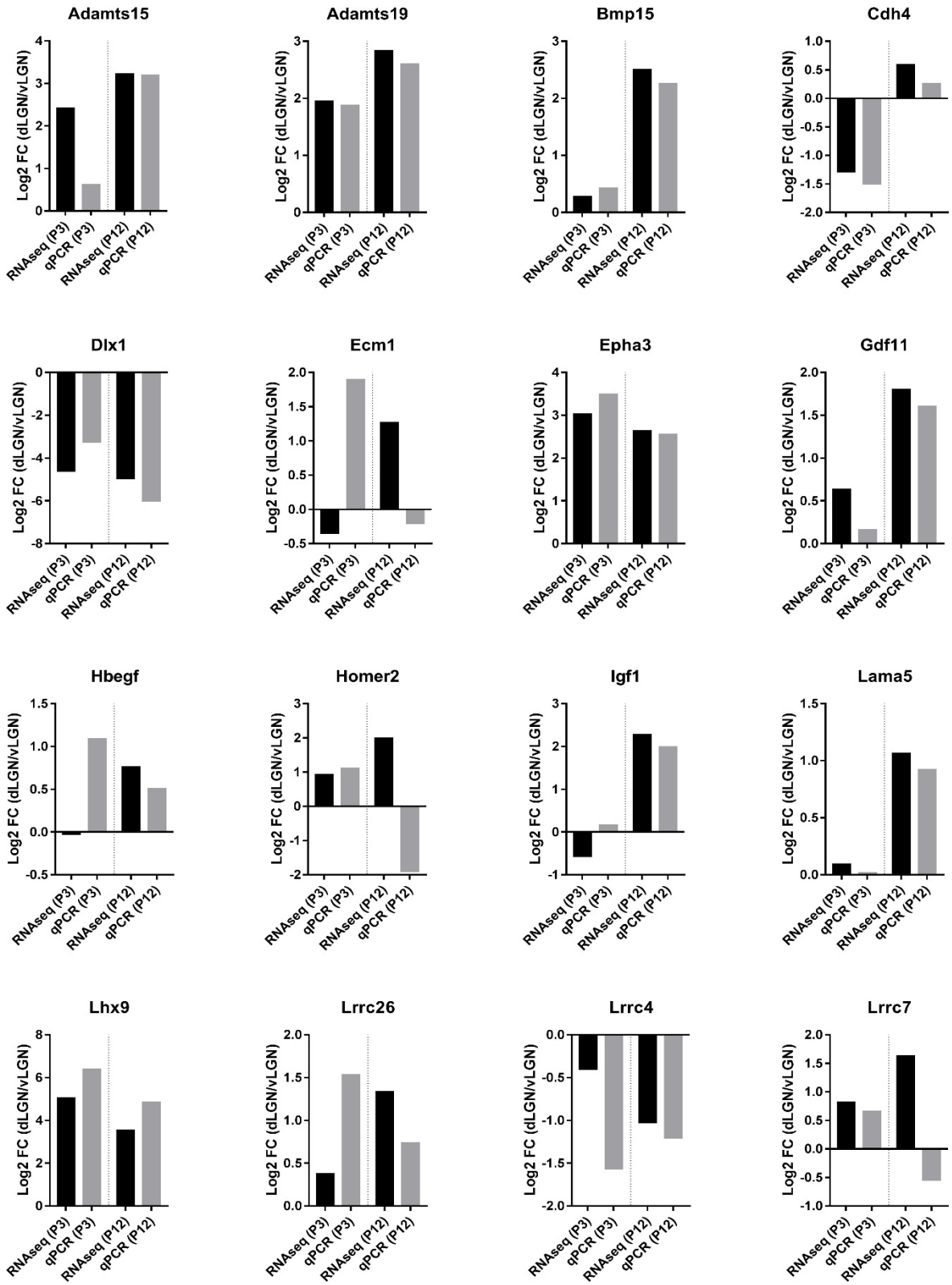
Adamts15
Adamts19
Bmp15
Cdh4
Dlx1
Ecm1
Epha3
Gdf11
Hbegf
Homer2
Igf1
Lama5
Lhx9
Lrrc26
Lrrc4
Lrrc7
Log2 FC (dLGN/vLGN)
RNAseq (P3)
qPCR (P3)
RNAseq (P12)
qPCR (P12)

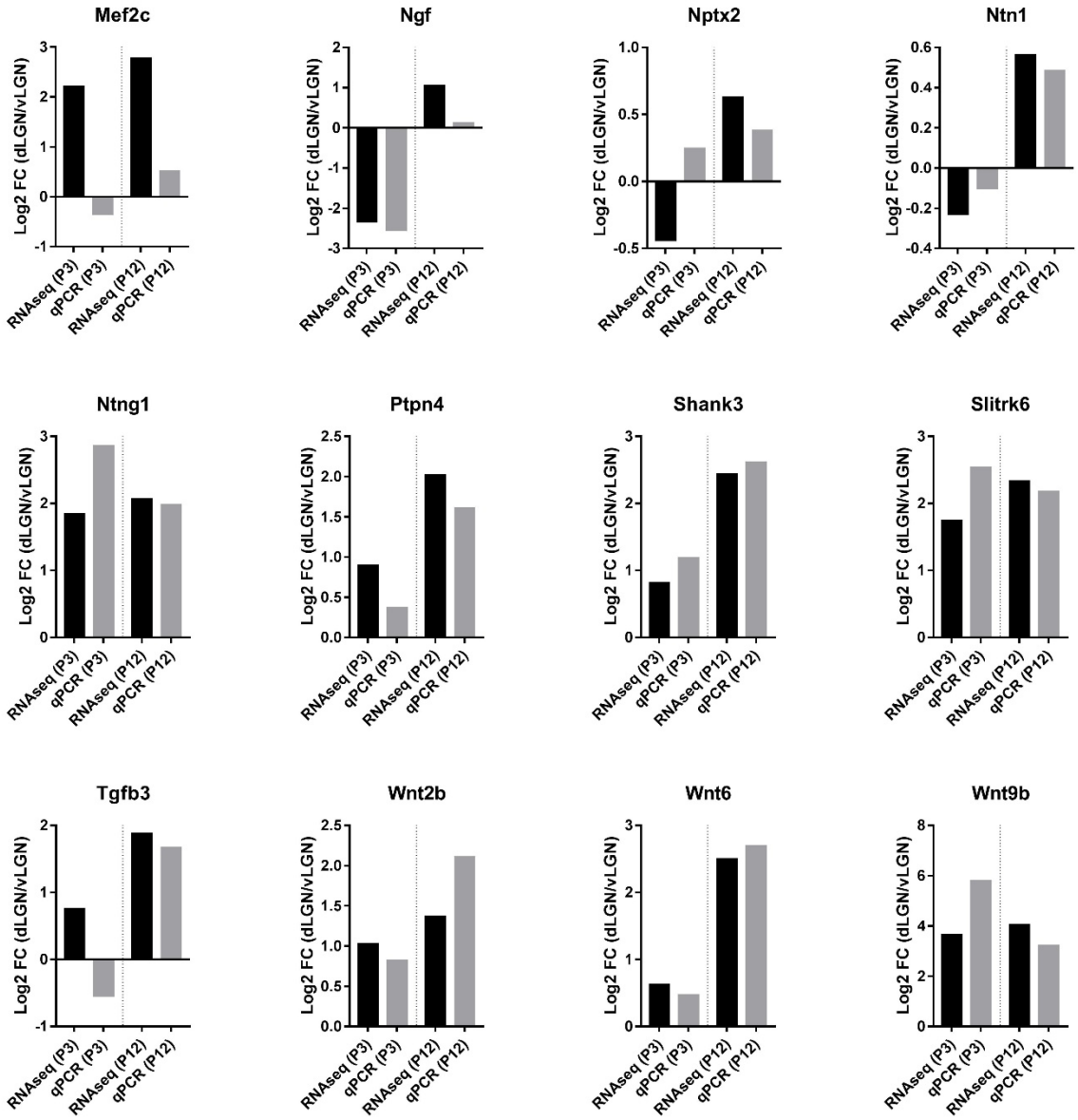
Mef2c
Ngf
Nptx2
Ntn1
Ntng1
Ptpn4
Shank3
Slitrk6
Tgfb3
Wnt2b
Wnt6
Wnt9b
Log2 FC (dLGN/vLGN)
RNAseq (P3)
qPCR (P3)
RNAseq (P12)
qPCR (P12)

References

Altman, J., and Bayer, S.A. (1989). Development of the rat thalamus: VI. The posterior lobule of the thalamic neuroepithelium and the time and site of origin and settling pattern of neurons of the lateral geniculate and lateral posterior nuclei. Journal of Comparative Neurology *284*, 581-601.

Arcelli, P., Frassoni, C., Regondi, M., Biasi, S., and Spreafico, R. (1997). GABAergic neurons in mammalian thalamus: a marker of thalamic complexity? Brain research bulletin *42*, 27-37.

Baden, T., Berens, P., Franke, K., Rosón, M.R., Bethge, M., and Euler, T. (2016). The functional diversity of retinal ganglion cells in the mouse. Nature *529*, 345-350.

Baden, T., Schubert, T., Chang, L., Wei, T., Zaichuk, M., Wissinger, B., and Euler, T. (2013). A tale of two retinal domains: near-optimal sampling of achromatic contrasts in natural scenes through asymmetric photoreceptor distribution. Neuron *80*, 1206-1217.

Benowitz, L.I., He, Z., and Goldberg, J.L. (2017). Reaching the brain: advances in optic nerve regeneration. Experimental neurology *287*, 365-373.

Bickford, M.E. (2015). Thalamic circuit diversity: modulation of the driver/modulator framework. Frontiers in neural circuits *9*.

Bickford, M.E., Slusarczyk, A., Dilger, E.K., Krahe, T.E., Kucuk, C., and Guido, W. (2010). Synaptic development of the mouse dorsal lateral geniculate nucleus. The Journal of comparative neurology *518*, 622-635.

Bickford, M.E., Zhou, N., Krahe, T.E., Govindaiah, G., and Guido, W. (2015). Retinal and tectal "driver-like" inputs converge in the shell of the mouse dorsal lateral geniculate nucleus. The Journal of Neuroscience *35*, 10523-10534.

Born, G., and Schmidt, M. (2007). GABAergic pathways in the rat subcortical visual system: a comparative study in vivo and in vitro. European Journal of Neuroscience *26*, 1183-1192.

Braak, H., and Bachmann, A. (1985). The percentage of projection neurons and interneurons in the human lateral geniculate nucleus. Human neurobiology *4*, 91-95.

Briggs, F., and Usrey, W.M. (2008). Emerging views of corticothalamic function. Current opinion in neurobiology *18*, 403-407.

Brooks, J.M., Su, J., Levy, C., Wang, J.S., Seabrook, T.A., Guido, W., and Fox, M.A. (2013). A Molecular Mechanism Regulating the Timing of Corticogeniculate Innervation. Cell reports *5*, 573-581.

Brose, N. (2009). Synaptogenic proteins and synaptic organizers: "many hands make light work". Neuron *61*, 650-652.

Bukalo, O., and Dityatev, A. (2012). Synaptic cell adhesion molecules. In Synaptic Plasticity (Springer), pp. 97-128.

Campbell, G., and Frost, D.O. (1987). Target-controlled differentiation of axon terminals and synaptic organization. Proceedings of the National Academy of Sciences *84*, 6929-6933.

Campbell, G., and Frost, D.O. (1988). Synaptic organization of anomalous retinal projections to the somatosensory and auditory thalamus: Target-controlled morphogenesis of axon terminals and synaptic glomeruli. Journal of Comparative Neurology *272*, 383-408.

Cang, J., and Feldheim, D.A. (2013). Developmental mechanisms of topographic map formation and alignment. Annual review of neuroscience *36*, 51-77.

Cantallops, I., Haas, K., and Cline, H.T. (2000). Postsynaptic CPG15 promotes synaptic maturation and presynaptic axon arbor elaboration in vivo. Nature neuroscience *3*, 1004-1011.

Cappelletti, G., Galbiati, M., Ronchi, C., Maggioni, M.G., Onesto, E., and Poletti, A. (2007). Neuritin (cpg15) enhances the differentiating effect of NGF on neuronal PC12 cells. Journal of neuroscience research *85*, 2702-2713.

Cetin, A., and Callaway, E.M. (2014). Optical control of retrogradely infected neurons using drug-regulated "TLoop" lentiviral vectors. Journal of neurophysiology *111*, 2150-2159.

Chandler, D., Dragovic, M., Cooper, M., Badcock, J.C., Mullin, B.H., Faulkner, D., Wilson, S.G., Hallmayer, J., Howell, S., Rock, D., *et al.* (2010). Impact of Neuritin 1 (NRN1) polymorphisms on fluid intelligence in schizophrenia. American journal of medical genetics Part B, Neuropsychiatric genetics : the official publication of the International Society of Psychiatric Genetics *153B*, 428-437.

Chen, C., and Regehr, W.G. (2000). Developmental remodeling of the retinogeniculate synapse. Neuron *28*, 955-966.

Chia, P.H., Li, P., and Shen, K. (2013). Cellular and molecular mechanisms underlying presynapse formation. The Journal of cell biology *203*, 11-22.

Christopherson, K.S., Ullian, E.M., Stokes, C.C., Mullowney, C.E., Hell, J.W., Agah, A., Lawler, J., Mosher, D.F., Bornstein, P., and Barres, B.A. (2005). Thrombospondins are astrocyte-secreted proteins that promote CNS synaptogenesis. Cell *120*, 421-433.

Cleland, B., Dubin, M., and Levick, W. (1971). Simultaneous recording of input and output of lateral geniculate neurones. Nature *231*, 191-192.

Cleland, B., and Lee, B. (1985). A comparison of visual responses of cat lateral geniculate nucleus neurones with those of ganglion cells afferent to them. The Journal of physiology *369*, 249-268.

Corriveau, R.A., Shatz, C.J., and Nedivi, E. (1999). Dynamic regulation of cpg15 during activity-dependent synaptic development in the mammalian visual system. The Journal of neuroscience *19*, 7999-8008.

Crabtree, J.W., and Killackey, H.P. (1989). The topographic organization and axis of projection within the visual sector of the rabbit's thalamic reticular nucleus. European Journal of Neuroscience *1*, 94-109.

Crair, M.C., and Mason, C.A. (2016). Reconnecting eye to brain. J Neurosci *36*, 10707-10722.

Cruz-Martín, A., El-Danaf, R.N., Osakada, F., Sriram, B., Dhande, O.S., Nguyen, P.L., Callaway, E.M., Ghosh, A., and Huberman, A.D. (2014). A dedicated circuit links direction-selective retinal ganglion cells to the primary visual cortex. Nature *507*, 358-361.

De Lima, A.D., and Singer, W. (1987). The serotoninergic fibers in the dorsal lateral geniculate nucleus of the cat: distribution and synaptic connections demonstrated with immunocytochemistry. Journal of Comparative Neurology *258*, 339-351.

de Lima, D.A., Montero, V., and Singer, W. (1985). The cholinergic innervation of the visual thalamus: an EM immunocytochemical study. Experimental brain research *59*, 206-212.

de Wit, J., Sylwestrak, E., O'Sullivan, M.L., Otto, S., Tiglio, K., Savas, J.N., Yates, J.R., 3rd, Comoletti, D., Taylor, P., and Ghosh, A. (2009). LRRTM2 interacts with Neurexin1 and regulates excitatory synapse formation. Neuron *64*, 799-806.

Dhande, O.S., Estevez, M.E., Quattrochi, L.E., El-Danaf, R.N., Nguyen, P.L., Berson, D.M., and Huberman, A.D. (2013). Genetic dissection of retinal inputs to brainstem nuclei controlling image stabilization. The Journal of Neuroscience *33*, 17797-17813.

Dhande, O.S., Hua, E.W., Guh, E., Yeh, J., Bhatt, S., Zhang, Y., Ruthazer, E.S., Feller, M.B., and Crair, M.C. (2011). Development of single retinofugal axon arbors in normal and β2 knock-out mice. The Journal of Neuroscience *31*, 3384-3399.

Dhande, O.S., and Huberman, A.D. (2014). Retinal ganglion cell maps in the brain: implications for visual processing. Current opinion in neurobiology *24*, 133-142.

Dubin, M.W., and Cleland, B.G. (1977). Organization of visual inputs to interneurons of lateral geniculate nucleus of the cat. Journal of Neurophysiology *40*, 410-427.

Ellis, E.M., Gauvain, G., Sivyer, B., and Murphy, G.J. (2016). Shared and Distinct Retinal Input to the Mouse Superior Colliculus and Dorsal Lateral Geniculate Nucleus. Journal of neurophysiology, jn. 00227.02016.

Emerson, V., Chalupa, L., Thompson, I., and Talbot, R. (1982). Behavioural, physiological, and anatomical consequences of monocular deprivation in the golden hamster (Mesocricetus auratus). Experimental brain research *45*, 168-178.

Erzurumlu, R.S., Jhaveri, S., and Schneider, G.E. (1988). Distribution of morphologically different retinal axon terminals in the hamster dorsal lateral geniculate nucleus. Brain research *461*, 175-181.

Euler, T., Haverkamp, S., Schubert, T., and Baden, T. (2014). Retinal bipolar cells: elementary building blocks of vision. Nature Reviews Neuroscience *15*, 507-519.

Feldheim, D.A., Vanderhaeghen, P., Hansen, M.J., Frisén, J., Lu, Q., Barbacid, M., and Flanagan, J.G. (1998). Topographic guidance labels in a sensory projection to the forebrain. Neuron *21*, 1303-1313.

Flavell, S.W., and Greenberg, M.E. (2008). Signaling mechanisms linking neuronal activity to gene expression and plasticity of the nervous system. Annual review of neuroscience *31*, 563.

Fox, M.A., Sanes, J.R., Borza, D.-B., Eswarakumar, V.P., Fässler, R., Hudson, B.G., John, S.W., Ninomiya, Y., Pedchenko, V., and Pfaff, S.L. (2007). Distinct target-derived signals organize formation, maturation, and maintenance of motor nerve terminals. Cell *129*, 179-193.

Fox, M.A., and Umemori, H. (2006). Seeking long-term relationship: axon and target communicate to organize synaptic differentiation. Journal of neurochemistry *97*, 1215-1231.

Francks, C., Maegawa, S., Laurén, J., Abrahams, B.S., Velayos-Baeza, A., Medland, S.E., Colella, S., Groszer, M., McAuley, E., and Caffrey, T.M. (2007). LRRTM1 on chromosome 2p12 is a maternally suppressed gene that is associated paternally with handedness and schizophrenia. Molecular psychiatry *12*, 1129-1139.

Friedlander, M., Lin, C., and Sherman, S. (1980). Dendritic and axonal morphology of physiological classes of geniculo-cortical relay cells. Paper presented at: Experimental Brain Research (Springer).

Friedlander, M., Lin, C., Stanford, L., and Sherman, S.M. (1981). Morphology of functionally identified neurons in lateral geniculate nucleus of the cat. Journal of Neurophysiology *46*, 80-129.

Fujino, T., Leslie, J.H., Eavri, R., Chen, J.L., Lin, W.C., Flanders, G.H., Borok, E., Horvath, T.L., and Nedivi, E. (2011). CPG15 regulates synapse stability in the developing and adult brain. Genes & development *25*, 2674-2685.

Gabbott, P.L., and Bacon, S.J. (1994). Two types of interneuron in the dorsal lateral geniculate nucleus of the rat: a combined NADPH diaphorase histochemical and GABA immunocytochemical study. Journal of Comparative Neurology *350*, 281-301.

Gaillard, F., Karten, H.J., and Sauvé, Y. (2013). Retinorecipient areas in the diurnal murine rodent Arvicanthis niloticus: a disproportionally large superior colliculus. Journal of Comparative Neurology *521*, 1699-1726.

Gill, K.P., Hung, S.S., Sharov, A., Lo, C.Y., Needham, K., Lidgerwood, G.E., Jackson, S., Crombie, D.E., Nayagam, B.A., and Cook, A.L. (2016). Enriched retinal ganglion cells derived from human embryonic stem cells. Scientific reports *6*, 30552.

Godement, P., Salaün, J., and Imbert, M. (1984). Prenatal and postnatal development of retinogeniculate and retinocollicular projections in the mouse. Journal of Comparative Neurology *230*, 552-575.

Goldberg, J.L., and Guido, W. (2016). Report on the National Eye Institute Audacious Goals Initiative: Regenerating the Optic NerveReport on NEI Audacious Goals Initiative. Investigative ophthalmology & visual science *57*, 1271-1275.

Golding, B., Pouchelon, G., Bellone, C., Murthy, S., Di Nardo, A.A., Govindan, S., Ogawa, M., Shimogori, T., Lüscher, C., and Dayer, A. (2014). Retinal input directs the recruitment of inhibitory interneurons into thalamic visual circuits. Neuron *81*, 1057-1069.

Grant, E., Hoerder-Suabedissen, A., and Molnár, Z. (2016). The Regulation of Corticofugal Fiber Targeting by Retinal Inputs. Cerebral Cortex, bhv315.

Grubb, M.S., and Thompson, I.D. (2004). Biochemical and anatomical subdivision of the dorsal lateral geniculate nucleus in normal mice and in mice lacking the β2 subunit of the nicotinic acetylcholine receptor. Vision research *44*, 3365-3376.

Guido, W. (2008). Refinement of the retinogeniculate pathway. The Journal of physiology *586*, 4357-4362.

Guillery, R. (1969). The organization of synaptic interconnections in the laminae of the dorsal lateral geniculate nucleus of the cat. Zeitschrift für Zellforschung und mikroskopische Anatomie *96*, 1-38.

Guillery, R., and Harting, J.K. (2003). Structure and connections of the thalamic reticular nucleus: advancing views over half a century. Journal of Comparative Neurology *463*, 360-371.

Guillery, R., and Scott, G. (1971). Observations on synaptic patterns in the dorsal lateral geniculate nucleus of the cat: the C laminae and the perikaryal synapses. Experimental brain research *12*, 184-203.

Hale, P., Sefton, A.J., Baur, L., and Cottee, L. (1982). Interrelations of the rat's thalamic reticular and dorsal lateral geniculate nuclei. Experimental brain research *45*, 217-229.

Hallanger, A.E., Levey, A.I., Lee, H.J., Rye, D.B., and Wainer, B.H. (1987). The origins of cholinergic and other subcortical afferents to the thalamus in the rat. Journal of Comparative Neurology *262*, 105-124.

Hammer, S., Carrillo, G.L., Govindaiah, G., Monavarfeshani, A., Bircher, J.S., Su, J., Guido, W., and Fox, M.A. (2014). Nuclei-specific differences in nerve terminal distribution, morphology, and development in mouse visual thalamus. Neural development *9*, 1.

Hammer, S., Monavarfeshani, A., Lemon, T., Su, J., and Fox, M.A. (2015). Multiple retinal axons converge onto relay cells in the adult mouse thalamus. Cell reports *12*, 1575-1583.

Hamos, J.E., Van Horn, S.C., Raczkowski, D., and Sherman, S.M. (1987). Synaptic circuits involving an individual retinogeniculate axon in the cat. Journal of Comparative Neurology *259*, 165-192.

Harting, J.K., Huerta, M.F., Hashikawa, T., and van Lieshout, D.P. (1991a). Projection of the mammalian superior colliculus upon the dorsal lateral geniculate nucleus: organization of tectogeniculate pathways in nineteen species. Journal of comparative neurology *304*, 275-306.

Harting, J.K., Van Lieshout, D., Hashikawa, T., and Weber, J. (1991b). The parabigeminogeniculate projection: connectional studies in eight mammals. Journal of comparative neurology *305*, 559-581.

Hattar, S., Kumar, M., Park, A., Tong, P., Tung, J., Yau, K.W., and Berson, D.M. (2006). Central projections of melanopsin-expressing retinal ganglion cells in the mouse. Journal of Comparative Neurology *497*, 326-349.

Hong, Y.K., and Chen, C. (2011). Wiring and rewiring of the retinogeniculate synapse. Current opinion in neurobiology *21*, 228-237.

Huberman, A.D., Feller, M.B., and Chapman, B. (2008a). Mechanisms underlying development of visual maps and receptive fields. Annual review of neuroscience *31*, 479-509.

Huberman, A.D., Manu, M., Koch, S.M., Susman, M.W., Lutz, A.B., Ullian, E.M., Baccus, S.A., and Barres, B.A. (2008b). Architecture and activity-mediated refinement of axonal projections from a mosaic of genetically identified retinal ganglion cells. Neuron *59*, 425-438.

Huberman, A.D., Wei, W., Elstrott, J., Stafford, B.K., Feller, M.B., and Barres, B.A. (2009). Genetic identification of an On-Off direction-selective retinal ganglion cell subtype reveals a layer-specific subcortical map of posterior motion. Neuron *62*, 327-334.

Irvin, G.E., Casagrande, V.A., and Norton, T.T. (1993). Center/surround relationships of magnocellular, parvocellular, and koniocellular relay cells in primate lateral geniculate nucleus. Visual neuroscience *10*, 363-373.

Jacobs, G.H., Williams, G.A., and Fenwick, J.A. (2004). Influence of cone pigment coexpression on spectral sensitivity and color vision in the mouse. Vision research *44*, 1615-1622.

Jager, P., Ye, Z., Yu, X., Zagoraiou, L., Prekop, H.-T., Partanen, J., Jessell, T.M., Wisden, W., Brickley, S.G., and Delogu, A. (2016). Tectal-derived interneurons contribute to phasic and tonic inhibition in the visual thalamus. Nature Communications *7*.

Jaubert-Miazza, L., Green, E., Lo, F., Bui, K., Mills, J., and Guido, W. (2005). Structural and functional composition of the developing retinogeniculate pathway in the mouse. Visual neuroscience *22*, 661.

Jones, E., and Powell, T. (1969). Electron microscopy of synaptic glomeruli in the thalamic relay nuclei of the cat. Proceedings of the Royal Society of London B: Biological Sciences *172*, 153-171.

Jones, E.G. (2012). The thalamus (Springer Science & Business Media).

Jones, E.G., and Rubenstein, J.L. (2004). Expression of regulatory genes during differentiation of thalamic nuclei in mouse and monkey. Journal of Comparative Neurology *477*, 55-80.

Jurgens, C.W., Bell, K.A., McQuiston, A.R., and Guido, W. (2012). Optogenetic stimulation of the corticothalamic pathway affects relay cells and GABAergic neurons differently in the mouse visual thalamus. PLoS One *7*, e45717.

Kaas, J., Guillery, R., and Allman, J. (1972). Some Principles of Organization in the Dorsal Lateral Geniculate Nucleus; pp. 283–299. Brain, Behavior and Evolution *6*, 283-299.

Kay, J.N., De la Huerta, I., Kim, I.-J., Zhang, Y., Yamagata, M., Chu, M.W., Meister, M., and Sanes, J.R. (2011). Retinal ganglion cells with distinct directional preferences differ in molecular identity, structure, and central projections. The Journal of Neuroscience *31*, 7753-7762.

Kim, I.-J., Zhang, Y., Meister, M., and Sanes, J.R. (2010). Laminar restriction of retinal ganglion cell dendrites and axons: subtype-specific developmental patterns revealed with transgenic markers. The Journal of Neuroscience *30*, 1452-1462.

Kim, I.-J., Zhang, Y., Yamagata, M., Meister, M., and Sanes, J.R. (2008). Molecular identification of a retinal cell type that responds to upward motion. Nature *452*, 478-482.

Ko, J., Fuccillo, M.V., Malenka, R.C., and Sudhof, T.C. (2009a). LRRTM2 functions as a neurexin ligand in promoting excitatory synapse formation. Neuron *64*, 791-798.

Ko, J., Soler-Llavina, G.J., Fuccillo, M.V., Malenka, R.C., and Sudhof, T.C. (2011). Neuroligins/LRRTMs prevent activity- and Ca2+/calmodulin-dependent synapse elimination in cultured neurons. The Journal of cell biology *194*, 323-334.

Köberlein, J., Beifus, K., Schaffert, C., and Finger, R.P. (2013). The economic burden of visual impairment and blindness: a systematic review. BMJ open *3*, e003471.

Kong, L., Fry, M., Al-Samarraie, M., Gilbert, C., and Steinkuller, P.G. (2012). An update on progress and the changing epidemiology of causes of childhood blindness worldwide. Journal of American Association for Pediatric Ophthalmology and Strabismus *16*, 501-507.

Krahe, T.E., El-Danaf, R.N., Dilger, E.K., Henderson, S.C., and Guido, W. (2011). Morphologically distinct classes of relay cells exhibit regional preferences in the dorsal lateral geniculate nucleus of the mouse. The Journal of Neuroscience *31*, 17437-17448.

Laurén, J., Airaksinen, M.S., Saarma, M., and õnis Timmusk, T. (2003). A novel gene family encoding leucine-rich repeat transmembrane proteins differentially expressed in the nervous system. Genomics *81*, 411-421.

Lee, S.H., and Sheng, M. (2000). Development of neuron–neuron synapses. Current opinion in neurobiology *10*, 125-131.

Leist, M., Datunashvilli, M., Kanyshkova, T., Zobeiri, M., Aissaoui, A., Cerina, M., Romanelli, M.N., Pape, H.-C., and Budde, T. (2016). Two types of interneurons in the mouse lateral geniculate nucleus are characterized by different h-current density. Scientific reports *6*.

Ling, C., Hendrickson, M.L., and Kalil, R.E. (2012). Morphology, classification, and distribution of the projection neurons in the dorsal lateral geniculate nucleus of the rat. PloS one *7*, e49161.

Linhoff, M.W., Lauren, J., Cassidy, R.M., Dobie, F.A., Takahashi, H., Nygaard, H.B., Airaksinen, M.S., Strittmatter, S.M., and Craig, A.M. (2009). An unbiased expression screen for synaptogenic proteins identifies the LRRTM protein family as synaptic organizers. Neuron *61*, 734-749.

López-Bendito, G., and Molnár, Z. (2003). Thalamocortical development: how are we going to get there? Nature Reviews Neuroscience *4*, 276-289.

Ludwig, K.U., Mattheisen, M., Muhleisen, T.W., Roeske, D., Schmal, C., Breuer, R., Schulte-Korne, G., Muller-Myhsok, B., Nothen, M.M., Hoffmann, P., *et al.* (2009). Supporting evidence for LRRTM1 imprinting effects in schizophrenia. Molecular psychiatry *14*, 743-745.

Lund, R., and Cunningham, T. (1972). Aspects of synaptic and laminar organization of the mammalian lateral geniculate body. Invest Ophthalmol *11*, 291-302.

Mackay-Sim, A., Sefton, A.J., and Martin, P.R. (1983). Subcortical projections to lateral geniculate and thalamic reticular nuclei in the hooded rat. Journal of comparative neurology *213*, 24-35.

Macosko, E.Z., Basu, A., Satija, R., Nemesh, J., Shekhar, K., Goldman, M., Tirosh, I., Bialas, A.R., Kamitaki, N., and Martersteck, E.M. (2015). Highly parallel genome-wide expression profiling of individual cells using nanoliter droplets. Cell *161*, 1202-1214.

Maekawa, Y., Onishi, A., Matsushita, K., Koide, N., Mandai, M., Suzuma, K., Kitaoka, T., Kuwahara, A., Ozone, C., and Nakano, T. (2016). Optimized culture system to induce neurite outgrowth from retinal ganglion cells in three-dimensional retinal aggregates differentiated from mouse and human embryonic stem cells. Current eye research *41*, 558-568.

Martersteck, E.M., Hirokawa, K.E., Evarts, M., Bernard, A., Duan, X., Li, Y., Ng, L., Oh, S.W., Ouellette, B., and Royall, J.J. (2017). Diverse Central Projection Patterns of Retinal Ganglion Cells. Cell Reports *18*, 2058-2072.

Masland, R.H. (2001). The fundamental plan of the retina. Nature neuroscience *4*, 877-886.

McCormick, D.A. (1992). Neurotransmitter actions in the thalamus and cerebral cortex and their role in neuromodulation of thalamocortical activity. Progress in neurobiology *39*, 337-388.

Monavarfeshani, A., Sabbagh, U., and Fox, M.A. (2017). Not a one-trick pony: Diverse connectivity and functions of the rodent lateral geniculate complex. Visual Neuroscience *34*.

Montera, V., and Zempel, J. (1985). Evidence for two types of GABA-containing interneurons in the A-laminae of the cat lateral geniculate nucleus: a double-label HRP and GABA-immunocytochemical study. Experimental brain research *60*, 603-609.

Montero, V., and Singer, W. (1985). Ultrastructural identification of somata and neural processes immunoreactive to antibodies against glutamic acid decarboxylase (GAD) in the dorsal lateral geniculate nucleus of the cat. Experimental brain research *59*, 151-165.

Morgan, J.L., Berger, D.R., Wetzel, A.W., and Lichtman, J.W. (2016). The Fuzzy Logic of Network Connectivity in Mouse Visual Thalamus. Cell *165*, 192-206.

Morin, L.P., and Studholme, K.M. (2014). Retinofugal projections in the mouse. Journal of Comparative Neurology *522*, 3733-3753.

Muir-Robinson, G., Hwang, B.J., and Feller, M.B. (2002). Retinogeniculate axons undergo eye-specific segregation in the absence of eye-specific layers. The Journal of neuroscience *22*, 5259-5264.

Naeve, G.S., Ramakrishnan, M., Kramer, R., Hevroni, D., Citri, Y., and Theill, L.E. (1997). Neuritin: a gene induced by neural activity and neurotrophins that promotes neuritogenesis. Proceedings of the National Academy of Sciences *94*, 2648-2653.

Nakano, T., Ando, S., Takata, N., Kawada, M., Muguruma, K., Sekiguchi, K., Saito, K., Yonemura, S., Eiraku, M., and Sasai, Y. (2012). Self-formation of optic cups and storable stratified neural retina from human ESCs. Cell stem cell *10*, 771-785.

Nassi, J.J., and Callaway, E.M. (2009). Parallel processing strategies of the primate visual system. Nature Reviews Neuroscience *10*, 360-372.

Nedivi, E. (1998). Promotion of Dendritic Growth by CPG15, an Activity-Induced Signaling Molecule. Science *281*, 1863-1866.

Nedivi, E., Fieldust, S., Theill, L.E., and Hevron, D. (1996). A set of genes expressed in response to light in the adult cerebral cortex and regulated during development. Proceedings of the National Academy of Sciences *93*, 2048-2053.

Nedivi, E., Hevroni, D., Naot, D., Israeli, D., and Citri, Y. (1993). Numerous candidate plasticity-related genes revealed by differential cDNA cloning. Nature *363*, 718-722.

Ohlemacher, S.K., Sridhar, A., Xiao, Y., Hochstetler, A.E., Sarfarazi, M., Cummins, T.R., and Meyer, J.S. (2016). Stepwise differentiation of retinal ganglion cells from human pluripotent stem cells enables analysis of glaucomatous neurodegeneration. Stem Cells *34*, 1553-1562.

Olsen, S.R., Bortone, D.S., Adesnik, H., and Scanziani, M. (2012). Gain control by layer six in cortical circuits of vision. Nature *483*, 47-52.

Ortín-Martínez, A., Nadal-Nicolás, F.M., Jiménez-López, M., Alburquerque-Béjar, J.J., Nieto-López, L., García-Ayuso, D., Villegas-Pérez, M.P., Vidal-Sanz, M., and Agudo-Barriuso, M. (2014). Number and distribution of mouse retinal cone photoreceptors: differences between an albino (Swiss) and a pigmented (C57/BL6) strain. PLoS One *9*, e102392.

Papadopoulos, G.C., and Parnavelas, J.G. (1990a). Distribution and synaptic organization of dopaminergic axons in the lateral geniculate nucleus of the rat. Journal of Comparative Neurology *294*, 356-361.

Papadopoulos, G.C., and Parnavelas, J.G. (1990b). Distribution and synaptic organization of serotoninergic and noradrenergic axons in the lateral geniculate nucleus of the rat. Journal of Comparative Neurology *294*, 345-355.

Petrof, I., and Sherman, S.M. (2013). Functional significance of synaptic terminal size in glutamatergic sensory pathways in thalamus and cortex. The Journal of physiology *591*, 3125-3131.

Pfeiffenberger, C., Yamada, J., and Feldheim, D.A. (2006). Ephrin-As and patterned retinal activity act together in the development of topographic maps in the primary visual system. The Journal of neuroscience *26*, 12873-12884.

Pinault, D. (2004). The thalamic reticular nucleus: structure, function and concept. Brain research reviews *46*, 1-31.

Puelles, L., and Rubenstein, J.L. (2003). Forebrain gene expression domains and the evolving prosomeric model. Trends in neurosciences *26*, 469-476.

Rafols, J.A., and Valverde, F. (1973). The structure of the dorsal lateral geniculate nucleus in the mouse. A Golgi and electron microscopic study. Journal of Comparative Neurology *150*, 303-331.

Reese, B. (1988). 'Hidden lamination'in the dorsal lateral geniculate nucleus: the functional organization of this thalamic region in the rat. Brain research reviews *13*, 119-137.

Reese, B., and Cowey, A. (1983). Projection lines and the ipsilateral retino-geniculate pathway in the hooded rat. Neuroscience *10*, 1233-1247.

Reichman, S., Terray, A., Slembrouck, A., Nanteau, C., Orieux, G., Habeler, W., Nandrot, E.F., Sahel, J.-A., Monville, C., and Goureau, O. (2014). From confluent human iPS cells to self-

forming neural retina and retinal pigmented epithelium. Proceedings of the National Academy of Sciences *111*, 8518-8523.

Rein, D.B., Zhang, P., Wirth, K.E., Lee, P.P., Hoerger, T.J., McCall, N., Klein, R., Tielsch, J.M., Vijan, S., and Saaddine, J. (2006). The economic burden of major adult visual disorders in the United States. Archives of ophthalmology *124*, 1754-1760.

Rivlin-Etzion, M., Zhou, K., Wei, W., Elstrott, J., Nguyen, P.L., Barres, B.A., Huberman, A.D., and Feller, M.B. (2011). Transgenic mice reveal unexpected diversity of on-off direction-selective retinal ganglion cell subtypes and brain structures involved in motion processing. The Journal of Neuroscience *31*, 8760-8769.

Robles, E., Filosa, A., and Baier, H. (2013). Precise lamination of retinal axons generates multiple parallel input pathways in the tectum. J Neurosci *33*, 5027-5039.

Rompani, S.B., Müllner, F.E., Wanner, A., Zhang, C., Roth, C.N., Yonehara, K., and Roska, B. (2017). Different Modes of Visual Integration in the Lateral Geniculate Nucleus Revealed by Single-Cell-Initiated Transsynaptic Tracing. Neuron *93*, 767-776. e766.

Ryabets-Lienhard, A., Stewart, C., Borchert, M., and Geffner, M.E. (2016). The Optic Nerve Hypoplasia Spectrum: Review of the Literature and Clinical Guidelines. Advances in pediatrics *63*, 127.

Sanes, J.R., and Lichtman, J.W. (2001). Induction, assembly, maturation and maintenance of a postsynaptic apparatus. Nature Reviews Neuroscience *2*, 791-805.

Sanes, J.R., and Masland, R.H. (2015). The types of retinal ganglion cells: current status and implications for neuronal classification. Annual review of neuroscience *38*, 221-246.

Sanes, J.R., and Yamagata, M. (2009). Many paths to synaptic specificity. Annual review of cell and developmental biology *25*, 161-195.

Sato, H., Fukutani, Y., Yamamoto, Y., Tatara, E., Takemoto, M., Shimamura, K., and Yamamoto, N. (2012). Thalamus-derived molecules promote survival and dendritic growth of developing cortical neurons. The Journal of neuroscience : the official journal of the Society for Neuroscience *32*, 15388-15402.

Seabrook, T.A., El-Danaf, R.N., Krahe, T.E., Fox, M.A., and Guido, W. (2013a). Retinal input regulates the timing of corticogeniculate innervation. The Journal of Neuroscience *33*, 10085-10097.

Seabrook, T.A., Krahe, T.E., Govindaiah, G., and Guido, W. (2013b). Interneurons in the mouse visual thalamus maintain a high degree of retinal convergence throughout postnatal development. Neural development *8*, 1.

Shanks, J.A., Ito, S., Schaevitz, L., Yamada, J., Chen, B., Litke, A., and Feldheim, D.A. (2016). Corticothalamic Axons Are Essential for Retinal Ganglion Cell Axon Targeting to the Mouse Dorsal Lateral Geniculate Nucleus. The Journal of Neuroscience *36*, 5252-5263.

Shekhar, K., Lapan, S.W., Whitney, I.E., Tran, N.M., Macosko, E.Z., Kowalczyk, M., Adiconis, X., Levin, J.Z., Nemesh, J., and Goldman, M. (2016). Comprehensive classification of retinal bipolar neurons by single-cell transcriptomics. Cell *166*, 1308-1323. e1330.

Sherman, S.M. (1985). Functional organization of the W-, X-, and Y-cell pathways in the cat: a review and hypothesis. Progress in psychobiology and physiological psychology *11*, 233-314.

Sherman, S.M. (2004). Interneurons and triadic circuitry of the thalamus. Trends in neurosciences *27*, 670-675.

Sherman, S.M. (2005). Thalamic relays and cortical functioning. Progress in brain research *149*, 107-126.

Sherman, S.M. (2016). Thalamus plays a central role in ongoing cortical functioning. Nature neuroscience *16*, 533-541.

Sherman, S.M., and Guillery, R. (2002). The role of the thalamus in the flow of information to the cortex. Philosophical Transactions of the Royal Society of London Series B: Biological Sciences *357*, 1695-1708.

Siddiqui, T.J., and Craig, A.M. (2011). Synaptic organizing complexes. Current opinion in neurobiology *21*, 132-143.

Siddiqui, T.J., Pancaroglu, R., Kang, Y., Rooyakkers, A., and Craig, A.M. (2010). LRRTMs and neuroligins bind neurexins with a differential code to cooperate in glutamate synapse development. The Journal of neuroscience : the official journal of the Society for Neuroscience *30*, 7495-7506.

Sieving, P.A. (2012). NEI Audacious Goals Initiative to Catalyze Innovation Editorial. Investigative ophthalmology & visual science *53*, 7149-7150.

Sincich, L.C., Adams, D.L., Economides, J.R., and Horton, J.C. (2007). Transmission of spike trains at the retinogeniculate synapse. The Journal of Neuroscience *27*, 2683-2692.

Singh, R., Su, J., Brooks, J., Terauchi, A., Umemori, H., and Fox, M.A. (2011). Fibroblast growth factor 22 contributes to the development of retinal nerve terminals in the dorsal lateral geniculate nucleus. Frontiers in molecular neuroscience *4*.

Singh, R., Su, J., Brooks, J., Terauchi, A., Umemori, H., and Fox, M.A. (2012). Fibroblast growth factor 22 contributes to the development of retinal nerve terminals in the dorsal lateral geniculate nucleus.

So, K.-F., Campbell, G., and Lieberman, A. (1985). Synaptic organization of the dorsal lateral geniculate nucleus in the adult hamster. Anatomy and embryology *171*, 223-234.

Soler-Llavina, G.J., Fuccillo, M.V., Ko, J., Südhof, T.C., and Malenka, R.C. (2011). The neurexin ligands, neuroligins and leucine-rich repeat transmembrane proteins, perform convergent and divergent synaptic functions in vivo. Proceedings of the National Academy of Sciences *108*, 16502-16509.

Stevens, G.A., White, R.A., Flaxman, S.R., Price, H., Jonas, J.B., Keeffe, J., Leasher, J., Naidoo, K., Pesudovs, K., and Resnikoff, S. (2013). Global prevalence of vision impairment and blindness: magnitude and temporal trends, 1990–2010. Ophthalmology *120*, 2377-2384.

Takashima, N., Odaka, Y.S., Sakoori, K., Akagi, T., Hashikawa, T., Morimura, N., Yamada, K., and Aruga, J. (2011). Impaired cognitive function and altered hippocampal synapse morphology in mice lacking Lrrtm1, a gene associated with schizophrenia. PLoS One *6*, e22716.

Terauchi, A., Johnson-Venkatesh, E.M., Toth, A.B., Javed, D., Sutton, M.A., and Umemori, H. (2010). Distinct FGFs promote differentiation of excitatory and inhibitory synapses. Nature *465*, 783-787.

Tham, Y.-C., Li, X., Wong, T.Y., Quigley, H.A., Aung, T., and Cheng, C.-Y. (2014). Global prevalence of glaucoma and projections of glaucoma burden through 2040: a systematic review and meta-analysis. Ophthalmology *121*, 2081-2090.

Thompson, A.D., Picard, N., Min, L., Fagiolini, M., and Chen, C. (2016). Cortical Feedback Regulates Feedforward Retinogeniculate Refinement. Neuron *91*, 1021-1033.

Towns, L.C., Burton, S., Kimberly, C., and Fetterman, M. (1982). Projections of the dorsal lateral geniculate and lateral posterior nuclei to visual cortex in the rabbit. Journal of Comparative Neurology *210*, 87-98.

Triplett, J.W., Wei, W., Gonzalez, C., Sweeney, N.T., Huberman, A.D., Feller, M.B., and Feldheim, D.A. (2014). Dendritic and axonal targeting patterns of a genetically-specified class of retinal ganglion cells that participate in image-forming circuits. Neural development *9*, 2.

Umemori, H., Linhoff, M.W., Ornitz, D.M., and Sanes, J.R. (2004). FGF22 and its close relatives are presynaptic organizing molecules in the mammalian brain. Cell *118*, 257-270.

Usrey, W.M., Reppas, J.B., and Reid, R.C. (1999). Specificity and strength of retinogeniculate connections. Journal of Neurophysiology *82*, 3527-3540.

Van Hooser, S.D., and Nelson, S.B. (2006). The squirrel as a rodent model of the human visual system. Visual neuroscience *23*, 765-778.

Virolainen, S.-M., Achim, K., Peltopuro, P., Salminen, M., and Partanen, J. (2012). Transcriptional regulatory mechanisms underlying the GABAergic neuron fate in different diencephalic prosomeres. Development *139*, 3795-3805.

Voikar, V., Kulesskaya, N., Laakso, T., Lauren, J., Strittmatter, S.M., and Airaksinen, M.S. (2013). LRRTM1-deficient mice show a rare phenotype of avoiding small enclosures--a tentative mouse model for claustrophobia-like behaviour. Behavioural brain research *238*, 69-78.

Vue, T.Y., Aaker, J., Taniguchi, A., Kazemzadeh, C., Skidmore, J.M., Martin, D.M., Martin, J.F., Treier, M., and Nakagawa, Y. (2007). Characterization of progenitor domains in the developing mouse thalamus. Journal of Comparative Neurology *505*, 73-91.

Waites, C.L., Craig, A.M., and Garner, C.C. (2005). Mechanisms of vertebrate synaptogenesis. Annu Rev Neurosci *28*, 251-274.

Wang, Q., Sporns, O., and Burkhalter, A. (2012). Network analysis of corticocortical connections reveals ventral and dorsal processing streams in mouse visual cortex. J Neurosci *32*, 4386-4399.

Wang, S., Eisenback, M., Datskovskaia, A., Boyce, M., and Bickford, M.E. (2002). GABAergic pretectal terminals contact GABAergic interneurons in the cat dorsal lateral geniculate nucleus. Neuroscience letters *323*, 141-145.

Wässle, H. (2004). Parallel processing in the mammalian retina. Nature Reviews Neuroscience *5*, 747-757.

Wilson, J., Friedlander, M., and Sherman, S. (1984). Fine structural morphology of identified X- and Y-cells in the cat's lateral geniculate nucleus. Proceedings of the Royal Society of London Series B, Biological Sciences, 411-436.

Yamagata, M., Sanes, J.R., and Weiner, J.A. (2003). Synaptic adhesion molecules. Current opinion in cell biology *15*, 621-632.

Yeh, C.-I., Stoelzel, C.R., Weng, C., and Alonso, J.-M. (2009). Functional consequences of neuronal divergence within the retinogeniculate pathway. Journal of neurophysiology *101*, 2166-2185.

Yogev, S., and Shen, K. (2014). Cellular and molecular mechanisms of synaptic specificity. Annual review of cell and developmental biology *30*, 417-437.

Yucel, Y.H., and Gupta, N. (2015). A framework to explore the visual brain in glaucoma with lessons from models and man. Experimental eye research *141*, 171-178.

Zhang, J., Ackman, J.B., Xu, H.-P., and Crair, M.C. (2012). Visual map development depends on the temporal pattern of binocular activity in mice. Nature neuroscience *15*, 298-307.

Zhong, X., Gutierrez, C., Xue, T., Hampton, C., Vergara, M.N., Cao, L.-H., Peters, A., Park, T.-S., Zambidis, E.T., and Meyer, J.S. (2014). Generation of three dimensional retinal tissue with functional photoreceptors from human iPSCs. Nature communications *5*, 4047.

Zito, A., Cartelli, D., Cappelletti, G., Cariboni, A., Andrews, W., Parnavelas, J., Poletti, A., and Galbiati, M. (2012). Neuritin 1 promotes neuronal migration. Brain structure & function.

2. Multiple retinal axons converge onto relay cells in the adult mouse thalamus

Authors:

Sarah Hammer,[1,5] Aboozar Monavarfeshani,[1,2,5] Tyler Lemon,[1] Jianmin Su,[1] and Michael Andrew Fox1,2,3*

[1]Virginia Tech Carilion Research Institute, Roanoke, VA 24016, USA

[2]Department of Biological Sciences, Virginia Tech, Blacksburg, VA 24061, USA

[3]Department of Pediatrics, Virginia Tech Carilion School of Medicine, Roanoke, VA [2]4016, USA

[5]Co-first author

[*]Correspondence: mafox1@vtc.vt.edu

http://dx.doi.org/10.1016/j.celrep.2015.08.003

Highlights:

Brainbow-based technology can be used to differentially label retinal terminals

Clusters of retinal terminals originate from numerous uniquely labeled RGCs

Complex retinogeniculate synapses contain terminals from >10 distinct retinal axons

A higher level of convergence exists on relay cells than previously appreciated

2.1. Summary

Activity-dependent refinement of neural circuits is a fundamental principle of neural development. This process has been well studied at retinogeniculate synapses – synapses that form between retinal ganglion cells (RGCs) and relay cells within the dorsal lateral geniculate nucleus. Physiological studies suggest that shortly after birth inputs from ~20 RGCs converge onto relay cells. Subsequently, all but just 1-2 of these inputs is eliminated. Despite widespread acceptance this notion is at odds with ultrastructural studies showing numerous retinal terminals clustering onto relay cell dendrites in the adult. Here we explored this discrepancy using brainbow AAVs and serial block face scanning electron microscopy (SBFSEM). Results with both approaches demonstrate that terminals from numerous RGCs cluster onto relay cell dendrites, challenging the notion that only 1-2 RGCs innervate each relay cell. These findings force us to re-evaluate our understanding of subcortical visual circuitry.

2.2. Introduction

Initially an exuberant number of axons generate synapses with target neurons in the brain only to have a large number of these supernumerary inputs eliminated in an activity-dependent fashion. This process, termed synapse elimination, has been well studied in the mouse visual thalamus, where synapses form between retinal projection neurons (i.e. retinal ganglion cells [RGCs]) and thalamic relay cells within the dorsal lateral geniculate nucleus (dLGN). Physiological studies over the past decade have suggested that retinal inputs to dLGN relay cells undergo an extensive amount of refinement during early postnatal development. While as many as 20 RGCs may innervate relay cells in the first week of mouse development, this number is reduced to just 1-2 RGCs by the end of the 3rd postnatal week of rodent development (Chen and Regehr, 2000; Hong and Chen, 2011; Hooks and Chen, 2006; Jaubert-Miazza et al., 2005).

Furthermore, single electrode recordings in mature primate LGN have been interpreted to indicate that retinal-derived excitatory postsynaptic potentials in relay cells arise from just 1 RGC (Sincich et al., 2007). Based upon these studies and the near unitary matching of retinal input to thalamic relay cell in the adult dLGN, the retinogeniculate synapse has emerged as a model for our understanding of activity-dependent refinement in the brain.

It is important to note, however, that these conclusions appear at odds with a series of four-decade old ultrastructural studies that characterized two distinct types of retinogeniculate synapses in dLGN: “simple encapsulated” retinogeniculate synapses are composed of single, large retinal terminals that contact large diameter relay cell dendrites and “complex encapsulated” retinogeniculate synapses that are composed of as many as ten distinct retinal terminals all converging on the same region of relay cell dendrite (Jones and Powell, 1969) (Guillery and Scott, 1971; Lund and Cunningham, 1972). If multiple retinal terminals converge at these synaptic sites, how can a near unitary matching of RGC axons to relay cells exist? A recent study by Hong et al. began to shed light on this paradox by revealing that the dramatic decrease in retinal convergence onto relay cells was accompanied by retinal terminals from single axonal arbors clustering onto postsynaptic sites in dLGN (Hong et al., 2014). This suggests that the numerous retinal terminals in “complex encapsulated” retinogeniculate synapses arise from branches of the same terminal arbor. To test this hypothesis we employed “brainbow” adeno-associated viral vectors (brainbow AAVs) (Cai et al., 2013), a technique that permits the differential labeling of RGCs and their terminals with unique combinations of fluorescent reporter proteins. To our surprise this approach revealed that clusters of retinal terminals originated from numerous, distinct RGCs. To test whether these clustered retinal terminals represented true synaptic connections with the same relay cell we used serial block

face scanning electron microscopy (SBFSEM), a technique that permits the 3D reconstruction of pre- and postsynaptic elements at high resolution (Denk and Horstmann, 2004). These analyses provide further evidence that terminals from numerous axons converged onto the same dendrite in “complex encapsulated” retinogeniculate synapses. These results challenge the notion that only 1-2 RGCs contact each dLGN relay cell and suggest we need to re-evaluate our understanding of the anatomy and development of subcortical visual circuitry.

2.3. Results

To assess whether clusters of retinal terminals originate from single RGC axons we employed “brainbow” AAVs to differentially label RGCs with unique combinations of four fluorescent proteins – farnesylated Tag-blue fluorescent protein (BFP), enhanced yellow fluorescent protein (EYFP), monomeric Cherry fluorescent protein (mChe), and monomeric teal fluorescent protein (mTFP) (Cai et al., 2013). Brainbow-based technologies have previously been used successfully to trace axonal projections, including retinal projections, in a variety of vertebrate species (Cai et al., 2013; Livet et al., 2007; Pan et al., 2013; Robles et al., 2013). Each brainbow AAV is capable of driving the expression of two different fluorescent proteins (see Figure 1A), however as each cell may express different levels of all 4 fluorescent proteins a nearly limitless possibility of colors is achievable with these constructs (Cai et al., 2013). Since brainbow AAVs are Cre-dependent, we injected a 1:1 mixture of both brainbow AAVs into the vitreous chamber of postnatal day 12-14 (P12-14) *calb2-cre* transgenic mice (Taniguchi et al., 2011). Cre recombinase is expressed by a large subset of RGCs in these mice (Zhu et al., 2014). After 3 weeks, mice were euthanized and RGCs were examined with confocal microscopy. Analysis in retinal cross-sections and whole mounts revealed four important points: 1).

Intraocular delivery of brainbow AAVs successfully labeled a large number of RGCs in *calb2-cre* mice (referred to here as brainbow AAV::*calb2-cre* mice) (Figure 1B,C); 2). By examining dendritic stratification of uniquely labeled RGCs in brainbow AAV::*calb2-cre* mice it was clear that multiple classes of RGCs were labeled in these mice; 3). Unique combinations of fluorescent reporter proteins were evenly distributed throughout retinal axons in brainbow AAV::*calb2-cre* mice. This point is of particular importance since a key requirement for this "brainbow"-based approach to be successful is that there must be a uniform distribution of the entire constellation of fluorescent proteins within the axon and terminal arbor (so that color can be used as a marker of RGC origin of an axon). Previous studies on zebrafish RGCs have demonstrated that the distribution of brainbow-based fluorescent proteins remain uniformly distributed in both axonal and terminal compartments of the same cell (Robles et al., 2013). To be entirely sure that this was the case for retinal projections in mice we analyzed color distribution in RGC axons in retinal whole-mounts of brainbow AAV::*calb2-cre* mice. Data presented here confirmed that the distribution of the entire constellation of fluorescent molecules expressed by a single RGC in brainbow AAV::*calb2-cre* mice was evenly distributed throughout RGC axons in the retina (Figure 1D,E). This data supports the feasibility of using differential labeling of RGC terminals in brainbow AAV::*calb2-cre* dLGN to probe whether "complex encapsulated" retinogeniculate synapses arise from branches of the same terminal arbor.

To answer whether clusters of retinal terminals in dLGN arise from the same RGC we turned our attention to the dLGN of P35 brainbow AAV::*calb2-cre* mice. It is important to note that only a sparse population of retinal axons and terminals in dLGN were labeled with this approach (Figure 2). Regardless of this sparse labeling, we discovered that most terminal clusters contained numerous uniquely colored elements (Figures 1H,I and 2). Since the "core" and

"shell" regions of dLGN contain distinct types of relay cells and receive input from distinct types of RGCs (Dhande and Huberman, 2014; Hong and Chen, 2011; Krahe et al., 2011), we addressed whether multi-colored terminal clusters were present in both regions of P35 brainbow AAV::*calb2-cre* mice dLGN. Analysis with anterograde tracers and immunohistochemistry with retinal-terminal specific markers both suggested that terminal clusters were present in both regions, but that clusters appeared larger and more widespread in the "shell" region of dLGN where axons from direction-selective RGCs arborize (Supplemental Figure 1). Analysis in the P35 brainbow AAV::*calb2-cre* mice revealed multi-colored terminal clusters in both "core" and "shell" regions of dLGN (Figure 1H and 2).

In contrast to the diversity of uniquely colored elements in these terminal clusters, retinal axons traversing this region of dLGN displayed consistent distributions of fluorescent proteins (see arrowheads in Figure 2A). This suggests that the numerous colored elements at terminal clusters represented axonal terminals originating from different RGCs. Importantly, when we analyzed individual retinal arbors in dLGN we found uniform expression of fluorescent proteins in each bouton of a single retinal axon arbor (Figure 1F,G), again suggesting that terminal clusters containing multiple differently colored retinal terminals reflected clusters containing terminals from multiple RGCs.

While these results indicate that clusters of retinal terminals originate from multiple RGCs, they do not indicate whether these boutons contact the same dendrite or even the same relay cell. The gold standard for identifying such synaptic connections is with the use of high-resolution electron microscopy (EM) – the technique that first identified the complex encapsulated retinogeniculate synapses more than 4 decades ago (Guillery and Scott, 1971; Jones and Powell, 1969; Lund and Cunningham, 1972). The problem with traditional EM approaches

has been the difficulty in obtaining large volumes of serially sectioned EM images and in aligning and registering all of these images. Without large volumes of serially sectioned tissue it has been impossible to identify the axonal origins of each presynaptic bouton at these complex retinogeniculate synapses. For this reason, we applied Serial Block Face Scanning Electron Microscopy (SBFSEM) to reconstruct retinogeniculate synapses at high resolution (5nm/pixel) in P42 mouse dLGN. In electron micrographs, retinal terminals were identified based on the presence of pale-colored mitochondria and dense clusters of spherical synaptic vesicles, relay cell dendrites were identified based on the lack of synaptic vesicles, dark mitochondria and microtubules, and synaptic sites between terminals and dendrites were identified by the presence of an identifiable active zone (Bickford et al., 2010; Hammer et al., 2014; Lund and Cunningham, 1972).

In total 71 retinal axons (and all of their terminal boutons within the volumes of tissue) were traced and reconstructed in the "shell" region of dLGN. These reconstructed axons generated 344 distinct synaptic sites onto the dendrites of relay cells and the average length of axon traced was 27.6 µm (+/- 22 µm [SD]). Importantly, we observed single dendrites that received input from both simple and complex retinogeniculate synapses, suggesting single relay cells have the potential to be innervated by both types of retinal synapses (data not shown). Terminal boutons from 17 of these retinal axons participated in large, "simple encapsulated" retinogeniculate synapses (see Figure 3). Although only one of these axons generated terminal boutons that participated in both "simple encapsulated" retinogeniculate synapses and "complex encapsulated" retinogeniculate synapses (data not shown), this observation suggests that RGCs have the potential to generate both types of retinogeniculate synapses. Of the remaining 16 axons that generated large, "simple encapsulated" synapses, not a single example was identified in

which terminals clustered around a single segment of dendrite. Instead we observed single axons contacting multiple dendrites (Figure 3D-F) and multiple retinal axons converging onto different regions of the same dendrite (Figure 3A-C). The longest reconstructed retinal axon that contributed to simple retinogeniculate synapses measured 116.9 µm in length. It is important to point out, however, that in both cases it remains possible that these axons or dendrites may have originated from branches of the same RGC or relay cell, respectively, that branched outside of the volume of tissue reconstructed.

The remaining 54 retinal axons reconstructed generated boutons that contributed to "complex encapsulated" retinogeniculate synapses (Figure 4). In contrast to those retinal axons that generated "simple encapsulated" synapses, these 54 axons generated clusters of boutons that made synaptic contact with multiple, adjacent regions of the same dendrite (see blue and orange retinal terminals in Figure 4A-H and bright green retinal terminals in Figure 4I-O). The longest reconstructed retinal axon that contributed to complex retinogeniculate synapses measured 80.6 µm in length. These axons also generated boutons that made synaptic contact onto inhibitory interneuron dendrites (which were distinguished from relay cell dendrites by the presence of synaptic vesicles) (Bickford et al., 2010; Lund and Cunningham, 1972) that were also identified in "complex encapsulated" synapses (see orange retinal terminals and purple inhibitory dendrite in Figure 4A-H).

Although the bulk of SBFSEM analysis was performed on the "shell" region of dLGN, we also generated datasets from the "core" region of dLGN. Both simple and complex retinogeniculate synapses were observed in these datasets and boutons in the complex synapse appeared to originate from distinct retinal axons (Supplemental Figure 1).

Next, we quantified different features of simple and complex retinogeniculate synapses. We found that retinal boutons participating in complex retinogeniculate synapses were smaller than their counterparts in simple synapses (Supplemental Figure 2). Moreover, boutons in these complex synapses contained ~50% fewer active zones and ~50% fewer dendritic protrusions than boutons in simple retinogeniculate synapses (Supplemental Figure 2). These differences were not merely the result of terminals being smaller in size, since there was a statistically significant difference in the active zone: bouton diameter ratio at these two synapse types (Supplemental Figure 2).

While these results were expected based on previous studies (Bickford et al., 2010; Hong et al., 2014; Lund and Cunningham, 1972), the number of retinal axons that contribute to these clusters of retinal terminals was unexpected. In most cases we observed terminal boutons originating from 3-8 different retinal axons in these reconstructions (Figure 4A-H), however in a few cases we observed clusters that contained boutons from more than a dozen different retinal axons (Figure 4I-O). While results from single retinal axon tracing studies could be interpreted to indicate that these clustered terminals originated from distant branches of 1 or 2 retinal axons (Dhande et al., 2011; Hong et al., 2014), our own studies of terminal clusters in brainbow AAV::*calb2-cre* mice suggest that many of these terminal boutons do in fact originate from distinct RGCs (Figure 2). Therefore, taken together, these results and those describe above in brainbow AAV::*calb2-cre* mice, indicate that numerous retinal inputs converge onto relay cells in the adult mouse dLGN.

2.4. Discussion

The retinogeniculate synapse has emerged as one of the most widely used models for studying activity-dependent refinement in the developing brain. In mice, physiological studies have suggested that as retinal axons initially innervate dLGN as many as 20 distinct RGC inputs converge onto the dendrites of relay cells, but over the first few weeks of postnatal development, most supernumerary retinal inputs are eliminated so that each relay cell receives input from just 1-2 RGCs in the adult animal (Chen and Regehr, 2000; Hong and Chen, 2011). A concept so well entrenched it has made its way into widely used textbooks (Squire et al., 2012).

Here we applied two relatively novel technologies to examine the clustering of retinal terminals at retinogeniculate synapses. Our hope was to provide an explanation for why "complex encapsulated" retinogeniculate synapses exist if each relay cell receives input from just 1-2 RGCs. While our initial hypothesis was that each retinal terminal within a "complex encapsulated" retinogeniculate synapse originated from branches of a single RGCs, our data indicate that presynaptic terminals from numerous retinal axons converge onto relay cells in the mature rodent dLGN. These results raise an obvious question: *what is the actual number of RGCs that innervate each relay cell*? Unfortunately an exact number cannot be determined since the studies described here focused on small regions of retinal arbors or dendritic trees, limiting the ability to reconstruct every single axon that synapses onto a given relay cell. That being said, for many relay cells the number of retinal inputs likely will approach or exceed a dozen. While this statement (and the results demonstrated here) contrasts the widely-accepted concept of a near unitary matching of RGC to relay cell, these results are supported (at least in part) by previous studies that have suggested a modestly larger number of retinal inputs on relay cells than just 1-2 (Cleland and Lee, 1985; Sincich et al., 2007; Usrey et al., 1999).

We are therefore left pondering why anatomical and functional studies produce such differing conclusions. *Is this discrepancy a technical issue with the approaches applied?* Certainly this is a possibility, as all experimental approaches have shortcomings. *Are these complex synapses leaky, so that the release of glutamate from one terminal activates all of the postsynaptic receptors within this synaptic cluster?* Certainly the latter is a possibility since the presence and consequence of synaptic spillover has been demonstrated in both simulations and with experimental approaches at complex retinogeniculate synapses (Budisantoso et al., 2012). *Do some classes of relay cells in mouse dLGN receive input from only one type of retinogeniculate synapse, so that some relay cells receive input from just 1-2 RGCs while other classes receive input from large numbers of RGCs?* This possibility is supported in part by a heroic study by Sherman and colleagues in which a single retinal axon was labeled with HRP and its connectivity with 4 LGN relay cells was examined with serial electron microscopy (Hamos et al., 1987). The HRP-labeled axon accounted for 100% of the retinal inputs onto the proximal dendrites of one of the relay cells, but only 49%, 33%, and 2% of the retinal inputs of the other 3 relay cells, suggesting levels of convergence on relay cells may vary widely (Hamos et al., 1987). Moreover, the morphology of retinal terminals generated by this single HRP-labeled axon differed between the cells, suggesting a role for the postsynaptic neuron in determining the architecture of the retinogeniculate synapse (Hamos et al., 1987). However, our reconstructions identified cases in which single relay cells were innervated by both simple and complex retinogeniculate synapses, arguing against the possibility of different classes of relay cells receiving just one type of retinal synapse. *Are "complex encapsulated" retinogeniculate synapses considerably weaker than the large, "simple encapsulated" synapses, so that their influence on postsynaptic activity is negligible?* The reduced number of active zones and

dendritic protrusions in retinal boutons associated with complex retinogeniculate, shown by us here and by Budisantoso et al. (2012) in the rat dLGN, suggest that the strength of terminals may be weaker at complex synapses. Unfortunately we do not know the answers to all of these questions yet but one can certainly imagine a number of possibilities that will need to be addressed in future studies.

Results from our studies also raise interesting questions regarding how different classes of RGCs participate in retinal terminal clustering in dLGN. Only a single retinal axon was reconstructed that participated in both complex and simple type retinogeniculate synapses. While this may reflect a sampling issue, it may also indicate that different classes of RGCs generate different types of retinogeniculate synapses. Just as different classes of retinal axons arborize in unique domains of dLGN (Dhande and Huberman, 2014; Hong and Chen, 2011), it is tempting to speculate that some classes of retinal axons cluster their terminals into complex retinogeniculate synapses (like observed in Hong et al. 2014) while others do not use this mechanism of refinement and reorganization.

Finally, it is important to discuss an implication that these studies may have on using the retinogeniculate synapse as a model of activity-dependent refinement. Many groups use this model synapse to explore the cellular and molecular underpinnings of activity-dependent refinement at brain synapses. Such studies are based on the assumption that inputs from ~20 RGCs initially converge on relay cells, but that most of these inputs are eliminated during development. But, what if this is not the case? What if retinal convergence persists (at least anatomically) in the mature visual system? Our results lead us to think that this is the case and indicate we need to re-evaluate our understanding of the architecture and flow of visual information through retinogeniculate circuits.

2.5. Experimental Procedures

2.5.1. Mice

Wild-type C57 mice were obtained from Charles River. Calb2-cre mice were obtained from Jackson Laboratory (Stock #010774). All analyses conformed to National Institutes of Health guidelines and protocols approved by the Virginia Polytechnic Institute and State University Institutional Animal Care and Use Committees.

2.5.2. Intraocular injections of brainbow AAVs

The following brainbow AAVs were obtained from the University of Pennsylvania Vector Core (http://www.med.upenn.edu/gtp/vectorcore/): AAV9.hEF1a.lox.TagBFP.lox.eYFP.lox.WPRE.hGH-InvBYF (lot #V3809TI-R) and AAV9.hEF1a.lox.mCherry.lox.mTFP1.lox.WPRE.hGH-InvCheTF (lot #V3530TI-R). Each brainbow AAV is capable of driving the expression of two different fluorescent proteins (see Figure 1A). Intraocular injection of brainbow AAVs was performed as described previously for the intraocular delivery of cholera toxin subunit B (Jaubert-Miazza et al., 2005; Su et al., 2011). Briefly, mice were anesthetized with isoflurane vapors at P12-14. The sclera was pierced with a sharp-tipped glass pipette and excess vitreous was drained. Another pipette, filled with a 1:1 mixture of both brainbow AAVs, was inserted into the hole made by the first pipette. The pipette containing the AAVs was attached to a Picospritzer and a prescribed volume (3–5 μl) of solution was injected into the eye. After 21 days, mice were euthanized, transcardially perfused with PBS and 4% paraformaldehyde, and retinas and brains were post-fixed in 4% paraformaldehyde for 12 hours. Fixed brains were coronally sectioned (80-100 μm) on a vibratome (Microm HM 650V, Thermo Scientific) and mounted in ProLong Gold (Invitrogen). Fixed retinas were either

prepared as whole-mounts or were sectioned on a Leica CM1850 cryostat (16µm cross-sections) and in either case were mounted in ProLong Gold (Invitrogen) (Su et al., 2011). RGCs and retinal projections were analyzed from 6 animals. Images were acquired on a Zeiss LSM 700 confocal microscope and color analysis of maximum projections images was performed in Photoshop.

2.5.3. Serial Block Face Scanning Electron Microscopy

Mice were transcardially perfused sequentially with PBS and 4% paraformaldehyde / 2% glutaradehyde in 0.1M cacodylate buffer. Brains were immediately removed, vibratomed (300 µm coronal sections) and dLGN were dissected. Tissues were then stained, embedded, sectioned and imaged by Renovo Neural Inc. (Cleveland, OH). Images were acquired at a resolution of 5 nm/pixel and image sets included > 200 serial sections (with each section representing 75 nm in the z axis). SBFSEM data sets were 40µm x 40 µm x 12-20 µm. 4 data sets were analyzed for each region (from a total of 3 P42 wild-type mice). Data sets were traced and analyzed in TrakEM2 (Cardona et al., 2012). Retinal terminals were identified (and distinguished from non-retinal terminals) by the presence of synaptic vesicles and pale mitochondria as previously described (Bickford et al., 2010; Hammer et al., 2014; Lund and Cunningham, 1972). Synaptic sites were identified by the presence of active zones and postsynaptic densities. Analysis of data sets was performed independently by three researchers to ensure unbiased results.

Acknowledgements

This work was supported in part by the National Institutes of Health – National Eye Institute grant EY021222 (MAF). We thank Dr. G. Valdez for helpful comments on the

manuscript and for providing assistance with the brainbow AAVs. We also thank Dr. A. Cardona for advice in tracing retinal axon length in SBFSEM datasets.

Figure 2.1. Labeling of RGCs and retinal axons with brainbow AAVs.

A. Schematic representing the constructs of each of the two brainbow AAVs used in these studies. Following Cre recombination these two constructs generate either farnesylated Tag-blue fluorescent protein (BFP) or enhanced yellow fluorescent protein (EYFP), or monomeric Cherry fluorescent protein (mChe) or monomeric teal fluorescent protein (mTFP). EF1 represent regulatory elements from the elongation 1α gene and W represents elements from the woodchuck hepatitis virus posttranscriptional regulatory element. Lox site mutants are depicted with grey triangles. For additional details see Cai et al. 2013. B. Confocal image of a P35 retinal cross section following intraocular injection of brainbow AAV into calb2-cre mice. Note the ability to delineate the dendritic arbor of the green-labeled RGC from adjacent fluorescently labeled RGCs. C. Confocal image of a P35 retinal whole mount following intraocular injection of brainbow AAV into calb2-cre mice. D. Confocal image of differentially labeled RGC axons in a P35 retinal whole mount brainbow AAV::calb2-cre mouse. E. Color analysis at five locations (1-5) along the 6 axons labeled in D (labeled A-F). The color boxes represent the colors at each point highlighted along the axons. Numbers in the boxes represent the red (R), green (G), and blue (B) color intensity values at each point along the axons. Note the relative similar distribution of "color" along each axon. E,F. A single retinal axon labeled with brainbow AAVs in dLGN of a P35 calb2-cre mice. F depicts color analysis for the three boutons highlighted by arrows in E. H,I. Terminals from 3 distinct retinal axons converging at a single cluster following labeling with brainbow AAVs in dLGN of a P35 calb2-cre mice. I depicts color analysis for the three boutons highlighted in H. Scale bar in B = 50 μm for B,D and in C = 100 μm.

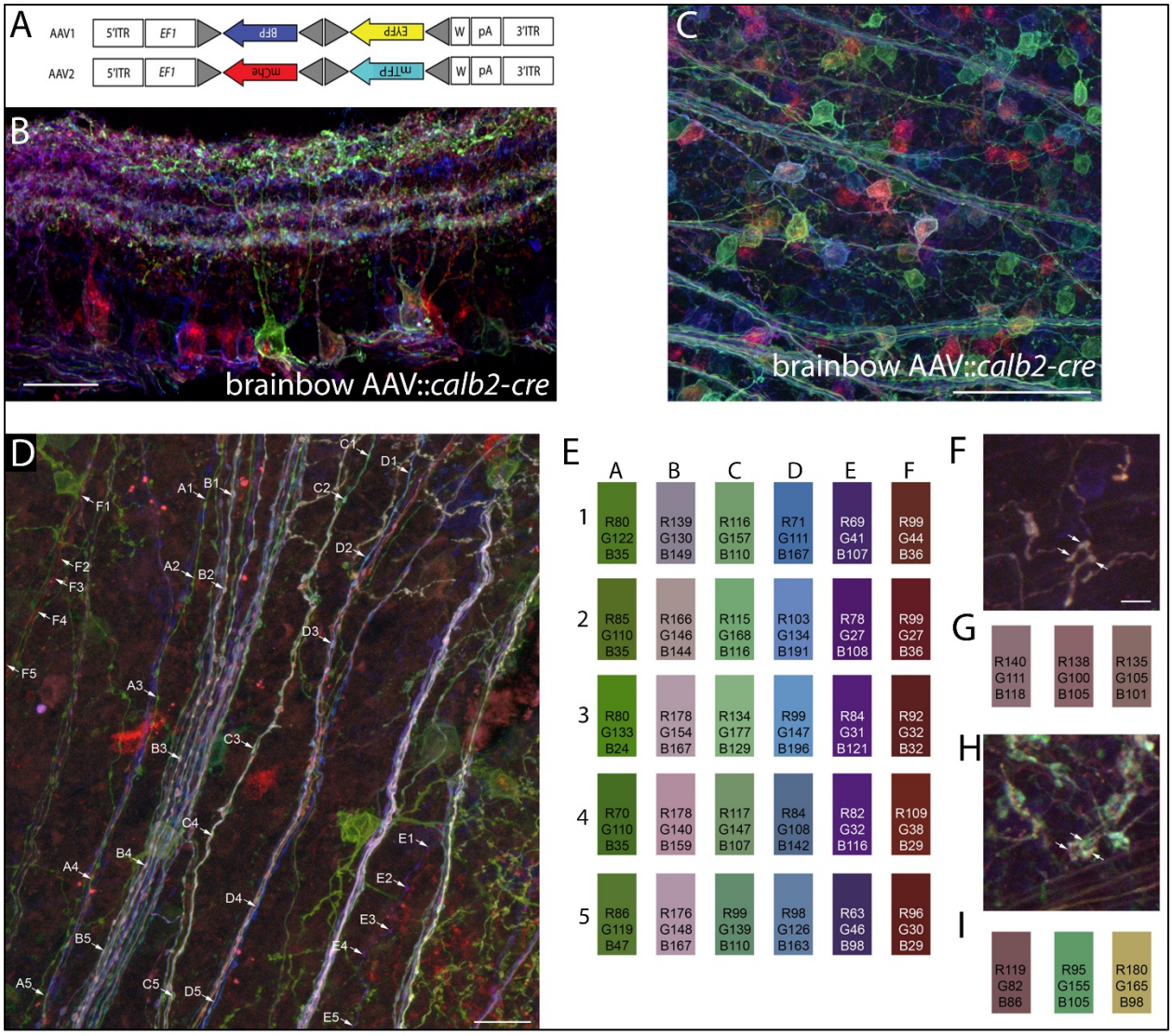
A
AAV1
5'ITR
EF1
BFP
EYFP
W
pA
3'ITR
AAV2
5'ITR
EF1
mCh
mTFP
W
pA
3'ITR
B
brainbow AAV::calb2-cre
C
brainbow AAV::calb2-cre
D
A1
B1
C1
D1
F1
C2
D2
F2
A2
B2
F3
F4
D3
F5
A3
B3
C3
C4
E1
B4
A4
E2
D4
E3
B5
E4
A5
C5
D5
E5
E
A
B
C
D
E
F
1
R80 G122 B35
R139 G130 B149
R116 G157 B110
R71 G111 B167
R69 G41 B107
R99 G44 B36
2
R85 G110 B35
R166 G146 B144
R115 G168 B116
R103 G134 B191
R78 G27 B108
R99 G27 B36
3
R80 G133 B24
R178 G154 B167
R134 G177 B129
R99 G147 B196
R84 G31 B121
R92 G32 B32
4
R70 G110 B35
R178 G140 B159
R117 G147 B107
R84 G108 B142
R82 G32 B116
R109 G38 B29
5
R86 G119 B47
R176 G148 B167
R99 G139 B110
R98 G126 B163
R63 G46 B98
R96 G30 B29
F
G
R140 G111 B118
R138 G100 B105
R135 G105 B101
H
I
R119 G82 B86
R95 G155 B105
R180 G165 B98

Figure 2.2. Clusters of retinal terminals in dLGN contain boutons from multiple retinal axons.

Maximum projection, confocal image of retinal axons and terminals labeled with brainbow AAVs in dLGN of P35 *calb2-cre* mice. Arrowheads highlight retinal axons traversing this region of dLGN. **B-K**. High magnification images of the retinal boutons indicated by arrows in **A**. **B'-K'** color analysis for terminals highlighted with arrowheads in B-K. Scale bar in **A** = 20 μm for **A** and 7 μm for **B-K**.

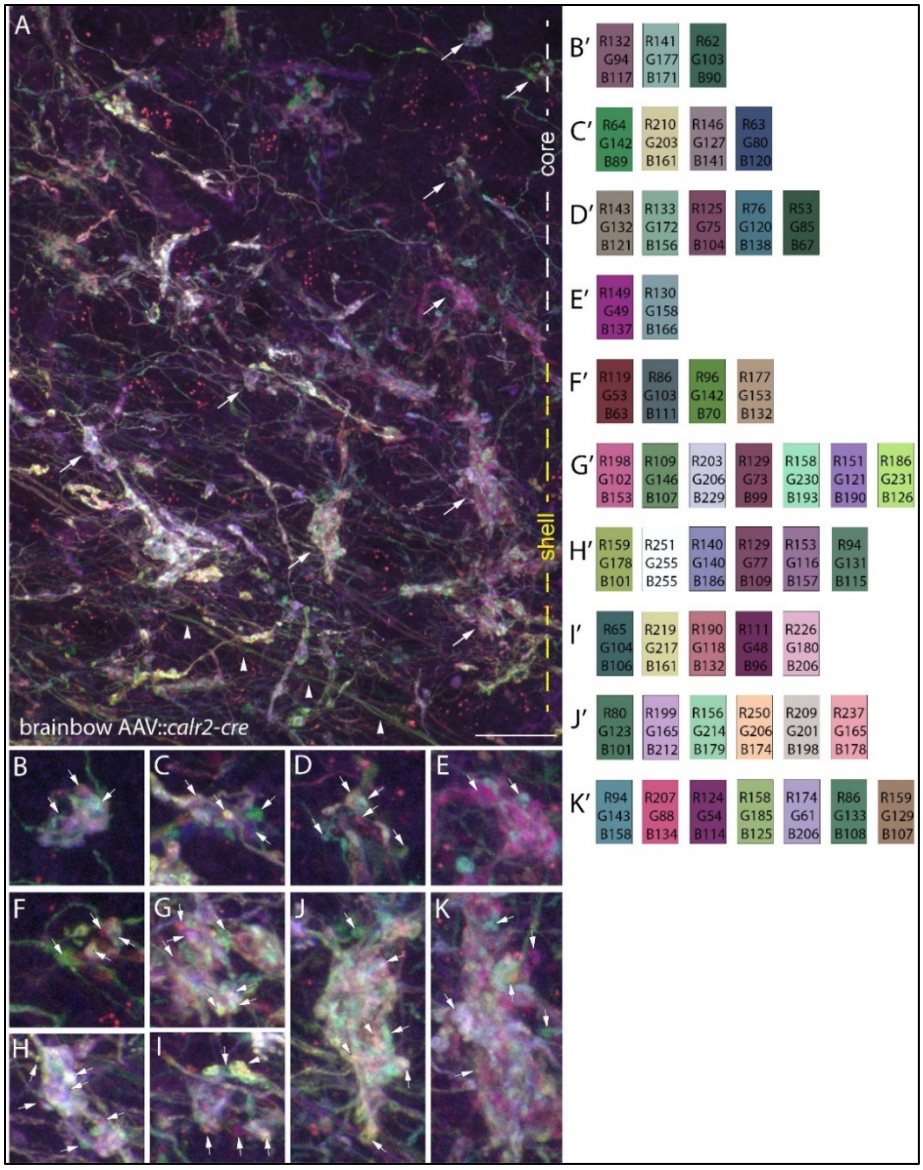
A
core
shell
brainbow AAV::calr2-cre
B
C
D
E
F
G
J
K
H
I
B′ R132 G94 B117 R141 G177 B171 R62 G103 B90
C′ R64 G142 B89 R210 G203 B161 R146 G127 B141 R63 G80 B120
D′ R143 G132 B121 R133 G172 B156 R125 G75 B104 R76 G120 B138 R53 G85 B67
E′ R149 G49 B137 R130 G158 B166
F′ R119 G53 B63 R86 G103 B111 R96 G142 B70 R177 G153 B132
G′ R198 G102 B153 R109 G146 B107 R203 G206 B229 R129 G73 B99 R158 G230 B193 R151 G121 B190 R186 G231 B126
H′ R159 G178 B101 R251 G255 B255 R140 G140 B186 R129 G77 B109 R153 G116 B157 R94 G131 B115
I′ R65 G104 B106 R219 G217 B161 R190 G118 B132 R111 G48 B96 R226 G180 B206
J′ R80 G123 B101 R199 G165 B212 R156 G214 B179 R250 G206 B174 R209 G201 B198 R237 G165 B178
K′ R94 G143 B158 R207 G88 B134 R124 G54 B114 R158 G185 B125 R174 G61 B206 R86 G133 B108 R159 G129 B107

Figure 2.3. Ultrastructural analysis and reconstruction of retinal axons contributing to "simple encapsulated" retinogeniculate synapses in dLGN.

A,B. SBFSEM images of two retinal terminals synapsing onto the same relay cell dendrite. **C.** 3D reconstruction of the 2 RGC terminal boutons from **A,B** converging on a single relay cell dendrite. **D,E.** SBFSEM images of two retinal terminals from the same RGC axon making synaptic contact with two distinct relay cell dendrites. **F.** 3D reconstruction of the retinal axon and relay cell dendrites from **D,E**. Scale bar in **B** = 1.5 µm for **A,B** and in **E** = 1.5 µm for **D,E**.

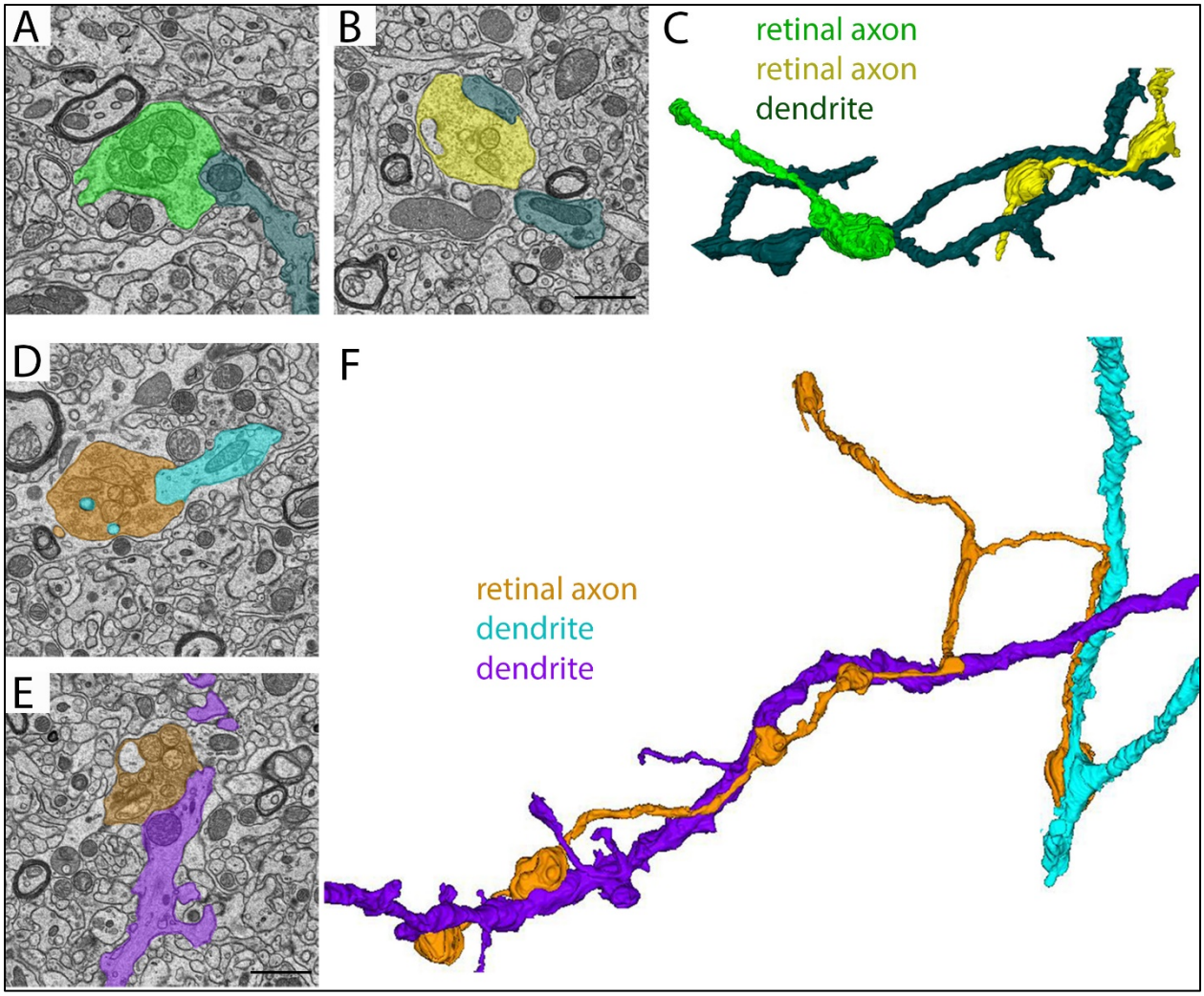
A
B
C
retinal axon
retinal axon
dendrite
D
E
F
retinal axon
dendrite
dendrite

Figure 2.4. Ultrastructural analysis and reconstruction of retinal axons contributing to "complex encapsulated" retinogeniculate synapses in dLGN.

A-D. SBFSEM images of 6 retinal terminals synapsing onto the same relay cell dendrite (pseudo-colored in bright green). **E**. Key indicates the types of cellular elements pseudo-colored in **A-D** and **F-H**. **F.** 3D reconstruction of all of the elements pseudo-colored in **A-D**. **G.** 3D reconstruction of 3 RGC axons, an inhibitory interneuron dendrite and the relay cell dendrite in **A-D. H.** 3D reconstruction of a single RGC axon and the relay cell dendrite in **A-D.** Arrow indicates a retinal bouton that makes synaptic contact with an element other that the relay cell dendrite pseudo-colored bright green. **I-K.** SBFSEM images of 14 retinal terminals synapsing onto the same relay cell dendrite (pseudo-colored in bright yellow). **L.** Key indicates the types of cellular elements pseudo-colored in **I-K** and **M-O**. **M.** 3D reconstruction of all of the elements pseudo-colored in **I-K**. **N.** 3D reconstruction of 3 RGC axons and the relay cell dendrite in **I-K. O.** 3D reconstruction of a single RGC axon and the relay cell dendrite in **I-K.** Arrow indicates a retinal bouton that makes synaptic contact with an element other that the relay cell dendrite pseudo-colored bright yellow. Scale bar in **D** = 1.5 μm for **A-D**. and in **K** = 1.5 μm for **I-K**.

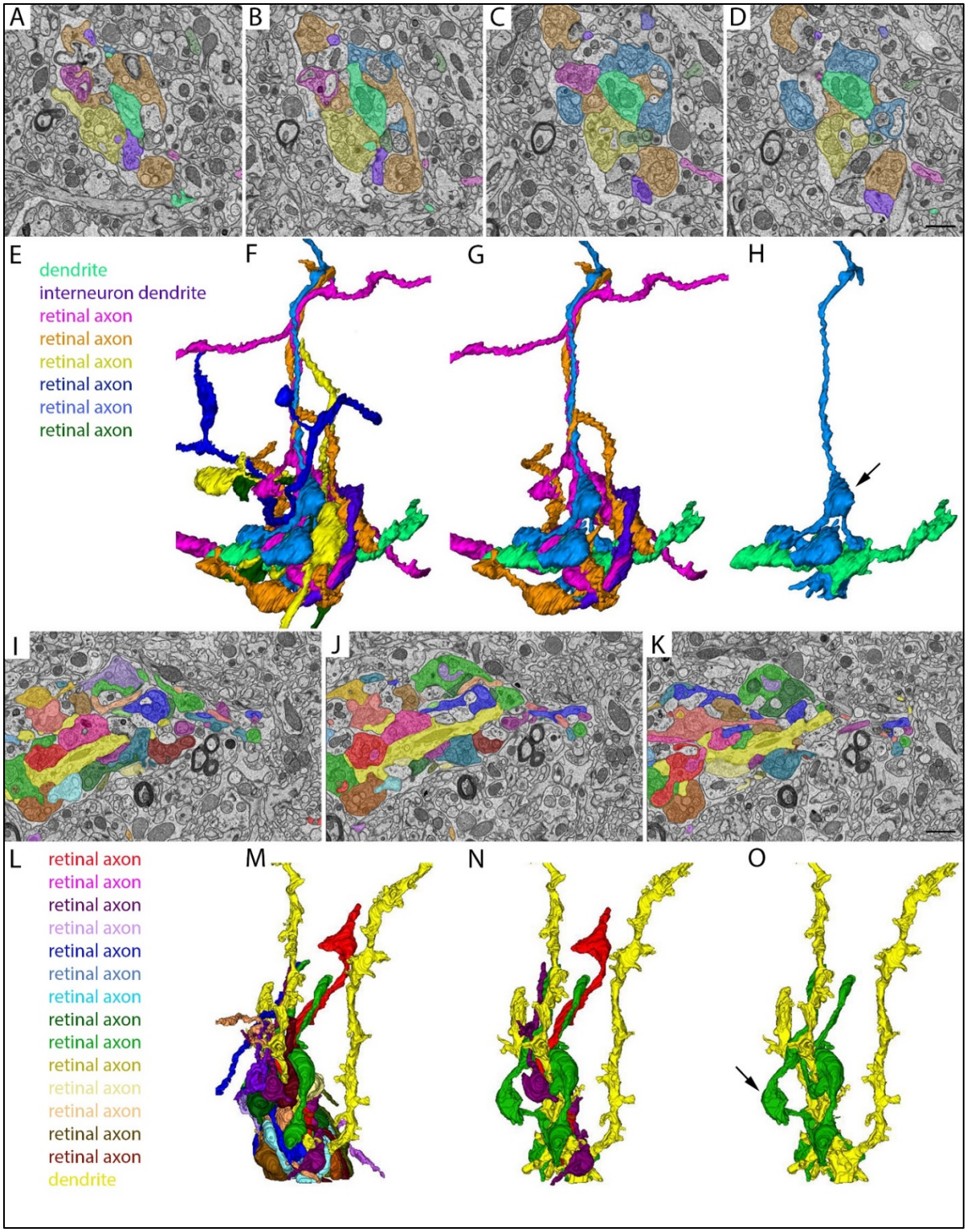
A
B
C
D
E
dendrite
interneuron dendrite
retinal axon
retinal axon
retinal axon
retinal axon
retinal axon
retinal axon
F
G
H
I
J
K
L
retinal axon
retinal axon
retinal axon
retinal axon
retinal axon
retinal axon
retinal axon
retinal axon
retinal axon
retinal axon
retinal axon
retinal axon
retinal axon
retinal axon
dendrite
M
N
O

Figure 2.5. Supplemental Figure 1

Supports the results shown in Figure 2 by revealing (with anterograde tracing, IHC and SBFSEM) that simple and complex retinal synapses are present in both the “core” and “shell” regions of dLGN.

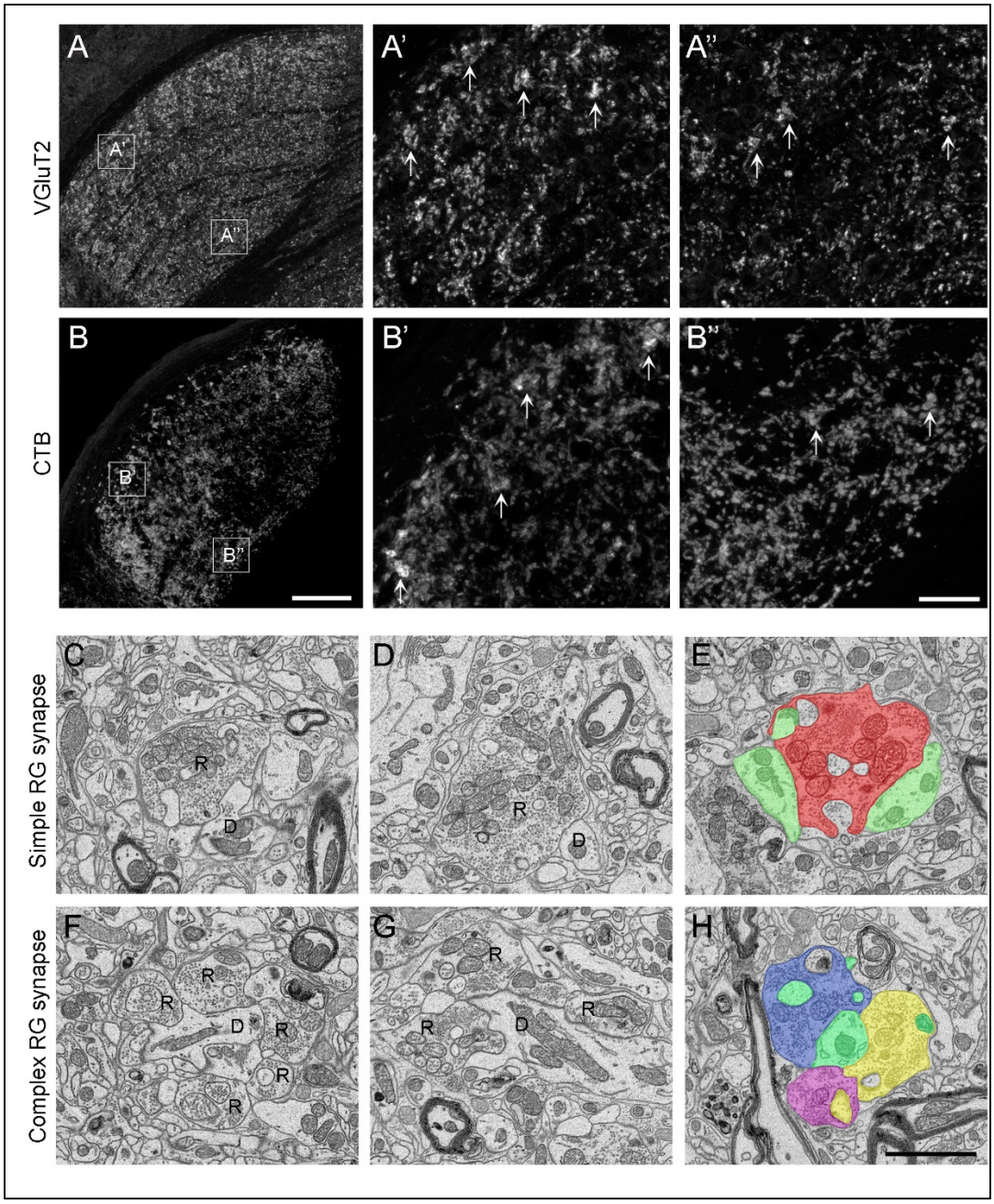
VGluT2
CTB
Simple RG synapse
Complex RG synapse
A
A'
A''
B
B'
B''
C
D
E
F
G
H
R
D

Figure 2.6. Supplemental Figure 2

Supports the results shown in Figures 3 and 4 by demonstrating non-pseudo-colored simple and complex retinogeniculate synapses in the shell of dLGN. These images demonstrate synaptic release sites and show statistically significant differences in the number of active zones, bouton diameter, and dendritic protrusions in these two types of synapses.

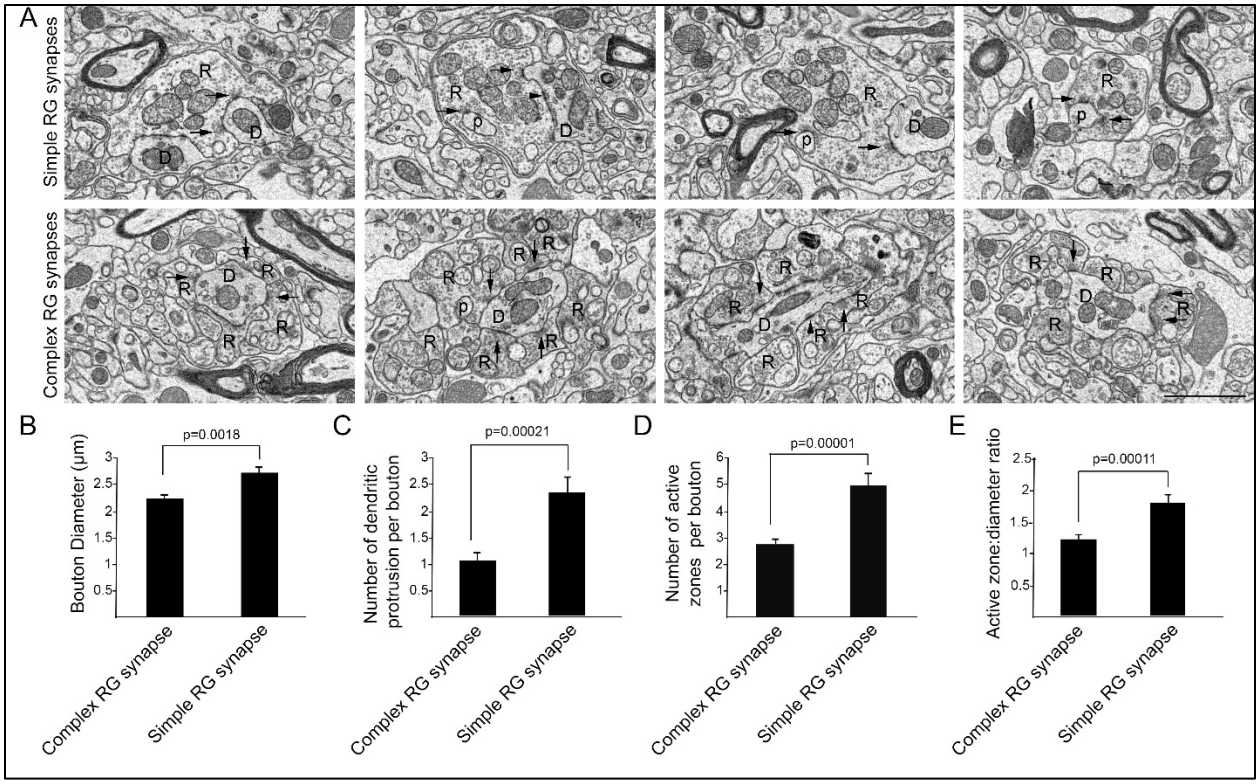
A
Simple RG synapses
Complex RG synapses
R
D
p
B
Bouton Diameter (µm)
p=0.0018
Complex RG synapse
Simple RG synapse
C
Number of dendritic protrusion per bouton
p=0.00021
D
Number of active zones per bouton
p=0.00001
E
Active zone:diameter ratio
p=0.00011

References

Bickford, M.E., Slusarczyk, A., Dilger, E.K., Krahe, T.E., Kucuk, C., and Guido, W. (2010). Synaptic development of the mouse dorsal lateral geniculate nucleus. The Journal of comparative neurology *518*, 622-635.

Budisantoso, T., Matsui, K., Kamasawa, N., Fukazawa, Y., and Shigemoto, R. (2012). Mechanisms underlying signal filtering at a multisynapse contact. J Neurosci *32*, 2357-2376.

Cai, D., Cohen, K.B., Luo, T., Lichtman, J.W., and Sanes, J.R. (2013). Improved tools for the Brainbow toolbox. Nature methods *10*, 540-547.

Cardona, A., Saalfeld, S., Schindelin, J., Arganda-Carreras, I., Preibisch, S., Longair, M., Tomancak, P., Hartenstein, V., and Douglas, R.J. (2012). TrakEM2 software for neural circuit reconstruction. PLoS One *7*, e38011.

Chen, C., and Regehr, W.G. (2000). Developmental remodeling of the retinogeniculate synapse. Neuron *28*, 955-966.

Cleland, B., and Lee, B. (1985). A comparison of visual responses of cat lateral geniculate nucleus neurones with those of ganglion cells afferent to them. The Journal of physiology *369*, 249-268.

Denk, W., and Horstmann, H. (2004). Serial block-face scanning electron microscopy to reconstruct three-dimensional tissue nanostructure. PLoS biology *2*, e329.

Dhande, O.S., Hua, E.W., Guh, E., Yeh, J., Bhatt, S., Zhang, Y., Ruthazer, E.S., Feller, M.B., and Crair, M.C. (2011). Development of single retinofugal axon arbors in normal and β2 knock-out mice. The Journal of Neuroscience *31*, 3384-3399.

Dhande, O.S., and Huberman, A.D. (2014). Retinal ganglion cell maps in the brain: implications for visual processing. Current opinion in neurobiology *24*, 133-142.

Guillery, R., and Scott, G. (1971). Observations on synaptic patterns in the dorsal lateral geniculate nucleus of the cat: the C laminae and the perikaryal synapses. Experimental brain research *12*, 184-203.

Hammer, S., Carrillo, G.L., Govindaiah, G., Monavarfeshani, A., Bircher, J.S., Su, J., Guido, W., and Fox, M.A. (2014). Nuclei-specific differences in nerve terminal distribution, morphology, and development in mouse visual thalamus. Neural development *9*, 1.

Hamos, J.E., Van Horn, S.C., Raczkowski, D., and Sherman, S.M. (1987). Synaptic circuits involving an individual retinogeniculate axon in the cat. Journal of Comparative Neurology *259*, 165-192.

Hong, Y.K., and Chen, C. (2011). Wiring and rewiring of the retinogeniculate synapse. Current opinion in neurobiology *21*, 228-237.

Hong, Y.K., Park, S., Litvina, E.Y., Morales, J., Sanes, J.R., and Chen, C. (2014). Refinement of the retinogeniculate synapse by bouton clustering. Neuron *84*, 332-339.

Hooks, B.M., and Chen, C. (2006). Distinct roles for spontaneous and visual activity in remodeling of the retinogeniculate synapse. Neuron *52*, 281-291.

Jaubert-Miazza, L., Green, E., Lo, F., Bui, K., Mills, J., and Guido, W. (2005). Structural and functional composition of the developing retinogeniculate pathway in the mouse. Visual neuroscience *22*, 661.

Jones, E., and Powell, T. (1969). Electron microscopy of synaptic glomeruli in the thalamic relay nuclei of the cat. Proceedings of the Royal Society of London B: Biological Sciences *172*, 153-171.

Krahe, T.E., El-Danaf, R.N., Dilger, E.K., Henderson, S.C., and Guido, W. (2011). Morphologically distinct classes of relay cells exhibit regional preferences in the dorsal lateral geniculate nucleus of the mouse. The Journal of Neuroscience *31*, 17437-17448.

Livet, J., Weissman, T.A., Kang, H., Draft, R.W., Lu, J., Bennis, R.A., Sanes, J.R., and Lichtman, J.W. (2007). Transgenic strategies for combinatorial expression of fluorescent proteins in the nervous system. Nature *450*, 56-62.

Lund, R., and Cunningham, T. (1972). Aspects of synaptic and laminar organization of the mammalian lateral geniculate body. Invest Ophthalmol *11*, 291-302.

Pan, Y.A., Freundlich, T., Weissman, T.A., Schoppik, D., Wang, X.C., Zimmerman, S., Ciruna, B., Sanes, J.R., Lichtman, J.W., and Schier, A.F. (2013). Zebrabow: multispectral cell labeling for cell tracing and lineage analysis in zebrafish. Development *140*, 2835-2846.

Robles, E., Filosa, A., and Baier, H. (2013). Precise lamination of retinal axons generates multiple parallel input pathways in the tectum. J Neurosci *33*, 5027-5039.

Sincich, L.C., Adams, D.L., Economides, J.R., and Horton, J.C. (2007). Transmission of spike trains at the retinogeniculate synapse. The Journal of Neuroscience *27*, 2683-2692.

Squire, L., Berg, D., Bloom, F.E., Du Lac, S., Ghosh, A., and Spitzer, N.C. (2012). Fundamental neuroscience (Academic Press).

Su, J., Haner, C.V., Imbery, T.E., Brooks, J.M., Morhardt, D.R., Gorse, K., Guido, W., and Fox, M.A. (2011). Reelin is required for class-specific retinogeniculate targeting. The Journal of Neuroscience *31*, 575-586.

Taniguchi, H., He, M., Wu, P., Kim, S., Paik, R., Sugino, K., Kvitsani, D., Fu, Y., Lu, J., and Lin, Y. (2011). A resource of Cre driver lines for genetic targeting of GABAergic neurons in cerebral cortex. Neuron *71*, 995-1013.

Usrey, W.M., Reppas, J.B., and Reid, R.C. (1999). Specificity and strength of retinogeniculate connections. Journal of Neurophysiology *82*, 3527-3540.

Zhu, Y., Xu, J., Hauswirth, W.W., and DeVries, S.H. (2014). Genetically targeted binary labeling of retinal neurons. J Neurosci *34*, 7845-7861.

3. LRRTM1 underlies synaptic convergence in visual thalamus

Aboozar Monavarfeshani[1,2], Gail Stanton[1,3], Jonathan Van Name[1], Kaiwen Su[1], William A. Mills III[1,4], Kenya Swilling[1], Alicia Kerr[1,4], Jianmin Su[1], Michael A. Fox[1,2,3]

[1]Developmental and Translational Neurobiology Center, Virginia Tech Carilion Research Institute, 2 Riverside Circle, Roanoke, VA 24016

[2]Department of Biological Sciences, Virginia Tech, Blacksburg, VA 24061

[3]Virginia Tech Carilion School of Medicine, Roanoke, VA

[4]Translational Biology, Medicine, and Health Graduate Program, Virginia Tech, Blacksburg, VA

Lead contact and corresponding author:

Michael A. Fox

Director, Developmental and Translational Neurobiology Center

Virginia Tech Carilion Research Institute

2 Riverside Circle

Roanoke, VA 24016

mafox1@vtc.vt.edu

3.1. Abstract

It has long been thought that the mammalian visual system is organized into parallel pathways, with incoming visual signals being parsed in the retina based on feature (e.g. color, contrast and motion) and then transmitted to the brain in unmixed, feature-specific channels. To faithfully convey feature-specific information from retina to cortex, thalamic relay cells must receive inputs from only a small number of functionally similar retinal ganglion cells. However, recent studies challenged this by revealing substantial levels of retinal convergence onto relay cells. Here, we sought to identify mechanisms responsible for the assembly of such convergence. Using an unbiased transcriptomics approach and targeted mutant mice, we discovered a critical role for the synaptic adhesion molecule Leucine Rich Repeat Transmembrane Neuronal 1 (LRRTM1) in the emergence of retinothalamic convergence. Importantly, LRRTM1 mutant mice display impairment in visual behaviors, suggesting a functional role of retinothalamic convergence in vision.

3.2. Introduction

Over thirty classes of functionally and morphologically distinct retinal ganglion cells (RGCs) exist in mammals, each responsible for conveying different features of the visual world and each with unique projections to retinorecipient nuclei within the brain (Baden et al., 2016; Martersteck et al., 2017; Sanes and Masland, 2015). As a group, RGCs innervate over 40 retinorecipient brain regions (Monavarfeshani et al., 2017; Morin and Studholme, 2014). However, only a subset of RGCs (~50%) innervate relay cells in the visual thalamus (i.e. the dorsal lateral geniculate nucleus [dLGN]) and provide the principle pathway for image-forming visual information to reach the cerebral cortex (Dhande et al., 2015; Seabrook et al., 2017) (Fig. 1A). The recent development of transgenic tools to label these classes of RGCs has revealed that their inputs are segregated into distinct class-specific sublamina within visual thalamus (Hong and Chen, 2011; Huberman et al., 2008a; Huberman et al., 2009; Kay et al., 2011; Kim et al., 2010; Kim et al., 2008; Monavarfeshani et al., 2017), supporting the longstanding belief that different features of the visual field are transmitted through the subcortical visual system in parallel, unmixed anatomical channels (Cruz-Martín et al., 2014; Dhande et al., 2015).

In addition to being segregated based on class, retinal projections in dLGN are unique in that they form structurally and functionally distinct synapses compared to their counterparts in other retinorecipient nuclei (Hammer et al., 2014). RTs in dLGN are prototypic "driver" inputs which are dramatically large (compared to adjacent non-retinal inputs) and are capable of generating strong excitatory postsynaptic responses in thalamic relay cells. Until recently, it was thought that the level of convergence of retinal inputs onto these relay cells was exceptionally low with only a few (1-5) RGCs innervating each relay cell (Chen and Regehr, 2000; Cleland et al., 1971; Cleland and Lee, 1985; Hamos et al., 1987; Jaubert-Miazza et al., 2005; Mastronarde,

1992; Rathbun et al., 2016; Rathbun et al., 2010; Sincich et al., 2007; Usrey et al., 1999; Weyand, 2016; Yeh et al., 2009). This low level of retinal convergence allows relay cells to faithfully transfer information from RGCs to visual cortex in an unaltered form, also adding support to the notion that information regarding different features of the visual field flow through the thalamus in parallel channels.

Recently, however, a series of anatomical studies in mice have challenged the concept of feature-specific, parallel visual channels by revealing a level of retinal convergence onto relay cells that is more than an order of magnitude higher than previously described (Hammer et al., 2015; Howarth et al., 2014; Morgan et al., 2016; Rompani et al., 2017). Not only is there a high level of retinogeniculate (RG) convergence in mice, but some relay cells receive input from many functionally distinct classes of RGCs (Rompani et al., 2017) raising new questions about the role of thalamus in processing visual information before it reaches visual cortex.

Part of this newly appreciated retinal convergence stems from a set of unique RG synapses (termed complex RG synapses) that contain numerous retinal axons whose terminals aggregate on shared regions of relay cell dendrites (Hammer et al., 2015; Lund and Cunningham, 1972; Morgan et al., 2016). Complex RG synapses have been reported in both rodents and higher mammals (Campbell and Frost, 1987; Guillery and Scott, 1971; Jones and Powell, 1969; Lund and Cunningham, 1972; So et al., 1985; Wilson et al., 1984). Similar to the more classical simple RG synapses (which contain a single retinal terminal on a given portion of a relay cell dendrite), these complex RG synapses are absent from other retinorecipient regions of brain (Hammer et al., 2014) (Fig. S1). Since branches of dLGN-projecting RGCs also innervate other retinorecipient nuclei (Dhande et al., 2015), we interpret this to suggest that target-derived

signals must be generated in dLGN to pattern the unique transformation of retinal axons into simple and complex RG synapses.

In the present study, we sought to identify such target-derived signals. Using next generation sequencing, we discovered that relay cells in dLGN (but not principal neurons in other retinorecipient nuclei) express Leucine Rich Repeat Transmembrane Neuronal 1 (LRRTM1), a known inducer of excitatory synaptogenesis (de Wit et al., 2009; Linhoff et al., 2009). Genetic deletion of LRRTM1 led to a loss of complex RG synapses and thus reduced retinal convergence in visual thalamus. While mutants lacking LRRTM1 and complex RG synapse exhibit normal visual acuity and contrast sensitivity, they display impaired performance in a set of more complex visual tasks that require processing multiple distinct elements of the visual field. Taken together, these results not only identify a novel mechanism underlying the establishment of retinal convergence in visual thalamus, but importantly provide the first insight into the functional significance of complex RG synapses (and, possibly, retinal convergence) in vision.

3.3. Results

3.3.1. Unique transformation of retinal terminals in dLGN coincides with eye-opening

To examine the emergence of the unique morphology of retinal terminals in developing mouse dLGN, two approaches were applied: retinal terminals were either immunolabeled with antibodies against vesicular glutamate transporter 2 (VGluT2, a synaptic vesicular component only present in retinal terminals in visual thalamus) (Hammer et al., 2014; Land et al., 2004), or were anterogradely labeled by intraocular injection of fluorescent-conjugated Cholera Toxin B (CTB) (Muscat et al., 2003) (Fig. 1B-1H and S1A-S1H). Shortly after their initial formation (P3-

P8), VGluT2- or CTB-labeled terminals appeared similar in size and morphology in dLGN and the adjacent retinorecipient ventral lateral geniculate nucleus (vLGN). However, by eye-opening (P12-P14), terminals in dLGN underwent significant enlargement compared to those in vLGN and other (Hammer et al., 2014) retinorecipient nuclei (Fig. 1B-1H and S1A-S1H). The unique developmental transformation of retinal terminals in dLGN at eye-opening (rather than at their initial formation), suggested that this was not the result of purely cell intrinsic mechanisms in dLGN-projecting classes of RGCs.

To test this hypothesis we assessed retinal terminals generated by a single class of ON-OFF direction-selective RGCs whose axons branch to innervate both dLGN and superior colliculus (SC) (Dhande et al., 2015; Kim et al., 2010). This class of RGC is specifically labeled in *hb9-gfp* mice (Trenholm et al., 2011). Despite originating from branches of individual retinal axons, those terminals present in dLGN were dramatically larger than those in SC (Fig. 1I). These data suggest that target-derived cues are generated in dLGN around the time of eye-opening to pattern the transformation of retinal terminals.

The approaches described above do not provide the resolution required to differentiate simple and complex RG synapses, therefore, we used serial block-face scanning electron microscopy (SBFSEM) to identify whether both simple and complex RG synapses emerged at eye-opening. While our SBFSEM ultrastructural analysis revealed the presence of both simple and complex RG synapses shortly after eye-opening (P14) we were only able to identify simple-like RG synapses in the developing dLGN (P8) (Fig. 1J). Moreover, we delivered brainbow AAVs (Fig. 1K) intraocularly in *calb2-cre* mice (in which a large proportion of RGCs express Cre recombinase) to generate multi-colored RGCs and assess the development of complex RG synapses (Hammer et al., 2015). Similar to SBFSEM analysis, brainbow AAV-labeling failed to

detect clusters of retinal terminals at P8 (Fig. 1L), but clearly revealed clusters of retinal terminals originating from distinct RGCs as early as P10 and P14 (Fig. 1M and 1N). Thus, around eye-opening, dLGN-specific molecular mechanisms must emerge to induce the unique transformation of both simple and complex RG synapses.

3.3.2. Identification of target-derived synaptic organizing molecules in dLGN

To identify target-derived synaptic organizers present at eye-opening in dLGN (but not other retinorecipient regions), we performed next-generation transcriptome analysis of developing mouse visual thalamus (Fig. 2A). We assessed four different developmental time points, two before eye-opening (P3 and P8), and two at (P12) or after (P25) eye-opening (Fig. 1). Comparing gene expression profiles in both dLGN and vLGN revealed hundreds of differentially and developmentally expressed mRNAs (Fig. 2B). We focused our attention on a small subset of genes that were significantly enriched in dLGN (compared to vLGN) and whose highest expression coincided with eye-opening and the emergence of simple and complex RG synapses. Two genes with well-established roles in inducing excitatory synapses fit those criteria: *lrrtm1* and *neuritin 1* (*nrn1*) (Fig. 2C-2E) (Javaherian and Cline, 2005; Linhoff et al., 2009). We confirmed the enrichment of these genes at eye-opening in dLGN (but not vLGN) by qPCR, *in situ* hybridization and western blot (Fig. 2F-2I, 3A-3D and S2A-S2C). In addition to their low expression level in vLGN, it is important to point out that *lrrtm1* and *nrn1* mRNAs were either absent or only weakly expressed in other retinorecipient nuclei, such as the SC and suprachiasmatic nucleus (SCN) (Fig. 3E, S2D and S2E). There were, however, significant differences in the distribution of *lrrtm1* and *nrn1* mRNAs in other regions of the visual system. *Lrrtm1* was not generated by RGCs (although it was expressed in the INL) or by many cells in

primary visual cortex (vCTX) (Fig. 3E and 3F), whereas *nrn1* was robustly expressed by both RGCs and by cells in vCTX (Fig. 3E and 3F) (see also Fujino et al., 2008; Nedivi, 1998).

Finally, we sought to address the cell-specific expression of *lrrtm1* and *nrn1* in visual thalamus. Since *lrrtm1* encodes a transmembrane cell adhesion molecule and *nrn1* encodes a GPI-linked membrane associated extracellular molecules (Linhoff et al., 2009; Naeve et al., 1997), we assumed dLGN relay cells must generate these molecules for them to act post-synaptically at RG synapses. We combined *in situ* hybridization analysis using riboprobes against these two genes with molecular and genetic approaches to label different cell types in dLGN. First, we demonstrated that both *lrrtm1* and *nrn1* mRNAs are generated by neurons and not glia since they were co-expressed by *syt1*-expressing neurons but not by Iba1-expressing microglia or GFP-labeled astrocytes in *aldh1l1-gfp* mice (Fig. 4A-4F). Next, to differentiate which types of neurons generate these synaptogenic cues, we assessed *lrrtm1* and *nrn1* mRNA expression in glutamate decarboxylase (GAD67)-expressing inhibitory interneurons and in *crh-cre::tdt* transgenic mice in which excitatory thalamocortical relay cells are fluorescently labeled (Taniguchi et al., 2011). Results revealed *lrrtm1* and *nrn1* are exclusively produced by dLGN relay cells (Fig. 4G-4J). Based on their developmental and cell-specific expression, these molecules therefore represented prime candidates to influence the development of simple and complex RG synapses.

3.3.3. LRRTM1 is required for the development of complex RG synapses

Previous studies have reported roles for both LRRTM1 and NRN1 (also called Candidate Plasticity Gene 15, CPG15) in inducing the formation and maturation of excitatory synapses (Cantallops et al., 2000; Ko et al., 2011; Linhoff et al., 2009; Nedivi, 1998; Soler-Llavina et al.,

2011). In addition, NRN1 contributes to the development and maturation of retinal arbors (Cantallops et al., 2000). To test whether these molecules are necessary for the development of retinal terminals, we assessed the morphology of retinal terminals in dLGN of mice lacking LRRTM1 (Linhoff et al., 2009) or NRN1 (Fujino et al., 2011) using VGluT2 immunostaining and CTB anterograde labeling. These studies revealed a significant decrease in the number of large $VGluT2^{+}$ and CTB^{+} puncta in dLGN of *lrrtm1*$^{-/-}$ mice at and after eye-opening (Fig. 5A-5C, S3A), suggesting a role for this molecule in the maturation and/or refinement of RG circuitry. Retinal terminals in neonatal dLGN (i.e. before eye-opening) or in vLGN were not affected by the loss of LRRTM1 (Fig. 5A-5E and S3B). Since retinal projections account for only a small proportion (5-10%) of all projections innervating relay cells residing in dLGN (Monavarfeshani et al., 2017), we also assessed whether the loss of LRRTM1 altered other types of terminals in dLGN. None of the non-retinal inputs examined appeared affected in *lrrtm1*$^{-/-}$ mutant mice (Fig. S3C). Similar analysis in *nrn1*$^{-/-}$ mutants failed to identify developmental deficits in the density, size or distribution of retinal terminal in dLGN (Fig. S4A and S4B).

As described earlier, an important limitation of these techniques is that they cannot differentiate simple or complex RG synapses. It was therefore unclear whether individual retinal terminals were smaller in *lrrtm1*$^{-/-}$ mice, or clusters of retinal terminals were absent in these mutants. To overcome this technical limitation, we employed both SBFSEM and multicolor brainbow-AAV labeling of retinal axons in dLGN of *lrrtm1*$^{-/-}$ mutant and control mice. In SBFSEM, retinal terminals were distinguished from all other synaptic terminals by their round vesicles and pale mitochondria (Bickford et al., 2010; Hammer et al., 2014; Rafols and Valverde, 1973) and were traced throughout the entire volume of the imaged tissues. In total, 534 retinal terminals were analyzed in *lrrtm1*$^{-/-}$ mice and 646 in controls (n = 3 mice per genotypes). While

only a small fraction (<10%) of all retinal terminals were categorized as simple RG synapses in controls, the majority (about 63%) of retinal terminals fell into this category in *lrrtm1*$^{-/-}$ mutant dLGN (Fig. 6A-6C, S5A and S5B). Conversely, only 37% of RG synapses in mutants were classified as complex versus 90% in controls (Fig. 6C). Similarly, analysis of multicolor-labeled retinal terminals by brainbow AAVs showed fewer and smaller clustered retinal terminals in dLGN of lrrtm1$^{-/-}$ mice (Fig. 6E-6G). The majority of retinal terminal clusters in mutants (82.6%) contained less than 4 distinct inputs (i.e. colors). In contrast, the majority (80%) of clusters in controls contained more than 4 distinct retinal terminals.

Thus, there was a significant loss of complex RG synapse in the absence of LRRTM1. In fact, these numbers underrepresent the loss of retinal convergence in mutants, since our criteria for defining a complex RG synapse requires the presence of just two distinct retinal inputs. Not only was there a significant loss of complex RG synapses in mutants, but those complex synapses that remained contained significantly fewer retinal terminals. In control dLGN about 86% of complex RG synapses contained between 4-14 retinal terminals, whereas the majority of complex RG synapses in *lrrtm1*$^{-/-}$ mutants contained only 2 or 3 inputs (Fig. 6C). While the reduced number of complex RG synapses (and retinal inputs at the few persisting complex RG synapses) might be caused by fewer retinal axons in mutants, we failed to observe a significant loss of RGC axons in the optic nerves of *lrrtm1*$^{-/-}$ mice (Fig. S5D-S5H). Surprisingly, we also observed an increase in individual retinal terminal size in both simple and complex RG synapses in *lrrtm1*$^{-/-}$ mice (Fig. 6D).

3.3.4. Impaired visual behaviors in mice lacking LRRTM1

The functional consequence of LRRTM1 deletion and the loss of complex RG synapses was assessed by a two-alternative forced swim test (Huberman and Niell, 2011; Prusky et al., 2000; Wong and Brown, 2006). In this test, mice learn to associate a visual cue with a hidden platform that allows them to escape the water (Fig. 7A). In order to confirm the necessity of vision for performing this task we asked whether *math5*$^{-/-}$ mice, which are genetically blind (Wang et al., 2001), can detect the positive visual cue and find the hidden platform. *Math5*$^{-/-}$ mice were unable to perform this task, demonstrating the importance of vision in this assay (Fig. S6A).

To explore the role of LRRTM1 (and complex RG synapses) in vision, mice were trained for 8 days to detect a vertical grating (0.17 cycle per degree, cpd) on S+ monitor positioned above the hidden platform, compared with a gray screen or a horizontal grating display on the S- monitor (Fig. 7A). Mice that exceeded 70% accuracy in locating the hidden platform were considered capable of detecting and discriminating the visual cues (Prusky et al., 2000). *Lrrtm1*$^{-/-}$ mutants and controls displayed equal abilities to detect the vertical grating (positive visual cue) against the gray screen or horizontal grating at the end of training, although the initial learning phase of *lrrtm1*$^{-/-}$ mice was moderately impaired (Fig. 7B and 7C), which is in agreement with previous findings showing a delayed response of *lrrtm1*$^{-/-}$ mutant mice to new environment (Takashima et al., 2011). In order to demonstrate that control or mutant mice were not capable of detecting the hidden platform itself (instead of associating it to the visual cue), we trained control and mutant mice (for 8 days) to associate the positive visual cue (S+) (with near 100% accuracy) with the platform. We then moved the platform below the negative (S-) visual cue and tested each mouse for 10 trials in day 9. Mutants and controls swam toward the positive visual cue that lacked the rescue platform, confirming they could not detect the hidden platform (Fig. S6B).

By changing the frequency of the vertical bars, we next tested visual acuity in *lrrtm1*$^{-/-}$ mutants. Results indicate that acuity was similar between mutants and controls, both falling below the 70% correct criteria at spatial frequencies above 0.57 cpd. There was a statistically significant difference between *lrrtm1*$^{-/-}$ and control mice at a single spatial frequency (0.62 cpd), however, at this frequency both performed poorly in the task (Fig. 7D). Next, we altered the contrast of the vertical grating bars rather than the spatial frequency or orientation. Similarly, *lrrtm1*$^{-/-}$ mutants failed to show significant differences compared to wild type mice (Fig. 7E). Taken together these results suggest *lrrtm1*$^{-/-}$ mutants do not exhibit deficits in visual acuity, simple pattern recognition or contrast sensitivity.

Next, we exposed mice to more complex visual tasks in which multiple features of the visual scene were altered at once. There are conflicting data indicating spatial memory deficits in mice lacking LRRTM1 (Takashima et al., 2011; Voikar et al., 2013). For this reason, we adjusted our experimental design to rule out the influence of spatial memory impairment on performing task performance. After 8 days of training, pattern discrimination was tested while also increasing the spatial frequency or decreasing the contrast of both vertical and horizontal gratings. After each day of testing, we checked the ability of mice to perform the initial, standard discrimination task (i.e. to discriminating vertical and horizontal grating with 0.17 cpd and 100% contrast). Throughout the experiments, *lrrtm1*$^{-/-}$ mice failed to show any signs of memory deficits in this task. Interestingly, while control mice were able to discriminate vertical and horizontal bars at a spatial frequency of 0.32 cpd, *lrrtm1*$^{-/-}$ mice performance dropped significantly under the 70% threshold during these more complex tasks (Fig. 7F). Similarly, at lower contrast (i.e. 25% and 10%) mutant mice lacked the sensitivity to discriminate vertical and horizontal grating patterns (Fig. 7G). As another set of controls, we repeated these behaviors task with *nrn1*$^{-/-}$

mutants and found no deficit in their performance in either the simple or complex visual tasks (Fig. S6C-S6H). Taken together, these results indicate that mice lacking LRRTM1 and complex RG synapses exhibit abnormalities in performing more complex visual tasks.

3.4. Discussion

For decades it has been thought that the mammalian visual system was assembled into a number of parallel pathways, each conveying a specific feature of the visual field (e.g. contrast, color, motion, etc.) in a separate channel from the retina to the thalamus and then to primary visual areas of the cerebral cortex. An important characteristic of such parallel pathways is that the thalamus must act as a relay that passes on feature-specific visual information to the cerebral cortex without mixing these different channels of information. Thus, relay cells in the visual thalamus must receive input from a small number of retinal neurons, all of which belong to the same subclass of RGCs. Electrophysiological data has largely supported this hypothesis by demonstrating that few retinal axons (1-5) innervate each relay cell in the mature brain (Chen and Regehr, 2000; Cleland et al., 1971; Cleland and Lee, 1985; Hong and Chen, 2011; Hooks and Chen, 2006; Jaubert-Miazza et al., 2005; Mastronarde, 1992; Rathbun et al., 2016; Rathbun et al., 2010; Usrey et al., 1999; Weyand, 2016; Yeh et al., 2009). Recently, however, a series of studies have challenged this notion by demonstrating a shockingly high level of convergence onto thalamic relay cells, with some relay cells receiving inputs from as many as 90 RGCs (Hammer et al., 2015; Hamos et al., 1987; Morgan et al., 2016; Rompani et al., 2017). Not only do retinal inputs from multiple classes of RGCs innervate single relay cells (Rompani et al., 2017), but nerve terminals from more than a dozen distinct RGCs clusters at shared synaptic sites on dendrites of individual relay cell (Hammer et al., 2015; Morgan et al., 2016). Interestingly,

using ontogenetic stimulation of retinal terminals expressing channelrhodopsin (ChR2) Litvina and Chen (Litvina and Chen, 2017b) have recently confirmed a higher level functional retinal convergence onto dLGN relay cells. Here, we sought to understand the molecular mechanisms underlying this newly appreciated convergence in visual thalamus. Using an unbiased screen, we identified LRRTM1 as a target-derived cue necessary for the formation of retinal convergence onto dLGN relay cells. Analysis in LRRTM1-deficient mice revealed that the lack of this synaptic adhesion molecule and complex RG synapses led to impaired visual function.

3.4.1. LRRTM1 as a target-derived synaptic organizer in visual thalamus

LRRTMs are transmembrane proteins that act as transsynaptic signals to trigger excitatory synaptogenesis (de Wit and Ghosh, 2014; de Wit et al., 2009; Linhoff et al., 2009; Um et al., 2016). When present in the postsynaptic membrane, LRRTM1 binds to the extracellular domain of neurexins to induce presynaptic differentiation in contacting axons (Linhoff et al., 2009; Siddiqui et al., 2010). In visual thalamus, LRRTM1 is specifically expressed by relay cells (and not other cells) and its transsynaptic partners, neurexins, are generated by RGCs (Fig. S7) (Sajgo et al., 2017; Shigeoka et al., 2016). Therefore, based on our results, we hypothesized that LRRTM1-neurexin interactions are critical for the formation of complex RG synapses. Although the necessity of neurexins in retinogeniculate connectivity has yet to be thoroughly examined, the loss of CASK, a MAGUK protein necessary for trafficking neurexins to the presynaptic membrane, leads to abnormal retinogeniculate connectivity and optic nerve hypoplasia (LaConte et al., 2016; Liang et al., 2017; Moog et al., 2011; Srivastava et al., 2016).

It is important to point out that neurexins have other postsynaptic partners expressed in visual thalamus, including neuroligins and other LRRTMs (Fig. S7) (Laurén et al., 2003;

Varoqueaux et al., 2006), each capable of inducing excitatory synaptogenesis elsewhere in the brain or *in vitro* (Craig et al., 2006; Fox and Umemori, 2006; Ko et al., 2009a; Siddiqui et al., 2010). The presence of LRRTM1, other LRRTMs, and neuroligins in dLGN raises an interesting possibility that simple and complex RG synapse may be assembled through different postsynaptic interactions with neurexins. As such, astrocytes may also contribute to the signals that regulate simple or complex RG synapses. Retinal terminals in simple RG synapse are ensheathed by astrocytic processes (Bickford et al., 2010; Hammer et al., 2014) and these astrocytes are known to produce extracellular factors capable of bridging neurexin-neuroligin interactions to facilitate excitatory synaptogenesis (Kucukdereli et al., 2011; Singh et al., 2016).

The presence of multiple postsynaptic neurexins partners in dLGN also raises the possibility that their abundance (or overabundance) may prevent some level of activity dependent refinement in dLGN. Overexpression of different combinations of neurexin-binding partners in postsynaptic neurons has been shown to impair synapse elimination *in vitro* (Ko et al., 2011). The emergence of complex RG synapse at eye-opening may therefore represent synapses with an overabundance of neurexin-binding receptors, in which strong trans-synaptic adhesion prevent complete activity-dependent RG refinement. While certainly possible, we see this as unlikely given the dramatic refinement of retinal arbors around eye-opening in mice and since this RG refinement itself gives rise to retinal bouton clustering (Dhande et al., 2011; Hong et al., 2014).

3.4.2. Retinal convergence: artifact or by design?

The discovery of an extraordinary level of retinal convergence on mouse relay cells has left the field pondering whether such convergence is an artifact of impaired refinement (as

described above) or whether there is functional significance to such “fuzzy” connectivity (as one group has termed this retinogeniculate convergence) (Morgan et al., 2016). It is easy to discount the importance of retinal convergence onto relay cells and the role that complex RG synapses may play in vision, since many groups (including our own (Hammer et al., 2014)) have demonstrated that relay cells receive a very small number of strong, functional inputs from the retina (Chen and Regehr, 2000; Hooks and Chen, 2006; Jaubert-Miazza et al., 2005; Litvina and Chen, 2017b). Many of the techniques used to identify high levels of retinogeniculate convergence in mice have been anatomical in nature (e.g. ultrastructural analysis, anterograde multicolor labeling of RGCs and retrograde trans-synaptic tracing) (Hammer et al., 2015; Morgan et al., 2016; Rompani et al., 2017), leading to the possibility that “form” does not fit “function” in mouse visual thalamus. Recent optogenetic analysis of the RG circuit in mice has revealed a substantially higher level of functional retinal convergence on rely cells, however the strength of these inputs widely varies (Litvina and Chen, 2017b). Functional roles for weak RG synapses remain unclear.

In the present study, we took advantage of the loss of complex RG synapses in *lrrtm1*$^{-/-}$ mice to begin to shed light on the functional significance of retinal convergence on thalamic relay cells. While the ability of *lrrtm1*$^{-/-}$ mice to perform tasks with simple visual cues appeared unaltered compared with controls, they performed poorly on tasks where more than one feature of the visual scenes was altered at once. Although these mice lack LRRTM1 globally, such deficits are likely the direct result of impaired RG circuitry for several reasons. First, LRRTM1 is largely absent from retina and visual cortex, sites whose function are required for the performance of these visual tasks. Second, global deletion of LRRTM1 failed to result in synaptic or cytoarchitectural changes in other brain regions that process visual information (Fig.

S7). For these reasons, we believe that results presented here provide the first clues that complex RG synapses (and retinal convergence) are not functionally insignificant artifacts of impaired or incomplete activity dependent refinement, but rather are an important component of processing and relaying visual information from the retina to visual cortex.

3.5. Materials and methods

3.5.1. Animals

CD1 and C57/BL6 mice were obtained from Charles River (Wilmington, MA) or Harlan (Indianapolis, IN). Lrrtm1$^{-/-}$ mice were obtained from MMRRC (stock # 031619-UCD), Nrn1$^{-/-}$ (stock # 018402), Calb2-Cre (stock # 010774) and Rosa-stop-tdT mice (stock # 007905) were all obtained from Jackson Laboratory. Crh-Cre (stock # 030850-UCD) and Aldh1l1-EGFP (stock # 011015-UCD) mice were obtained from W. Guido (University of Louisville) and S. Robel (Virginia Tech), respectively. Math5$^{-/-}$ (stock# 042298-UCD) were obtained from S. W. Wang and were described previously (Wang et al., 2001). Mice were housed in a 12 hr dark/light cycle and had *ad libitum* access to food and water. All experiments were performed in compliance with National Institutes of Health (NIH) guidelines and protocols and were approved by the Virginia Polytechnic Institute and State University IACUC.

3.5.2. Immunohistochemistry (IHC)

Anesthetized mice were transcardially perfused with phosphate-buffered saline (PBS; pH 7.4) and 4% paraformaldehyde in PBS (PFA; pH 7.4). Dissected brains and eyes were post-fixed in 4% PFA for 12-16 hours at 4°C. Tissues were cryopreserved in 30% sucrose solution for 2-3 days, embedded in Tissue Freezing Medium (Electron Microscopy Sciences, Hatfield, PA), and

cryosectioned (16 μm sections). Sections were air-dried onto Superfrost Plus slides (Fisher Scientific, Pittsburgh, PA) and frozen at -80°C until further processing. For IHC, slides were incubated in blocking buffer (2.5% bovine serum albumin, 5% Normal Goat Serum, 0.1% Triton-X in PBS) for 1 hr. Primary antibodies were diluted in blocking buffer as following: GAD67 (Millipore MAB5406) 1:700; IBA1 (Wako 019-19741) 1:1000; VGluT2 (Synaptic Systems 135511) 1:500; VGluT1 (Synaptic Systems 135402) 1:700; mGluR1a (Frontier Institute co. AB_2571799) 1:250 and incubated on tissue sections for >12 hr at 4°C. After washing three times in PBS, fluorescently conjugated secondary antibodies (1:1000 in blocking buffer) were incubated on sections for 1 hr at room temperature. After five washes with PBS, sections were stained with DAPI (1:5000 in water) and were mounted with Vectashield (Vector Laboratories, Burlingame, CA). Images were acquired on a Zeiss LSM 700 confocal microscope. When comparing sections from different age groups or genotypes, images were acquired with identical parameters. A minimum of three animals (per genotype and per age) were compared in all IHC experiments.

3.5.3. Riboprobe production

pCMV-SPORT6 Plasmids carrying *syt1* (cat # 5363062), *nrn1* (cat # 5367281), and *lrrtm1* (cat # 5321979) were obtained from GE Dharmacon. *gad1* 1Kb cDNA (corresponding to nucleotides 1099-2081) was generated using Superscript II Reverse Transcriptase First Strand cDNA Synthesis kit (cat # 18064014, Invitrogen, La Jolla, CA) according to the manufacturer manual, amplified by PCR using primers mentioned in the primers list, gel purified, and then cloned into a pGEM®-T Easy Vector using pGEM®-T Easy Vector kit, (cat # A1360, Promega, Madison, WI) according to the kit manual. Sense and anti-sense riboprobes against *gad1, syt1,*

nrn1, and *lrrtm1* were synthesized from 5 µg linearized plasmids using digoxigenin-(DIG) or fluorescein-labeled uridylyltransferase (UTP) (cat # 11685619910, cat # 11277073910, Roche, Mannheim, Germany) and the MAXIscript in vitro Transcription Kit (cat # AM1312, Ambion, Austin, TX) according to the kit manual. 5 µg of Riboprobes (20 µl) were hydrolyzed into ~0.5 kb fragments by adding 80 µl of water, 4 µl of NaHCO3 (1 M), 6 µl Na2CO3 (1 M) and incubating the mixture in 60°C for specific amounts of time determined for each probe by the following formula: Time=$(X_{kb}-0.5)/(X_{kb}*0.055)$, where X is the full length of the RNA probe. RNA fragments were finally precipitated in 250 µl 100% ethanol containing 5 µl Acetic acid, 10 µl NaCl (5 M) and 1 µl glycogen (5 mg/ml). Finally, the pellet dissolved in 50 µl of RNAase-free water.

3.5.4. In situ hybridization (ISH)

ISH was performed on 16 µm sections prepared as described above. Sections were fixed in 4% PFA for 10 min, washed with PBS for 15 min, incubated in proteinase K solution (1 µg/ml in 50 mM Tris PH 7.5, 5 mM EDTA) for 10 min, washed with PBS for 5 min, incubated in 4% PFA for 5 min, washed with PBS for 15 min, incubated in acetylation solution (196.6 ml water, 2.6ml triethanolamin, 0.35 ml HCl, 0.5 ml acetic acid) for 10 min, washed with PBS for 10 min, incubated in 0.1% triton (in PBS) for 30 min, washed with PBS for 40 min, incubated in 0.3% H_2O_2 (in water) for 30 min, washed with PBS for 10 min, pre-hybridized with hybridization solution (50 ml of Sigma 2X prehyb solution, 25 mg Roche yeast RNA and 8 mg heparin) for 1 hr, hybridized with 50 µl of heat-denatured diluted riboprobes (1-2 µl of riboprobe in 50 µl hybridization solution heated for 10 min in 70°C), mounted with cover slips and kept at 60°C overnight. On day 2, coverslips were gently removed in 60°C preheated 2X saline-sodium citrate

(SSC) buffer, and slides were washed 5 times in 60°C preheated 0.2X SSC buffer for 2-3 hr at 60°C. Slides were washed 3 times with Tris-buffered saline (TBS) and blocked for 1 hr with blocking buffer (0.2% Roche blocking reagent, 10% lamb serum in TBS) prior to overnight 4°C incubation with horseradish peroxidase (POD)-conjugated anti-DIG or anti-fluorescent antibodies (cat # 11426346910 and cat # 11207733910, Roche). On day 3, bound riboprobes were detected by staining with Tyramide Signal Amplification (TSA) system (cat # NEL75300 1KT, PerkinElmer, Shelton, CT). For double ISH, sections were washed in TBS after the TSA reaction, then incubated in 0.3% H_2O_2 for 30 min, washed with TBS for 10 min, incubated with the second POD-conjugated antibody in blocking buffer and detected with TSA system as described above. Images were obtained on a Zeiss LSM700 confocal microscope. A minimum of three animals per genotype and age were compared in ISH experiments.

3.5.5. Quantitative real time PCR (qPCR)

Pooled tissues (5-7 animals per sample) were isolated from P3, P8, P12 and P25 mice, and RNA was purified using the Aurum™ Total RNA Fatty and Fibrous Tissue kit (cat # 7326870, BioRad) according to the kit manual. cDNAs were generated with Superscript II RT (Invitrogen). qPCR was performed on a CFX Connect real time system (BioRad) using iTaq SYBRGreen Supermix (cat # 1725124, BioRad) according to the kit protocol. The following cycling conditions were used with 12.5 ng of cDNA: 95°C for 30 s and 42 cycles of amplification (95°C for 10 s, 60°C for 30 s) followed by a melting curve analysis. Relative quantities of RNA were determined using the ΔΔ-CT method (Schmittgen and Livak, 2008). A minimum of n=3 biological replicates (each in triplicate) was run for each gene. Each individual

run included separate Glyceraldehyde-3-Phosphate Dehydrogenase (*gapdh*), Actin, or 18s rRNA control reactions. qPCR primers can be found in the primer list.

3.5.6. Western blot

Mice were perfused with PBS, brains removed, and d- and vLGN were dissected separately in ice-cold PBS. Tissues were pooled from >5 littermates per group and subsequenctly lysed in modified loading buffer containing 50 mM Tris–HCl (pH 6.8), 2% sodium dodecyl sulfate (SDS), 10% glycerol, and protease inhibitors (1 mM PMSF). Samples were homogenized, boiled for 10 min, and insoluble material was removed. Protein concentrations were determined by Micro BCA™ Protein Assay Kit (cat # 23235, Pierce, Rockford, IL). Equal amounts of protein were loaded and separated by SDS-PAGE and transferred to a PVDF membrane as described previously (Fox et al., 2007). After blocking in 5% non-fat milk in PBS (containing 0.05% Tween), PVDF membranes were incubated with primary antibodies (LRRTM1 [Synaptic Systems AF4897], Actin [EMD Millipore MAB1501]), followed by HRP-conjugated secondary antibodies. Immunoblotted proteins were detected with Amersham ECL Prime Western Blotting Detection Reagent (cat # RPN2236).

3.5.7. Intraocular injection of anterograde tracers and AAVs

For intraocular injections, mice were anesthetized with isoflurane or hypothermia, and 1-2 µl of 1 mg/ml CTB was injected into the eye intravitreally with a fine glass pipette attached to a picospritzer. After 2 days, perfused and PFA fixed brains were sectioned (90 µm) using a Vibratome (HM650v, ThermoFisher). Sections were stained with DAPI and mounted with Vectashield (Vector Laboratories, Burlingame, CA). Images were acquired on a Zeiss LSM 700

confocal microscope. A similar approach was used to inject 1-2 µl of a 1:1 mixture of the following AAVs: AAV9.hEF1a.lox.TagBFP.lox.eYFP.lox.WPRE.hGH-InvBYF (AV-9-PV2453) and AAV9.hEF1a.lox.mCherry.lox.mTFP1.lox.WPRE.hGH-InvCheTF (AV-9-PV2454). At P0 or P10 AAVs were injected into the eyes and 2-3 weeks after the injections, mice were anesthetized, perfused, and their brains were fixed in 4% PFA overnight. Brains were then sectioned (90µm) using a Vibratome and sections were mounted with Vectashield. Images were acquired on a Zeiss LSM 700 confocal microscope.

3.5.8. Serial block-face scanning electron microscopy

Mice were perfused with 0.1M sodium cacodylate buffer containing 4% PFA and 2.5% glutaraldehyde. Brains were immediately vibratomed (300-µm coronal sections), and dLGN tissues were dissected and shipped to Renovo Neural (Cleveland, OH). Processing and image acquisition were performed as described in detail previously (Hammer et al., 2014; Mukherjee et al., 2016). Serial image stacks were analyzed using TrakEM2 in Fiji (Cardona et al., 2012). Presence of synaptic vesicles and pale mitochondria have been used as features to distinguished retinal terminals from non-retinal terminals in dLGN (Bickford et al., 2010; Hammer et al., 2014). Analysis of data sets were performed independently by four researchers to ensure unbiased results.

3.5.9. RNA sequencing

RNA was isolated from vLGN and dLGN at four different ages (P3, P8, P12 and P25) and was shipped to the Genomics Research Laboratory at Virginia Tech's Biocomplexity Institute for RNAseq analysis. Quality of total RNA was checked on Agilent BioAnalyzer 2100

(Agilent Technologies, Santa Clara CA). Libraries were generated using Apollo 324 Robot (Wafergen, CA). 500 ng of total RNA (with RIN ≥ 9.0) was enriched for polyA RNA using PrepX PolyA mRNA Isolation Kit (cat # 400047, Wafergen, Fremont, CA) and was then onverted into a library of template molecules using the PrepX RNA-Seq for Illumina Library Kit (cat # 400046, Wafergen, Fremont, CA). Validation of the 280-300bp libraries (160-180 bp insert) was completed using an Agilent 2100 Bioanalyzer and quantitated using Quant-iT dsDNA HS Kit (cat # Q33120, Invitrogen). Eight individually indexed cDNA libraries were pooled and sequenced on an Illumina HiSeq, resulting in a minimum of 40-50 million reads. Libraries were clustered onto a flow cell using Illumina's TruSeq PE Cluster Kit v3-cBOT-HS (cat # PE-401-3001), and sequenced 2 x 100 PE using TruSeq SBS Kit v3-HS (200-cycles) (cat # FC-401-3001). Low quality base calls, sequences with low complexity tails, and adaptor sequences were removed using a combination of Btrim and EA-utils. Sequencing reads were then aligned to the mouse genome (Tophat2/Bowtie) and expression determined via HTSeq counting. DESeq2 has been used to determine fold change and statistical significance of changes between samples.

3.5.10. Visual behavior tasks

Two alternative forced swim tasks were performed in a trapezoid shaped pool (sides a = 25 cm, b = 80 cm, c and d = 143cm) with two side-by-side monitors (19 inches, V196L, Acer) placed at the wide end (b) of the tank and separated by a black divider (42 cm). Detailed instructions for the apparatus were described previously (Prusky et al., 2000). A rescue platform (37 cm × 13 cm × 14 cm) was hidden under water below the monitor with the positive visual cue (termed the S+ side). Visual cues (i.e. different grating pattern) were generated in the Gabor-patch generator (https://www.cogsci.nl/gabor-generator). The visual cue and hidden platform

were moved to the right or left screens in a pseudorandom manner with the following orders: LRLLRLRRLR, RLRRLRLLRL, RRLRLLRLRL and LLRLRRLRLR. During the behavioral tasks the room was dark, but a 60-W bulb was positioned above the holding cages. Three mice were housed per cage, and during the visual tasks each mouse was transferred to a separate cage which was placed on a heat pad and lined with paper towels. A day before starting experiments, mice were acclimated to the experimenter and the pool through plain handling of mice, 1-2 min period of direct contact with the hidden platform at either arms, and submersion into the water at gradually-increasing distances from the hidden platform. The ability of mice to detect and associate a S+ vertical grating display with the rescue platform (in contrast to the lack of a platform beneath the S- screen that displayed either a gray or horizontal grating) was assessed. Behavioral tasks included a training phase (8 days) and a testing phase (10-12 days). For training phases, mice were placed at the release chute and given one minute to find the platform. A trial was recorded as a correct choice if a mouse passed the choice line on the S+ side, while passing the choice line on the S- side was recorded as an incorrect choice. After arriving at the rescue platform, mice were placed back into their individual cages only if they made the correct choice. When a mouse made an incorrect choice, it was placed back at the release chute to perform another trial immediately before going back to its home cage. After 8 sessions of training, mice learned to find the visual cue with a >80% accuracy. To test visual acuity and contrast sensitivity, we increased the spatial frequency and decreased the contrast of the grating, respectively. In the testing phase of the detection tasks, 10 trials of a given task were performed in 10 consecutive days (one per day). For the testing phase of discrimination tasks, 10 trials were given in a single day. No more than 6 animals were tested in a given session. Each mouse (P56-

90) performed 8-10 trials per session. Final values represent average values for 10-20 animals per genotype.

3.5.11. Quantifications and statistics

For quantifying the size of retinal terminals labeled with fluorescent CTB or VGluT2 immunostaining, the area of isolated puncta (which may contain one or more RGC terminals) were measured in 20x or 40X confocal images of dLGN and vLGN sections by semi-manual selection of the puncta in the ImageJ. 3-7 animals (3 sections per animals) were analyzed per age and genotype and the cumulative frequencies of different terminal sizes were obtained. Two-way ANOVA analysis was used to determine any significant change in the distribution of retinal terminal sizes between groups.

Intensity and density of the signals in immunostained images of dLGN, vLGN and vCTX were measured in ImageJ. 3-7 animals (3 sections per animals) were analyzed per genotype and age and the mean values were compared between groups. T-test or ANOVA were used to determine any significant difference of the mean values between groups.

Retinal terminals were identified by their unique ultrastructural features including the presence of round synaptic vesicles and pale mitochondria (Bickford et al., 2010; Hammer et al., 2014). Retinal terminals clustering onto the same portion of a dendritic branch were classified as complex RG synapses if the membranes of terminals touched each other and were not isolated from each other by glial processes. On the other hand, a retinal terminal isolated from other retinal terminals was classified as a simple RG synapse. In each mouse, retinal terminals were identified regardless of their simple or complex designation and were then assigned to one of these two classes. The proportion of retinal terminals participating in each class was averaged

from data sets obtained from the dLGN of three mice per genotype (2-3 data sets were obtained per mouse). T-test or ANOVA analysis were used to determine any significant difference of the mean values between groups.

The performance of a mouse in the training sessions was reported as the percentage of correct choices the mouse made out of 8 or 10 trials per day (e.g. day 1), and then an average of daily performances were calculated for each group of mice. The performance of a mouse in the test phase of both detection and discrimination tasks were reported as the percentage of correct choices the mouse made out of 10 trials per given task (e.g. for 10% contrast) and these values were used to calculate the mean for a group of mice (e.g. control group). T-test or ANOVA analysis were used to determine any significant difference of the mean values between groups.

Acknowledgments

This work was supported in part by the National Institutes of Health – National Eye Institute grants EY021222 and EY024712 (M.A.F.), an Independent Investigator grant from the Brain and Behavior Foundation (M.A.F.), and a fellowship from the VTCRI Medical Research Scholars Program (A.M.). The authors are grateful to Drs. G. Valdez, K. Mukherjee and Y.A. Pan for helpful comments and discussions. We also thank Drs. S. Robel (VTCRI) and W. Guido (U. Louisville) for generously supplying *aldh1l1-gfp* and *crh-cre* mice, respectively.

Competing financial interests

The authors declare no competing financial interests.

Figure 3.1. Retinal projections develop into unique terminal types in dLGN

(A) Schematic of the mouse brain highlighting the main retinorecipient regions including dLGN.

(B) Development of VGluT2-positive retinal terminals in dLGN and vLGN in wild type mice.

(C-G) Cumulative (cum.) distribution of VGluT2-positive puncta size in P3 (C), P8 (D), P14 (E), P25 (F) and P62 (G) dLGN (orange) and vLGN (blue). Data are shown as Mean ± SEM.

(H) Average total VGluT2-positive terminal size in developing dLGN and vLGN. Data are shown as Mean ± SEM, *$p<0.01$, **$p<0.001$ by ANOVA.

(I) GFP-positive retinal terminals in dLGN and superior colliculus (SC) of *hb9-gfp* mice. Red arrowheads denote some of the gfp-labeled retinal terminals.

(J) SBFSEM of retinogeniculate synapses in dLGN of P8 and P14 mice. 3D reconstruction of retinal terminals and relay cell dendrite are depicted below each micrograph. The black arrows denote the location of retinal terminals depicted in the above micrographs.

(K) Schematic representation of brainbow-AAV constructs.

(L-N) Examples of brainbow-labeled clusters of retinal terminals in dLGN of P8 (L), P10 (M) and P14 (N) *calb2-cre* mice. Arrowheads denote terminals labeled by different colors.

Scale bars, 20 μm (B and I), 5 μm (J), 10 μm (L).

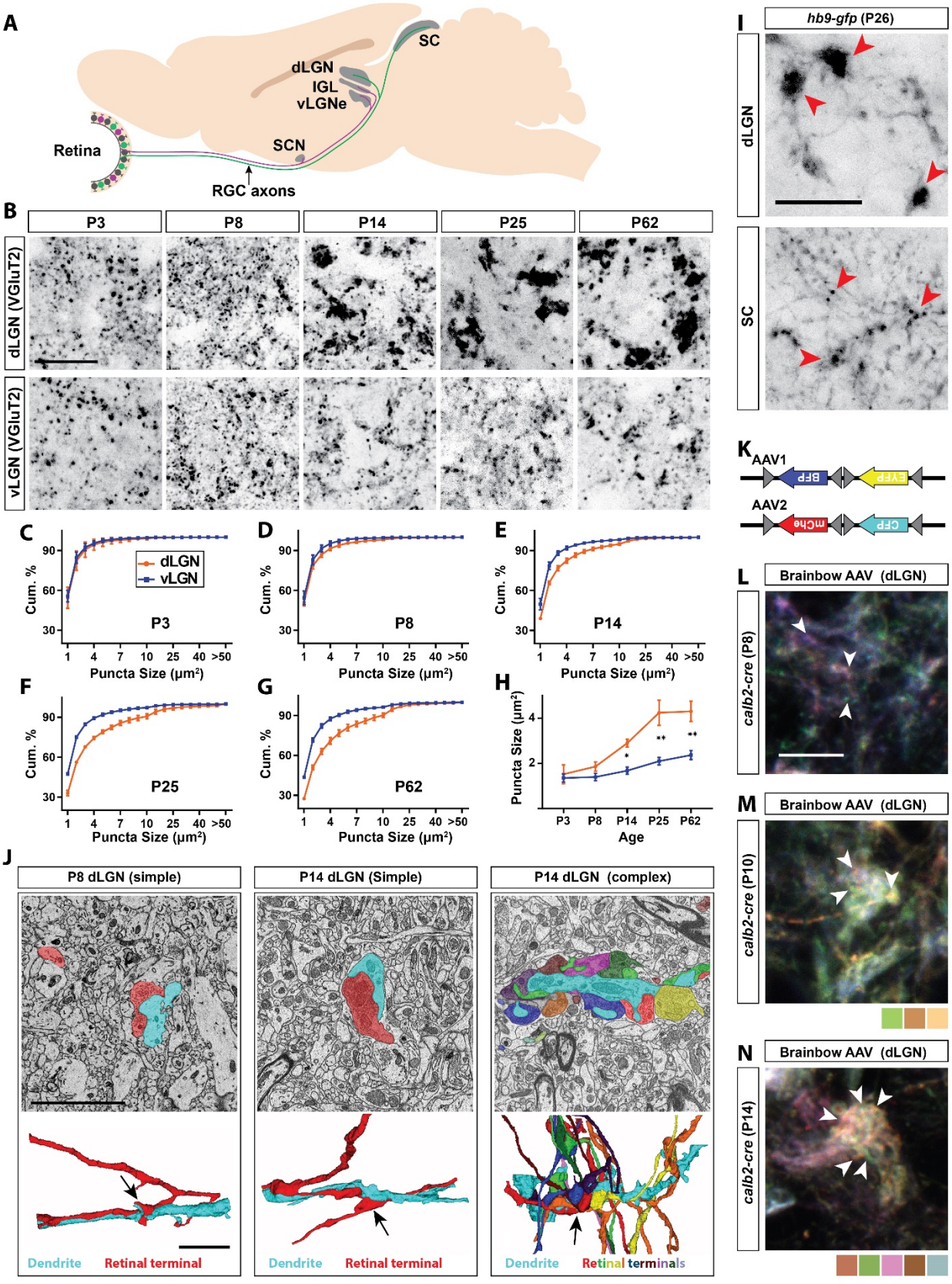
A
SC
dLGN
IGL
vLGNe
SCN
Retina
RGC axons
B
P3
P8
P14
P25
P62
dLGN (VGluT2)
vLGN (VGluT2)
C
D
E
F
G
H
dLGN
vLGN
Cum. %
Puncta Size (μm²)
Puncta Size (μm²)
Age
I
hb9-gfp (P26)
dLGN
SC
K
AAV1
AAV2
BFP
EYFP
mCherry
CFP
L
Brainbow AAV (dLGN)
calb2-cre (P8)
M
Brainbow AAV (dLGN)
calb2-cre (P10)
N
Brainbow AAV (dLGN)
calb2-cre (P14)
J
P8 dLGN (simple)
P14 dLGN (Simple)
P14 dLGN (complex)
Dendrite
Retinal terminal
Retinal terminals

Figure 3.2. Identification of *lrrtm1* and *nrn1* as candidate synaptic organizing cues in dLGN

(A) Next generation RNAseq was performed on RNA isolated from dLGN and vLGN at P3, P8, P12 and P25.

(B) Volcano scatter plots show differentially expressed mRNAs in the developing dLGN.

(C) Relative *lrrtm1* and *nrn1* mRNA levels in dLGN at P8, P12 and P25 compared to P3 by RNAseq. Data are relative values comparing different ages, *P<0.0001 by Wald Chi-Squared Test (DESeq2).

(D and E) Enrichment of *lrrtm1* (D) and *nrn1* (E) mRNAs in dLGN compared to vLGN at four ages in wild type mice. Data are relative values comparing dLGN and vLGN, *P<0.0001 by Wald Chi-Squared Test (DESeq2).

(F and G) Developmental expression of *lrrtm1* (F) and *nrn1* (G) mRNAs in wild type dLGN by qPCR. Data are shown as Mean ± SEM; ***p<0.0001, **p<0.01, *p<0.05 by ANOVA.

(H and I) ISH for *lrrtm1* (F) and *nrn1* (G) mRNAs in coronal sections of wild type P25 mouse brains.

Scale bar, 1mm (H and I).

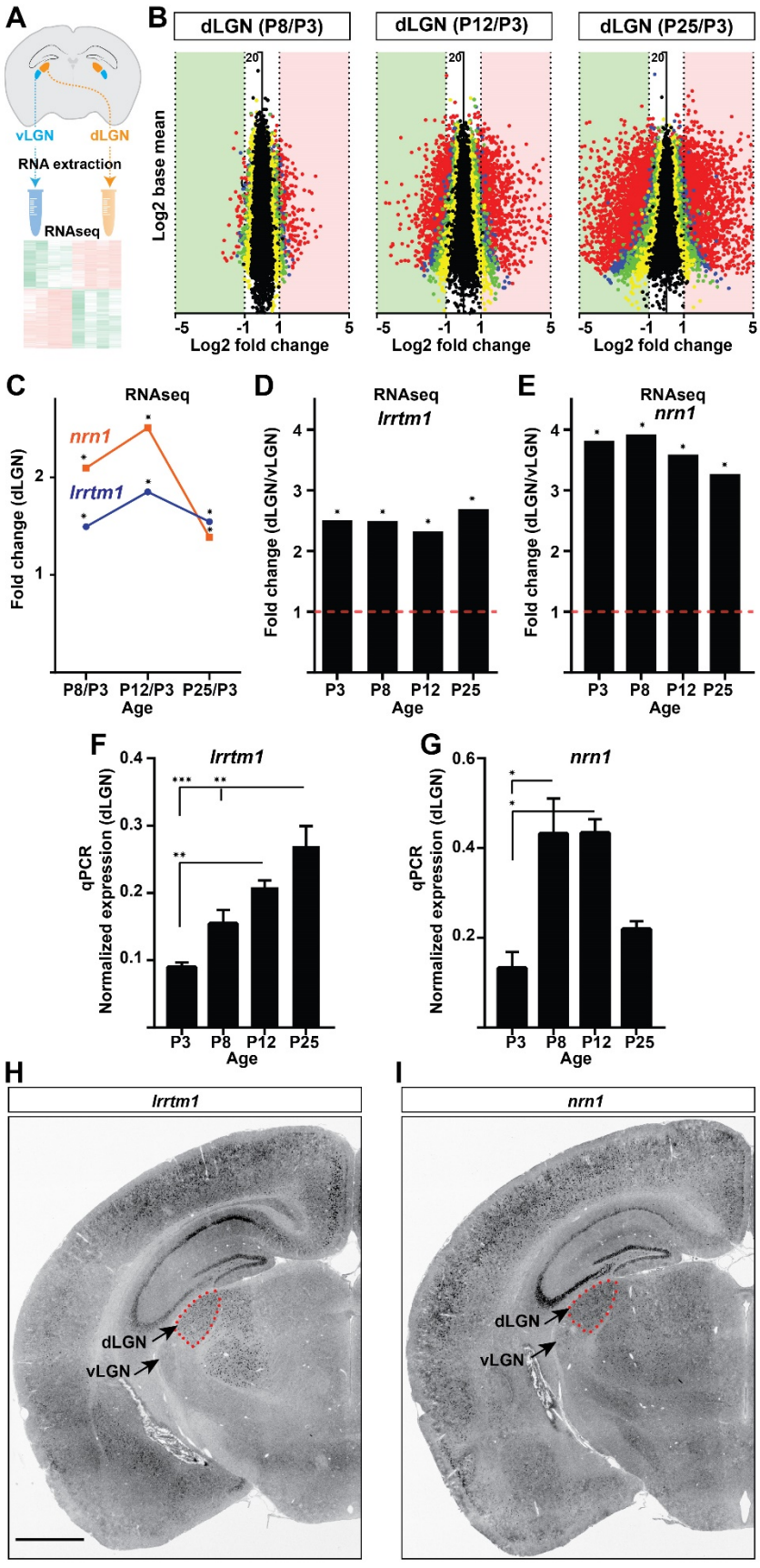
A
vLGN
dLGN
RNA extraction
RNAseq
B
dLGN (P8/P3)
dLGN (P12/P3)
dLGN (P25/P3)
Log2 base mean
Log2 fold change
C
RNAseq
nrn1
lrrtm1
Fold change (dLGN)
P8/P3 P12/P3 P25/P3
Age
D
RNAseq
lrrtm1
Fold change (dLGN/vLGN)
P3 P8 P12 P25
Age
E
RNAseq
nrn1
Fold change (dLGN/vLGN)
P3 P8 P12 P25
Age
F
lrrtm1
qPCR
Normalized expression (dLGN)
P3 P8 P12 P25
Age
G
nrn1
qPCR
Normalized expression (dLGN)
P3 P8 P12 P25
Age
H
lrrtm1
dLGN
vLGN
I
nrn1
dLGN
vLGN

Figure 3.3. Developmental and region-specific expression of lrrtm1 and nrn1

(A) ISH for *lrrtm1* and *nrn1* mRNAs in the developing visual thalamus. dLGN encircled by red dots.

(B-D) Western blots show LRRTM1 protein level is higher in dLGN than vLGN (B) and increases in the dLGN postnatally (C and D). Data are shown as Mean ± SEM; ***p<0.0001, **p<0.01, *p<0.05 by ANOVA.

(E) Expression of *lrrtm1* and *nrn1* mRNAs in coronal sections of P25 mouse brains. Boxes in visual cortex (vCTX) and superior colliculus (SC) are shown in higher magnifications on the right.

(F) Expression of *lrrtm1* and *nrn1* mRNAs in retina. Yellow arrowheads denote mRNA expression. ONL, outer nuclear layer; INL, inter nuclear layer; GCL, ganglion cell layer.

Scale bars, 200 μm (A), 500 μm (E), 50 μm (insets of vCTX and SC and F).

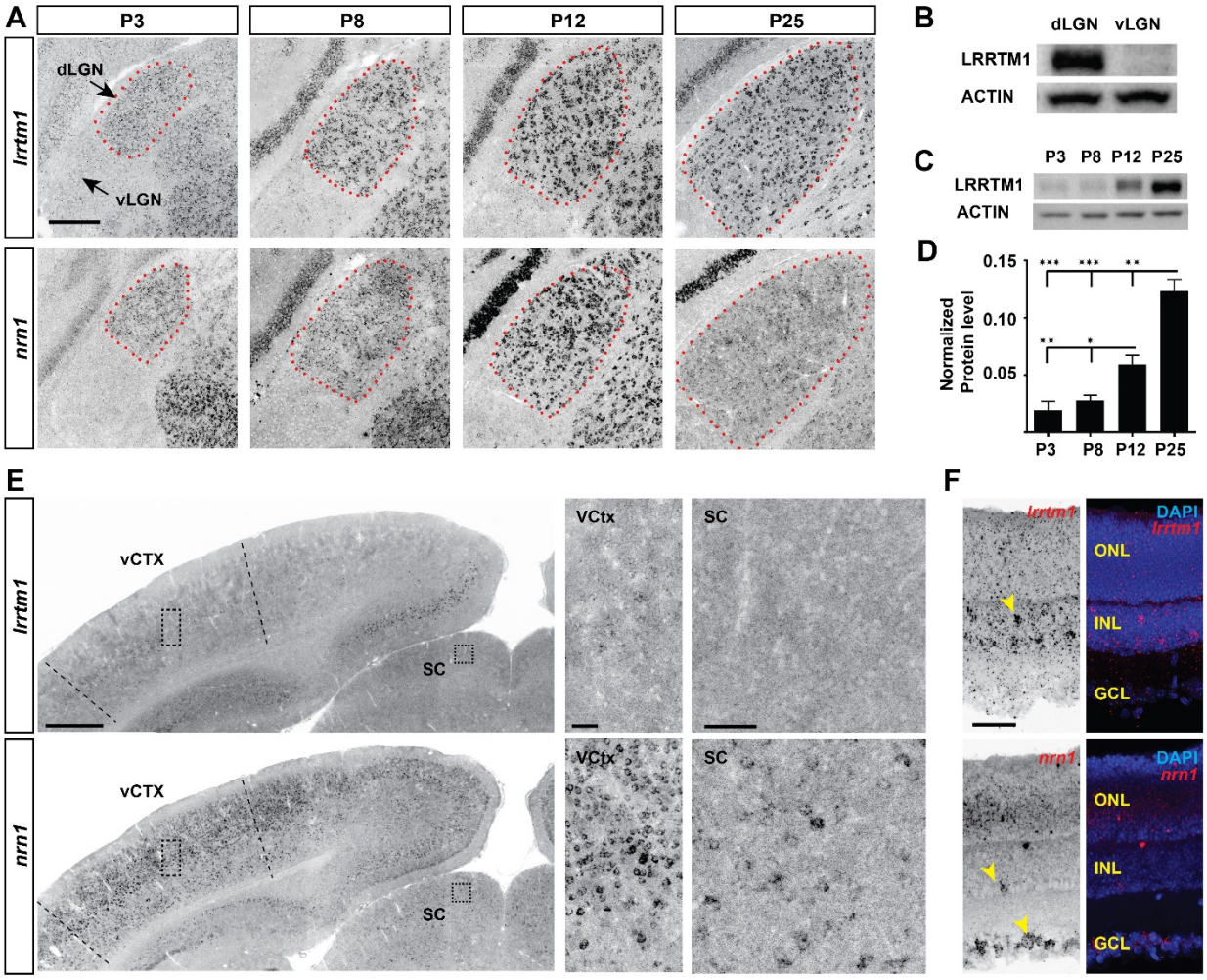
A
P3
P8
P12
P25
lrrtm1
nrn1
dLGN
vLGN
B
dLGN
vLGN
LRRTM1
ACTIN
C
P3
P8
P12
P25
LRRTM1
ACTIN
D
Normalized Protein level
0.15
0.10
0.05
***
***
**
**
*
P3
P8
P12
P25
E
lrrtm1
nrn1
vCTX
SC
VCtx
SC
F
lrrtm1
nrn1
DAPI
ONL
INL
GCL

Figure 3.4. dLGN relay cells generate *lrrtm1* and *nrn1*

(A and B) Double *in situ* hybridization (ISH) for *syt1* and either *lrrtm1* (A) or *nrn1* (B) in P14 wild type dLGN.

(C and D) ISH for either *lrrtm1* (C) or *nrn1* (D) in dLGN of P14 *aldh1l1-gfp* mice revealed no astrocytic expression of these mRNAs.

(E and F) ISH for *lrrtm1* (C) or *nrn1* (D) and immunostaining (IHC) for the microglia marker Iba1 in P14 wild type dLGN.

(G and H) ISH for *lrrtm1* (C) or *nrn1* (D) and IHC for GAD67 in P14 wild type mice revealed no expression by inhibitory interneurons.

(I and J) Double ISH for either *lrrtm1* (C) or *nrn1* (D) and *gad1* in P25 *crh-cre::tdt* dLGN revealed expression by relay cells.

Scale bar, 20 μm (A-J).

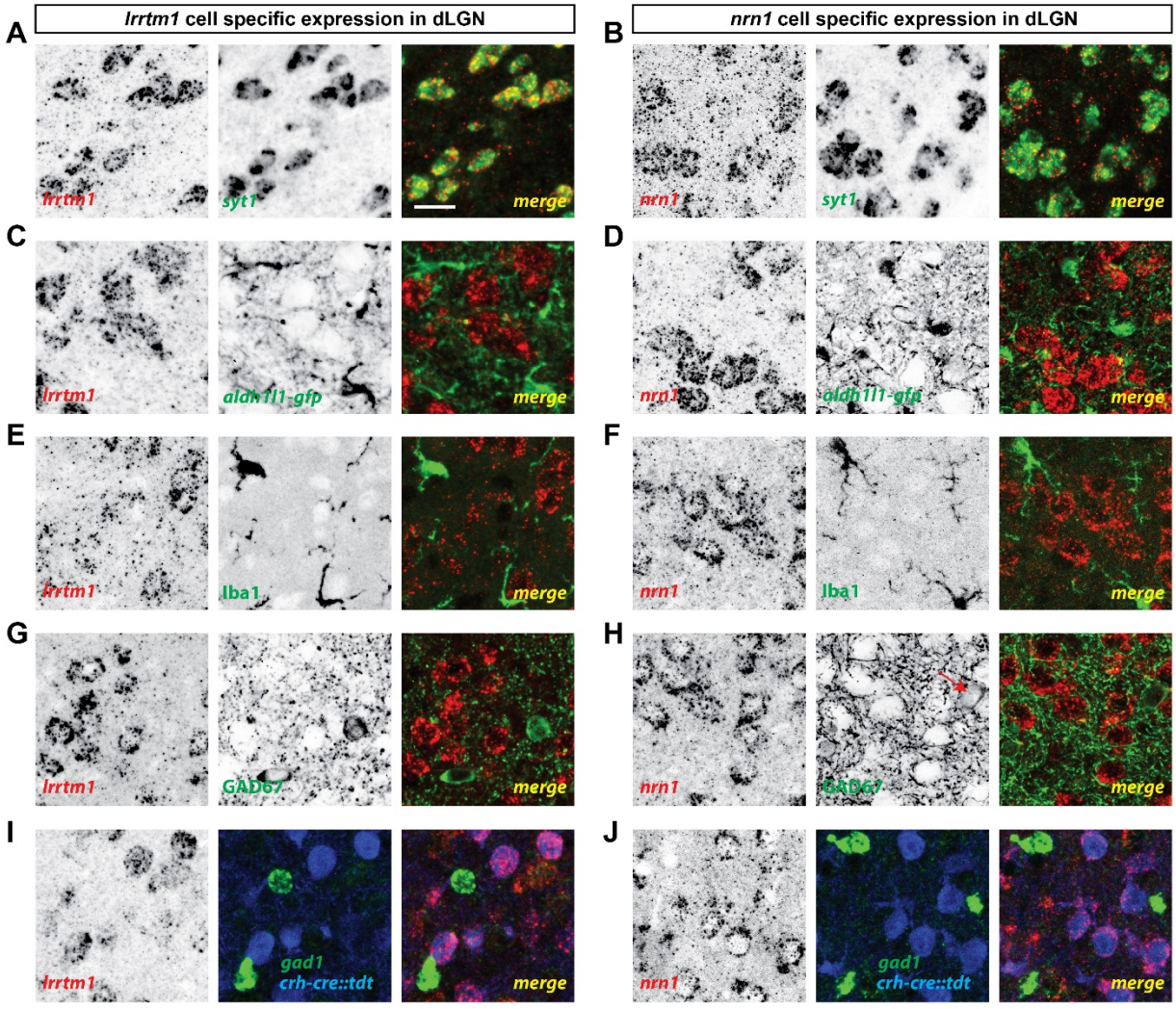
A
lrrtm1 cell specific expression in dLGN
lrrtm1
syt1
merge
B
nrn1 cell specific expression in dLGN
nrn1
syt1
merge
C
lrrtm1
aldh1l1-gfp
merge
D
nrn1
aldh1l1-gfp
merge
E
lrrtm1
Iba1
merge
F
nrn1
Iba1
merge
G
lrrtm1
GAD67
merge
H
nrn1
GAD67
merge
I
lrrtm1
gad1
crh-cre::tdt
merge
J
nrn1
gad1
crh-cre::tdt
merge

Figure 3.5. Loss of *lrrtm1* results in smaller vglut2-positive puncta in dLGN but not vLGN

(A and D) Immunostaining of VGluT2-positive retinal terminals in dLGN (A) and vLGN (D) of littermate control and *lrrtm1*$^{-/-}$ mice at P3, P8, P14 and P25. Red boxes in P25 panels are shown in higher magnification on the right.

(B and E) Cumulative (cum.) distribution of VGluT2-positive puncta size in control and *lrrtm1*$^{-/-}$ mice dLGN (B) and vLGN (E).

(C and F) Average total VGluT2-positive puncta size in control and *lrrtm1*$^{-/-}$ mice dLGN (C) and vLGN (F). Data represent Mean ± SEM; ***p<0.0001, **p<0.01, *p<0.05 by ANOVA.

Scale bar, 20 μm (A and C), 10 μm (insets).

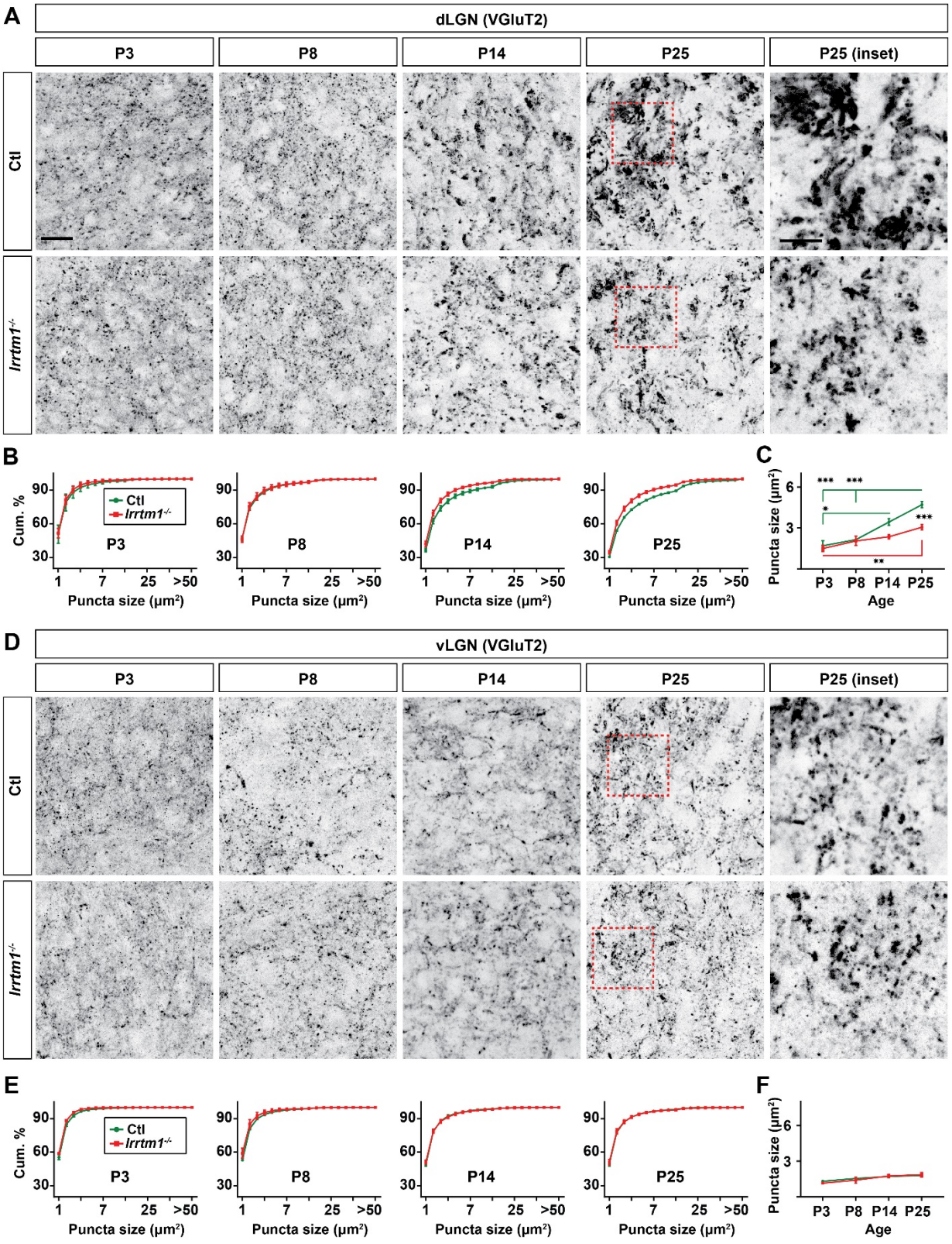
A
dLGN (VGluT2)
P3
P8
P14
P25
P25 (inset)
Ctl
Irrtm1-/-
B
Cum. %
Ctl
Irrtm1-/-
P3
P8
P14
P25
Puncta size (µm²)
C
Puncta size (µm²)
Age
D
vLGN (VGluT2)
E
F

Figure 3.6. Loss of complex RG synapses in *lrrtm1*$^{-/-}$ mice

(A and B) SBFSEM images of retinal terminals in P42 control (A, labeled in green) and *lrrtm1*$^{-/-}$ (B, labeled in red) dLGN. RG synapses are depicted in insets a1-a4 (ctl) and b1-b4 (*lrrtm1*$^{-/-}$). In insets, each retinal terminal is depicted in a unique color, however, similar colors in different insets do not represent axonal branches of the same RGC. 3D reconstruction of retinal terminals and relay cell dendrite are depicted on the right. The black arrows denote the position of dendrites stemming from relay cells somas.

(C) Percentage of retinal terminals contributing to forming RG synapses with 1, 2, 3 or ≥4 distinct retinal terminals in P42 lrrtm1-/- and control dLGN. Data represent Mean ± SEM; ***p<0.0001, by ANOVA.

(D) Quantification of terminal size in simple and complex RG synapse (syn.) in dLGN of *lrrtm1*$^{-/-}$ and control mice. Data represent Mean ± SEM; ***p<0.0001, by ANOVA.

(E and F) Retinal terminals were multicolor-labeled by injecting 1-2 µl brainbow AAVs into the vitreous humor of *lrrtm1*$^{-/-}$*::calb2-cre* and control mice.

(G) Color analysis of clustered retinal terminals in wild type and *lrrtm1*$^{-/-}$ mutants revealed a lower level of complex RG synapses in mutants.

Scale bar, 10 µm (A and B and 3D images), 20 µm (E), 1 µm (insets).

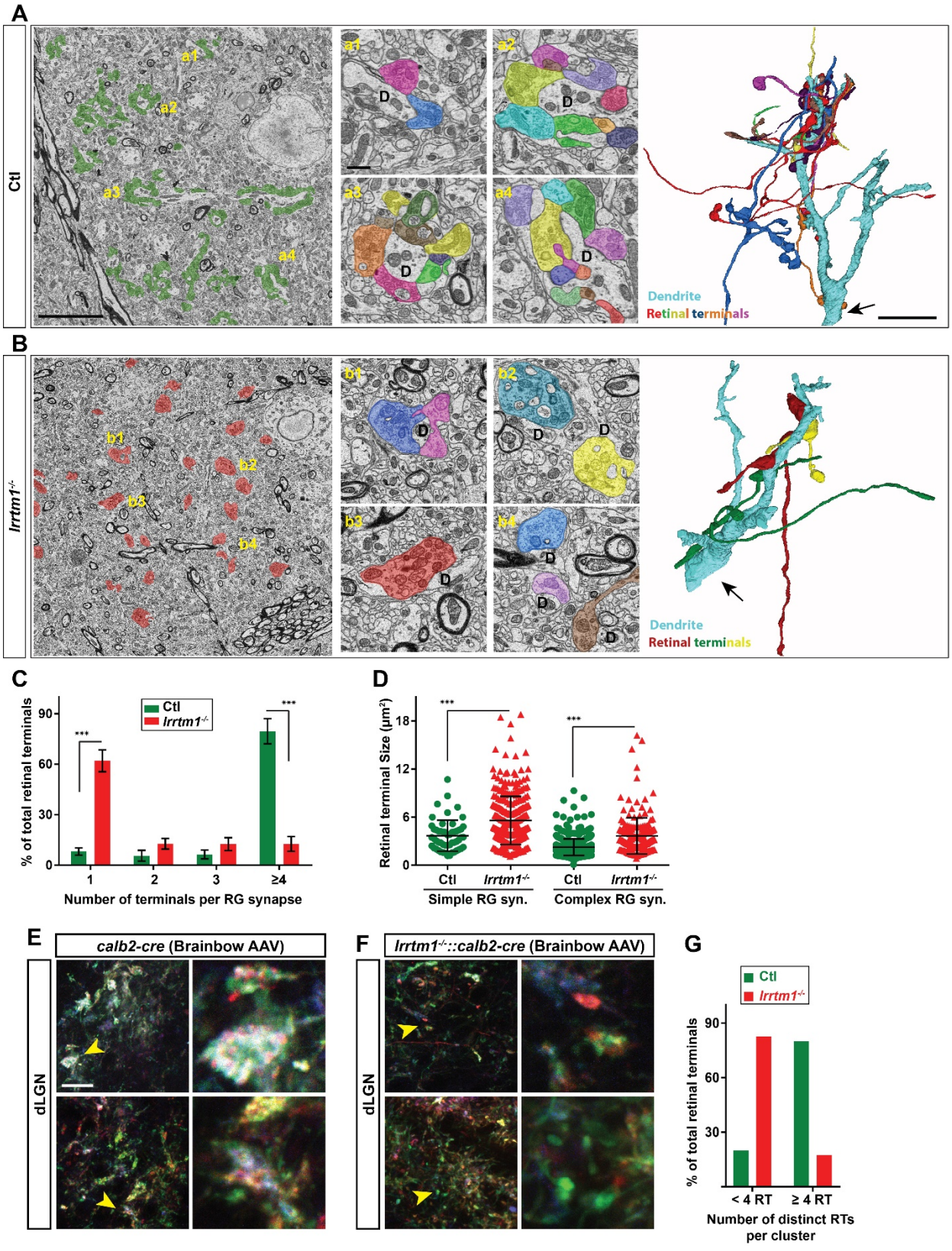
A
Ctl
a1
a2
a3
a4
D
Dendrite
Retinal terminals
B
Irrtm1-/-
b1
b2
b3
b4
D
Dendrite
Retinal terminals
C
Ctl
Irrtm1-/-
% of total retinal terminals
90
60
30
0
***
***
1
2
3
≥4
Number of terminals per RG synapse
D
Retinal terminal Size (µm²)
18
12
6
0
***
***
Ctl
Irrtm1-/-
Ctl
Irrtm1-/-
Simple RG syn.
Complex RG syn.
E
calb2-cre (Brainbow AAV)
dLGN
F
Irrtm1-/-::calb2-cre (Brainbow AAV)
dLGN
G
Ctl
Irrtm1-/-
% of total retinal terminals
90
60
30
< 4 RT
≥ 4 RT
Number of distinct RTs per cluster

Figure 3.7. Complex RG synapses are required for visual behaviors

(A) Schematic diagrams depicting the two-alternative forced swim behavior task. A' depicts a mouse's view of the visual displays (e.g. vertical gratings).

(B and C) Training *lrrtm1*$^{-/-}$ (red) and control (green) mice to detect a vertical grating display versus a gray screen (B) or horizontal grating display (C). Examples of visual displays are depicted in B' and C'.

(D and E) Percentage of correct choices made by *lrrtm1*$^{-/-}$ (red) and control (green) mice for detection of vertical gratings with increasing spatial frequency (D; cpd, cycle per degree) or decreasing contrast versus a gray screen (E). Examples of visual displays are depicted in D' and E'.

(F and G) Correct choices made by *lrrtm1*$^{-/-}$ (red) and control (green) mice for discriminating vertical grating from horizontal grating either with increasing spatial frequency (F) or with decreasing contrast (G). D1-D7 are the consecutive days of the test phase. Examples of visual displays are depicted in F' and G'.

For B-G, dash line represents the 70% correct threshold for successful completion of task. All data are shown as Mean ± SEM; ***$p<0.0001$, **$p<0.01$, *$p<0.05$ by ANOVA.

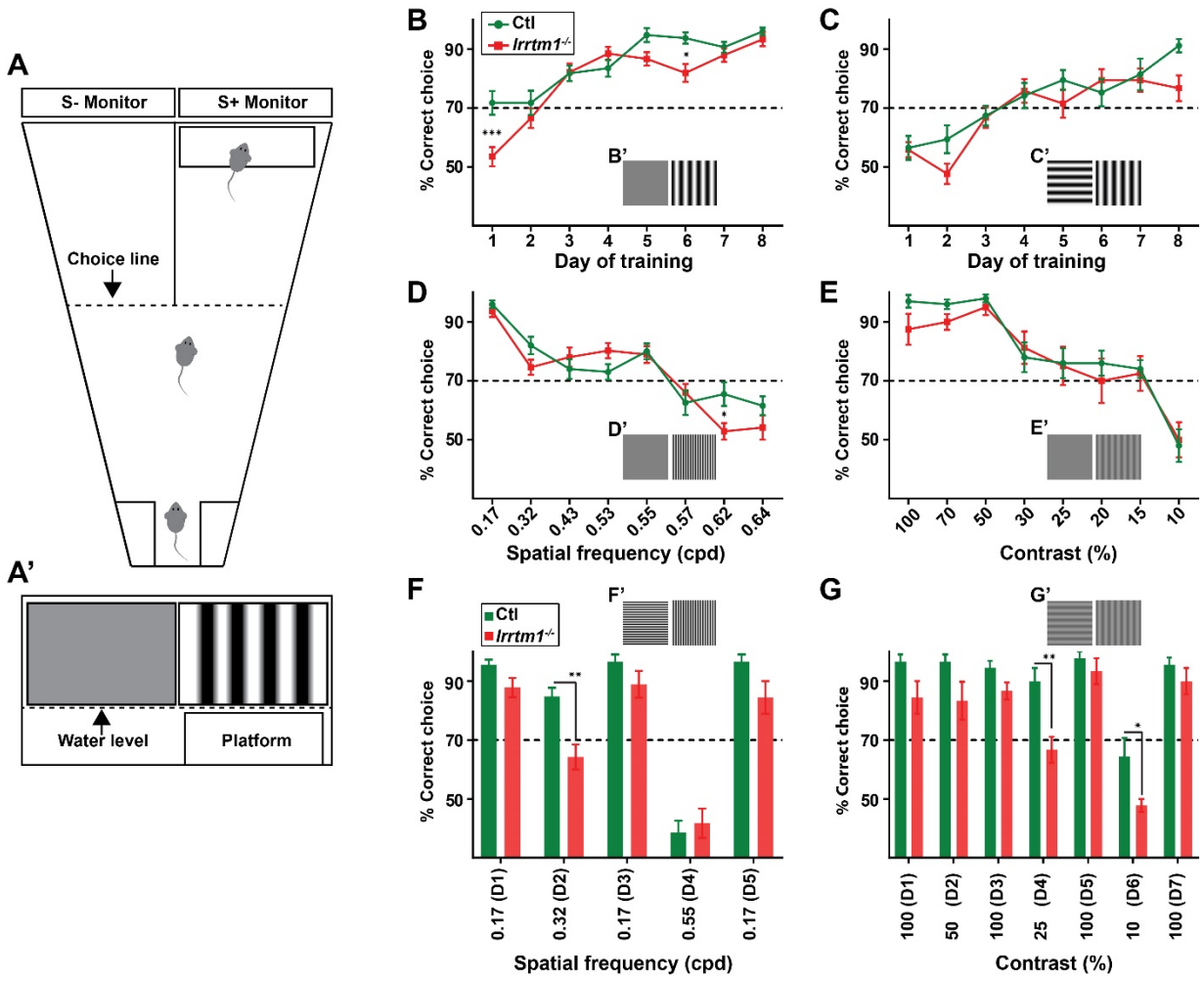
A
S- Monitor
S+ Monitor
Choice line
A'
Water level
Platform
B
Ctl
Irrtm1-/-
% Correct choice
Day of training
B'
C
C'
D
D'
Spatial frequency (cpd)
E
E'
Contrast (%)
F
F'
0.17 (D1)
0.32 (D2)
0.17 (D3)
0.55 (D4)
0.17 (D5)
G
G'
100 (D1)
50 (D2)
100 (D3)
25 (D4)
100 (D5)
10 (D6)
100 (D7)

Supplementary Figure 3.1: CTB-tracing of RGC projections revealed unique enlargement of retinal terminals in dLGN. Related to Figure 1.

(A) Intraocular injection of CTB was used to study the developmental transformation of retinal terminals in dLGN and vLGN in wild type mice. Similar to VGluT2 study (Figure 1A) retinal terminals in dLGN undergo a significant enlargement at eye-opening which is absent from the vLGN.

(B-F) Cumulative distribution of CTB-filled terminal size in the developing mouse dLGN (orange) and vLGN (blue) showing different distribution of retinal terminal size in dLGN compared to vLGN at and after eye-opening. Data are shown as Mean ± SEM.

(G) Average total CTB-filled terminal size in developing dLGN (orange) and vLGN (blue) showing significant enlargement of retinal terminals in dLGN at and after eye-opening (and the absence of comparable changes in vLGN). Data represent Mean ± SEM; *$p<0.0001$ by ANOVA.

(H) SBFSEM of types of retinogeniculate synapses in dLGN and vLGN of P42 mice. 3D reconstruction of retinal terminals and relay cell dendrite are depicted below each micrograph.

Scale bars, 10 μm (A), 5 μm (H).

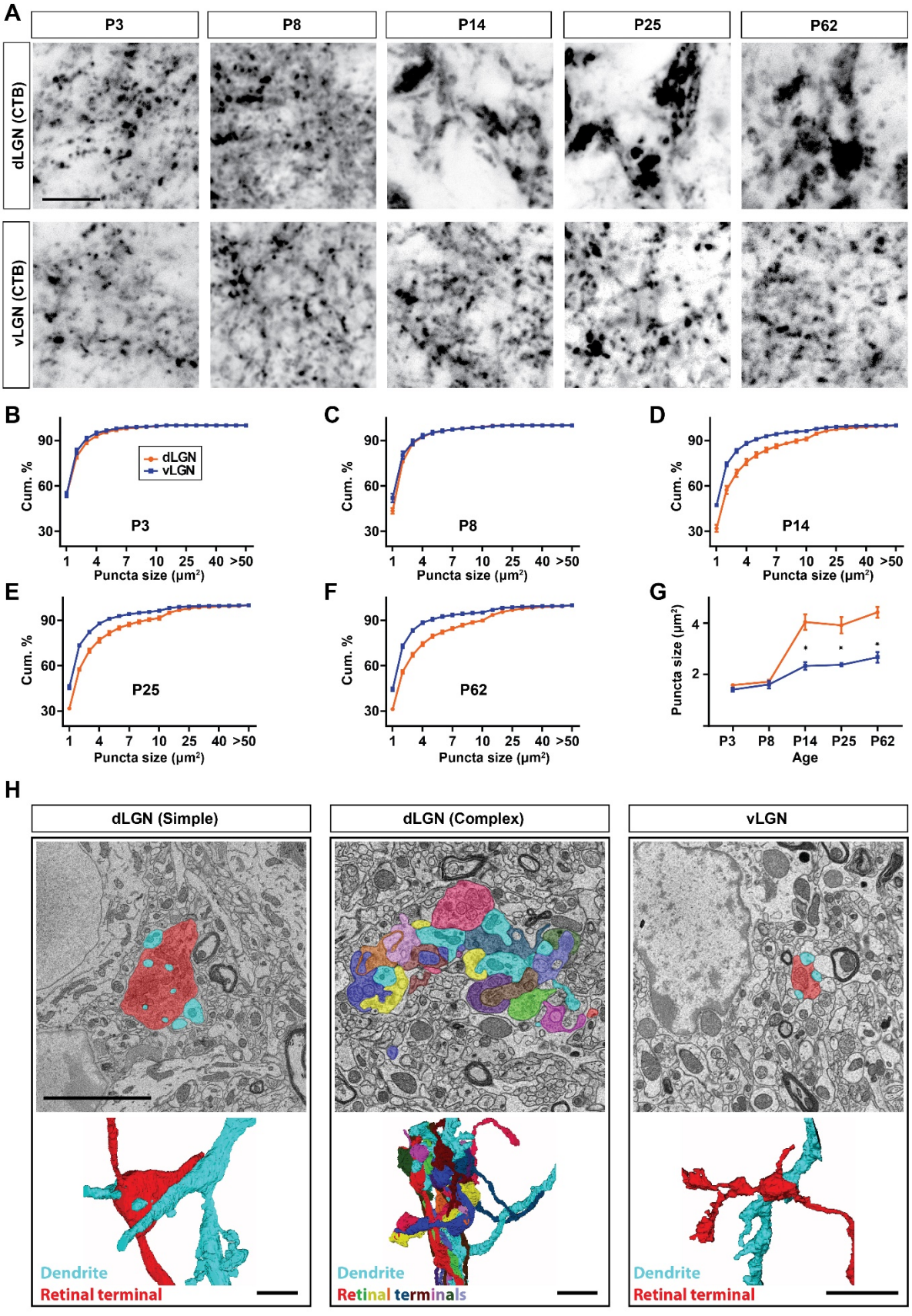
A
P3
P8
P14
P25
P62
dLGN (CTB)
vLGN (CTB)
B
C
D
E
F
G
dLGN
vLGN
Cum. %
Puncta size (μm²)
1 4 7 10 25 40 >50
90
60
30
P3
P8
P14
P25
P62
Puncta size (μm²)
Age
H
dLGN (Simple)
dLGN (Complex)
vLGN
Dendrite
Retinal terminal
Retinal terminals

Supplementary Figure 3.2: lrrtm1 and nrn1 are not expressed in SCN. Related to Figures 2 & 3.

(A and B) The specificity of antisense riboprobes against *lrrtm1* (C) and *nrn1* (D) used in this study was confirmed by comparing them to their sense riboprobes. Red dash line indicated ventral border of dLGN.

(C) dLGN tissue of *lrrtm1*$^{-/-}$ mutants and wild type mice were subjected to western blot analysis to confirm that LRRTM1 antibody (which is an antibody raised against human LRRTM1) specifically recognizes LRRTM1 protein in mouse.

(D and E) Absence of *lrrtm1* (A) and *nrn1* (B) mRNAs in SCN, the main retinorecipient nucleus involved in regulating circadian clock. Red dash line indicated SCN in the hypothalamus.

Scale bars, 200 μm (A and B), 100 μm (C and D).

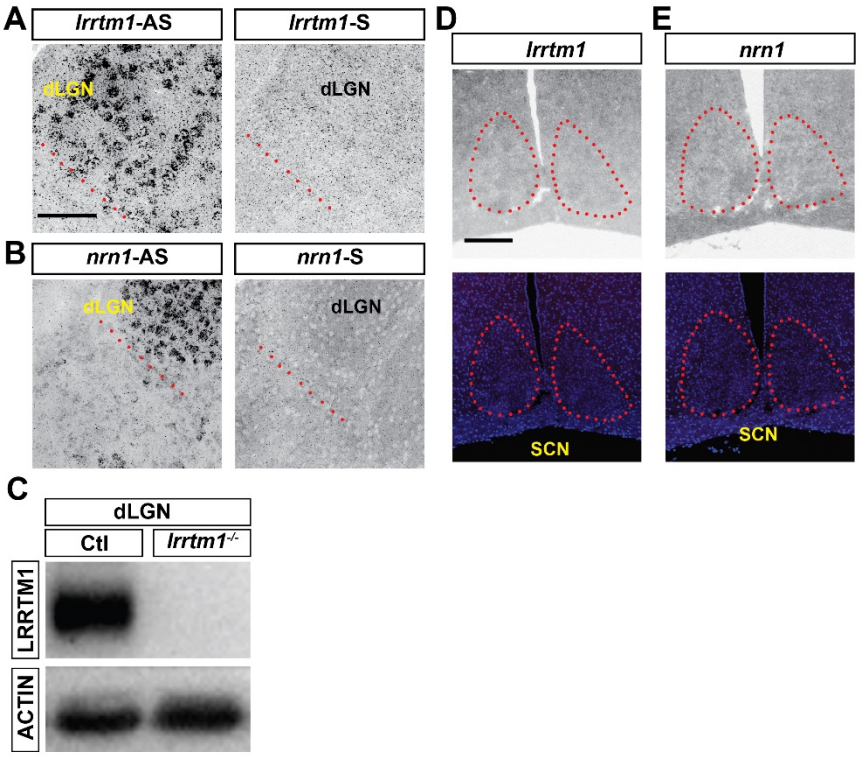
A
lrrtm1-AS
lrrtm1-S
dLGN
dLGN
B
nrn1-AS
nrn1-S
dLGN
dLGN
C
dLGN
Ctl
lrrtm1-/-
LRRTM1
ACTIN
D
lrrtm1
SCN
E
nrn1
SCN

Supplementary Figure 3.3: Lack of *lrrtm1* affects retinogeniculate synapses but not other synapses in dLGN. Related to Figure 5.

(A and B) CTB labeling of retinal terminals in dLGN (A) and vLGN (B) of littermate control (green) and *lrrtm1*$^{-/-}$ mice (red) at P3, P8, P14 and P25. Cumulative (cum.) distribution of CTB-filled terminal size in dLGN (A') and vLGN (B') as well as the average size of CTB puncta in dLGN (A'') and vLGN (B'') demonstrated smaller CTB puncta size in *lrrtm1*$^{-/-}$ mice. Data represent Mean ± SEM; ***$p<0.0001$, **$p<0.01$ by ANOVA.

(C) dLGN sections of control and *lrrtm1*$^{-/-}$ mice at P25 immunostained with VGluT1, mGluR1 and GAD67. Quantification of the florescence signal intensity (C') and fraction of the total dLGN area occupied by the signal (C'') for each staining are depicted on the right. All data are shown as Mean ± SEM. No significant changes has been observed for these non-retinal synaptic markers in *lrrtm1*$^{-/-}$ mice.

Scale bars, 20 µm (A and B), 250 µm (C).

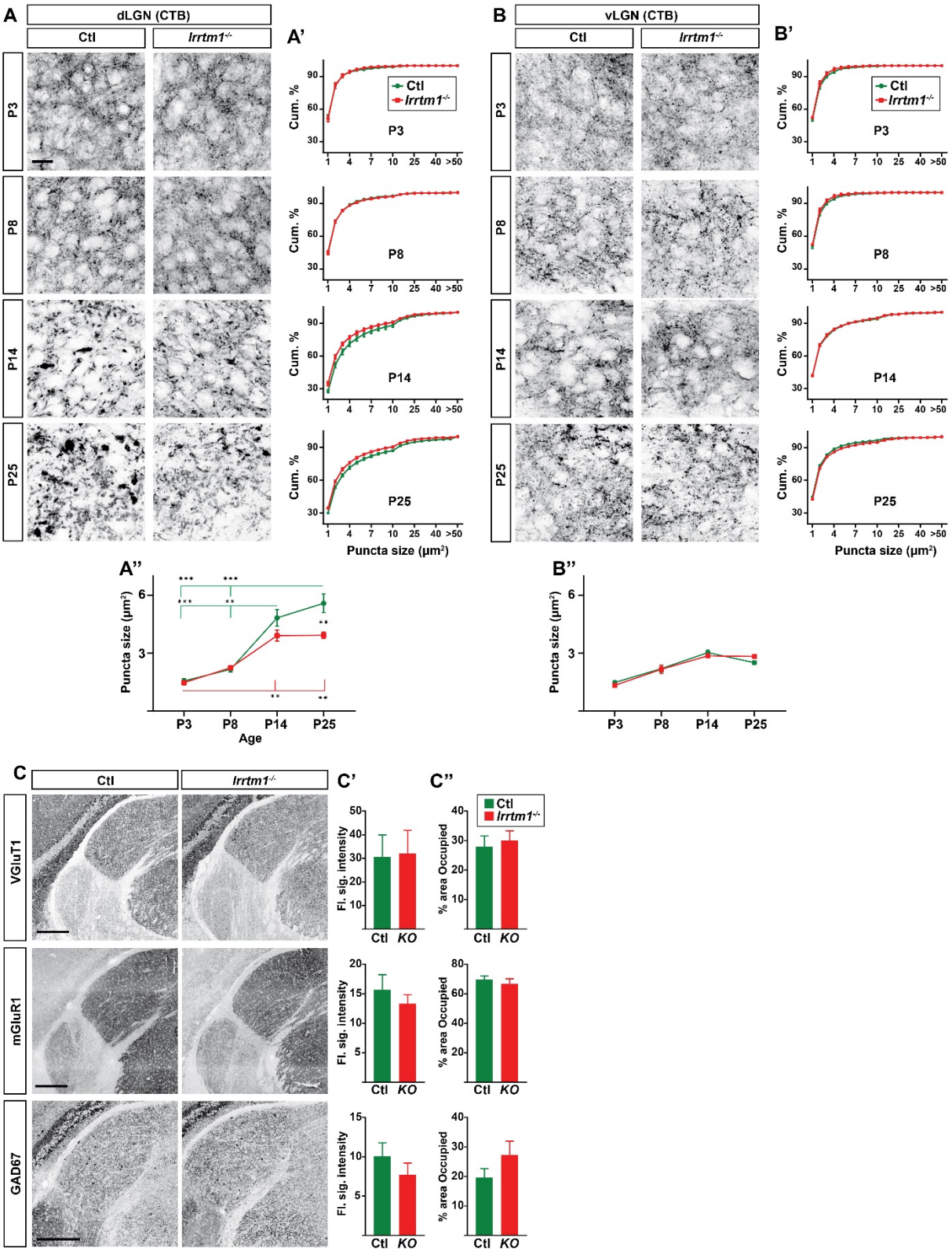
A
dLGN (CTB)
Ctl
Irrtm1-/-
P3
P8
P14
P25
A'
Cum. %
Puncta size (µm²)
A''
Puncta size (µm²)
Age
B
vLGN (CTB)
B'
B''
C
VGluT1
mGluR1
GAD67
C'
Fl. sig. intensity
C''
% area Occupied
KO

Supplementary Figure 3.4: Lack of *nrn1* did not affect retinogeniculate synapses. Related to Figure 5.

(A and B) Immunostaining of VGluT2-positive retinal terminals in dLGN (A) and vLGN (B) of littermate control and *nrn1*$^{-/-}$ mice at P8, P14 and P25. Cumulative (cum.) distribution of VGluT2-positive puncta size are depicted in A' (for dLGN) and B' (for vLGN). No significant difference in the size of retinal terminals has been observed in dLGN of mice lacking *nrn1*. All data are shown as Mean ± SEM.

Scale bars, 50 μm (A).

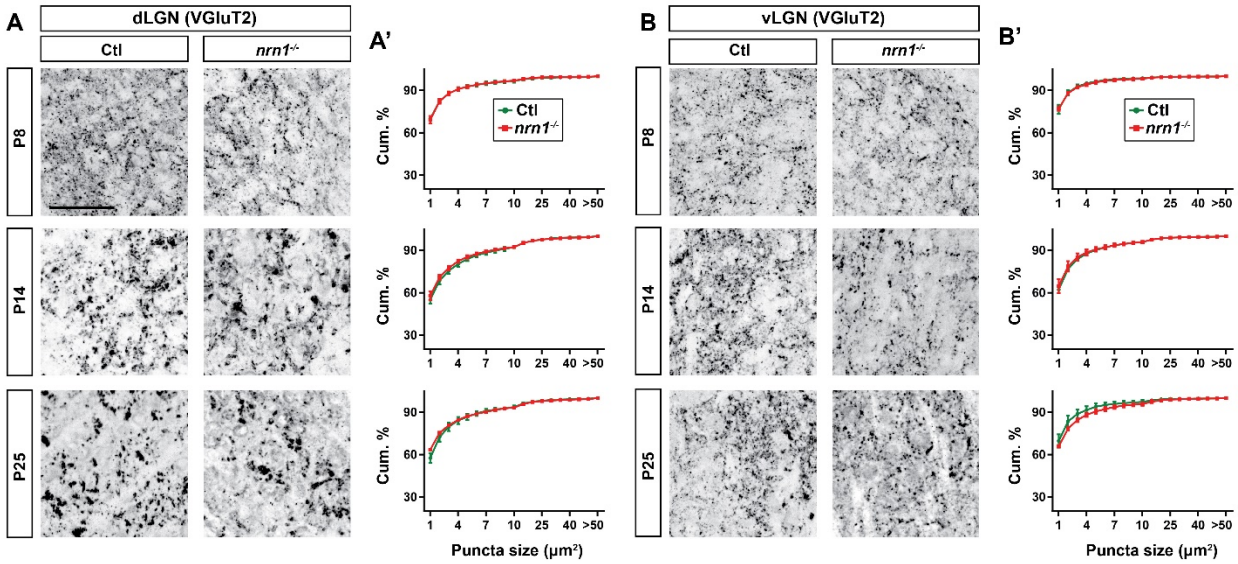
A
dLGN (VGluT2)
Ctl
nrn1-/-
P8
P14
P25
A'
Cum. %
Ctl
nrn1-/-
1 4 7 10 25 40 >50
Puncta size (µm²)
B
vLGN (VGluT2)
B'

Supplementary Figure 3.5: lack of *lrrtm1* resulted in a significant decrease in the number of complex RG synapses. Related to Figure 6.

(A and B) Three examples of dLGN SBFSEM micrographs in control (A) and *lrrtm1*$^{-/-}$ dLGN (B). All retinal terminals in the micrographs are pseudocolored in black and are depicted on the right, to simulate what these sections might look like with CTB or VGluT2 labeling. In the left micrographs, retinal terminals are labeled in green (A, control) and red (B, *lrrtm1*$^{-/-}$).

(C and D) Optic nerve (ON) cross section of control (C) and *lrrtm1*$^{-/-}$ (D) mice at P25 stained with toluidine blue. Higher magnification of the ON are depicted in C' (control) and D' (*lrrtm1*$^{-/-}$).

(E) Quantification of RGC axons in the ON showed similar number of axons in the ON of control (green) and *lrrtm1*$^{-/-}$ mice (red).

(F) Measuring cross section areas of the ON in control (green) and *lrrtm1*$^{-/-}$ mice (red) revealed no significant difference between mutant and control mice.

(G) Cumulative distribution of individual RGC axons size in control (green) and *lrrtm1*$^{-/-}$ mice (red) showed normal axon size (area of the individual axonal cross sections) in *lrrtm1*$^{-/-}$ mutants. All data are shown as Mean ± SEM.

Scale bars, 10 μm (A and B), 20 μm (C), 100 μm (D and E), 10 μm (D' and E').

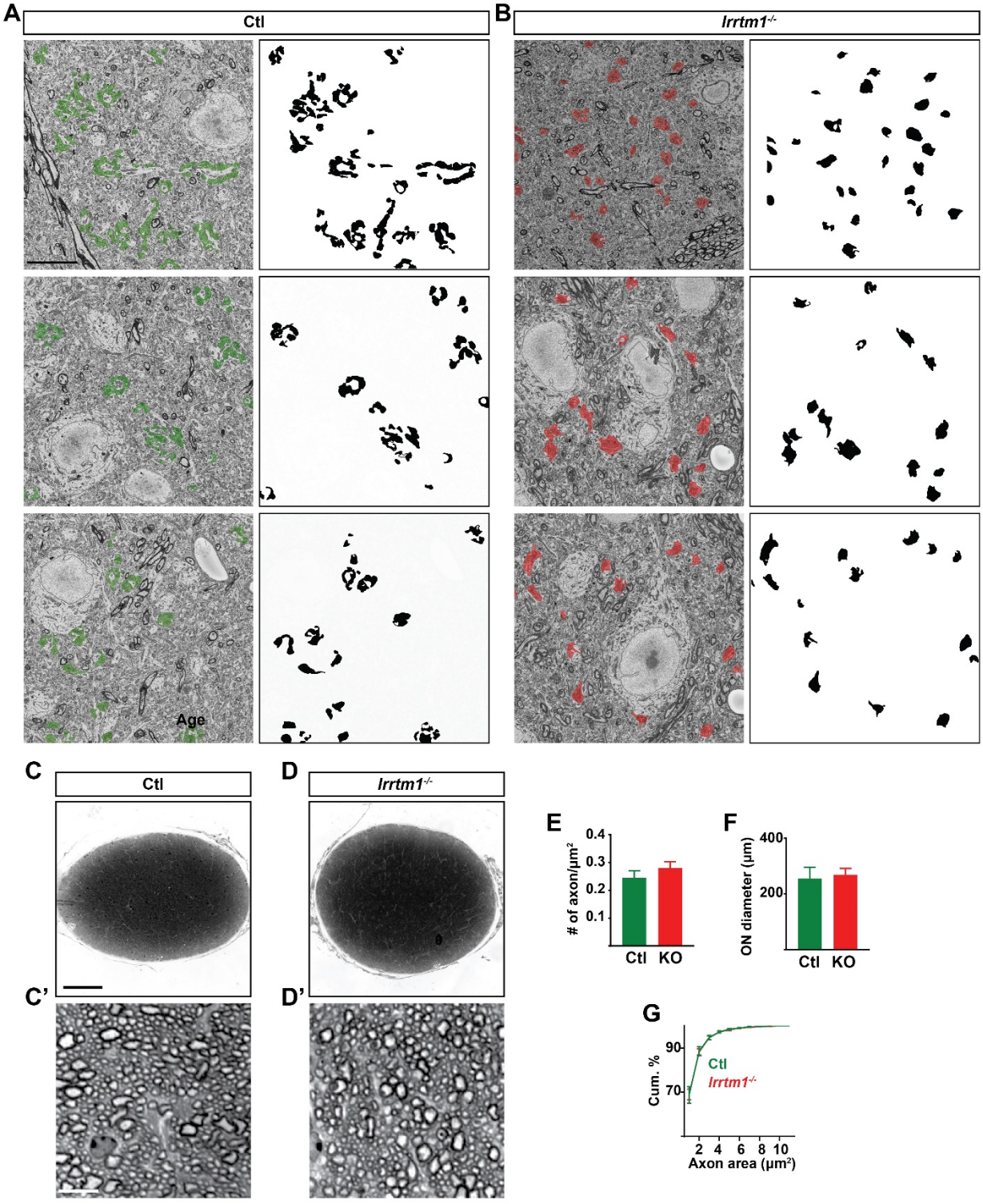
A
Ctl
B
Irrtm1-/-
Age
C
Ctl
C'
D
Irrtm1-/-
D'
E
# of axon/µm²
0.4
0.3
0.2
0.1
Ctl
KO
F
ON diameter (µm)
400
200
Ctl
KO
G
Cum. %
90
70
Ctl
Irrtm1-/-
2
4
6
8
10
Axon area (µm²)

Supplementary Figure 3.6: *Nrn1*$^{-/-}$ mice did not show a deficit in visual behavior. Related to Figure 7.

(A) Genetically blind *math5*$^{-/-}$ mice did not learn to perform the visual detection task confirming the necessity of vision for performing this assay. Dash line indicate the 70% threshold for successful performance in task.

(B) The percentage of correct choices made by control (green) or *lrrtm1*$^{-/-}$ mice (red) in a normal test when hidden platform positioned on the S+ side (vertical grating) and in a reverse test when hidden platform placed on the S- (horizontal grating). Results confirmed that accurate performance in this assay depend on association of the visual cues with the hidden platform rather than detecting the hidden platform itself.

(C and D) Training *nrn1*$^{-/-}$ (red) and control (green) mice to detect vertical grating versus a gray screen (B) or horizontal grating (C). *Nrn1*$^{-/-}$ Mutants showed a slight improved learning performance compared to wild types. Examples of visual displays are depicted in C' and D'.

(E and F) Percentage of correct choices made by *nrn1*$^{-/-}$ (red) and control (green) mice for detection of vertical gratings with increasing spatial frequency (E; cpd, cycle per degree) or decreasing contrast (F). Examples of visual displays are depicted in E' and F'.

(G and H) Comparison of correct choices made by *lrrtm1*$^{-/-}$ (red) *nrn1*$^{-/-}$ (blue) and control (green) mice for discriminating vertical grating from horizontal grating either with increasing spatial frequency (G) or with decreasing contrast (H). Results indicated abnormal visual behavior in *lrrtm1*$^{-/-}$ mice for performing more complex visual task. Examples of visual displays are depicted in G' and H'. D1-D5 indicates the consecutive days of the test phase.

For D-H, dash line represents the 70% correct threshold for successful completion of the task. All data are shown as Mean ± SEM; ***$p<0.0001$, **$p<0.01$, *$p<0.05$ by ANOVA.

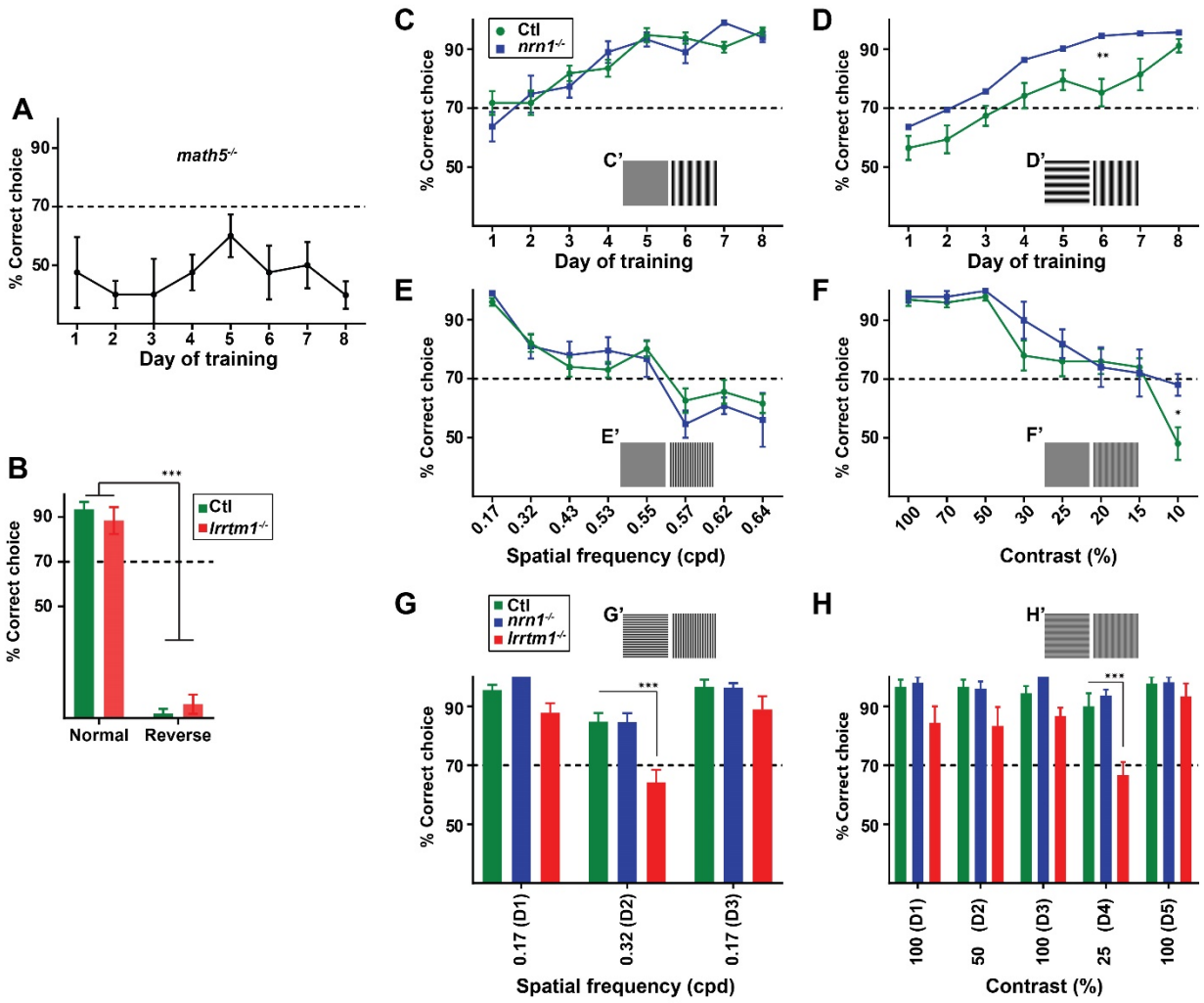
A
math5-/-
% Correct choice
Day of training
B
Ctl
lrrtm1-/-
Normal
Reverse
C
Ctl
nrn1-/-
C'
D
D'
E
E'
Spatial frequency (cpd)
F
F'
Contrast (%)
G
G'
0.17 (D1)
0.32 (D2)
0.17 (D3)
H
H'
100 (D1)
50 (D2)
100 (D3)
25 (D4)
100 (D5)

Supplementary Figure 3.7: Loss of *lrrtm1*$^{-/-}$ did not affect visual cortex. Related to Figures 5 & 7.

(A and B) Examples of visual cortex sections immunostained for VGluT1 and VGluT2 excitatory synaptic markers in control and *lrrtm1*$^{-/-}$ mice at P14 (A) and P25 (B). Quantification of florescence signal intensity and fraction of the total dLGN area occupied by the signal for each staining are depicted on the bottom in A' and B' (KO = *lrrtm1*$^{-/-}$ mutants). Results indicated that visual behavior deficits observed in *lrrtm1*$^{-/-}$ mutants were caused by loss of complex RG synapses in visual thalamus rather than abnormalities in other parts of the brain involved in processing visual information (e.g. visual cortex). In P25 tissues, Syt2 used to label cells in layer V of the cortex. Data are shown as Mean ± SEM.

(C) A pan-neurexin antibody revealed the presence of neurexins, the presynaptic binding partner of *lrrtm1*, in the RGCs. Yellow arrowhead denotes neurexin protein expression in RGCs. Brn3a is used here as a marker for RGCs and GAD67 to identify INL and inner plexiform layer.

(D-E) RNAseq analysis revealed the presence several neurexin-binding proteins such as *lrrtms* (D) and neuroligins (E) in dLGN. Higher level of *lrrtm1* at eye-opening and its enrichment in dLGN compared to vLGN made *lrrtm1* the prime candidate capable of influencing the transformation of RG synapses in dLGN. Data are shown as RNA raw reads (D and E) and expression relative values obtained by comparing dLGN to vLGN (D' and E') or different ages (D'' and E'').

Scale bars, 50 μm (A and C).

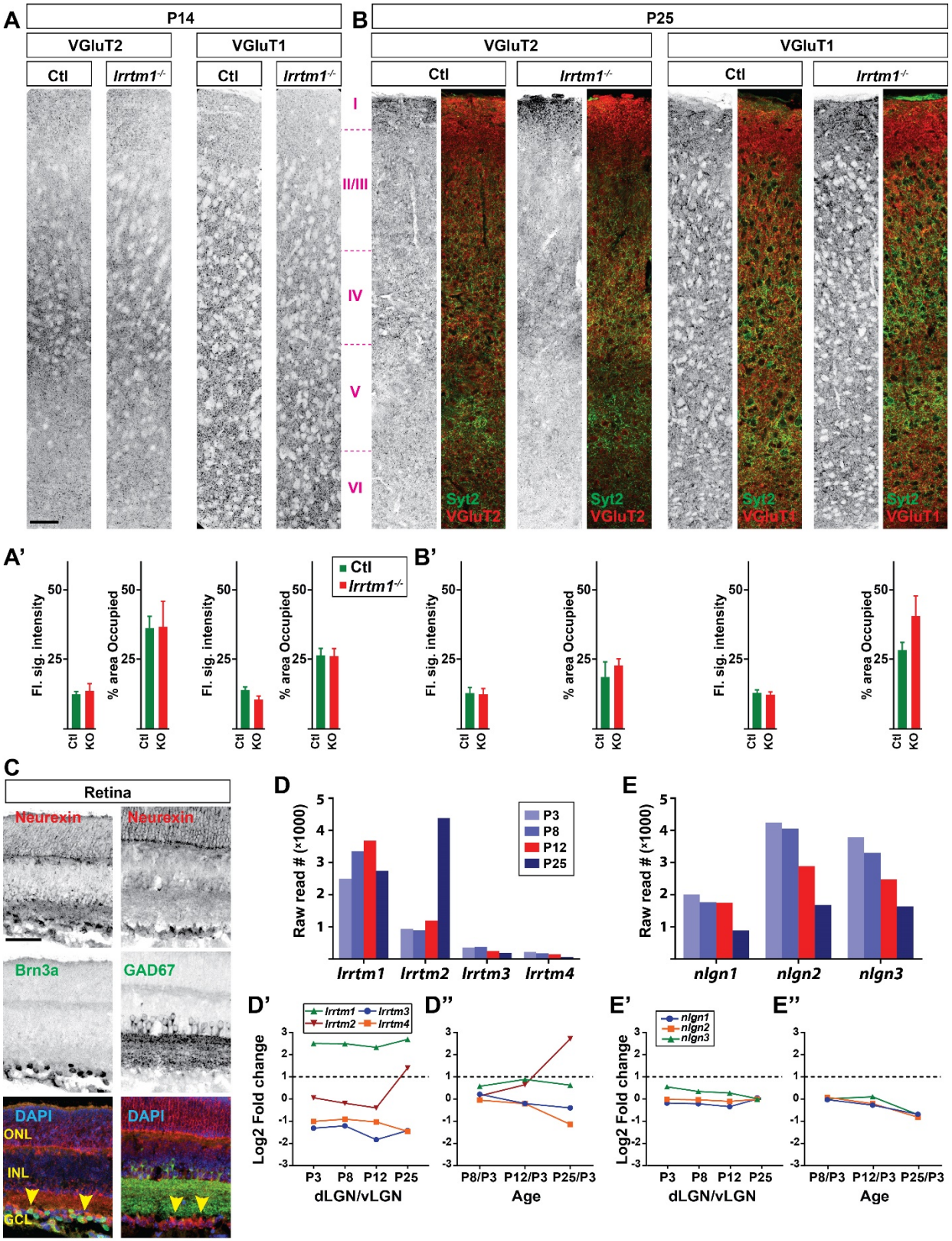
A
P14
VGluT2
VGluT1
Ctl
Irrtm1-/-
B
P25
I
II/III
IV
V
VI
Syt2
VGluT2
VGluT1
A'
B'
Fl. sig. intensity
% area Occupied
Ctl
KO
C
Retina
Neurexin
Brn3a
GAD67
DAPI
ONL
INL
GCL
D
Raw read # (×1000)
P3
P8
P12
P25
Irrtm1
Irrtm2
Irrtm3
Irrtm4
E
Nlgn1
Nlgn2
Nlgn3
D'
D''
E'
E''
Log2 Fold change
dLGN/vLGN
Age
P8/P3
P12/P3
P25/P3

References

Baden, T., Berens, P., Franke, K., Rosón, M.R., Bethge, M., and Euler, T. (2016). The functional diversity of retinal ganglion cells in the mouse. Nature *529*, 345-350.

Bickford, M.E., Slusarczyk, A., Dilger, E.K., Krahe, T.E., Kucuk, C., and Guido, W. (2010). Synaptic development of the mouse dorsal lateral geniculate nucleus. The Journal of comparative neurology *518*, 622-635.

Campbell, G., and Frost, D.O. (1987). Target-controlled differentiation of axon terminals and synaptic organization. Proceedings of the National Academy of Sciences *84*, 6929-6933.

Cantallops, I., Haas, K., and Cline, H.T. (2000). Postsynaptic CPG15 promotes synaptic maturation and presynaptic axon arbor elaboration in vivo. Nature neuroscience *3*, 1004-1011.

Cardona, A., Saalfeld, S., Schindelin, J., Arganda-Carreras, I., Preibisch, S., Longair, M., Tomancak, P., Hartenstein, V., and Douglas, R.J. (2012). TrakEM2 software for neural circuit reconstruction. PLoS One *7*, e38011.

Chen, C., and Regehr, W.G. (2000). Developmental remodeling of the retinogeniculate synapse. Neuron *28*, 955-966.

Cleland, B., Dubin, M., and Levick, W. (1971). Simultaneous recording of input and output of lateral geniculate neurones. Nature *231*, 191-192.

Cleland, B., and Lee, B. (1985). A comparison of visual responses of cat lateral geniculate nucleus neurones with those of ganglion cells afferent to them. The Journal of physiology *369*, 249-268.

Craig, A.M., Graf, E.R., and Linhoff, M.W. (2006). How to build a central synapse: clues from cell culture. Trends in neurosciences *29*, 8-20.

Cruz-Martín, A., El-Danaf, R.N., Osakada, F., Sriram, B., Dhande, O.S., Nguyen, P.L., Callaway, E.M., Ghosh, A., and Huberman, A.D. (2014). A dedicated circuit links direction-selective retinal ganglion cells to the primary visual cortex. Nature *507*, 358-361.

de Wit, J., and Ghosh, A. (2014). Control of neural circuit formation by leucine-rich repeat proteins. Trends in neurosciences *37*, 539-550.

de Wit, J., Sylwestrak, E., O'Sullivan, M.L., Otto, S., Tiglio, K., Savas, J.N., Yates, J.R., 3rd, Comoletti, D., Taylor, P., and Ghosh, A. (2009). LRRTM2 interacts with Neurexin1 and regulates excitatory synapse formation. Neuron *64*, 799-806.

Dhande, O.S., Hua, E.W., Guh, E., Yeh, J., Bhatt, S., Zhang, Y., Ruthazer, E.S., Feller, M.B., and Crair, M.C. (2011). Development of single retinofugal axon arbors in normal and β2 knock-out mice. The Journal of Neuroscience *31*, 3384-3399.

Dhande, O.S., Stafford, B.K., Lim, J.-H.A., and Huberman, A.D. (2015). Contributions of Retinal Ganglion Cells to Subcortical Visual Processing and Behaviors. Annual Review of Vision Science *1*, 291-328.

Fox, M.A., Sanes, J.R., Borza, D.-B., Eswarakumar, V.P., Fässler, R., Hudson, B.G., John, S.W., Ninomiya, Y., Pedchenko, V., and Pfaff, S.L. (2007). Distinct target-derived signals organize formation, maturation, and maintenance of motor nerve terminals. Cell *129*, 179-193.

Fox, M.A., and Umemori, H. (2006). Seeking long-term relationship: axon and target communicate to organize synaptic differentiation. Journal of neurochemistry *97*, 1215-1231.

Fujino, T., Leslie, J.H., Eavri, R., Chen, J.L., Lin, W.C., Flanders, G.H., Borok, E., Horvath, T.L., and Nedivi, E. (2011). CPG15 regulates synapse stability in the developing and adult brain. Genes & development *25*, 2674-2685.

Guillery, R., and Scott, G. (1971). Observations on synaptic patterns in the dorsal lateral geniculate nucleus of the cat: the C laminae and the perikaryal synapses. Experimental brain research *12*, 184-203.

Hammer, S., Carrillo, G.L., Govindaiah, G., Monavarfeshani, A., Bircher, J.S., Su, J., Guido, W., and Fox, M.A. (2014). Nuclei-specific differences in nerve terminal distribution, morphology, and development in mouse visual thalamus. Neural development *9*, 1.

Hammer, S., Monavarfeshani, A., Lemon, T., Su, J., and Fox, M.A. (2015). Multiple retinal axons converge onto relay cells in the adult mouse thalamus. Cell reports *12*, 1575-1583.

Hamos, J.E., Van Horn, S.C., Raczkowski, D., and Sherman, S.M. (1987). Synaptic circuits involving an individual retinogeniculate axon in the cat. Journal of Comparative Neurology *259*, 165-192.

Hong, Y.K., and Chen, C. (2011). Wiring and rewiring of the retinogeniculate synapse. Current opinion in neurobiology *21*, 228-237.

Hong, Y.K., Park, S., Litvina, E.Y., Morales, J., Sanes, J.R., and Chen, C. (2014). Refinement of the retinogeniculate synapse by bouton clustering. Neuron *84*, 332-339.

Hooks, B.M., and Chen, C. (2006). Distinct roles for spontaneous and visual activity in remodeling of the retinogeniculate synapse. Neuron *52*, 281-291.

Howarth, M., Walmsley, L., and Brown, T.M. (2014). Binocular integration in the mouse lateral geniculate nuclei. Current Biology *24*, 1241-1247.

Huberman, A.D., Feller, M.B., and Chapman, B. (2008a). Mechanisms underlying development of visual maps and receptive fields. Annual review of neuroscience *31*, 479-509.

Huberman, A.D., and Niell, C.M. (2011). What can mice tell us about how vision works? Trends in neurosciences *34*, 464-473.

Huberman, A.D., Wei, W., Elstrott, J., Stafford, B.K., Feller, M.B., and Barres, B.A. (2009). Genetic identification of an On-Off direction-selective retinal ganglion cell subtype reveals a layer-specific subcortical map of posterior motion. Neuron *62,* 327-334.

Jaubert-Miazza, L., Green, E., Lo, F., Bui, K., Mills, J., and Guido, W. (2005). Structural and functional composition of the developing retinogeniculate pathway in the mouse. Visual neuroscience *22,* 661.

Javaherian, A., and Cline, H.T. (2005). Coordinated motor neuron axon growth and neuromuscular synaptogenesis are promoted by CPG15 in vivo. Neuron *45,* 505-512.

Jones, E., and Powell, T. (1969). Electron microscopy of synaptic glomeruli in the thalamic relay nuclei of the cat. Proceedings of the Royal Society of London B: Biological Sciences *172,* 153-171.

Kay, J.N., De la Huerta, I., Kim, I.-J., Zhang, Y., Yamagata, M., Chu, M.W., Meister, M., and Sanes, J.R. (2011). Retinal ganglion cells with distinct directional preferences differ in molecular identity, structure, and central projections. The Journal of Neuroscience *31,* 7753-7762.

Kim, I.-J., Zhang, Y., Meister, M., and Sanes, J.R. (2010). Laminar restriction of retinal ganglion cell dendrites and axons: subtype-specific developmental patterns revealed with transgenic markers. The Journal of Neuroscience *30,* 1452-1462.

Kim, I.-J., Zhang, Y., Yamagata, M., Meister, M., and Sanes, J.R. (2008). Molecular identification of a retinal cell type that responds to upward motion. Nature *452,* 478-482.

Ko, J., Fuccillo, M.V., Malenka, R.C., and Sudhof, T.C. (2009a). LRRTM2 functions as a neurexin ligand in promoting excitatory synapse formation. Neuron *64,* 791-798.

Ko, J., Soler-Llavina, G.J., Fuccillo, M.V., Malenka, R.C., and Sudhof, T.C. (2011). Neuroligins/LRRTMs prevent activity- and Ca2+/calmodulin-dependent synapse elimination in cultured neurons. The Journal of cell biology *194,* 323-334.

Kucukdereli, H., Allen, N.J., Lee, A.T., Feng, A., Ozlu, M.I., Conatser, L.M., Chakraborty, C., Workman, G., Weaver, M., and Sage, E.H. (2011). Control of excitatory CNS synaptogenesis by astrocyte-secreted proteins Hevin and SPARC. Proceedings of the National Academy of Sciences *108,* E440-E449.

LaConte, L.E., Chavan, V., Liang, C., Willis, J., Schönhense, E.-M., Schoch, S., and Mukherjee, K. (2016). CASK stabilizes neurexin and links it to liprin-α in a neuronal activity-dependent manner. Cellular and Molecular Life Sciences *73,* 3599-3621.

Land, P.W., Kyonka, E., and Shamalla-Hannah, L. (2004). Vesicular glutamate transporters in the lateral geniculate nucleus: expression of VGLUT2 by retinal terminals. Brain research *996,* 251-254.

Laurén, J., Airaksinen, M.S., Saarma, M., and õnis Timmusk, T. (2003). A novel gene family encoding leucine-rich repeat transmembrane proteins differentially expressed in the nervous system. Genomics *81*, 411-421.

Liang, C., Kerr, A., Qiu, Y., Cristofoli, F., Van Esch, H., Fox, M.A., and Mukherjee, K. (2017). Optic Nerve Hypoplasia Is a Pervasive Subcortical Pathology of Visual System in Neonates. Investigative Ophthalmology & Visual Science *58*, 5485-5496.

Linhoff, M.W., Lauren, J., Cassidy, R.M., Dobie, F.A., Takahashi, H., Nygaard, H.B., Airaksinen, M.S., Strittmatter, S.M., and Craig, A.M. (2009). An unbiased expression screen for synaptogenic proteins identifies the LRRTM protein family as synaptic organizers. Neuron *61*, 734-749.

Litvina, E.Y., and Chen, C. (2017b). Functional Convergence at the Retinogeniculate Synapse. Neuron *96*, 330-338. e335.

Lund, R., and Cunningham, T. (1972). Aspects of synaptic and laminar organization of the mammalian lateral geniculate body. Invest Ophthalmol *11*, 291-302.

Martersteck, E.M., Hirokawa, K.E., Evarts, M., Bernard, A., Duan, X., Li, Y., Ng, L., Oh, S.W., Ouellette, B., and Royall, J.J. (2017). Diverse Central Projection Patterns of Retinal Ganglion Cells. Cell Reports *18*, 2058-2072.

Mastronarde, D.N. (1992). Nonlagged relay cells and interneurons in the cat lateral geniculate nucleus: receptive-field properties and retinal inputs. Visual neuroscience *8*, 407-441.

Monavarfeshani, A., Sabbagh, U., and Fox, M.A. (2017). Not a one-trick pony: Diverse connectivity and functions of the rodent lateral geniculate complex. Visual Neuroscience *34*.

Moog, U., Kutsche, K., Kortüm, F., Chilian, B., Bierhals, T., Apeshiotis, N., Balg, S., Chassaing, N., Coubes, C., and Das, S. (2011). Phenotypic spectrum associated with CASK loss-of-function mutations. Journal of medical genetics, jmedgenet-2011-100218.

Morgan, J.L., Berger, D.R., Wetzel, A.W., and Lichtman, J.W. (2016). The Fuzzy Logic of Network Connectivity in Mouse Visual Thalamus. Cell *165*, 192-206.

Morin, L.P., and Studholme, K.M. (2014). Retinofugal projections in the mouse. Journal of Comparative Neurology *522*, 3733-3753.

Mukherjee, K., Clark, H.R., Chavan, V., Benson, E.K., Kidd, G.J., and Srivastava, S. (2016). Analysis of Brain Mitochondria Using Serial Block-Face Scanning Electron Microscopy. JoVE (Journal of Visualized Experiments), e54214-e54214.

Muscat, L., Huberman, A.D., Jordan, C.L., and Morin, L.P. (2003). Crossed and uncrossed retinal projections to the hamster circadian system. Journal of Comparative Neurology *466*, 513-524.

Naeve, G.S., Ramakrishnan, M., Kramer, R., Hevroni, D., Citri, Y., and Theill, L.E. (1997). Neuritin: a gene induced by neural activity and neurotrophins that promotes neuritogenesis. Proceedings of the National Academy of Sciences *94*, 2648-2653.

Nedivi, E. (1998). Promotion of Dendritic Growth by CPG15, an Activity-Induced Signaling Molecule. Science *281*, 1863-1866.

Prusky, G.T., West, P.W., and Douglas, R.M. (2000). Behavioral assessment of visual acuity in mice and rats. Vision research *40*, 2201-2209.

Rafols, J.A., and Valverde, F. (1973). The structure of the dorsal lateral geniculate nucleus in the mouse. A Golgi and electron microscopic study. Journal of Comparative Neurology *150*, 303-331.

Rathbun, D.L., Alitto, H.J., Warland, D.K., and Usrey, W.M. (2016). Stimulus contrast and retinogeniculate signal processing. Frontiers in neural circuits *10*.

Rathbun, D.L., Warland, D.K., and Usrey, W.M. (2010). Spike timing and information transmission at retinogeniculate synapses. J Neurosci *30*, 13558-13566.

Rompani, S.B., Müllner, F.E., Wanner, A., Zhang, C., Roth, C.N., Yonehara, K., and Roska, B. (2017). Different Modes of Visual Integration in the Lateral Geniculate Nucleus Revealed by Single-Cell-Initiated Transsynaptic Tracing. Neuron *93*, 767-776. e766.

Sajgo, S., Ghinia, M.G., Brooks, M., Kretschmer, F., Chuang, K., Hiriyanna, S., Wu, Z., Popescu, O., and Badea, T.C. (2017). Molecular codes for cell type specification in Brn3 retinal ganglion cells. Proceedings of the National Academy of Sciences, 201618551.

Sanes, J.R., and Masland, R.H. (2015). The types of retinal ganglion cells: current status and implications for neuronal classification. Annual review of neuroscience *38*, 221-246.

Schmittgen, T.D., and Livak, K.J. (2008). Analyzing real-time PCR data by the comparative CT method. Nature protocols *3*, 1101-1108.

Seabrook, T., Burbridge, T., Crair, M., and Huberman, A. (2017). Architecture, Function, and Assembly of the Mouse Visual System. Annual review of neuroscience *40*, 499.

Shigeoka, T., Jung, H., Jung, J., Turner-Bridger, B., Ohk, J., Lin, J.Q., Amieux, P.S., and Holt, C.E. (2016). Dynamic axonal translation in developing and mature visual circuits. Cell *166*, 181-192.

Siddiqui, T.J., Pancaroglu, R., Kang, Y., Rooyakkers, A., and Craig, A.M. (2010). LRRTMs and neuroligins bind neurexins with a differential code to cooperate in glutamate synapse development. The Journal of neuroscience : the official journal of the Society for Neuroscience *30*, 7495-7506.

Sincich, L.C., Adams, D.L., Economides, J.R., and Horton, J.C. (2007). Transmission of spike trains at the retinogeniculate synapse. The Journal of Neuroscience *27*, 2683-2692.

Singh, S.K., Stogsdill, J.A., Pulimood, N.S., Dingsdale, H., Kim, Y.H., Pilaz, L.-J., Kim, I.H., Manhaes, A.C., Rodrigues, W.S., and Pamukcu, A. (2016). Astrocytes assemble thalamocortical synapses by bridging NRX1α and NL1 via Hevin. Cell *164*, 183-196.

So, K.-F., Campbell, G., and Lieberman, A. (1985). Synaptic organization of the dorsal lateral geniculate nucleus in the adult hamster. Anatomy and embryology *171*, 223-234.

Soler-Llavina, G.J., Fuccillo, M.V., Ko, J., Südhof, T.C., and Malenka, R.C. (2011). The neurexin ligands, neuroligins and leucine-rich repeat transmembrane proteins, perform convergent and divergent synaptic functions in vivo. Proceedings of the National Academy of Sciences *108*, 16502-16509.

Srivastava, S., McMillan, R., Willis, J., Clark, H., Chavan, V., Liang, C., Zhang, H., Hulver, M., and Mukherjee, K. (2016). X-linked intellectual disability gene CASK regulates postnatal brain growth in a non-cell autonomous manner. Acta neuropathologica communications *4*, 30.

Takashima, N., Odaka, Y.S., Sakoori, K., Akagi, T., Hashikawa, T., Morimura, N., Yamada, K., and Aruga, J. (2011). Impaired cognitive function and altered hippocampal synapse morphology in mice lacking Lrrtm1, a gene associated with schizophrenia. PLoS One *6*, e22716.

Taniguchi, H., He, M., Wu, P., Kim, S., Paik, R., Sugino, K., Kvitsani, D., Fu, Y., Lu, J., and Lin, Y. (2011). A resource of Cre driver lines for genetic targeting of GABAergic neurons in cerebral cortex. Neuron *71*, 995-1013.

Trenholm, S., Johnson, K., Li, X., Smith, R.G., and Awatramani, G.B. (2011). Parallel mechanisms encode direction in the retina. Neuron *71*, 683-694.

Um, J.W., Choi, T.Y., Kang, H., Cho, Y.S., Choii, G., Uvarov, P., Park, D., Jeong, D., Jeon, S., Lee, D., *et al.* (2016). LRRTM3 Regulates Excitatory Synapse Development through Alternative Splicing and Neurexin Binding. Cell Rep *14*, 808-822.

Usrey, W.M., Reppas, J.B., and Reid, R.C. (1999). Specificity and strength of retinogeniculate connections. Journal of Neurophysiology *82*, 3527-3540.

Varoqueaux, F., Aramuni, G., Rawson, R.L., Mohrmann, R., Missler, M., Gottmann, K., Zhang, W., Südhof, T.C., and Brose, N. (2006). Neuroligins determine synapse maturation and function. Neuron *51*, 741-754.

Voikar, V., Kulesskaya, N., Laakso, T., Lauren, J., Strittmatter, S.M., and Airaksinen, M.S. (2013). LRRTM1-deficient mice show a rare phenotype of avoiding small enclosures--a tentative mouse model for claustrophobia-like behaviour. Behavioural brain research *238*, 69-78.

Wang, S.W., Kim, B.S., Ding, K., Wang, H., Sun, D., Johnson, R.L., Klein, W.H., and Gan, L. (2001). Requirement for math5 in the development of retinal ganglion cells. Genes & development *15*, 24-29.

Weyand, T.G. (2016). The multifunctional lateral geniculate nucleus. Reviews in the neurosciences *27*, 135-157.

Wilson, J., Friedlander, M., and Sherman, S. (1984). Fine structural morphology of identified X- and Y-cells in the cat's lateral geniculate nucleus. Proceedings of the Royal Society of London Series B, Biological Sciences, 411-436.

Wong, A., and Brown, R. (2006). Visual detection, pattern discrimination and visual acuity in 14 strains of mice. Genes, Brain and Behavior *5*, 389-403.

Yeh, C.-I., Stoelzel, C.R., Weng, C., and Alonso, J.-M. (2009). Functional consequences of neuronal divergence within the retinogeniculate pathway. Journal of neurophysiology *101*, 2166-2185.

4. Discussion and Future Perspective

In my PhD, I undertook a series of studies that revealed new aspects of retinogeniculate circuitry in the dLGN. I discovered a novel molecular mechanism that underlies the development of this circuit. In this section, I discuss why learning about mechanisms underlying the development of neural circuit in the mouse visual system, particularly dLGN, is important (from a translational perspective) and how my findings fit with the existing literature regarding circuitry and information processing mechanisms in the subcortical visual system (from a basic science perspective).

4.1. Rebuilding vision through regenerative therapies

Our visual ability relies on properly wired neural circuits that connect the retina to different visual centers in the brain. Retinal ganglion cells (RGCs) send visual information to several different subcortical nuclei in the brain, including the dorsal Lateral Geniculate Nucleus (dLGN) of the thalamus and the Superior Colliculus (SC) of the midbrain (Berson, 2008; Morin and Studholme, 2014). From subcortical regions, visual information is transferred to higher cortical areas and transformed into visual perceptions (Dhande and Huberman, 2014). Traumatic injuries to the optic nerve and neurodegenerative diseases of the visual system such as glaucoma (Danesh-Meyer and Levin, 2015; Gupta and Yücel, 2007) and optic nerve hypoplasia (Borchert, 2012; Kaur et al., 2013), disrupt the retinofugal pathway between retina and brain and lead to permanent and irreversible loss of vision. While there are currently no effective treatments for these debilitating conditions, regenerative strategies with the aim of repairing or replacing these damaged neuronal circuits are one of the most promising options for restoring partial or full visual function (Crair and Mason, 2016; Goldberg and Guido, 2016). *What information do we*

need and how should we implement it in order to rebuild or repair a disrupted visual circuit? Although my discussion is focused on conditions that impair RGCs and their projections to subcortical regions, these regenerative strategies can be applied to impairments and injuries which affect other neural circuits in the visual system or other sensory systems.

Two main regenerative strategies are being investigated depending on the type of damage to the visual circuit (Benowitz et al., 2017; Mead et al., 2015). In the first approach, damaged or lost RGCs are replaced with new cells through transplantation of stem cell-derived RGCs. Different sources of stem cells can be used in this approach, such as bone marrow derived mesenchymal stem cells (BMSC), neural stem cells or embryonic/induced pluripotent stem cells. A major difficulty with replacing RGCs in the retina is the generation of all different classes of RGCs, which exceed 40. Theoretically, each distinct class of RGCs requires a unique stem cell differentiation protocol.

In the second approach, the regeneration capacity of damaged RGCs is activated so they can regrow their severed axons and re-innervate the retinorecipient target regions in the brain (Crair and Mason, 2016; Gao et al., 2012). However, axonal regeneration approaches can be combined with stem cell transplantation so that stem cells act as a source of neurotrophic factors. To regrow, injured axons must form new growth cones and must have a permissive environment. Yet, in the case of injured RGCs, neither intrinsic intracellular mechanisms nor extracellular environment are in favor of regeneration. RGC axonal regeneration is prevented by the initiation of intrinsic mechanisms which repress growth cone formation, and by an unfavorable environment around the injury site due to glial scarring (Yiu and He, 2006). Therefore, both intrinsic and extrinsic mechanisms of axonal regrowth need to be reprogrammed into a state that favors appropriate regrowth of the axons. While the process of axonal outgrowth in early

development is mainly through “tethered growth”, the regrowth of injured RGC axons in a mature neural circuit is completely *de novo*. This *de novo* outgrowth requires a constant supply of energy and continuous transport of axonal building blocks (e.g. lipids, proteins etc.) from the cell body to the growth cone. Moreover, newly formed growth cones must travel a long way through optic nerve and optic tract to reach their destinations which may take them several weeks or months (He and Jin, 2016). The optic nerve and optic tract environments should also permit the myelination of the regrown axons. After arriving at the correct regions, RGC axons need to select one or more distinct types of cells and even specific subcellular parts of the target cells (e.g. proximal versus distal dendrites). On the other hand, target regions of newly innervating axons must permit the formation, maturation and refinement of new synapses. In dLGN, retinal projections make up only a small portion of (5-10%) of the total inputs onto relay cells and majority of the inputs arise from non-retinal projections (e.g. cortical feedback inputs, tectal inputs and brainstem inputs). During development, these non-retinal projections influence the formation and organization of retinal inputs.

Therefore, regeneration of the whole circuit in a mature visual system requires the reactivation (or replacement) of many of these intrinsic and extrinsic developmentally-regulated targeting and differentiation mechanisms. This suggests, the regeneration of the whole visual circuits is only possible if regeneration capacity of all different parts of the circuit is reactivated. However, it is important to ask whether we need to rebuild the whole circuit or only a small portion of the circuit in order to achieve a functional and beneficial outcome (Moore and Goldberg, 2010).

Despite remarkable progress in regenerating retinal axons and identifying axonal guidance cues (Bei et al., 2016; de Lima et al., 2012a; de Lima et al., 2012b; Duan et al., 2015;

Fox and Guido, 2011; Lim et al., 2016; Liu et al., 2011; Lu et al., 2014; Park et al., 2008; Singh et al., 2011; Su et al., 2011), regenerated axons fail to assemble fully-functional synapses and restore normal visual behaviors, creating a vital need for a better understanding of the synaptic assembly mechanisms in retinorecipient nuclei. Our studies (Hammer et al., 2014; Hammer et al., 2015) and others (Morgan et al., 2016) showed that, in the dLGN, RTs not only form larger retinogeniculate (RG) synapses (compared to other target regions in the mouse brain), they participate in forming "complex" RG synapses in which several distinct RTs converge onto a short length of a thalamic cell dendrite. *How do RTs in dLGN obtain their unique morphology? What is the functional significance of these differences synaptic organizations?* Answers to these questions are critical for regeneration of functional RG synapses in dLGN, which are the main and most important conduits of image-forming visual information from retina to the primary visual cortex (V1). Although both RGC- and dLGN-derived cues can play roles in the differentiation of RG synapses, in this dissertation (chapter 3), I focused on identification and characterization of target-derived signals. To do that, I compared the whole transcriptome of the dLGN and its adjacent nucleus, vLGN, (both of which receive dense retinal inputs) during different stages of RG synapse development in mice. My RNAseq screen revealed *Lrrtm1* as an important factor required for development of complex RG synapses in dLGN.

In order to understand if *Lrrtm1* is truly a potential candidate for regenerative therapies aimed at restoring RG circuit further studies are needed to investigate its mechanism of action as well as its role in higher mammals such non-human primates and humans. For example, *is expression of exogenous LRRTM1 in other retinorecipient nuclei (e.g. vLGN and SC) sufficient to induce complex RG synapse formation? Does the primate and human dLGN contain LRRTM1 and complex RG synapses? Do complex RG synapses play an important role in primate or*

human vision? Are there safe ways to express this exogenous transmembrane protein in human dLGN relay cells? While studies in cats and rats have shown the presence of complex RG synapse in dLGN, currently no data is available on the existence and prevalence of complex RG synapses in non-human primates and humans. Moreover, in cats and rats it is not completely understood what fraction of total RG synapses belong to complex RG synapses. Our data in mice indicates that majority of RTs participate in forming complex RG synapse. With the aim of answering some of the questions that I mentioned above, I generated lentivirus and adeno-associated viruses (AAVs) that contain plasmid constructs of mouse LRRTM1 and GFP reporter proteins. While *in vitro* experiments showed that infected HEK cells with these viruses are producing LRRTM1 protein, we could not show that the translated LRRTM1 proteins are correctly inserted in the plasma membrane. More studies are needed on the mechanism of LRRTM1 transportation to the plasma membrane in order to make sure that the overexpressed protein is placed in the right compartment of the neural processes.

4.2. Convergence of RG synapse: anatomical versus functional studies

Until recently, the dLGN has been known as a simple relay center connecting retinal ganglion cells to primary visual cortex. For dLGN to act as a mere relay center, dLGN relay cells must preserve the retinal information, and then send that information to visual cortex without modifying it. In this relay mode, first, a heterogeneous population of relay cells must be present in dLGN in order to carry distinct visual information passed to them by retinal inputs. Second, the local circuitry of dLGN cells must be simple in order to prevent processing and modification of received visual signals. Third, functional properties of dLGN cells (e.g. their receptive field) are expected to be similar to those of RGCs. Fourth, retinal input onto relay cells must arise from

one class of RGCs and even a few number of RGCs (~1-3). Emerging anatomical and physiological studies in mice, however, do not fully support this relay mode (Kerschensteiner and Guido, 2017; Litvina and Chen, 2017a; Monavarfeshani et al., 2017; Morgan, 2017; Morgan et al., 2016).

So far, only three groups of dLGN relay cells have been characterized based on their morphology and their physiological responses to visual stimuli. These groups of cells resemble those identified in other mammals (e.g. X, Y and W cells of cat dLGN) and they show region-specific distribution in the mouse dLGN. X-like cells are more present on the shell of the dLGN, Y-like cells are found more in the core region of the dLGN and X-like cells (as well as local interneurons) were dispersed throughout the dLGN. While the presence of these three groups of relay cells suggests at least three channels of visual information exist in dLGN, they are far fewer than the number of distinct classes retinal ganglion cells in retina which is around 40. If different image-forming classes of RGCs send feature-specific visual information to relay cells in dLGN, there should be more than three classes of relay cells in dLGN in order to transmit that information to the visual cortex through parallel, unmixed channels. New advances in single cell sequencing and tracing techniques will help to investigate whether more unidentified classes of relay cells exist.

The circuitry of the dLGN exhibits a high level of complexity. dLGN receives many other inputs (reviewed in the introduction section) from a variety of other sources beside retinal inputs. Complex circuity of the dLGN endows this nucleus with the ability to shape and process retinal information before passing them to primary visual cortex. In most mammals, dLGN relay cells are responsive to distinct visual features (e.g. direction and orientation of movement) (Cheong et al., 2013; Cruz-Martín et al., 2014; Ling et al., 2015; Marshel et al., 2012; Piscopo et

al., 2013; Scholl et al., 2013; Zhao et al., 2013), which previously have been thought to be generated through cortical processing (Alonso et al., 2001; Hubel and Wiesel, 1972).

Moreover, recent studies, including our own (chapter 1), revealed a high level of retinal convergence onto dLGN relay cells, both anatomically and functionally (Hammer et al., 2015; Litvina and Chen; Morgan et al., 2016; Rompani et al., 2017). Thus, visual information in dLGN may undergoes striking transformation (i.e. integration of distinct retinal inputs and many other non-retinal inputs).

Two approaches have been applied to investigate the functional connectivity in the retinogeniculate pathway. In the first approach, a stimulating electrode is placed on the surface of the optic tract, and 0.6-1.2 mm away from that, a recording electrode is patched onto a dLGN relay cell. Various intensities of the stimulus are applied to the optic tract to identify two parameters; the minimum stimulus intensity capable of evoking an EPSC in a dLGN relay cell and the maximum stimulus intensity required to generate the maximum EPSC in that dLGN relay cell. The EPSC triggered by minimum stimulus intensity is suggested to be driven by a single RGC axon while the maximum EPSC by all of the RGC inputs to that given dLGN cell. The fraction of single axon EPCS to all axon EPSC (called fiber fraction) is used to estimate the number of functional inputs onto a dLGN cell (Chen and Regehr, 2000; Hooks and Chen, 2006; Jaubert-Miazza et al., 2005). Likewise, a plot of EPSP against the stimulus intensity is drawn and the number of steps in the graph is used to estimate the number of axons. Using fiber fraction value, it has been estimated that between 10 to 20 weak RGC inputs converge onto a dLGN relay cells prior to the eye-opening (p12-p14). However, after eye-opening and during the adulthood many of this weak inputs disappear and only a few (1-3) RGC inputs remain which can strongly

drive large amplitude EPSP in the geniculate cells. I should note that most of these experiments have been done on brain tissues *in vitro* and in rodents.

In another approach which have mainly been applied *in vivo* and in higher mammals (e.g. monkeys and cats), the activity of a dLGN relay cells is recorded extracellularly in anesthetized animals while its paired RGC is stimulated by light signals. A visual stimulus is delivered to the center of one RGC receptive field and recording electrode(s) is advanced down gradually in the tissue until it encounters a strong EPSP that can drive a dLGN relay cell to spike. Recording electrodes are inserted into the dLGN through a guide tube positioned 5 mm above the LGN. A cohort of studies (Cleland et al., 1971; Cleland and Lee, 1985; Mastronarde, 1992; Sincich et al., 2007; Usrey et al., 1999; Weyand, 2007; Yeh et al., 2009) using different versions of this approach suggested that spikes of one RGC can diverge onto as many as 10 (X cells in cats) to 20 (Y cells in cats) dLGN relay cells. On the other hand, one dLGN relay cell can receive converging inputs from 1-4 RGCs. These studies demonstrated that about 90% of spikes in a dLGN relay cell is driven by one dominant RGC inputs, suggesting that the actual functional ratio of RGC-dLGN connection is close to 1:1 and the other converging RGC inputs are weak and non-driving retinal inputs. Considering the degree of retinal divergence, the number of dLGN relay cells (estimated to be around 500K cells) and the number of RGCs in the retina (estimated to be around 100K cells), a high level (80%) of synchronicity is expected among dLGN relay cells. However, the maximum level of correlated spiking activity that has been observed between two X cells in dLGN of cats was around 40% (with an average of 10%) (Yeh et al., 2009). This suggest a lower functional divergence compared to the observed divergence of retinal projections.

Convergence and divergence of retinal projections in dLGN are mechanisms that endow relay cells with a higher processing power. It enables them to alter retinal information so they can extract specific features of the visual scene (e.g. novel receptive field) (Sherman, 2016; Weyand, 2016). Early electron microscopy observations in cats dLGN indicated the presence of convergent and divergent retinal projections in a cell-specific way, with Y cells receiving more convergent inputs (~10 RGC inputs) than X cells (1 RGC input) (Hamos et al., 1987; Robson, 1993). Recently, serial block-face scanning electron microscopy has made it possible to reconstruct neural circuits in 3D and obtain a more precise anatomical view of the circuits. Using SBFSEM, we and others (Hammer et al., 2015; Morgan et al., 2016) discovered a high level of retinal convergence onto dLGN relay cells in mice. Our EM reconstruction data (chapter 2) revealed more than a dozen of distinct RGC axons converging at a shared region of a single dLGN relay cell dendrite. These sites of retinal convergence have been observed previously in cats. Although less obvious than astrocytic wrapping around simple encapsulated RG synapses, astrocytic process are present around these complex RG synapses. Morgan *et al*. reconstructed a large number of full dLGN relay cells and their RGC projections in mouse dLGN (400*600*280 μm) and found that up to 40 RGC axons can converge onto different dendritic branches of a single dLGN relay cell (convergence at a cellular level). Similar to our finding (Hammer et al. 2015), they also reported up to a dozen distinct retinal terminal clustered at the site of complex RG synapses (convergence at a subcellular level). One important limitation of these EM studies is that the reconstructed neural circuits are still only a small portion of the whole visual circuit. It is possible that RGC axons split into multiple branches in the optic tract or even optic nerve (which is not included in the reconstructed area) and these distinct retinal terminals in complex RG synapses are actually different axonal segments of a single RGC axon. To overcome this

issue, we used brainbow tract-tracing (chapter 2) by injecting AAVs into the vitreous humor of mice that express Cre recombinase in their RGCs. The brainbow AAVs has been shown to distinctively label infected neurons (an in this case, RGCs) with different and distinct colors (Cai et al., 2013; Robles et al., 2013). Our brainbow labeling of axons suggested that individual axons that cluster together and form complex RG synapses are in fact coming from distinct RGCs. The subcellular convergence of retinal projections at the site of complex RG synapse may serves as a substrate for the refinement and reorganization of RG synapses in dLGN during development. It has been shown that axonal arbors of a single RGC can undergo refinement through reorganization and clustering of synaptic boutons along the arbors instead of extension or retraction of axonal branches (Hong et al., 2014).

More recently, another group (Rompani et al., 2017) used retrograde trans-synaptic rabies virus and traced one single dLGN cell and all RGCs that innervate that cell. Their data revealed a significantly high level of retinal convergence onto dLGN cells. Their data suggested three modes of visual information transfer in the dLGN. First, a classic relay mode in which 1-5 RGCs from a same class project to a dLGN relay cell. However, the name “relay” still does not seem suitable considering all other non-retinal inputs onto each dLGN relay cells. Second, a combination mode, in which 6-36 RGCs make synapses onto a single dLGN cell and interestingly their morphological properties, suggested that these RGCs are from different classes. Third, a binocular combination-mode in which up to 91 RGCs from both eyes projects to one dLGN cells. Interestingly, in the binocular combination mode the RGCs form contralateral eye found to be from different classes (based on morphological clustering of the labeled RGCs) but the ipsilateral eye from same class. It should be noted that the efficacy and fidelity of the trans-synaptic viral transmission, and the approach by which identified RGCs have been

assigned to a different RGC classes, are two limiting factor of this trans-synaptic tracing technique that might have impacted the reported numbers in this unexpected results. It would be interesting to find out whether binocular inputs onto dLGN cells converge at the site of complex RG synapses or they are distributed on different dendritic branches of relay cells. Regardless of the anatomical organization, convergence of retinal inputs from both eyes to relay cells (Grieve, 2005; Howarth et al., 2014; Rompani et al., 2017) can provide a substrate for experience-dependent ocular dominance plasticity in the dLGN of mice. In a recent study by Jaepel et al. (2017), the activity of relay cell axonal boutons in the layer 1 of V1 has been recorded using two-photon Ca^{2+} imaging in live animals for 4 weeks. They chronically recorded eye-specific activity from relay cell boutons before and after monocular deprivation and found a significant ocular dominance shift in dLGN cells. Despite having an elegant design, I think this study failed to prove that they only recorded from geniculocortical boutons.

Important questions arise from these anatomical studies: *Are all these convergent retinal inputs functional and capable of modifying dLGN activity? Is information content of converging retinal inputs different from each other? Is this convergence has any functional significance for vision?* In a recent study, using optogenetics, Litviana and Chen (2017b) identified around 10 functional retinal inputs onto a single dLGN relay cell, a number five times larger than what they have reported before. However, using a computational simulation, they estimated that only 30% of all convergent inputs onto one relay cell are capable of driving the relay cell to spike and the rest of retinal inputs are weak and perhaps modulatory. Unfortunately, the criteria used to define a “strong” driving retinal input is quite different from those used to assess driving inputs in early development, making it an inconsistent threshold to use. Therefore, it is unclear whether the “cut

off" used in this study to identify strong retinal inputs is reliable or not. Overall, results from this study revealed the existence of functional retinal convergence in dLGN.

Following the recognition of parallel pathways for the transmission of somatosensory information from the peripheral nerves to the brain, a similar parallel organization in the visual system has been predicted (Bishop, 1933). This prediction was based on variation in the size and conduction velocity of retinal axon in the optic nerve. The concept of parallel pathways in the visual system had been strengthened by continuously growing discoveries expanding the list of morphologically and functionally distinct classes of retinal ganglion cells in the retina (Stone, 2013). Moreover, in all main animal models used for studying the visual system (i.e. non-human primates, cats and rodents) at least three groups of neurons (parallel channels) in the dLGN have been identified. In primate dLGN, M cells provide a channel for visual information about motion and contrast, P cells carry information relevant to form, color and spatial frequency and K cells provide channels for a mixture of visual properties such orientation and color (Hendry and Reid, 2000). X, Y and W cells in cats and X-like, Y-like and W-like cells in rodents are different classes of dLGN cells resembling primate M, P and K cells, respectively. Most studies in mammals agree upon the existence of parallel visual sensory pathways in the retina until they reaches to the dLGN. However, how many pathways exist in subcortical visual system and how dLGN convey feature-specific visual information to primary visual cortex is not well understood.

A question that arises from these findings is: *how many features are parsed out in the retina and how many of them are transferred through parallel pathways to visual cortex?* Recent findings mentioned above, and findings included in this dissertation, which show a high degree of retinal convergence in dLGN, indicate the possibility of mixing different visual information in dLGN (at a subcortical level) which is in contract to the more classical view of parallel pathway

that proposes V1 as the sole site for integration of different visual pathways (Denman and Contreras, 2016; Gao et al., 2010) .

For this parallel organization concept to work in dLGN of mice, distinct relay cells must show specificity for different features of the sensory visual information they receive. Theoretically, they should show variation in their morphology (similar to what we see among RGCs). However, anatomical tracing studies in dLGN have yet to reveal such diversity in the morphology of relay cells. From a spatial perspective, the presence of topographic organization among both RGC axons, in the dLGN, and dLGN relay cells axons, in the primary visual cortex, indicates that there are, certainly, unmixed pathways which carry space-specific visual information regarding different locations of the visual field. These space-specific pathways enable the visual system to preserve a continues representation of spatial information from retina to brain (Cang and Feldheim, 2013; Feldheim et al., 1998; Huberman et al., 2008a; Pfeiffenberger et al., 2006). If other features of the visual information require parallel channels, then, each of these space-specific channels needs to contain several feature-specific sub-pathways. Homogenous distribution of distinct RGC classes (e.g. ON-OFF direction selective RGCs) suggests an anatomical framework for parallel processing of visual information in the retina. However, evidence for the existence of similar pathways in dLGN to the primary visual cortex is in pale. Only three classes of relay cells have been identified and their spatial distribution is not completely resolved.

Electrophysiological recording of the dLGN relay cells shows a near unitary matching between RGCs and dLGN cells, suggesting a one-to-one relationship between RGCs and dLGN relay cells and, therefore, supporting the existence of parallel pathways (Glees and le Gros Clark, 1941; Piscopo et al., 2013). Moreover, functional properties of the neurons in the dLGN

(Denman and Contreras, 2016) and primary visual cortex (Gao et al., 2010) of mice suggest separation of functional channels from the dLGN to the primary visual cortex. In the dLGN most of the cells (a ratio of 9:1) showed linear spatial summation which is similar to the number of RGCs exhibiting linearity of spatial summation within their receptive field (Denman and Contreras, 2016; Stone and Pinto, 1993). Overall, so far, current electrophysiological recording in dLGN and V1 suggest that integration and mixing of visual information ocuurs mainly in V1. Recent advances in optogenetics and recording approaches, as well as in anatomical tracing techniques, will help to shed light on the discrepancies between anatomical observation and functional recording data.

4.3. Lrrtm1 mechanism of action

Leucine-rich repeat transmembrane proteins (LRRTM1-4) (de Wit et al., 2009; Ko et al., 2009a; Linhoff et al., 2009; Siddiqui et al., 2010; Siddiqui et al., 2013) and neuroligins (NL1-4) (Budreck and Scheiffele, 2007; Chih et al., 2005; Chubykin et al., 2007; Craig and Kang, 2007; Graf et al., 2004; Ichtchenko et al., 1995; Ichtchenko et al., 1996; Ko et al., 2009b; Varoqueaux et al., 2006; Varoqueaux et al., 2004) are located at the postsynaptic membranes and interact with three members of presynaptic neurexins (NXN1-3). These interactions have been shown to be important for the assembly, maturation, and maintenance of synapses. Moreover, several members of these protein families are associated with neurological disorders such as autism and schizophrenia (de Wit and Ghosh, 2014, 2015; de Wit et al., 2011; Francks et al., 2007; Sousa et al., 2010; Südhof, 2008). In chapter 3, I showed that LRRTM1, which is generated by postsynaptic relay cells, is important for the development of complex retinogeniculate synapses

around the time of eye-opening in dLGN of mice. *How does lack of this transmembrane adhesion molecule can cause a dramatic reduction in the number of complex RG synapses?*

While *in vitro* overexpression of *Lrrtm1* led to increased synapse formation (Linhoff et al., 2009), *Lrrtm1* knock down experiments did not result in any alteration in synapse density (Ko et al., 2011). However, simultaneous knock down of other neurexin binding partners (i.e. Lrrtm2, NL1 and NL3) along with *Lrrtm1* led to a significant reduction in synapse density in cultured neurons. This suggests an overlapping and compensatory relationship among these neurexin binding partners. Interestingly, this synapse reduction in cultured neurons was prevented by blocking synaptic activity, suggesting that the synapse loss induced by removal of LRRTMs and NLs is due to increased synapse elimination and not due to decreased synapse formation (Ko et al., 2011). Overall *in vitro* studies suggested that *Lrrtm1* can prevent activity-dependent refinement of excitatory synapses. In chapter 3, I showed the lack of LRRTM1 can reduce the number of clustered (smaller) RTs and instead increase the number of simple and larger RTs.

It is plausible to hypothesize that the removal of *Lrrtm1* from relay cells leads to an increased rate, or more effective, experience-dependent refinement of retinal terminals in the retinogeniculate circuit. Our time course anatomical study of retinal terminals indicates that the reduction in the number of larger RG synapses in mice lacking LRRTM1 start around eye-opening (despite reaching a statistical significance level), the time that coincide with a surge in the expression of LRRTM1. Comparing mutant and control mice using SBFSEM and brainbow tracing will help to confirm at what time point during development of retinogeniculate circuit this reduction of complex RG synapses occurs. Thus, it is possible that in wild type mice LRRTM1 is promoting clustering of RTs and keeping dLGN in a more unrefined and plastic

state. If this is true, *Lrrtm1* can potentially increase the rewiring capacity of the retinogeniculate circuit. I can assume that *Lrrtm1* expression (and complex RG synapses) are a way of conserving a readily available anatomical substrate for functional reorganization of synapses. Therefore, it would be interesting to remove *Lrrtm1* at different time points during development using conditional *Lrrtm1* mutant mice in order to study the exact role of *Lrrtm1* in the refinement of retinogeniculate circuit. Increases in the expression of *Lrrtm1* mRNA and protein around eye-opening suggest that the expression of this gene might be regulated through an activity-dependent mechanism. While, an *in vitro* study showed that *Lrrtm1* expression is indeed regulated by neural activity and nuclear calcium singling (Hayer and Bading, 2015), our *in vivo* late dark rearing of mice (for 10 days) did not reveal any changes in the expression of *Lrrtm1* mRNA. In the future, measuring *Lrrtm1* expression after complete removal of retinal activity (e.g. using enucleation or testing it in transgenically blind *Math5*$^{-/-}$ mice) may answer whether *Lrrtm1* level of expression depends on retinal activity and shed more light on novel roles that this synaptic organizer may play in activity-dependent refinement of retinogeniculate circuit.

References

Alonso, J.-M., Usrey, W.M., and Reid, R.C. (2001). Rules of connectivity between geniculate cells and simple cells in cat primary visual cortex. J Neurosci *21*, 4002-4015.

Bei, F., Lee, H.H.C., Liu, X., Gunner, G., Jin, H., Ma, L., Wang, C., Hensch, T.K., Frank, E., and Sanes, J.R. (2016). Restoration of Visual Function by Enhancing Conduction in Regenerated Axons. Cell *164*, 219-232.

Benowitz, L.I., He, Z., and Goldberg, J.L. (2017). Reaching the brain: advances in optic nerve regeneration. Experimental neurology *287*, 365-373.

Berson, D. (2008). Retinal ganglion cell types and their central projections. The senses: a comprehensive reference *1*, 491-520.

Bishop, G. (1933). Fiber groups in the optic nerve. American Journal of Physiology--Legacy Content *106*, 460-474.

Borchert, M. (2012). Reappraisal of the optic nerve hypoplasia syndrome. Journal of Neuro-ophthalmology *32*, 58-67.

Budreck, E.C., and Scheiffele, P. (2007). Neuroligin-3 is a neuronal adhesion protein at GABAergic and glutamatergic synapses. European Journal of Neuroscience *26*, 1738-1748.

Cai, D., Cohen, K.B., Luo, T., Lichtman, J.W., and Sanes, J.R. (2013). Improved tools for the Brainbow toolbox. Nature methods *10*, 540-547.

Cang, J., and Feldheim, D.A. (2013). Developmental mechanisms of topographic map formation and alignment. Annual review of neuroscience *36*, 51-77.

Chen, C., and Regehr, W.G. (2000). Developmental remodeling of the retinogeniculate synapse. Neuron *28*, 955-966.

Cheong, S.K., Tailby, C., Solomon, S.G., and Martin, P.R. (2013). Cortical-like receptive fields in the lateral geniculate nucleus of marmoset monkeys. J Neurosci *33*, 6864-6876.

Chih, B., Engelman, H., and Scheiffele, P. (2005). Control of excitatory and inhibitory synapse formation by neuroligins. Science *307*, 1324-1328.

Chubykin, A.A., Atasoy, D., Etherton, M.R., Brose, N., Kavalali, E.T., Gibson, J.R., and Südhof, T.C. (2007). Activity-dependent validation of excitatory versus inhibitory synapses by neuroligin-1 versus neuroligin-2. Neuron *54*, 919-931.

Cleland, B., Dubin, M., and Levick, W. (1971). Simultaneous recording of input and output of lateral geniculate neurones. Nature *231*, 191-192.

Cleland, B., and Lee, B. (1985). A comparison of visual responses of cat lateral geniculate nucleus neurones with those of ganglion cells afferent to them. The Journal of physiology *369*, 249-268.

Craig, A.M., and Kang, Y. (2007). Neurexin–neuroligin signaling in synapse development. Current opinion in neurobiology *17*, 43-52.

Crair, M.C., and Mason, C.A. (2016). Reconnecting eye to brain. J Neurosci *36*, 10707-10722.

Cruz-Martín, A., El-Danaf, R.N., Osakada, F., Sriram, B., Dhande, O.S., Nguyen, P.L., Callaway, E.M., Ghosh, A., and Huberman, A.D. (2014). A dedicated circuit links direction-selective retinal ganglion cells to the primary visual cortex. Nature *507*, 358-361.

Danesh-Meyer, H.V., and Levin, L.A. (2015). Glaucoma as a Neurodegenerative Disease. Journal of Neuro-Ophthalmology *35*, S22-S28.

de Lima, S., Habboub, G., and Benowitz, L.I. (2012a). Combinatorial therapy stimulates long-distance regeneration, target reinnervation, and partial recovery of vision after optic nerve injury in mice. International review of neurobiology *106*, 153-172.

de Lima, S., Koriyama, Y., Kurimoto, T., Oliveira, J.T., Yin, Y., Li, Y., Gilbert, H.-Y., Fagiolini, M., Martinez, A.M.B., and Benowitz, L. (2012b). Full-length axon regeneration in the adult mouse optic nerve and partial recovery of simple visual behaviors. Proceedings of the National Academy of Sciences *109*, 9149-9154.

de Wit, J., and Ghosh, A. (2014). Control of neural circuit formation by leucine-rich repeat proteins. Trends in neurosciences *37*, 539-550.

de Wit, J., and Ghosh, A. (2015). Specification of synaptic connectivity by cell surface interactions. Nature Reviews Neuroscience.

de Wit, J., Hong, W., Luo, L., and Ghosh, A. (2011). Role of leucine-rich repeat proteins in the development and function of neural circuits. Annual review of cell and developmental biology *27*, 697-729.

de Wit, J., Sylwestrak, E., O'Sullivan, M.L., Otto, S., Tiglio, K., Savas, J.N., Yates, J.R., 3rd, Comoletti, D., Taylor, P., and Ghosh, A. (2009). LRRTM2 interacts with Neurexin1 and regulates excitatory synapse formation. Neuron *64*, 799-806.

Denman, D.J., and Contreras, D. (2016). On Parallel Streams through the Mouse Dorsal Lateral Geniculate Nucleus. Frontiers in neural circuits *10*.

Dhande, O.S., and Huberman, A.D. (2014). Retinal ganglion cell maps in the brain: implications for visual processing. Current opinion in neurobiology *24*, 133-142.

Duan, X., Qiao, M., Bei, F., Kim, I.-J., He, Z., and Sanes, J.R. (2015). Subtype-specific regeneration of retinal ganglion cells following axotomy: effects of osteopontin and mTOR signaling. Neuron *85*, 1244-1256.

Feldheim, D.A., Vanderhaeghen, P., Hansen, M.J., Frisén, J., Lu, Q., Barbacid, M., and Flanagan, J.G. (1998). Topographic guidance labels in a sensory projection to the forebrain. Neuron *21*, 1303-1313.

Fox, M.A., and Guido, W. (2011). Shedding light on class-specific wiring: development of intrinsically photosensitive retinal ganglion cell circuitry. Molecular neurobiology *44*, 321-329.

Francks, C., Maegawa, S., Laurén, J., Abrahams, B.S., Velayos-Baeza, A., Medland, S.E., Colella, S., Groszer, M., McAuley, E., and Caffrey, T.M. (2007). LRRTM1 on chromosome 2p12 is a maternally suppressed gene that is associated paternally with handedness and schizophrenia. Molecular psychiatry *12*, 1129-1139.

Gao, E., DeAngelis, G.C., and Burkhalter, A. (2010). Parallel input channels to mouse primary visual cortex. J Neurosci *30*, 5912-5926.

Gao, H., Zhang, H.L., Shou, J., Chen, L., Shen, Y., Tang, Q., Huang, J., and Zhu, J. (2012). Towards retinal ganglion cell regeneration. Regenerative medicine *7*, 865-875.

Glees, P., and le Gros Clark, W. (1941). The termination of optic fibres in the lateral geniculate body of the monkey. Journal of anatomy *75*, 295.

Goldberg, J.L., and Guido, W. (2016). Report on the National Eye Institute Audacious Goals Initiative: Regenerating the Optic NerveReport on NEI Audacious Goals Initiative. Investigative ophthalmology & visual science *57*, 1271-1275.

Graf, E.R., Zhang, X., Jin, S.-X., Linhoff, M.W., and Craig, A.M. (2004). Neurexins induce differentiation of GABA and glutamate postsynaptic specializations via neuroligins. Cell *119*, 1013-1026.

Grieve, K.L. (2005). Binocular visual responses in cells of the rat dLGN. The Journal of physiology *566*, 119-124.

Gupta, N., and Yücel, Y.H. (2007). Glaucoma as a neurodegenerative disease. Current opinion in ophthalmology *18*, 110-114.

Hammer, S., Carrillo, G.L., Govindaiah, G., Monavarfeshani, A., Bircher, J.S., Su, J., Guido, W., and Fox, M.A. (2014). Nuclei-specific differences in nerve terminal distribution, morphology, and development in mouse visual thalamus. Neural development *9*, 1.

Hammer, S., Monavarfeshani, A., Lemon, T., Su, J., and Fox, M.A. (2015). Multiple retinal axons converge onto relay cells in the adult mouse thalamus. Cell reports *12*, 1575-1583.

Hamos, J.E., Van Horn, S.C., Raczkowski, D., and Sherman, S.M. (1987). Synaptic circuits involving an individual retinogeniculate axon in the cat. Journal of Comparative Neurology *259*, 165-192.

Hayer, S.N., and Bading, H. (2015). Nuclear calcium signaling induces expression of the synaptic organizers Lrrtm1 and Lrrtm2. The Journal of biological chemistry *290*, 5523-5532.

He, Z., and Jin, Y. (2016). Intrinsic control of axon regeneration. Neuron *90*, 437-451.

Hendry, S.H., and Reid, R.C. (2000). The koniocellular pathway in primate vision. Annual review of neuroscience *23*, 127-153.

Hong, Y.K., Park, S., Litvina, E.Y., Morales, J., Sanes, J.R., and Chen, C. (2014). Refinement of the retinogeniculate synapse by bouton clustering. Neuron *84*, 332-339.

Hooks, B.M., and Chen, C. (2006). Distinct roles for spontaneous and visual activity in remodeling of the retinogeniculate synapse. Neuron *52*, 281-291.

Howarth, M., Walmsley, L., and Brown, T.M. (2014). Binocular integration in the mouse lateral geniculate nuclei. Current Biology *24*, 1241-1247.

Hubel, D.H., and Wiesel, T.N. (1972). Laminar and columnar distribution of geniculo-cortical fibers in the macaque monkey. Journal of Comparative Neurology *146*, 421-450.

Huberman, A.D., Feller, M.B., and Chapman, B. (2008a). Mechanisms underlying development of visual maps and receptive fields. Annual review of neuroscience *31*, 479-509.

Ichtchenko, K., Hata, Y., Nguyen, T., Ullrich, B., Missler, M., Moomaw, C., and Südhof, T.C. (1995). Neuroligin 1: a splice site-specific ligand for β-neurexins. Cell *81*, 435-443.

Ichtchenko, K., Nguyen, T., and Südhof, T.C. (1996). Structures, alternative splicing, and neurexin binding of multiple neuroligins. Journal of Biological Chemistry *271*, 2676-2682.

Jaepel, J., Hübener, M., Bonhoeffer, T., and Rose, T. (2017). Lateral geniculate neurons projecting to primary visual cortex show ocular dominance plasticity in adult mice. Nature neuroscience, 1.

Jaubert-Miazza, L., Green, E., Lo, F., Bui, K., Mills, J., and Guido, W. (2005). Structural and functional composition of the developing retinogeniculate pathway in the mouse. Visual neuroscience *22*, 661.

Kaur, S., Jain, S., Sodhi, H.B., and Rastogi, A. (2013). Optic nerve hypoplasia. Oman journal of ophthalmology *6*, 77.

Kerschensteiner, D., and Guido, W. (2017). Organization of the dorsal lateral geniculate nucleus in the mouse. Visual Neuroscience *34*.

Ko, J., Fuccillo, M.V., Malenka, R.C., and Sudhof, T.C. (2009a). LRRTM2 functions as a neurexin ligand in promoting excitatory synapse formation. Neuron *64*, 791-798.

Ko, J., Soler-Llavina, G.J., Fuccillo, M.V., Malenka, R.C., and Sudhof, T.C. (2011). Neuroligins/LRRTMs prevent activity- and Ca2+/calmodulin-dependent synapse elimination in cultured neurons. The Journal of cell biology *194*, 323-334.

Ko, J., Zhang, C., Arac, D., Boucard, A.A., Brunger, A.T., and Südhof, T.C. (2009b). Neuroligin-1 performs neurexin-dependent and neurexin-independent functions in synapse validation. The EMBO Journal *28*, 3244-3255.

Lim, J.-H.A., Stafford, B.K., Nguyen, P.L., Lien, B.V., Wang, C., Zukor, K., He, Z., and Huberman, A.D. (2016). Neural activity promotes long-distance, target-specific regeneration of adult retinal axons. Nature neuroscience.

Ling, S., Pratte, M.S., and Tong, F. (2015). Attention alters orientation processing in the human lateral geniculate nucleus. Nature neuroscience *18*, 496-498.

Linhoff, M.W., Lauren, J., Cassidy, R.M., Dobie, F.A., Takahashi, H., Nygaard, H.B., Airaksinen, M.S., Strittmatter, S.M., and Craig, A.M. (2009). An unbiased expression screen for synaptogenic proteins identifies the LRRTM protein family as synaptic organizers. Neuron *61*, 734-749.

Litvina, E.Y., and Chen, C. Functional Convergence at the Retinogeniculate Synapse. Neuron *96*, 330-338.e335.

Litvina, E.Y., and Chen, C. (2017a). An evolving view of retinogeniculate transmission. Visual Neuroscience *34*.

Litvina, E.Y., and Chen, C. (2017b). Functional Convergence at the Retinogeniculate Synapse. Neuron *96*, 330-338. e335.

Liu, K., Tedeschi, A., Park, K.K., and He, Z. (2011). Neuronal intrinsic mechanisms of axon regeneration. Annual review of neuroscience *34*, 131-152.

Lu, Y., Belin, S., and He, Z. (2014). Signaling regulations of neuronal regenerative ability. Current opinion in neurobiology *27*, 135-142.

Marshel, J.H., Kaye, A.P., Nauhaus, I., and Callaway, E.M. (2012). Anterior-posterior direction opponency in the superficial mouse lateral geniculate nucleus. Neuron *76*, 713-720.

Mastronarde, D.N. (1992). Nonlagged relay cells and interneurons in the cat lateral geniculate nucleus: receptive-field properties and retinal inputs. Visual neuroscience *8*, 407-441.

Mead, B., Berry, M., Logan, A., Scott, R.A., Leadbeater, W., and Scheven, B.A. (2015). Stem cell treatment of degenerative eye disease. Stem cell research *14*, 243-257.

Monavarfeshani, A., Sabbagh, U., and Fox, M.A. (2017). Not a one-trick pony: Diverse connectivity and functions of the rodent lateral geniculate complex. Visual Neuroscience *34*.

Moore, D.L., and Goldberg, J.L. (2010). Four steps to optic nerve regeneration. Journal of Neuro-Ophthalmology *30*, 347-360.

Morgan, J.L. (2017). A connectomic approach to the lateral geniculate nucleus. Visual Neuroscience *34*.

Morgan, J.L., Berger, D.R., Wetzel, A.W., and Lichtman, J.W. (2016). The Fuzzy Logic of Network Connectivity in Mouse Visual Thalamus. Cell *165*, 192-206.

Morin, L.P., and Studholme, K.M. (2014). Retinofugal projections in the mouse. Journal of Comparative Neurology *522*, 3733-3753.

Park, K.K., Liu, K., Hu, Y., Smith, P.D., Wang, C., Cai, B., Xu, B., Connolly, L., Kramvis, I., and Sahin, M. (2008). Promoting axon regeneration in the adult CNS by modulation of the PTEN/mTOR pathway. Science *322*, 963-966.

Pfeiffenberger, C., Yamada, J., and Feldheim, D.A. (2006). Ephrin-As and patterned retinal activity act together in the development of topographic maps in the primary visual system. The Journal of neuroscience *26*, 12873-12884.

Piscopo, D.M., El-Danaf, R.N., Huberman, A.D., and Niell, C.M. (2013). Diverse visual features encoded in mouse lateral geniculate nucleus. The Journal of Neuroscience *33*, 4642-4656.

Robles, E., Filosa, A., and Baier, H. (2013). Precise lamination of retinal axons generates multiple parallel input pathways in the tectum. J Neurosci *33*, 5027-5039.

Robson, J.A. (1993). Qualitative and quantitative analyses of the patterns of retinal input to neurons in the dorsal lateral geniculate nucleus of the cat. Journal of Comparative Neurology *334*, 324-336.

Rompani, S.B., Müllner, F.E., Wanner, A., Zhang, C., Roth, C.N., Yonehara, K., and Roska, B. (2017). Different Modes of Visual Integration in the Lateral Geniculate Nucleus Revealed by Single-Cell-Initiated Transsynaptic Tracing. Neuron *93*, 767-776. e766.

Scholl, B., Tan, A.Y., Corey, J., and Priebe, N.J. (2013). Emergence of orientation selectivity in the mammalian visual pathway. J Neurosci *33*, 10616-10624.

Sherman, S.M. (2016). Thalamus plays a central role in ongoing cortical functioning. Nature neuroscience *16*, 533-541.

Siddiqui, T.J., Pancaroglu, R., Kang, Y., Rooyakkers, A., and Craig, A.M. (2010). LRRTMs and neuroligins bind neurexins with a differential code to cooperate in glutamate synapse development. The Journal of neuroscience : the official journal of the Society for Neuroscience *30*, 7495-7506.

Siddiqui, T.J., Tari, P.K., Connor, S.A., Zhang, P., Dobie, F.A., She, K., Kawabe, H., Wang, Y.T., Brose, N., and Craig, A.M. (2013). An LRRTM4-HSPG complex mediates excitatory synapse development on dentate gyrus granule cells. Neuron *79*, 680-695.

Sincich, L.C., Adams, D.L., Economides, J.R., and Horton, J.C. (2007). Transmission of spike trains at the retinogeniculate synapse. The Journal of Neuroscience *27*, 2683-2692.

Singh, R., Su, J., Brooks, J., Terauchi, A., Umemori, H., and Fox, M.A. (2011). Fibroblast growth factor 22 contributes to the development of retinal nerve terminals in the dorsal lateral geniculate nucleus. Frontiers in molecular neuroscience *4*.

Sousa, I., Clark, T.G., Holt, R., Pagnamenta, A.T., Mulder, E.J., and Minderaa, R.B. (2010). Polymorphisms in leucine-rich repeat genes are associated with autism spectrum disorder susceptibility in populations of European ancestry.

Stone, C., and Pinto, L.H. (1993). Response properties of ganglion cells in the isolated mouse retina. Visual neuroscience *10*, 31-39.

Stone, J. (2013). Parallel processing in the visual system: the classification of retinal ganglion cells and its impact on the neurobiology of vision (Springer Science & Business Media).

Su, J., Haner, C.V., Imbery, T.E., Brooks, J.M., Morhardt, D.R., Gorse, K., Guido, W., and Fox, M.A. (2011). Reelin is required for class-specific retinogeniculate targeting. The Journal of Neuroscience *31*, 575-586.

Südhof, T.C. (2008). Neuroligins and neurexins link synaptic function to cognitive disease. Nature *455*, 903-911.

Usrey, W.M., Reppas, J.B., and Reid, R.C. (1999). Specificity and strength of retinogeniculate connections. Journal of Neurophysiology *82*, 3527-3540.

Varoqueaux, F., Aramuni, G., Rawson, R.L., Mohrmann, R., Missler, M., Gottmann, K., Zhang, W., Südhof, T.C., and Brose, N. (2006). Neuroligins determine synapse maturation and function. Neuron *51*, 741-754.

Varoqueaux, F., Jamain, S., and Brose, N. (2004). Neuroligin 2 is exclusively localized to inhibitory synapses. European journal of cell biology *83*, 449-456.

Weyand, T.G. (2007). Retinogeniculate transmission in wakefulness. Journal of neurophysiology *98*, 769-785.

Weyand, T.G. (2016). The multifunctional lateral geniculate nucleus. Reviews in the neurosciences *27*, 135-157.

Yeh, C.-I., Stoelzel, C.R., Weng, C., and Alonso, J.-M. (2009). Functional consequences of neuronal divergence within the retinogeniculate pathway. Journal of neurophysiology *101*, 2166-2185.

Yiu, G., and He, Z. (2006). Glial inhibition of CNS axon regeneration. Nature Reviews Neuroscience *7*, 617-627.

Zhao, X., Chen, H., Liu, X., and Cang, J. (2013). Orientation-selective responses in the mouse lateral geniculate nucleus. The Journal of Neuroscience *33*, 12751-12763.

Alonso, J.-M., Usrey, W.M., and Reid, R.C. (2001). Rules of connectivity between geniculate cells and simple cells in cat primary visual cortex. J Neurosci *21*, 4002-4015.

Altman, J., and Bayer, S.A. (1989). Development of the rat thalamus: VI. The posterior lobule of the thalamic neuroepithelium and the time and site of origin and settling pattern of neurons of the lateral geniculate and lateral posterior nuclei. Journal of Comparative Neurology *284*, 581-601.

Arcelli, P., Frassoni, C., Regondi, M., Biasi, S., and Spreafico, R. (1997). GABAergic neurons in mammalian thalamus: a marker of thalamic complexity? Brain research bulletin *42*, 27-37.

Baden, T., Berens, P., Franke, K., Rosón, M.R., Bethge, M., and Euler, T. (2016). The functional diversity of retinal ganglion cells in the mouse. Nature *529*, 345-350.

Baden, T., Schubert, T., Chang, L., Wei, T., Zaichuk, M., Wissinger, B., and Euler, T. (2013). A tale of two retinal domains: near-optimal sampling of achromatic contrasts in natural scenes through asymmetric photoreceptor distribution. Neuron *80*, 1206-1217.

Bei, F., Lee, H.H.C., Liu, X., Gunner, G., Jin, H., Ma, L., Wang, C., Hensch, T.K., Frank, E., and Sanes, J.R. (2016). Restoration of Visual Function by Enhancing Conduction in Regenerated Axons. Cell *164*, 219-232.

Benowitz, L.I., He, Z., and Goldberg, J.L. (2017). Reaching the brain: advances in optic nerve regeneration. Experimental neurology *287*, 365-373.

Berson, D. (2008). Retinal ganglion cell types and their central projections. The senses: a comprehensive reference *1*, 491-520.

Bickford, M.E. (2015). Thalamic circuit diversity: modulation of the driver/modulator framework. Frontiers in neural circuits *9*.

Bickford, M.E., Slusarczyk, A., Dilger, E.K., Krahe, T.E., Kucuk, C., and Guido, W. (2010). Synaptic development of the mouse dorsal lateral geniculate nucleus. The Journal of comparative neurology *518*, 622-635.

Bickford, M.E., Zhou, N., Krahe, T.E., Govindaiah, G., and Guido, W. (2015). Retinal and tectal "driver-like" inputs converge in the shell of the mouse dorsal lateral geniculate nucleus. The Journal of Neuroscience *35*, 10523-10534.

Bishop, G. (1933). Fiber groups in the optic nerve. American Journal of Physiology--Legacy Content *106*, 460-474.

Borchert, M. (2012). Reappraisal of the optic nerve hypoplasia syndrome. Journal of Neuro-ophthalmology *32*, 58-67.

Born, G., and Schmidt, M. (2007). GABAergic pathways in the rat subcortical visual system: a comparative study in vivo and in vitro. European Journal of Neuroscience *26*, 1183-1192.

Braak, H., and Bachmann, A. (1985). The percentage of projection neurons and interneurons in the human lateral geniculate nucleus. Human neurobiology *4*, 91-95.

Briggs, F., and Usrey, W.M. (2008). Emerging views of corticothalamic function. Current opinion in neurobiology *18*, 403-407.

Brooks, J.M., Su, J., Levy, C., Wang, J.S., Seabrook, T.A., Guido, W., and Fox, M.A. (2013). A Molecular Mechanism Regulating the Timing of Corticogeniculate Innervation. Cell reports *5*, 573-581.

Brose, N. (2009). Synaptogenic proteins and synaptic organizers: "many hands make light work". Neuron *61*, 650-652.

Budisantoso, T., Matsui, K., Kamasawa, N., Fukazawa, Y., and Shigemoto, R. (2012). Mechanisms underlying signal filtering at a multisynapse contact. J Neurosci *32*, 2357-2376.

Budreck, E.C., and Scheiffele, P. (2007). Neuroligin-3 is a neuronal adhesion protein at GABAergic and glutamatergic synapses. European Journal of Neuroscience *26*, 1738-1748.

Bukalo, O., and Dityatev, A. (2012). Synaptic cell adhesion molecules. In Synaptic Plasticity (Springer), pp. 97-128.

Cai, D., Cohen, K.B., Luo, T., Lichtman, J.W., and Sanes, J.R. (2013). Improved tools for the Brainbow toolbox. Nature methods *10*, 540-547.

Campbell, G., and Frost, D.O. (1987). Target-controlled differentiation of axon terminals and synaptic organization. Proceedings of the National Academy of Sciences *84*, 6929-6933.

Campbell, G., and Frost, D.O. (1988). Synaptic organization of anomalous retinal projections to the somatosensory and auditory thalamus: Target-controlled morphogenesis of axon terminals and synaptic glomeruli. Journal of Comparative Neurology *272*, 383-408.

Cang, J., and Feldheim, D.A. (2013). Developmental mechanisms of topographic map formation and alignment. Annual review of neuroscience *36*, 51-77.

Cantallops, I., Haas, K., and Cline, H.T. (2000). Postsynaptic CPG15 promotes synaptic maturation and presynaptic axon arbor elaboration in vivo. Nature neuroscience *3*, 1004-1011.

Cappelletti, G., Galbiati, M., Ronchi, C., Maggioni, M.G., Onesto, E., and Poletti, A. (2007). Neuritin (cpg15) enhances the differentiating effect of NGF on neuronal PC12 cells. Journal of neuroscience research *85*, 2702-2713.

Cardona, A., Saalfeld, S., Schindelin, J., Arganda-Carreras, I., Preibisch, S., Longair, M., Tomancak, P., Hartenstein, V., and Douglas, R.J. (2012). TrakEM2 software for neural circuit reconstruction. PLoS One *7*, e38011.

Cetin, A., and Callaway, E.M. (2014). Optical control of retrogradely infected neurons using drug-regulated "TLoop" lentiviral vectors. Journal of neurophysiology *111*, 2150-2159.

Chandler, D., Dragovic, M., Cooper, M., Badcock, J.C., Mullin, B.H., Faulkner, D., Wilson, S.G., Hallmayer, J., Howell, S., Rock, D., *et al.* (2010). Impact of Neuritin 1 (NRN1) polymorphisms on fluid intelligence in schizophrenia. American journal of medical genetics Part B, Neuropsychiatric genetics : the official publication of the International Society of Psychiatric Genetics *153B*, 428-437.

Chen, C., and Regehr, W.G. (2000). Developmental remodeling of the retinogeniculate synapse. Neuron *28*, 955-966.

Cheong, S.K., Tailby, C., Solomon, S.G., and Martin, P.R. (2013). Cortical-like receptive fields in the lateral geniculate nucleus of marmoset monkeys. J Neurosci *33*, 6864-6876.

Chia, P.H., Li, P., and Shen, K. (2013). Cellular and molecular mechanisms underlying presynapse formation. The Journal of cell biology *203*, 11-22.

Chih, B., Engelman, H., and Scheiffele, P. (2005). Control of excitatory and inhibitory synapse formation by neuroligins. Science *307*, 1324-1328.

Christopherson, K.S., Ullian, E.M., Stokes, C.C., Mullowney, C.E., Hell, J.W., Agah, A., Lawler, J., Mosher, D.F., Bornstein, P., and Barres, B.A. (2005). Thrombospondins are astrocyte-secreted proteins that promote CNS synaptogenesis. Cell *120*, 421-433.

Chubykin, A.A., Atasoy, D., Etherton, M.R., Brose, N., Kavalali, E.T., Gibson, J.R., and Südhof, T.C. (2007). Activity-dependent validation of excitatory versus inhibitory synapses by neuroligin-1 versus neuroligin-2. Neuron *54*, 919-931.

Cleland, B., Dubin, M., and Levick, W. (1971). Simultaneous recording of input and output of lateral geniculate neurones. Nature *231*, 191-192.

Cleland, B., and Lee, B. (1985). A comparison of visual responses of cat lateral geniculate nucleus neurones with those of ganglion cells afferent to them. The Journal of physiology *369*, 249-268.

Corriveau, R.A., Shatz, C.J., and Nedivi, E. (1999). Dynamic regulation of cpg15 during activity-dependent synaptic development in the mammalian visual system. The Journal of neuroscience *19*, 7999-8008.

Crabtree, J.W., and Killackey, H.P. (1989). The topographic organization and axis of projection within the visual sector of the rabbit's thalamic reticular nucleus. European Journal of Neuroscience *1*, 94-109.

Craig, A.M., Graf, E.R., and Linhoff, M.W. (2006). How to build a central synapse: clues from cell culture. Trends in neurosciences *29*, 8-20.

Craig, A.M., and Kang, Y. (2007). Neurexin–neuroligin signaling in synapse development. Current opinion in neurobiology *17*, 43-52.

Crair, M.C., and Mason, C.A. (2016). Reconnecting eye to brain. J Neurosci *36*, 10707-10722.

Cruz-Martín, A., El-Danaf, R.N., Osakada, F., Sriram, B., Dhande, O.S., Nguyen, P.L., Callaway, E.M., Ghosh, A., and Huberman, A.D. (2014). A dedicated circuit links direction-selective retinal ganglion cells to the primary visual cortex. Nature *507*, 358-361.

Danesh-Meyer, H.V., and Levin, L.A. (2015). Glaucoma as a Neurodegenerative Disease. Journal of Neuro-Ophthalmology *35*, S22-S28.

De Lima, A.D., and Singer, W. (1987). The serotoninergic fibers in the dorsal lateral geniculate nucleus of the cat: distribution and synaptic connections demonstrated with immunocytochemistry. Journal of Comparative Neurology *258*, 339-351.

de Lima, D.A., Montero, V., and Singer, W. (1985). The cholinergic innervation of the visual thalamus: an EM immunocytochemical study. Experimental brain research *59*, 206-212.

de Lima, S., Habboub, G., and Benowitz, L.I. (2012a). Combinatorial therapy stimulates long-distance regeneration, target reinnervation, and partial recovery of vision after optic nerve injury in mice. International review of neurobiology *106*, 153-172.

de Lima, S., Koriyama, Y., Kurimoto, T., Oliveira, J.T., Yin, Y., Li, Y., Gilbert, H.-Y., Fagiolini, M., Martinez, A.M.B., and Benowitz, L. (2012b). Full-length axon regeneration in the adult mouse optic nerve and partial recovery of simple visual behaviors. Proceedings of the National Academy of Sciences *109*, 9149-9154.

de Wit, J., and Ghosh, A. (2014). Control of neural circuit formation by leucine-rich repeat proteins. Trends in neurosciences *37*, 539-550.

de Wit, J., and Ghosh, A. (2015). Specification of synaptic connectivity by cell surface interactions. Nature Reviews Neuroscience.

de Wit, J., Hong, W., Luo, L., and Ghosh, A. (2011). Role of leucine-rich repeat proteins in the development and function of neural circuits. Annual review of cell and developmental biology *27*, 697-729.

de Wit, J., Sylwestrak, E., O'Sullivan, M.L., Otto, S., Tiglio, K., Savas, J.N., Yates, J.R., 3rd, Comoletti, D., Taylor, P., and Ghosh, A. (2009). LRRTM2 interacts with Neurexin1 and regulates excitatory synapse formation. Neuron *64*, 799-806.

Denk, W., and Horstmann, H. (2004). Serial block-face scanning electron microscopy to reconstruct three-dimensional tissue nanostructure. PLoS biology *2*, e329.

Denman, D.J., and Contreras, D. (2016). On Parallel Streams through the Mouse Dorsal Lateral Geniculate Nucleus. Frontiers in neural circuits *10*.

Dhande, O.S., Estevez, M.E., Quattrochi, L.E., El-Danaf, R.N., Nguyen, P.L., Berson, D.M., and Huberman, A.D. (2013). Genetic dissection of retinal inputs to brainstem nuclei controlling image stabilization. The Journal of Neuroscience *33*, 17797-17813.

Dhande, O.S., Hua, E.W., Guh, E., Yeh, J., Bhatt, S., Zhang, Y., Ruthazer, E.S., Feller, M.B., and Crair, M.C. (2011). Development of single retinofugal axon arbors in normal and β2 knock-out mice. The Journal of Neuroscience *31*, 3384-3399.

Dhande, O.S., and Huberman, A.D. (2014). Retinal ganglion cell maps in the brain: implications for visual processing. Current opinion in neurobiology *24*, 133-142.

Dhande, O.S., Stafford, B.K., Lim, J.-H.A., and Huberman, A.D. (2015). Contributions of Retinal Ganglion Cells to Subcortical Visual Processing and Behaviors. Annual Review of Vision Science *1*, 291-328.

Duan, X., Qiao, M., Bei, F., Kim, I.-J., He, Z., and Sanes, J.R. (2015). Subtype-specific regeneration of retinal ganglion cells following axotomy: effects of osteopontin and mTOR signaling. Neuron *85*, 1244-1256.

Dubin, M.W., and Cleland, B.G. (1977). Organization of visual inputs to interneurons of lateral geniculate nucleus of the cat. Journal of Neurophysiology *40*, 410-427.

Ellis, E.M., Gauvain, G., Sivyer, B., and Murphy, G.J. (2016). Shared and Distinct Retinal Input to the Mouse Superior Colliculus and Dorsal Lateral Geniculate Nucleus. Journal of neurophysiology, jn. 00227.02016.

Emerson, V., Chalupa, L., Thompson, I., and Talbot, R. (1982). Behavioural, physiological, and anatomical consequences of monocular deprivation in the golden hamster (Mesocricetus auratus). Experimental brain research *45*, 168-178.

Erzurumlu, R.S., Jhaveri, S., and Schneider, G.E. (1988). Distribution of morphologically different retinal axon terminals in the hamster dorsal lateral geniculate nucleus. Brain research *461*, 175-181.

Euler, T., Haverkamp, S., Schubert, T., and Baden, T. (2014). Retinal bipolar cells: elementary building blocks of vision. Nature Reviews Neuroscience *15*, 507-519.

Feldheim, D.A., Vanderhaeghen, P., Hansen, M.J., Frisén, J., Lu, Q., Barbacid, M., and Flanagan, J.G. (1998). Topographic guidance labels in a sensory projection to the forebrain. Neuron *21*, 1303-1313.

Flavell, S.W., and Greenberg, M.E. (2008). Signaling mechanisms linking neuronal activity to gene expression and plasticity of the nervous system. Annual review of neuroscience *31*, 563.

Fox, M.A., and Guido, W. (2011). Shedding light on class-specific wiring: development of intrinsically photosensitive retinal ganglion cell circuitry. Molecular neurobiology *44*, 321-329.

Fox, M.A., Sanes, J.R., Borza, D.-B., Eswarakumar, V.P., Fässler, R., Hudson, B.G., John, S.W., Ninomiya, Y., Pedchenko, V., and Pfaff, S.L. (2007). Distinct target-derived signals organize formation, maturation, and maintenance of motor nerve terminals. Cell *129*, 179-193.

Fox, M.A., and Umemori, H. (2006). Seeking long-term relationship: axon and target communicate to organize synaptic differentiation. Journal of neurochemistry *97*, 1215-1231.

Francks, C., Maegawa, S., Laurén, J., Abrahams, B.S., Velayos-Baeza, A., Medland, S.E., Colella, S., Groszer, M., McAuley, E., and Caffrey, T.M. (2007). LRRTM1 on chromosome 2p12 is a maternally suppressed gene that is associated paternally with handedness and schizophrenia. Molecular psychiatry *12*, 1129-1139.

Friedlander, M., Lin, C., and Sherman, S. (1980). Dendritic and axonal morphology of physiological classes of geniculo-cortical relay cells. Paper presented at: Experimental Brain Research (Springer).

Friedlander, M., Lin, C., Stanford, L., and Sherman, S.M. (1981). Morphology of functionally identified neurons in lateral geniculate nucleus of the cat. Journal of Neurophysiology *46*, 80-129.

Fujino, T., Leslie, J.H., Eavri, R., Chen, J.L., Lin, W.C., Flanders, G.H., Borok, E., Horvath, T.L., and Nedivi, E. (2011). CPG15 regulates synapse stability in the developing and adult brain. Genes & development *25*, 2674-2685.

Gabbott, P.L., and Bacon, S.J. (1994). Two types of interneuron in the dorsal lateral geniculate nucleus of the rat: a combined NADPH diaphorase histochemical and GABA immunocytochemical study. Journal of Comparative Neurology *350*, 281-301.

Gaillard, F., Karten, H.J., and Sauvé, Y. (2013). Retinorecipient areas in the diurnal murine rodent Arvicanthis niloticus: a disproportionally large superior colliculus. Journal of Comparative Neurology *521*, 1699-1726.

Gao, E., DeAngelis, G.C., and Burkhalter, A. (2010). Parallel input channels to mouse primary visual cortex. J Neurosci *30*, 5912-5926.

Gao, H., Zhang, H.L., Shou, J., Chen, L., Shen, Y., Tang, Q., Huang, J., and Zhu, J. (2012). Towards retinal ganglion cell regeneration. Regenerative medicine *7*, 865-875.

Gill, K.P., Hung, S.S., Sharov, A., Lo, C.Y., Needham, K., Lidgerwood, G.E., Jackson, S., Crombie, D.E., Nayagam, B.A., and Cook, A.L. (2016). Enriched retinal ganglion cells derived from human embryonic stem cells. Scientific reports *6*, 30552.

Glees, P., and le Gros Clark, W. (1941). The termination of optic fibres in the lateral geniculate body of the monkey. Journal of anatomy *75*, 295.

Godement, P., Salaün, J., and Imbert, M. (1984). Prenatal and postnatal development of retinogeniculate and retinocollicular projections in the mouse. Journal of Comparative Neurology *230*, 552-575.

Goldberg, J.L., and Guido, W. (2016). Report on the National Eye Institute Audacious Goals Initiative: Regenerating the Optic NerveReport on NEI Audacious Goals Initiative. Investigative ophthalmology & visual science *57*, 1271-1275.

Golding, B., Pouchelon, G., Bellone, C., Murthy, S., Di Nardo, A.A., Govindan, S., Ogawa, M., Shimogori, T., Lüscher, C., and Dayer, A. (2014). Retinal input directs the recruitment of inhibitory interneurons into thalamic visual circuits. Neuron *81*, 1057-1069.

Graf, E.R., Zhang, X., Jin, S.-X., Linhoff, M.W., and Craig, A.M. (2004). Neurexins induce differentiation of GABA and glutamate postsynaptic specializations via neuroligins. Cell *119*, 1013-1026.

Grant, E., Hoerder-Suabedissen, A., and Molnár, Z. (2016). The Regulation of Corticofugal Fiber Targeting by Retinal Inputs. Cerebral Cortex, bhv315.

Grieve, K.L. (2005). Binocular visual responses in cells of the rat dLGN. The Journal of physiology *566*, 119-124.

Grubb, M.S., and Thompson, I.D. (2004). Biochemical and anatomical subdivision of the dorsal lateral geniculate nucleus in normal mice and in mice lacking the β2 subunit of the nicotinic acetylcholine receptor. Vision research *44*, 3365-3376.

Guido, W. (2008). Refinement of the retinogeniculate pathway. The Journal of physiology *586*, 4357-4362.

Guillery, R. (1969). The organization of synaptic interconnections in the laminae of the dorsal lateral geniculate nucleus of the cat. Zeitschrift für Zellforschung und mikroskopische Anatomie *96*, 1-38.

Guillery, R., and Harting, J.K. (2003). Structure and connections of the thalamic reticular nucleus: advancing views over half a century. Journal of Comparative Neurology *463*, 360-371.

Guillery, R., and Scott, G. (1971). Observations on synaptic patterns in the dorsal lateral geniculate nucleus of the cat: the C laminae and the perikaryal synapses. Experimental brain research *12*, 184-203.

Gupta, N., and Yücel, Y.H. (2007). Glaucoma as a neurodegenerative disease. Current opinion in ophthalmology *18*, 110-114.

Hale, P., Sefton, A.J., Baur, L., and Cottee, L. (1982). Interrelations of the rat's thalamic reticular and dorsal lateral geniculate nuclei. Experimental brain research *45*, 217-229.

Hallanger, A.E., Levey, A.I., Lee, H.J., Rye, D.B., and Wainer, B.H. (1987). The origins of cholinergic and other subcortical afferents to the thalamus in the rat. Journal of Comparative Neurology *262*, 105-124.

Hammer, S., Carrillo, G.L., Govindaiah, G., Monavarfeshani, A., Bircher, J.S., Su, J., Guido, W., and Fox, M.A. (2014). Nuclei-specific differences in nerve terminal distribution, morphology, and development in mouse visual thalamus. Neural development *9*, 1.

Hammer, S., Monavarfeshani, A., Lemon, T., Su, J., and Fox, M.A. (2015). Multiple retinal axons converge onto relay cells in the adult mouse thalamus. Cell reports *12*, 1575-1583.

Hamos, J.E., Van Horn, S.C., Raczkowski, D., and Sherman, S.M. (1987). Synaptic circuits involving an individual retinogeniculate axon in the cat. Journal of Comparative Neurology *259*, 165-192.

Harting, J.K., Huerta, M.F., Hashikawa, T., and van Lieshout, D.P. (1991a). Projection of the mammalian superior colliculus upon the dorsal lateral geniculate nucleus: organization of tectogeniculate pathways in nineteen species. Journal of comparative neurology *304*, 275-306.

Harting, J.K., Van Lieshout, D., Hashikawa, T., and Weber, J. (1991b). The parabigeminogeniculate projection: connectional studies in eight mammals. Journal of comparative neurology *305*, 559-581.

Hattar, S., Kumar, M., Park, A., Tong, P., Tung, J., Yau, K.W., and Berson, D.M. (2006). Central projections of melanopsin-expressing retinal ganglion cells in the mouse. Journal of Comparative Neurology *497*, 326-349.

Hayer, S.N., and Bading, H. (2015). Nuclear calcium signaling induces expression of the synaptic organizers Lrrtm1 and Lrrtm2. The Journal of biological chemistry *290*, 5523-5532.

He, Z., and Jin, Y. (2016). Intrinsic control of axon regeneration. Neuron *90*, 437-451.

Hendry, S.H., and Reid, R.C. (2000). The koniocellular pathway in primate vision. Annual review of neuroscience *23*, 127-153.

Hong, Y.K., and Chen, C. (2011). Wiring and rewiring of the retinogeniculate synapse. Current opinion in neurobiology *21*, 228-237.

Hong, Y.K., Park, S., Litvina, E.Y., Morales, J., Sanes, J.R., and Chen, C. (2014). Refinement of the retinogeniculate synapse by bouton clustering. Neuron *84*, 332-339.

Hooks, B.M., and Chen, C. (2006). Distinct roles for spontaneous and visual activity in remodeling of the retinogeniculate synapse. Neuron *52*, 281-291.

Howarth, M., Walmsley, L., and Brown, T.M. (2014). Binocular integration in the mouse lateral geniculate nuclei. Current Biology *24*, 1241-1247.

Hubel, D.H., and Wiesel, T.N. (1972). Laminar and columnar distribution of geniculo-cortical fibers in the macaque monkey. Journal of Comparative Neurology *146*, 421-450.

Huberman, A.D., Feller, M.B., and Chapman, B. (2008a). Mechanisms underlying development of visual maps and receptive fields. Annual review of neuroscience *31*, 479-509.

Huberman, A.D., Manu, M., Koch, S.M., Susman, M.W., Lutz, A.B., Ullian, E.M., Baccus, S.A., and Barres, B.A. (2008b). Architecture and activity-mediated refinement of axonal projections from a mosaic of genetically identified retinal ganglion cells. Neuron *59*, 425-438.

Huberman, A.D., and Niell, C.M. (2011). What can mice tell us about how vision works? Trends in neurosciences *34*, 464-473.

Huberman, A.D., Wei, W., Elstrott, J., Stafford, B.K., Feller, M.B., and Barres, B.A. (2009). Genetic identification of an On-Off direction-selective retinal ganglion cell subtype reveals a layer-specific subcortical map of posterior motion. Neuron *62*, 327-334.

Ichtchenko, K., Hata, Y., Nguyen, T., Ullrich, B., Missler, M., Moomaw, C., and Südhof, T.C. (1995). Neuroligin 1: a splice site-specific ligand for β-neurexins. Cell *81*, 435-443.

Ichtchenko, K., Nguyen, T., and Südhof, T.C. (1996). Structures, alternative splicing, and neurexin binding of multiple neuroligins. Journal of Biological Chemistry *271*, 2676-2682.

Irvin, G.E., Casagrande, V.A., and Norton, T.T. (1993). Center/surround relationships of magnocellular, parvocellular, and koniocellular relay cells in primate lateral geniculate nucleus. Visual neuroscience *10*, 363-373.

Jacobs, G.H., Williams, G.A., and Fenwick, J.A. (2004). Influence of cone pigment coexpression on spectral sensitivity and color vision in the mouse. Vision research *44*, 1615-1622.

Jaepel, J., Hübener, M., Bonhoeffer, T., and Rose, T. (2017). Lateral geniculate neurons projecting to primary visual cortex show ocular dominance plasticity in adult mice. Nature neuroscience, 1.

Jager, P., Ye, Z., Yu, X., Zagoraiou, L., Prekop, H.-T., Partanen, J., Jessell, T.M., Wisden, W., Brickley, S.G., and Delogu, A. (2016). Tectal-derived interneurons contribute to phasic and tonic inhibition in the visual thalamus. Nature Communications *7*.

Jaubert-Miazza, L., Green, E., Lo, F., Bui, K., Mills, J., and Guido, W. (2005). Structural and functional composition of the developing retinogeniculate pathway in the mouse. Visual neuroscience *22*, 661.

Javaherian, A., and Cline, H.T. (2005). Coordinated motor neuron axon growth and neuromuscular synaptogenesis are promoted by CPG15 in vivo. Neuron *45*, 505-512.

Jones, E., and Powell, T. (1969). Electron microscopy of synaptic glomeruli in the thalamic relay nuclei of the cat. Proceedings of the Royal Society of London B: Biological Sciences *172*, 153-171.

Jones, E.G. (2012). The thalamus (Springer Science & Business Media).

Jones, E.G., and Rubenstein, J.L. (2004). Expression of regulatory genes during differentiation of thalamic nuclei in mouse and monkey. Journal of Comparative Neurology *477*, 55-80.

Jurgens, C.W., Bell, K.A., McQuiston, A.R., and Guido, W. (2012). Optogenetic stimulation of the corticothalamic pathway affects relay cells and GABAergic neurons differently in the mouse visual thalamus. PLoS One *7*, e45717.

Kaas, J., Guillery, R., and Allman, J. (1972). Some Principles of Organization in the Dorsal Lateral Geniculate Nucleus; pp. 283–299. Brain, Behavior and Evolution *6*, 283-299.

Kaur, S., Jain, S., Sodhi, H.B., and Rastogi, A. (2013). Optic nerve hypoplasia. Oman journal of ophthalmology *6*, 77.

Kay, J.N., De la Huerta, I., Kim, I.-J., Zhang, Y., Yamagata, M., Chu, M.W., Meister, M., and Sanes, J.R. (2011). Retinal ganglion cells with distinct directional preferences differ in molecular identity, structure, and central projections. The Journal of Neuroscience *31*, 7753-7762.

Kerschensteiner, D., and Guido, W. (2017). Organization of the dorsal lateral geniculate nucleus in the mouse. Visual Neuroscience *34*.

Kim, I.-J., Zhang, Y., Meister, M., and Sanes, J.R. (2010). Laminar restriction of retinal ganglion cell dendrites and axons: subtype-specific developmental patterns revealed with transgenic markers. The Journal of Neuroscience *30*, 1452-1462.

Kim, I.-J., Zhang, Y., Yamagata, M., Meister, M., and Sanes, J.R. (2008). Molecular identification of a retinal cell type that responds to upward motion. Nature *452*, 478-482.

Ko, J., Fuccillo, M.V., Malenka, R.C., and Sudhof, T.C. (2009a). LRRTM2 functions as a neurexin ligand in promoting excitatory synapse formation. Neuron *64*, 791-798.

Ko, J., Soler-Llavina, G.J., Fuccillo, M.V., Malenka, R.C., and Sudhof, T.C. (2011). Neuroligins/LRRTMs prevent activity- and Ca2+/calmodulin-dependent synapse elimination in cultured neurons. The Journal of cell biology *194*, 323-334.

Ko, J., Zhang, C., Arac, D., Boucard, A.A., Brunger, A.T., and Südhof, T.C. (2009b). Neuroligin-1 performs neurexin-dependent and neurexin-independent functions in synapse validation. The EMBO Journal *28*, 3244-3255.

Köberlein, J., Beifus, K., Schaffert, C., and Finger, R.P. (2013). The economic burden of visual impairment and blindness: a systematic review. BMJ open *3*, e003471.

Kong, L., Fry, M., Al-Samarraie, M., Gilbert, C., and Steinkuller, P.G. (2012). An update on progress and the changing epidemiology of causes of childhood blindness worldwide. Journal of American Association for Pediatric Ophthalmology and Strabismus *16*, 501-507.

Krahe, T.E., El-Danaf, R.N., Dilger, E.K., Henderson, S.C., and Guido, W. (2011). Morphologically distinct classes of relay cells exhibit regional preferences in the dorsal lateral geniculate nucleus of the mouse. The Journal of Neuroscience *31*, 17437-17448.

Kucukdereli, H., Allen, N.J., Lee, A.T., Feng, A., Ozlu, M.I., Conatser, L.M., Chakraborty, C., Workman, G., Weaver, M., and Sage, E.H. (2011). Control of excitatory CNS synaptogenesis by astrocyte-secreted proteins Hevin and SPARC. Proceedings of the National Academy of Sciences *108*, E440-E449.

LaConte, L.E., Chavan, V., Liang, C., Willis, J., Schönhense, E.-M., Schoch, S., and Mukherjee, K. (2016). CASK stabilizes neurexin and links it to liprin-α in a neuronal activity-dependent manner. Cellular and Molecular Life Sciences *73*, 3599-3621.

Land, P.W., Kyonka, E., and Shamalla-Hannah, L. (2004). Vesicular glutamate transporters in the lateral geniculate nucleus: expression of VGLUT2 by retinal terminals. Brain research *996*, 251-254.

Laurén, J., Airaksinen, M.S., Saarma, M., and õnis Timmusk, T. (2003). A novel gene family encoding leucine-rich repeat transmembrane proteins differentially expressed in the nervous system. Genomics *81*, 411-421.

Lee, S.H., and Sheng, M. (2000). Development of neuron–neuron synapses. Current opinion in neurobiology *10*, 125-131.

Leist, M., Datunashvilli, M., Kanyshkova, T., Zobeiri, M., Aissaoui, A., Cerina, M., Romanelli, M.N., Pape, H.-C., and Budde, T. (2016). Two types of interneurons in the mouse lateral geniculate nucleus are characterized by different h-current density. Scientific reports *6*.

Liang, C., Kerr, A., Qiu, Y., Cristofoli, F., Van Esch, H., Fox, M.A., and Mukherjee, K. (2017). Optic Nerve Hypoplasia Is a Pervasive Subcortical Pathology of Visual System in Neonates. Investigative Ophthalmology & Visual Science *58*, 5485-5496.

Lim, J.-H.A., Stafford, B.K., Nguyen, P.L., Lien, B.V., Wang, C., Zukor, K., He, Z., and Huberman, A.D. (2016). Neural activity promotes long-distance, target-specific regeneration of adult retinal axons. Nature neuroscience.

Ling, C., Hendrickson, M.L., and Kalil, R.E. (2012). Morphology, classification, and distribution of the projection neurons in the dorsal lateral geniculate nucleus of the rat. PloS one *7*, e49161.

Ling, S., Pratte, M.S., and Tong, F. (2015). Attention alters orientation processing in the human lateral geniculate nucleus. Nature neuroscience *18*, 496-498.

Linhoff, M.W., Lauren, J., Cassidy, R.M., Dobie, F.A., Takahashi, H., Nygaard, H.B., Airaksinen, M.S., Strittmatter, S.M., and Craig, A.M. (2009). An unbiased expression screen for synaptogenic proteins identifies the LRRTM protein family as synaptic organizers. Neuron *61*, 734-749.

Litvina, E.Y., and Chen, C. Functional Convergence at the Retinogeniculate Synapse. Neuron *96*, 330-338.e335.

Litvina, E.Y., and Chen, C. (2017a). An evolving view of retinogeniculate transmission. Visual Neuroscience *34*.

Litvina, E.Y., and Chen, C. (2017b). Functional Convergence at the Retinogeniculate Synapse. Neuron *96*, 330-338. e335.

Liu, K., Tedeschi, A., Park, K.K., and He, Z. (2011). Neuronal intrinsic mechanisms of axon regeneration. Annual review of neuroscience *34*, 131-152.

Livet, J., Weissman, T.A., Kang, H., Draft, R.W., Lu, J., Bennis, R.A., Sanes, J.R., and Lichtman, J.W. (2007). Transgenic strategies for combinatorial expression of fluorescent proteins in the nervous system. Nature *450*, 56-62.

López-Bendito, G., and Molnár, Z. (2003). Thalamocortical development: how are we going to get there? Nature Reviews Neuroscience *4*, 276-289.

Lu, Y., Belin, S., and He, Z. (2014). Signaling regulations of neuronal regenerative ability. Current opinion in neurobiology *27*, 135-142.

Ludwig, K.U., Mattheisen, M., Muhleisen, T.W., Roeske, D., Schmal, C., Breuer, R., Schulte-Korne, G., Muller-Myhsok, B., Nothen, M.M., Hoffmann, P., *et al.* (2009). Supporting evidence for LRRTM1 imprinting effects in schizophrenia. Molecular psychiatry *14*, 743-745.

Lund, R., and Cunningham, T. (1972). Aspects of synaptic and laminar organization of the mammalian lateral geniculate body. Invest Ophthalmol *11*, 291-302.

Mackay-Sim, A., Sefton, A.J., and Martin, P.R. (1983). Subcortical projections to lateral geniculate and thalamic reticular nuclei in the hooded rat. Journal of comparative neurology *213*, 24-35.

Macosko, E.Z., Basu, A., Satija, R., Nemesh, J., Shekhar, K., Goldman, M., Tirosh, I., Bialas, A.R., Kamitaki, N., and Martersteck, E.M. (2015). Highly parallel genome-wide expression profiling of individual cells using nanoliter droplets. Cell *161*, 1202-1214.

Maekawa, Y., Onishi, A., Matsushita, K., Koide, N., Mandai, M., Suzuma, K., Kitaoka, T., Kuwahara, A., Ozone, C., and Nakano, T. (2016). Optimized culture system to induce neurite

outgrowth from retinal ganglion cells in three-dimensional retinal aggregates differentiated from mouse and human embryonic stem cells. Current eye research *41*, 558-568.

Marshel, J.H., Kaye, A.P., Nauhaus, I., and Callaway, E.M. (2012). Anterior-posterior direction opponency in the superficial mouse lateral geniculate nucleus. Neuron *76*, 713-720.

Martersteck, E.M., Hirokawa, K.E., Evarts, M., Bernard, A., Duan, X., Li, Y., Ng, L., Oh, S.W., Ouellette, B., and Royall, J.J. (2017). Diverse Central Projection Patterns of Retinal Ganglion Cells. Cell Reports *18*, 2058-2072.

Masland, R.H. (2001). The fundamental plan of the retina. Nature neuroscience *4*, 877-886.

Mastronarde, D.N. (1992). Nonlagged relay cells and interneurons in the cat lateral geniculate nucleus: receptive-field properties and retinal inputs. Visual neuroscience *8*, 407-441.

McCormick, D.A. (1992). Neurotransmitter actions in the thalamus and cerebral cortex and their role in neuromodulation of thalamocortical activity. Progress in neurobiology *39*, 337-388.

Mead, B., Berry, M., Logan, A., Scott, R.A., Leadbeater, W., and Scheven, B.A. (2015). Stem cell treatment of degenerative eye disease. Stem cell research *14*, 243-257.

Monavarfeshani, A., Sabbagh, U., and Fox, M.A. (2017). Not a one-trick pony: Diverse connectivity and functions of the rodent lateral geniculate complex. Visual Neuroscience *34*.

Montera, V., and Zempel, J. (1985). Evidence for two types of GABA-containing interneurons in the A-laminae of the cat lateral geniculate nucleus: a double-label HRP and GABA-immunocytochemical study. Experimental brain research *60*, 603-609.

Montero, V., and Singer, W. (1985). Ultrastructural identification of somata and neural processes immunoreactive to antibodies against glutamic acid decarboxylase (GAD) in the dorsal lateral geniculate nucleus of the cat. Experimental brain research *59*, 151-165.

Moog, U., Kutsche, K., Kortüm, F., Chilian, B., Bierhals, T., Apeshiotis, N., Balg, S., Chassaing, N., Coubes, C., and Das, S. (2011). Phenotypic spectrum associated with CASK loss-of-function mutations. Journal of medical genetics, jmedgenet-2011-100218.

Moore, D.L., and Goldberg, J.L. (2010). Four steps to optic nerve regeneration. Journal of Neuro-Ophthalmology *30*, 347-360.

Morgan, J.L. (2017). A connectomic approach to the lateral geniculate nucleus. Visual Neuroscience *34*.

Morgan, J.L., Berger, D.R., Wetzel, A.W., and Lichtman, J.W. (2016). The Fuzzy Logic of Network Connectivity in Mouse Visual Thalamus. Cell *165*, 192-206.

Morin, L.P., and Studholme, K.M. (2014). Retinofugal projections in the mouse. Journal of Comparative Neurology *522*, 3733-3753.

Muir-Robinson, G., Hwang, B.J., and Feller, M.B. (2002). Retinogeniculate axons undergo eye-specific segregation in the absence of eye-specific layers. The Journal of neuroscience *22*, 5259-5264.

Mukherjee, K., Clark, H.R., Chavan, V., Benson, E.K., Kidd, G.J., and Srivastava, S. (2016). Analysis of Brain Mitochondria Using Serial Block-Face Scanning Electron Microscopy. JoVE (Journal of Visualized Experiments), e54214-e54214.

Muscat, L., Huberman, A.D., Jordan, C.L., and Morin, L.P. (2003). Crossed and uncrossed retinal projections to the hamster circadian system. Journal of Comparative Neurology *466*, 513-524.

Naeve, G.S., Ramakrishnan, M., Kramer, R., Hevroni, D., Citri, Y., and Theill, L.E. (1997). Neuritin: a gene induced by neural activity and neurotrophins that promotes neuritogenesis. Proceedings of the National Academy of Sciences *94*, 2648-2653.

Nakano, T., Ando, S., Takata, N., Kawada, M., Muguruma, K., Sekiguchi, K., Saito, K., Yonemura, S., Eiraku, M., and Sasai, Y. (2012). Self-formation of optic cups and storable stratified neural retina from human ESCs. Cell stem cell *10*, 771-785.

Nassi, J.J., and Callaway, E.M. (2009). Parallel processing strategies of the primate visual system. Nature Reviews Neuroscience *10*, 360-372.

Nedivi, E. (1998). Promotion of Dendritic Growth by CPG15, an Activity-Induced Signaling Molecule. Science *281*, 1863-1866.

Nedivi, E., Fieldust, S., Theill, L.E., and Hevron, D. (1996). A set of genes expressed in response to light in the adult cerebral cortex and regulated during development. Proceedings of the National Academy of Sciences *93*, 2048-2053.

Nedivi, E., Hevroni, D., Naot, D., Israeli, D., and Citri, Y. (1993). Numerous candidate plasticity-related genes revealed by differential cDNA cloning. Nature *363*, 718-722.

Ohlemacher, S.K., Sridhar, A., Xiao, Y., Hochstetler, A.E., Sarfarazi, M., Cummins, T.R., and Meyer, J.S. (2016). Stepwise differentiation of retinal ganglion cells from human pluripotent stem cells enables analysis of glaucomatous neurodegeneration. Stem Cells *34*, 1553-1562.

Olsen, S.R., Bortone, D.S., Adesnik, H., and Scanziani, M. (2012). Gain control by layer six in cortical circuits of vision. Nature *483*, 47-52.

Ortín-Martínez, A., Nadal-Nicolás, F.M., Jiménez-López, M., Alburquerque-Béjar, J.J., Nieto-López, L., García-Ayuso, D., Villegas-Pérez, M.P., Vidal-Sanz, M., and Agudo-Barriuso, M. (2014). Number and distribution of mouse retinal cone photoreceptors: differences between an albino (Swiss) and a pigmented (C57/BL6) strain. PLoS One *9*, e102392.

Pan, Y.A., Freundlich, T., Weissman, T.A., Schoppik, D., Wang, X.C., Zimmerman, S., Ciruna, B., Sanes, J.R., Lichtman, J.W., and Schier, A.F. (2013). Zebrabow: multispectral cell labeling for cell tracing and lineage analysis in zebrafish. Development *140*, 2835-2846.

Papadopoulos, G.C., and Parnavelas, J.G. (1990a). Distribution and synaptic organization of dopaminergic axons in the lateral geniculate nucleus of the rat. Journal of Comparative Neurology *294*, 356-361.

Papadopoulos, G.C., and Parnavelas, J.G. (1990b). Distribution and synaptic organization of serotoninergic and noradrenergic axons in the lateral geniculate nucleus of the rat. Journal of Comparative Neurology *294*, 345-355.

Park, K.K., Liu, K., Hu, Y., Smith, P.D., Wang, C., Cai, B., Xu, B., Connolly, L., Kramvis, I., and Sahin, M. (2008). Promoting axon regeneration in the adult CNS by modulation of the PTEN/mTOR pathway. Science *322*, 963-966.

Petrof, I., and Sherman, S.M. (2013). Functional significance of synaptic terminal size in glutamatergic sensory pathways in thalamus and cortex. The Journal of physiology *591*, 3125-3131.

Pfeiffenberger, C., Yamada, J., and Feldheim, D.A. (2006). Ephrin-As and patterned retinal activity act together in the development of topographic maps in the primary visual system. The Journal of neuroscience *26*, 12873-12884.

Pinault, D. (2004). The thalamic reticular nucleus: structure, function and concept. Brain research reviews *46*, 1-31.

Piscopo, D.M., El-Danaf, R.N., Huberman, A.D., and Niell, C.M. (2013). Diverse visual features encoded in mouse lateral geniculate nucleus. The Journal of Neuroscience *33*, 4642-4656.

Prusky, G.T., West, P.W., and Douglas, R.M. (2000). Behavioral assessment of visual acuity in mice and rats. Vision research *40*, 2201-2209.

Puelles, L., and Rubenstein, J.L. (2003). Forebrain gene expression domains and the evolving prosomeric model. Trends in neurosciences *26*, 469-476.

Rafols, J.A., and Valverde, F. (1973). The structure of the dorsal lateral geniculate nucleus in the mouse. A Golgi and electron microscopic study. Journal of Comparative Neurology *150*, 303-331.

Rathbun, D.L., Alitto, H.J., Warland, D.K., and Usrey, W.M. (2016). Stimulus contrast and retinogeniculate signal processing. Frontiers in neural circuits *10*.

Rathbun, D.L., Warland, D.K., and Usrey, W.M. (2010). Spike timing and information transmission at retinogeniculate synapses. J Neurosci *30*, 13558-13566.

Reese, B. (1988). ‘Hidden lamination’in the dorsal lateral geniculate nucleus: the functional organization of this thalamic region in the rat. Brain research reviews *13*, 119-137.

Reese, B., and Cowey, A. (1983). Projection lines and the ipsilateral retino-geniculate pathway in the hooded rat. Neuroscience *10*, 1233-1247.

Reichman, S., Terray, A., Slembrouck, A., Nanteau, C., Orieux, G., Habeler, W., Nandrot, E.F., Sahel, J.-A., Monville, C., and Goureau, O. (2014). From confluent human iPS cells to self-forming neural retina and retinal pigmented epithelium. Proceedings of the National Academy of Sciences *111*, 8518-8523.

Rein, D.B., Zhang, P., Wirth, K.E., Lee, P.P., Hoerger, T.J., McCall, N., Klein, R., Tielsch, J.M., Vijan, S., and Saaddine, J. (2006). The economic burden of major adult visual disorders in the United States. Archives of ophthalmology *124*, 1754-1760.

Rivlin-Etzion, M., Zhou, K., Wei, W., Elstrott, J., Nguyen, P.L., Barres, B.A., Huberman, A.D., and Feller, M.B. (2011). Transgenic mice reveal unexpected diversity of on-off direction-selective retinal ganglion cell subtypes and brain structures involved in motion processing. The Journal of Neuroscience *31*, 8760-8769.

Robles, E., Filosa, A., and Baier, H. (2013). Precise lamination of retinal axons generates multiple parallel input pathways in the tectum. J Neurosci *33*, 5027-5039.

Robson, J.A. (1993). Qualitative and quantitative analyses of the patterns of retinal input to neurons in the dorsal lateral geniculate nucleus of the cat. Journal of Comparative Neurology *334*, 324-336.

Rompani, S.B., Müllner, F.E., Wanner, A., Zhang, C., Roth, C.N., Yonehara, K., and Roska, B. (2017). Different Modes of Visual Integration in the Lateral Geniculate Nucleus Revealed by Single-Cell-Initiated Transsynaptic Tracing. Neuron *93*, 767-776. e766.

Ryabets-Lienhard, A., Stewart, C., Borchert, M., and Geffner, M.E. (2016). The Optic Nerve Hypoplasia Spectrum: Review of the Literature and Clinical Guidelines. Advances in pediatrics *63*, 127.

Sajgo, S., Ghinia, M.G., Brooks, M., Kretschmer, F., Chuang, K., Hiriyanna, S., Wu, Z., Popescu, O., and Badea, T.C. (2017). Molecular codes for cell type specification in Brn3 retinal ganglion cells. Proceedings of the National Academy of Sciences, 201618551.

Sanes, J.R., and Lichtman, J.W. (2001). Induction, assembly, maturation and maintenance of a postsynaptic apparatus. Nature Reviews Neuroscience *2*, 791-805.

Sanes, J.R., and Masland, R.H. (2015). The types of retinal ganglion cells: current status and implications for neuronal classification. Annual review of neuroscience *38*, 221-246.

Sanes, J.R., and Yamagata, M. (2009). Many paths to synaptic specificity. Annual review of cell and developmental biology *25*, 161-195.

Sato, H., Fukutani, Y., Yamamoto, Y., Tatara, E., Takemoto, M., Shimamura, K., and Yamamoto, N. (2012). Thalamus-derived molecules promote survival and dendritic growth of developing cortical neurons. The Journal of neuroscience : the official journal of the Society for Neuroscience *32*, 15388-15402.

Schmittgen, T.D., and Livak, K.J. (2008). Analyzing real-time PCR data by the comparative CT method. Nature protocols *3*, 1101-1108.

Scholl, B., Tan, A.Y., Corey, J., and Priebe, N.J. (2013). Emergence of orientation selectivity in the mammalian visual pathway. J Neurosci *33*, 10616-10624.

Seabrook, T., Burbridge, T., Crair, M., and Huberman, A. (2017). Architecture, Function, and Assembly of the Mouse Visual System. Annual review of neuroscience *40*, 499.

Seabrook, T.A., El-Danaf, R.N., Krahe, T.E., Fox, M.A., and Guido, W. (2013a). Retinal input regulates the timing of corticogeniculate innervation. The Journal of Neuroscience *33*, 10085-10097.

Seabrook, T.A., Krahe, T.E., Govindaiah, G., and Guido, W. (2013b). Interneurons in the mouse visual thalamus maintain a high degree of retinal convergence throughout postnatal development. Neural development *8*, 1.

Shanks, J.A., Ito, S., Schaevitz, L., Yamada, J., Chen, B., Litke, A., and Feldheim, D.A. (2016). Corticothalamic Axons Are Essential for Retinal Ganglion Cell Axon Targeting to the Mouse Dorsal Lateral Geniculate Nucleus. The Journal of Neuroscience *36*, 5252-5263.

Shekhar, K., Lapan, S.W., Whitney, I.E., Tran, N.M., Macosko, E.Z., Kowalczyk, M., Adiconis, X., Levin, J.Z., Nemesh, J., and Goldman, M. (2016). Comprehensive classification of retinal bipolar neurons by single-cell transcriptomics. Cell *166*, 1308-1323. e1330.

Sherman, S.M. (1985). Functional organization of the W-, X-, and Y-cell pathways in the cat: a review and hypothesis. Progress in psychobiology and physiological psychology *11*, 233-314.

Sherman, S.M. (2004). Interneurons and triadic circuitry of the thalamus. Trends in neurosciences *27*, 670-675.

Sherman, S.M. (2005). Thalamic relays and cortical functioning. Progress in brain research *149*, 107-126.

Sherman, S.M. (2016). Thalamus plays a central role in ongoing cortical functioning. Nature neuroscience *16*, 533-541.

Sherman, S.M., and Guillery, R. (2002). The role of the thalamus in the flow of information to the cortex. Philosophical Transactions of the Royal Society of London Series B: Biological Sciences *357*, 1695-1708.

Shigeoka, T., Jung, H., Jung, J., Turner-Bridger, B., Ohk, J., Lin, J.Q., Amieux, P.S., and Holt, C.E. (2016). Dynamic axonal translation in developing and mature visual circuits. Cell *166*, 181-192.

Siddiqui, T.J., and Craig, A.M. (2011). Synaptic organizing complexes. Current opinion in neurobiology *21*, 132-143.

Siddiqui, T.J., Pancaroglu, R., Kang, Y., Rooyakkers, A., and Craig, A.M. (2010). LRRTMs and neuroligins bind neurexins with a differential code to cooperate in glutamate synapse development. The Journal of neuroscience : the official journal of the Society for Neuroscience *30*, 7495-7506.

Siddiqui, T.J., Tari, P.K., Connor, S.A., Zhang, P., Dobie, F.A., She, K., Kawabe, H., Wang, Y.T., Brose, N., and Craig, A.M. (2013). An LRRTM4-HSPG complex mediates excitatory synapse development on dentate gyrus granule cells. Neuron *79*, 680-695.

Sieving, P.A. (2012). NEI Audacious Goals Initiative to Catalyze Innovation Editorial. Investigative ophthalmology & visual science *53*, 7149-7150.

Sincich, L.C., Adams, D.L., Economides, J.R., and Horton, J.C. (2007). Transmission of spike trains at the retinogeniculate synapse. The Journal of Neuroscience *27*, 2683-2692.

Singh, R., Su, J., Brooks, J., Terauchi, A., Umemori, H., and Fox, M.A. (2011). Fibroblast growth factor 22 contributes to the development of retinal nerve terminals in the dorsal lateral geniculate nucleus. Frontiers in molecular neuroscience *4*.

Singh, R., Su, J., Brooks, J., Terauchi, A., Umemori, H., and Fox, M.A. (2012). Fibroblast growth factor 22 contributes to the development of retinal nerve terminals in the dorsal lateral geniculate nucleus.

Singh, S.K., Stogsdill, J.A., Pulimood, N.S., Dingsdale, H., Kim, Y.H., Pilaz, L.-J., Kim, I.H., Manhaes, A.C., Rodrigues, W.S., and Pamukcu, A. (2016). Astrocytes assemble thalamocortical synapses by bridging NRX1α and NL1 via Hevin. Cell *164*, 183-196.

So, K.-F., Campbell, G., and Lieberman, A. (1985). Synaptic organization of the dorsal lateral geniculate nucleus in the adult hamster. Anatomy and embryology *171*, 223-234.

Soler-Llavina, G.J., Fuccillo, M.V., Ko, J., Südhof, T.C., and Malenka, R.C. (2011). The neurexin ligands, neuroligins and leucine-rich repeat transmembrane proteins, perform convergent and divergent synaptic functions in vivo. Proceedings of the National Academy of Sciences *108*, 16502-16509.

Sousa, I., Clark, T.G., Holt, R., Pagnamenta, A.T., Mulder, E.J., and Minderaa, R.B. (2010). Polymorphisms in leucine-rich repeat genes are associated with autism spectrum disorder susceptibility in populations of European ancestry.

Squire, L., Berg, D., Bloom, F.E., Du Lac, S., Ghosh, A., and Spitzer, N.C. (2012). Fundamental neuroscience (Academic Press).

Srivastava, S., McMillan, R., Willis, J., Clark, H., Chavan, V., Liang, C., Zhang, H., Hulver, M., and Mukherjee, K. (2016). X-linked intellectual disability gene CASK regulates postnatal brain growth in a non-cell autonomous manner. Acta neuropathologica communications *4*, 30.

Stevens, G.A., White, R.A., Flaxman, S.R., Price, H., Jonas, J.B., Keeffe, J., Leasher, J., Naidoo, K., Pesudovs, K., and Resnikoff, S. (2013). Global prevalence of vision impairment and blindness: magnitude and temporal trends, 1990–2010. Ophthalmology *120*, 2377-2384.

Stone, C., and Pinto, L.H. (1993). Response properties of ganglion cells in the isolated mouse retina. Visual neuroscience *10*, 31-39.

Stone, J. (2013). Parallel processing in the visual system: the classification of retinal ganglion cells and its impact on the neurobiology of vision (Springer Science & Business Media).

Su, J., Haner, C.V., Imbery, T.E., Brooks, J.M., Morhardt, D.R., Gorse, K., Guido, W., and Fox, M.A. (2011). Reelin is required for class-specific retinogeniculate targeting. The Journal of Neuroscience *31*, 575-586.

Südhof, T.C. (2008). Neuroligins and neurexins link synaptic function to cognitive disease. Nature *455*, 903-911.

Takashima, N., Odaka, Y.S., Sakoori, K., Akagi, T., Hashikawa, T., Morimura, N., Yamada, K., and Aruga, J. (2011). Impaired cognitive function and altered hippocampal synapse morphology in mice lacking Lrrtm1, a gene associated with schizophrenia. PLoS One *6*, e22716.

Taniguchi, H., He, M., Wu, P., Kim, S., Paik, R., Sugino, K., Kvitsani, D., Fu, Y., Lu, J., and Lin, Y. (2011). A resource of Cre driver lines for genetic targeting of GABAergic neurons in cerebral cortex. Neuron *71*, 995-1013.

Terauchi, A., Johnson-Venkatesh, E.M., Toth, A.B., Javed, D., Sutton, M.A., and Umemori, H. (2010). Distinct FGFs promote differentiation of excitatory and inhibitory synapses. Nature *465*, 783-787.

Tham, Y.-C., Li, X., Wong, T.Y., Quigley, H.A., Aung, T., and Cheng, C.-Y. (2014). Global prevalence of glaucoma and projections of glaucoma burden through 2040: a systematic review and meta-analysis. Ophthalmology *121*, 2081-2090.

Thompson, A.D., Picard, N., Min, L., Fagiolini, M., and Chen, C. (2016). Cortical Feedback Regulates Feedforward Retinogeniculate Refinement. Neuron *91*, 1021-1033.

Towns, L.C., Burton, S., Kimberly, C., and Fetterman, M. (1982). Projections of the dorsal lateral geniculate and lateral posterior nuclei to visual cortex in the rabbit. Journal of Comparative Neurology *210*, 87-98.

Trenholm, S., Johnson, K., Li, X., Smith, R.G., and Awatramani, G.B. (2011). Parallel mechanisms encode direction in the retina. Neuron *71*, 683-694.

Triplett, J.W., Wei, W., Gonzalez, C., Sweeney, N.T., Huberman, A.D., Feller, M.B., and Feldheim, D.A. (2014). Dendritic and axonal targeting patterns of a genetically-specified class of retinal ganglion cells that participate in image-forming circuits. Neural development *9*, 2.

Um, J.W., Choi, T.Y., Kang, H., Cho, Y.S., Choii, G., Uvarov, P., Park, D., Jeong, D., Jeon, S., Lee, D., *et al.* (2016). LRRTM3 Regulates Excitatory Synapse Development through Alternative Splicing and Neurexin Binding. Cell Rep *14*, 808-822.

Umemori, H., Linhoff, M.W., Ornitz, D.M., and Sanes, J.R. (2004). FGF22 and its close relatives are presynaptic organizing molecules in the mammalian brain. Cell *118*, 257-270.

Usrey, W.M., Reppas, J.B., and Reid, R.C. (1999). Specificity and strength of retinogeniculate connections. Journal of Neurophysiology *82*, 3527-3540.

Van Hooser, S.D., and Nelson, S.B. (2006). The squirrel as a rodent model of the human visual system. Visual neuroscience *23*, 765-778.

Varoqueaux, F., Aramuni, G., Rawson, R.L., Mohrmann, R., Missler, M., Gottmann, K., Zhang, W., Südhof, T.C., and Brose, N. (2006). Neuroligins determine synapse maturation and function. Neuron *51*, 741-754.

Varoqueaux, F., Jamain, S., and Brose, N. (2004). Neuroligin 2 is exclusively localized to inhibitory synapses. European journal of cell biology *83*, 449-456.

Virolainen, S.-M., Achim, K., Peltopuro, P., Salminen, M., and Partanen, J. (2012). Transcriptional regulatory mechanisms underlying the GABAergic neuron fate in different diencephalic prosomeres. Development *139*, 3795-3805.

Voikar, V., Kulesskaya, N., Laakso, T., Lauren, J., Strittmatter, S.M., and Airaksinen, M.S. (2013). LRRTM1-deficient mice show a rare phenotype of avoiding small enclosures--a tentative mouse model for claustrophobia-like behaviour. Behavioural brain research *238*, 69-78.

Vue, T.Y., Aaker, J., Taniguchi, A., Kazemzadeh, C., Skidmore, J.M., Martin, D.M., Martin, J.F., Treier, M., and Nakagawa, Y. (2007). Characterization of progenitor domains in the developing mouse thalamus. Journal of Comparative Neurology *505*, 73-91.

Waites, C.L., Craig, A.M., and Garner, C.C. (2005). Mechanisms of vertebrate synaptogenesis. Annu Rev Neurosci *28*, 251-274.

Wang, Q., Sporns, O., and Burkhalter, A. (2012). Network analysis of corticocortical connections reveals ventral and dorsal processing streams in mouse visual cortex. J Neurosci *32*, 4386-4399.

Wang, S., Eisenback, M., Datskovskaia, A., Boyce, M., and Bickford, M.E. (2002). GABAergic pretectal terminals contact GABAergic interneurons in the cat dorsal lateral geniculate nucleus. Neuroscience letters *323*, 141-145.

Wang, S.W., Kim, B.S., Ding, K., Wang, H., Sun, D., Johnson, R.L., Klein, W.H., and Gan, L. (2001). Requirement for math5 in the development of retinal ganglion cells. Genes & development *15*, 24-29.

Wässle, H. (2004). Parallel processing in the mammalian retina. Nature Reviews Neuroscience *5*, 747-757.

Weyand, T.G. (2007). Retinogeniculate transmission in wakefulness. Journal of neurophysiology *98*, 769-785.

Weyand, T.G. (2016). The multifunctional lateral geniculate nucleus. Reviews in the neurosciences *27*, 135-157.

Wilson, J., Friedlander, M., and Sherman, S. (1984). Fine structural morphology of identified X- and Y-cells in the cat's lateral geniculate nucleus. Proceedings of the Royal Society of London Series B, Biological Sciences, 411-436.

Wong, A., and Brown, R. (2006). Visual detection, pattern discrimination and visual acuity in 14 strains of mice. Genes, Brain and Behavior *5*, 389-403.

Yamagata, M., Sanes, J.R., and Weiner, J.A. (2003). Synaptic adhesion molecules. Current opinion in cell biology *15*, 621-632.

Yeh, C.-I., Stoelzel, C.R., Weng, C., and Alonso, J.-M. (2009). Functional consequences of neuronal divergence within the retinogeniculate pathway. Journal of neurophysiology *101*, 2166-2185.

Yiu, G., and He, Z. (2006). Glial inhibition of CNS axon regeneration. Nature Reviews Neuroscience *7*, 617-627.

Yogev, S., and Shen, K. (2014). Cellular and molecular mechanisms of synaptic specificity. Annual review of cell and developmental biology *30*, 417-437.

Yucel, Y.H., and Gupta, N. (2015). A framework to explore the visual brain in glaucoma with lessons from models and man. Experimental eye research *141*, 171-178.

Zhang, J., Ackman, J.B., Xu, H.-P., and Crair, M.C. (2012). Visual map development depends on the temporal pattern of binocular activity in mice. Nature neuroscience *15*, 298-307.

Zhao, X., Chen, H., Liu, X., and Cang, J. (2013). Orientation-selective responses in the mouse lateral geniculate nucleus. The Journal of Neuroscience *33*, 12751-12763.

Zhong, X., Gutierrez, C., Xue, T., Hampton, C., Vergara, M.N., Cao, L.-H., Peters, A., Park, T.-S., Zambidis, E.T., and Meyer, J.S. (2014). Generation of three dimensional retinal tissue with functional photoreceptors from human iPSCs. Nature communications *5*, 4047.

Zhu, Y., Xu, J., Hauswirth, W.W., and DeVries, S.H. (2014). Genetically targeted binary labeling of retinal neurons. J Neurosci *34*, 7845-7861.

Zito, A., Cartelli, D., Cappelletti, G., Cariboni, A., Andrews, W., Parnavelas, J., Poletti, A., and Galbiati, M. (2012). Neuritin 1 promotes neuronal migration. Brain structure & function.